Chem. Rev. 1985, 85, 69-201

Kinetics and Mechanisms of the Gas-Phase Reactions of the Hydroxyl Radical with Organic Compounds under Atmospheric Conditions

ROGER ATKINSON

Statewide Air Pollution Research Center, University of California, Riverside, California 92521

Received February 2, 1985 (Revised Manuscript Received July 1, 1985)

Contents

I.	Introduction	69
II.	Experimental Techniques	71
	A. Kinetics	71
	1. Absolute Techniques	71
	2. Relative Rate Techniques	73
	B. Mechanistic and Product Data	
III.	Kinetic, Mechanistic, and Product Data Obtained	75
	A. Alkanes	87
	1. Kinetics	87
	2. Mechanism	95
	3. Atmospheric Reactions	96
	B. Haloalkanes	98
	1. Kinetics	98
	2. Mechanism	113
	3. Mechanism under Atmospheric Conditions	113
	C. Alkenes	113
	1. Kinetics	113
	2. Mechanism	127
	3. Mechanism under Atmospheric Conditions	128
	D. Haloalkenes	129
	1. Kinetics	129
	2. Mechanism	131
	3. Mechanism under Atmospheric Conditions	132
	E. Alkynes	132
	1. Kinetics	132
	2. Mechanism	134
	3. Mechanism under Atmospheric Conditions	135
	F. Oxygen-Containing Organics	135
	1. Kinetics	135
	2. Mechanisms and Subsequent Reactions under Atmospheric Conditions	146
	G. Sulfur-Containing Organics	153
	1. Kinetics	153
	2. Mechanism and Subsequent Reactions under Atmospheric Conditions	156
	H. Nitrogen- and Phosphorus-Containing Organics	161
	1. Kinetics	161
	2. Mechanisms and Subsequent Reactions under Atmospheric Conditions	161
	I. Aromatic Compounds	172
	1. Kinetics	172
	2. Mechanism	178
	3. Mechanisms under Atmospheric Conditions	180
	J. Organometallic Compounds	182
	1. Kinetics	182
	2. Mechanisms and Reaction Products under Atmospheric Conditions	182
IV.	Discussion and Conclusions	182
	A. Rate Constant Trends and Correlations	182
	1. Correlation with $O(^3P)$ Atom, NO_3 Radical, and O_3 Rate Constants	182
	2. Further Correlations Involving OH Radical Rate Constants	184
	B. Estimation of OH Radical Rate Constants	185
	1. H-Atom Abstraction from Alkanes, Carbonyls, Alkyl Nitrates, and Other Saturated Organics	185
	2. OH Radical Addition to Unsaturated $>C{=}C<$ and $-C{\equiv}C-$ Bonds	188
	3. OH Radical Addition to Aromatic Rings	189
	C. Atmospheric Lifetimes	192
V.	Conclusions	193
VI.	Addendum	193
	A. Alkanes	193
	B. Haloalkanes and Other Halo Organics	194
	C. Alkenes	194
	D. Alkynes	194
	E. Oxygen-Containing Organics	194
	F. Sulfur-Containing Organics	195
	G. Aromatics	195
VII.	Acknowledgment	195
VIII.	References	195

I. Introduction

It is now well established that the hydroxyl (OH) radical plays an important role in both combustion and atmospheric chemistry.[1-10] With this recognition of the OH radical as a dominant reactive species in the degradation of organic compounds in both the natural and polluted troposphere[1-3] and in combustion processes,[4-10] accurate measurements of the kinetics of OH radical reactions and the elucidation of their mechanisms and products have been the focus of a large number of experimental investigations. The great majority of these kinetic, mechanistic and product studies have been

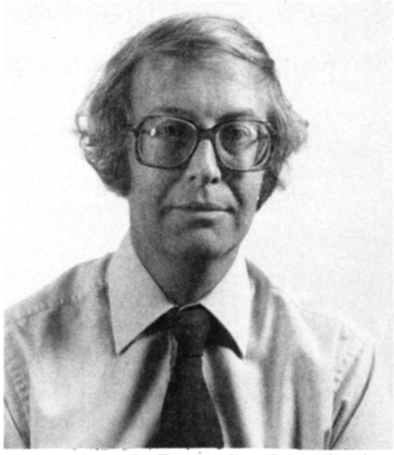

Roger Atkinson was born in England and received a B.A. in 1966 in Natural Sciences from the University of Cambridge and remained there to work for a Ph.D. degree in physical chemistry under the supervision of Dr. B. A. Thrush. After postdoctoral fellowships with Dr. R. J. Cvetanovic at the National Research Council of Canada, Ottawa, and Dr. K. H. Welge at the Centre for Research in Experimental Space Science, York University, Toronto, he moved in 1972 to the Statewide Air Pollution Research Center, University of California at Riverside, to study the kinetics and mechanisms of $O(^3P)$ atom and OH radical reactions with organics. During 1978–1980 he developed chemical computer models for detonation systems and photochemical air pollution at Thornton Research Centre, Shell Research Ltd., Chester, U.K., and Environmental Research and Technology, Inc., Westlake Village, CA. Dr. Atkinson then moved back to the Statewide Air Pollution Research Center at Riverside, where he is currently studying the kinetics and mechanisms of gas-phase O_3 and OH and NO_3 radical reactions of importance in tropospheric chemistry and in the degradation pathways of airborne toxic chemicals.

carried out since 1970, and in recent years detailed chemical computer modeling studies have aided in the elucidation of the reaction sequences operative under both atmospheric[3,11-17] and combustion conditions.[4-6,8-10]

In this paper the kinetics and mechanisms of the reactions of OH radicals with organic compounds under atmospheric conditions are emphasized, and discussion is generally limited to kinetic and mechanistic data obtained at temperatures $\lesssim$500 K. Hence flame, shock-tube, and high-temperature oxidation studies are in general not dealt with, although for studies in which kinetic measurements have encompassed wide temperature ranges (e.g., from $\sim$300 to $\gtrsim$1000 K) the high-temperature data obtained are presented and discussed.

With regard to atmospheric chemistry, Leighton[18] first suggested in 1961 that the OH radical could be an intermediate species playing an important role in photochemical air pollution. Subsequently, the first kinetic data for the reaction of OH radicals with organic compounds were obtained (for a series of alkanes) by Greiner[19,20] using a flash photolysis–kinetic spectroscopy technique. On the basis of these[19,20] and subsequent[21] data, Greiner postulated[21] that these reactions could be important in the formation of photochemical air pollution.

Heicklen and co-workers[22] and Weinstock and co-workers[23] then suggested that the reaction of OH radicals with CO could lead to a chain reaction consuming CO, converting NO to NO_2, and regenerating the OH radical.

$$OH + CO \rightarrow CO_2 + H$$

$$H + O_2 + M \rightarrow HO_2 + M$$

$$HO_2 + NO \rightarrow OH + NO_2$$

Subsequent studies[24-27] showed, however, that this chain reaction is only significant at CO concentrations sufficiently high that the rate of the OH radical reaction with CO is comparable to that with the organic compounds present. In the presence of organic compounds, chain reactions also occur to a certain extent, being initiated by OH radical reaction and propagated by various organic peroxy and alkoxy radicals, as shown below for methane, the simplest organic, under NO-rich conditions.

$$OH + CH_4 \rightarrow H_2O + \dot{C}H_3$$

$$\dot{C}H_3 + O_2 \xrightarrow{M} CH_3O_2\cdot$$

$$CH_3O_2\cdot + NO \rightarrow CH_3O\cdot + NO_2$$

$$CH_3O\cdot + O_2 \rightarrow HCHO + HO_2$$

$$HO_2 + NO \rightarrow OH + NO_2$$

Under conditions where the atmospheric concentrations of NO are $\lesssim$10 ppt (parts per trillion) [$\lesssim 2.4 \times 10^8$ molecule cm^{-3} at 298 K and 760 torr total pressure] the reactions of CH_3O_2 radicals with HO_2 and with other peroxy radicals (including, of course, CH_3O_2 itself) compete with the reaction of the CH_3O_2 radical with NO.[2]

For the longer chain alkanes this reaction mechanism becomes more complex due to isomerization and decomposition of the alkoxy radicals[3] and to the observation that the $\gtrsim C_3$ alkyl peroxy radicals can react with NO to yield directly alkyl nitrates, in competition with the reaction pathway yielding the alkoxy radical and NO_2.[3,28,29] The reaction mechanisms for the alkanes, alkenes, aromatics, and other classes of organics under atmospheric conditions are discussed in detail in later sections in this review.

Concurrently with these advances in the kinetic and mechanistic aspects of OH radical chemistry has been the elucidation of the atmospheric sources of OH radicals. In the troposphere, the important direct sources of OH radicals are from the reaction of $O(^1D)$ atoms, formed from the photodissociation of O_3 ($\lambda \lesssim 319$ nm),[3] with water vapor[3,30-32]

$$O_3 + h\nu \rightarrow O(^1D) + O_2(^1\Delta_g)$$

$$O(^1D) + M\ (M = O_2 + N_2) \rightarrow O(^3P) + M$$

$$O(^1D) + H_2O \rightarrow 2OH$$

and from the photodissociation of HONO.[3,30,31]

$$HONO + h\nu\ (\lambda \lesssim 400\ \text{nm}) \rightarrow OH + NO$$

The other important source of OH radicals arises from the reaction of HO_2 radicals with NO

$$HO_2 + NO \rightarrow OH + NO_2$$

with HO_2 radicals being generated from the photolysis of aldehydes and ketones, as for instance, from HCHO.[3]

$$HCHO + h\nu \rightarrow H + HCO$$

$$H + O_2 + M \rightarrow HO_2 + M$$

$$HCO + O_2 \rightarrow HO_2 + CO$$

At the higher altitudes applicable to the stratosphere and mesosphere, photodissociation of O_2 and N_2O are also sources of $O(^1D)$ atoms,[33-39] while the photodissociation of H_2O yields OH radicals directly, together with H atoms.

While numerous directly measured[40-54] and estimated[32,55-67] atmospheric OH radical concentrations have been reported, these atmospheric OH radical levels are still not well understood. Thus, due to experimental difficulties caused, at least in part, by artifactual formation of OH radicals during the measurement periods,[48,68-70] only in the past year or two have apparently reliable (but in many cases still only upper limit) experimental measurements of ambient tropospheric OH radical concentrations been reported.[48,51-54] In the lower troposphere these recent (and presumably more reliable) measurements using laser induced fluorescence and long path length ultraviolet absorption show that the OH radical concentrations are generally $\lesssim 5 \times 10^6$ molecule cm^{-3} and are often below the detection limits $[\sim(1-3) \times 10^6$ molecule $cm^{-3}]$ of the techniques used.[48,51-54]

Estimates of the average tropospheric OH radical concentrations have also been derived from the observed ambient tropospheric levels of trichloromethane ($CHCl_3$), 1,1,1-trichloroethane (CH_3CCl_3), and ^{14}CO.[56-61,65-67] Using the most recent kinetic data for the reaction of OH radicals with CH_3CCl_3,[71,72] these ambient measurements yield an average northern tropospheric OH radical concentration of $\sim 5 \times 10^5$ molecule cm^{-3}. More recently, Crutzen[32] has carried out calculations which predict that the annually averaged OH radical concentrations in the troposphere during a 24-h period are $\sim 5 \times 10^5$ molecule cm^{-3} and $\sim 6 \times 10^5$ molecule cm^{-3} for the northern and southern hemispheres, respectively. These calculated OH radical concentrations are in reasonably good agreement with those derived from the observed ambient concentrations of $CHCl_3$,[56] CH_3CCl_3,[56,57,59,65,66] and ^{14}CO[61] and hence define rather closely the yearly tropospheric 24-h average OH radical concentrations.

In the stratosphere the most definitive measurements are those of Anderson,[42,43] carried out at altitudes ranging from 30 to 43 km with corresponding OH radical concentrations ranging from $(4.5 \pm 1.6) \times 10^6$ molecule cm^{-3} at 30 km to $(2.8 \pm 1.0) \times 10^7$ molecule cm^{-3} at 43 km. More recently stratospheric OH radical concentrations, derived from satellite measurements of NO_2 and HNO_3 concentrations,[64] have been shown to be in reasonably good agreement with these earlier direct determinations.[42,43]

The actual OH radical concentrations in the troposphere and lower stratosphere are obviously of particular importance since reaction with the OH radical is an important, and in many cases dominant, loss process for organics of both natural and anthropogenic origin[1] and determines both the level of these organics in the troposphere and the amounts which are transported into the stratosphere.

In the following sections the major experimental techniques used in the kinetic and mechanistic studies carried out to date are briefly discussed, and the literature data (through early 1985) for the major classes of organic compounds are then dealt with individually.

II. Experimental Techniques

A. Kinetics

The experimental techniques used to study the kinetics of OH radical reactions with organics can be separated into two methods, namely, absolute and relative rate constant techniques. The absolute methods have involved mainly the discharge flow and flash photolysis techniques, with the modulation-phase shift and pulsed radiolysis methods being used in only a limited number of studies, while to date a variety of relative rate techniques have been used. These techniques are briefly discussed below.

1. Absolute Techniques

a. Discharge Flow. The detection of the OH radical by Oldenberg[73] from an electric discharge in water using ultraviolet absorption formed the first basis for the determination of OH radical kinetics. Avramenko and Lorenzo[74] subsequently developed a fast flow system with an electric discharge of water vapor as an OH radical source. The products from this discharge region then flowed along a tube designed to allow the addition of reactants downstream.[74] The absorption intensity at 306.4 nm due to OH radicals was monitored along the axis of the flow tube, and the difference in absorption intensity was related to the bimolecular rate constant for the reaction of OH radicals with the reactant. It was concluded by both Oldenberg[73] and Avramenko and Lorenzo[74] that the OH radical half-life in such a system was ~ 0.1 s.

The next major breakthrough in obtaining accurate kinetic information for OH radical reactions occurred from the work of Kaufman and Del Greco,[75-77] who showed that a discharge in water vapor gave rise to a complex chemical system in which OH radicals were produced downstream from the discharge, via secondary reactions such as

$$H + O_2 + M \rightarrow HO_2 + M$$

and

$$H + HO_2 \rightarrow 2OH$$

Furthermore, they showed[75-77] that the rapid reaction

$$H + NO_2 \rightarrow OH + NO$$

yielded a clean source of OH radicals which had an appreciably shorter half-life ($\sim 10^{-3}$ s), due, under the conditions investigated, to the fast bimolecular reaction

$$OH + OH \rightarrow H_2O + O(^3P)$$

All recent discharge flow investigations have utilized this reaction of H atoms with NO_2 as a source of OH radicals which, under the experimental conditions used, is free from interferences from vibrationally excited OH radicals.[78] For recent reviews of this general experimental technique, the articles of Howard[79] and Kaufman[80] should be consulted. Detection of the OH radical has typically been accomplished by resonance absorp-

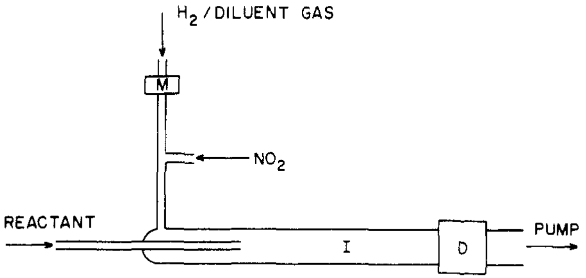

Figure 1. Schematic of a discharge flow system: (M) microwave discharge; (I) flow tube; (D) detection region.

tion (RA),[75-77] resonance fluorescence (RF),[81] electron paramagnetic resonance (EPR),[82-84] mass spectroscopy (MS),[85] laser magnetic resonance (LMR),[78,86] or laser-induced fluorescence (LIF).[87] The following OH radical concentrations employed are typical for these detection systems: resonance absorption, $\sim 10^{12}$–10^{14} molecule cm^{-3}; resonance fluorescence and laser-induced fluorescence, $\sim 10^{9}$–10^{12} molecule cm^{-3}; electron paramagnetic resonance, $\sim 10^{11}$–10^{13} molecule cm^{-3}; mass spectrometry, $\sim 10^{12}$–10^{13} molecule cm^{-3}; and laser magnetic resonance, $\sim 10^{9}$–10^{11} molecule cm^{-3}.

A schematic of a discharge flow system is shown in Figure 1. The major features are[79,80] (a) a microwave discharge of H_2 in a diluent gas (normally He or Ar) followed by admixture with a known amount of NO_2 to yield OH radicals, (b) a cylindrical flow tube, typically $\sim$50–100 cm in length with linear flow rates of typically 10^3–10^4 cm s^{-1}, (c) a moveable injector for introduction of reactants, and (d) an observation region utilizing one of the above detection techniques. The reactant concentration is normally in large excess over the initial OH radical concentration, and hence the decays of the OH radical concentration are pseudo first order. This then eliminates the necessity for determining absolute OH radical concentrations.

Using the movable injector system, kinetic problems associated with wall losses of OH radicals are normally avoided,[86,88,89] though obviously efforts should be taken to minimize wall losses.[90] Hydroxyl radical decay rates due to reaction with the added reactant are typically of the order of up to $\sim$500 s^{-1}, and total pressures are generally restricted to $\leq$10 torr,[79] although very recently Keyser[91] has used this technique to study the reaction of OH radicals with HCl up to a total pressure of helium of 100 torr. Hence extrapolation of the results to atmospheric pressure may give rise to significant uncertainties. As a recent example, this situation has become evident for the reaction of OH radicals with CO, which, although it has a nonzero bimolecular rate constant at low pressures, has been determined to have a pressure-dependent rate constant.[92-101]

At the higher OH radical concentrations encountered with EPR, MS, and RA detection, secondary reactions of OH radicals with reaction products can become important, necessitating the determination of stoichiometric factors in order to obtain the initial OH radical rate constants. Niki and co-workers[85,102,103] have successfully used a discharge flow-mass spectrometric technique to determine rate constants for the reaction of OH radicals with a series of organic compounds by monitoring the organic reactant decays in the presence of known excess OH radical concentrations, thus avoiding stoichiometric corrections. For details of the salient features and variations of the discharge flow technique, the references cited above should be consulted.

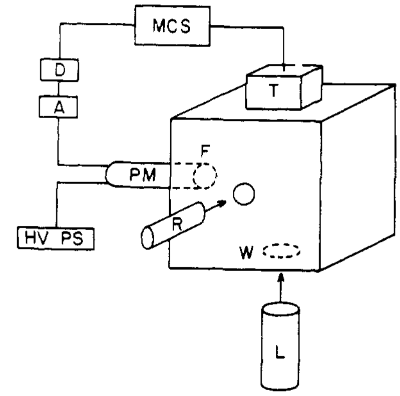

Figure 2. Schematic of a pulsed photolysis–resonance fluorescence system: (A) amplifier; (D) discriminator; (MSC) multichannel scaler; (PM) photomultiplier tube; (W) window; (F) interference filter; (L) flash lamp or photolysis laser; (R) resonance lamp or probe laser; (T) trigger unit; (HV PS) high voltage power supply.

b. Flash Photolysis. The flash photolysis technique, as first reported by Norrish and Porter[104] in 1949, was readily adapted to monitor OH radicals. In the earlier work of Horne and Norrish[105,106] and of Greiner,[19-21,107] the photodissociation of H_2O and H_2O_2 in the vacuum- and far-ultraviolet, respectively, was used to produce OH radicals. Hydroxyl radical concentrations were monitored by kinetic spectroscopy, using photographic plates to monitor the absorption of rotational lines in the $A^2\Sigma^+$ (v' = 0) $\leftarrow$ $X^2\Pi$ (v'' = 0) band.[19-21,105-107] Following this pioneering work of Greiner[19-21,107-111] in determining absolute OH and OD radical rate constants, the photographic plate–spectroscopic flash lamp combination was replaced by an OH radical resonance lamp (microwave discharge of H_2O in He or Ar at $\sim$1 torr total pressure)–photomultiplier combination[112]—that is, by resonance absorption with a fast data acquisition system. Most recently, Wahner and Zetzsch[100] have used an excimer laser as the pulsed photolysis source and a CW ring-dye laser, set at 308 nm, as the absorption probe beam.

The use of resonance fluorescence to monitor OH radicals as a function of time after the flash was pioneered by Stuhl and Niki[113,114] and has since been used by numerous groups to determine kinetic data for the reactions of OH radicals with a wide variety of inorganic and organic reactants. Discussions of the general flash photolysis–resonance absorption/fluorescence techniques have been given by Michael and Lee[115] and Kaufman.[80]

A schematic of a typical pulsed photolysis–resonance fluorescence system is shown in Figure 2. Hydroxyl radicals are typically produced from the pulsed photodissociation of H_2O[113] or HNO_3,[116,117] although other methods of producing OH radicals, such as the photolysis of N_2O–H_2,[118,119] O_3–H_2,[120] and NO_2–H_2[112] mixtures, have been used, where OH radicals are formed from the reaction of $O(^1D)$ atoms with H_2.

The pulsed ultraviolet or vacuum ultraviolet photolysis radiation is produced by means of flash lamps[113] or, more recently, by pulsed lasers[117,121,122] [these usually being the rare gas halogen excimer lasers, for example the ArF and KrF lasers, which lase at 193 nm (ArF) and 248 nm (KrF)]. The reaction cell is typically separated from the flash lamp by means of windows transmitting in the vacuum-ultraviolet region, such as LiF (transmitting $\lambda \gtrsim 105$ nm), MgF_2 (transmitting $\lambda \gtrsim 115$ nm), CaF_2 (transmitting $\lambda \gtrsim 125$ nm), sapphire (transmitting $\lambda \gtrsim 145$ nm), and Supracil (transmitting $\lambda \gtrsim 165$ nm). Hydroxyl radicals are monitored as a function of time after the pulsed flash lamp or laser radiation by resonance fluorescence using a CW microwave discharge in H_2O/He or H_2O/Ar mixtures[113] or by laser-induced fluorescence using a pulsed[123] or quasi-CW[122] laser to produce the probe irradiation beam. Photon counting techniques are generally necessary on account of the low signal levels employed.

Since 1975 slow flow systems have been routinely used so that the photolysis and reaction products do not build up in the reaction cell but are swept out of the cell.[124] Typically the residence times in the reaction cell (which have typically ranged in volume from ~150 to ~2000 cm^3) are of the order of ~1–10 s (~1–3 flashes). This approach also has the additional advantage of minimizing (or, hopefully, avoiding) losses of the reactant to the walls which has been observed to occur in metal (and possibly Pyrex) reaction vessels under nonflow conditions.

With the reactant concentration in large excess of the initial OH radical concentration, the bimolecular rate constants, k_2, are obtained from the observed pseudo-first-order OH radical decay rates, R, by use of the equation

$$R = k_1 + k_2[\text{reactant}] \qquad (1)$$

where k_1 is the first-order rate for removal of OH in the absence of added reactant (primarily attributed to diffusion out of the viewing zone and to reaction with the OH radical precursor or impurities in the diluent gas).

With RA and RF detection systems, typical OH radical concentrations in the reaction cell are ~ 10^{11}–10^{13} molecule cm^{-3} (~10^7 molecule cm^{-3} with laser absorption spectroscopy[100]) and ~10^9–10^{11} molecule cm^{-3}, respectively. Since, typically, the OH radical decay rates employed are up to ~10^4 and ~10^3 s^{-1} for RA and RF detection, respectively, the [reactant]/[OH] ratios are reasonably similar (though generally somewhat higher in the RF case). However, in earlier studies, because of the generally higher flash energies used with RA detection (~1000 J/flash compared with $\lesssim$100 J/flash for RF detection), secondary reactions of OH radicals with the larger amounts of photolysis products generated by the more intense flash may have been more important with the flash photolysis–resonance absorption techniques than for the flash photolysis–resonance fluorescence systems (see, for example, ref 125). Using the more recent pulsed laser photolysis–laser-induced fluorescence or laser absorption techniques,[100,122] the sensitivities for OH radical detection are sufficiently good that complications due to secondary reactions and/or photofragment formation are generally totally negligible.

A major advantage of the flash or laser photolysis technique is that a pressure range up to atmospheric pressure or greater can be employed, making this technique of great utility for investigating atmospherically important reactions. Because of problems associated with absorption of the flash lamp radiation, reactivity toward OH radicals, and quenching of the $OH(A^2\Sigma^+)$ state, He, Ar, N_2, and SF_6 are the diluent gases which have been commonly used.[96–98,122,123] The flash photolysis–resonance fluorescence technique has been used at total pressures of up to ~700 torr[96] (up to 8.6 atm using laser-induced fluorescence[123]), and with the advent of laser photolysis–laser-induced fluorescence systems[126] and laser photolysis–laser absorption techniques,[100] kinetic data can now be obtained up to and beyond atmospheric pressure in air. Similarly, the flash photolysis–resonance absorption technique has been routinely used up to approximately atmospheric pressure.[97] In recent years the maximum temperature of this flash photolysis technique has been raised to $\gtrsim$1000 K,[125,127,128] resulting in kinetic data being obtained in a single study over the temperature range $\leq$300 to $\geq$1000 K.[127,128]

c. Other Absolute Rate Constant Techniques. Two other absolute rate techniques have been utilized for the determination of rate constants for the reaction of OH radicals with organics, namely, the pulsed radiolysis[129] and modulation-phase shift[130] methods. Since these two techniques have been used in only a limited number of studies, they are not discussed here, but rather the reader is referred to ref 129 and 130 for further details.

2. Relative Rate Techniques

Numerous methods have been employed to obtain relative rate constant data for the reactions of OH radicals with organic compounds.[131–143] The major general technique used has been that of monitoring the relative rates of the disappearance of two or more organic compounds in chemical systems containing OH radicals. Clearly, in order to derive meaningful rate constant data from this experimental technique, either the organic loss processes must be solely due to reaction with the OH radical or, if another loss process (e.g., photolysis) occurs, its effect must be able to be accurately taken into account. While the potential for complicating reactive loss processes of the organic compounds other than by OH radical reaction exist in many of the chemical systems utilized for relative rate measurements, experimental tests can be carried out to ensure that these other loss processes are minimal. Furthermore, our knowledge of the chemistry of organic compounds, especially in irradiated NO_x–air systems, has progressed sufficiently so that in many cases the experimental conditions can be designed to minimize loss processes of the organics by reactive species other than the OH radical.

In general, if the sole loss processes of the organic being studied (the reactant organic) and the reference organic are via reaction with the OH radical

$$\text{OH} + \text{reactant organic} \rightarrow \text{products} \qquad (2)$$

$$\text{OH} + \text{reference organic} \rightarrow \text{products} \qquad (3)$$

and providing dilution is negligible, then

$$-\mathrm{d} \ln [\text{reactant organic}]/\mathrm{d}t = k_2[\text{OH}] \qquad (\text{I})$$

$$-\mathrm{d} \ln [\text{reference organic}]/\mathrm{d}t = k_3[\text{OH}] \qquad (\text{II})$$

Eliminating the OH radical concentration then leads to

$$\ln\left\{\frac{[\text{reactant organic}]_{t_0}}{[\text{reactant organic}]_t}\right\} = \frac{k_2}{k_3}\ln\left\{\frac{[\text{reference organic}]_{t_0}}{[\text{reference organic}]_t}\right\} \quad \text{(III)}$$

where $[\text{reactant organic}]_{t_0}$ and $[\text{reference organic}]_{t_0}$ are the concentrations of the reactant and reference organics, respectively, at time t_0, $[\text{reactant organic}]_t$ and $[\text{reference organic}]_t$ are the corresponding concentrations at time t, and k_2 and k_3 are the rate constants for reactions 2 and 3, respectively. Hence plots of ln $([\text{reactant organic}]_{t_0}/[\text{reactant organic}]_t)$ against ln $([\text{reference organic}]_{t_0}/[\text{reference organic}]_t)$ should yield a straight line of slope k_2/k_3 and zero intercept.

If dilution does occur, with the dilution factor at time t being D_t [where $D_t = \ln (C_{t_0}/C_t)$ and C_{t_0} and C_t would be the concentrations of a chemically nonreactive species at times t_0 and t, respectively], then eq III is modified to

$$\ln\left\{\frac{[\text{reactant organic}]_{t_0}}{[\text{reactant organic}]_t}\right\} - D_t = \frac{k_2}{k_3}\left[\ln\left\{\frac{[\text{reference organic}]_{t_0}}{[\text{reference organic}]_t}\right\} - D_t\right] \quad \text{(IV)}$$

Another situation commonly encountered occurs when the reactant organic photolyzes

$$\text{reactant organic} + h\nu \rightarrow \text{products} \quad (4)$$

In this case, assuming dilution to be negligible and that photolysis occurs at a constant rate (such as under conditions of constant light intensity), then

$$\frac{1}{(t - t_0)}\ln\left\{\frac{[\text{reactant organic}]_{t_0}}{[\text{reactant organic}]_t}\right\} = k_4 + \frac{k_2}{k_3(t - t_0)}\ln\left\{\frac{[\text{reference organic}]_{t_0}}{[\text{reference organic}]_t}\right\} \quad \text{(V)}$$

The above kinetic analyses have been general in that they are not limited to the case of a constant OH radical concentration. Obviously, if the OH radical concentration is constant or appears to be so within the measurement errors (i.e., from eq **II**), then plots of ln $([\text{reactant organic}]_{t_0}/[\text{reactant organic}]_t)$ and ln $([\text{reference organic}]_{t_0}/[\text{reference organic}]_t)$ against the reaction time $(t - t_0)$ will be linear, with slopes of $k_2[\text{OH}]$ and $k_3[\text{OH}]$, respectively. Their relative slopes then yield the desired rate constant ratio k_2/k_3. However, it is recommended that in all cases eq III, IV, and V, whichever is appropriate, be used. It should be noted that only relative measurements of the reactant and reference organic concentrations are necessary.

A variety of chemical systems, both photolytic and nonphotolytic, have been used for the measurement of relative rate constants.[131-143] During the 1970s the major photolytic chemical systems used to generate OH radicals were the photolysis of H_2O_2 at 253.7 nm, utilized by Gorse and Volman[131] [with a more complex derivation of the relevant rate data from the experimental data than that given above], the photolysis of nitrous acid[134,137]

$$\text{HONO} + h\nu \rightarrow \text{OH} + \text{NO}$$

and the photolysis of NO_x–organic–air mixtures.[133,136,138]

In the earlier relative rate constant determinations using irradiated NO_x–organic–air mixtures, the irradiations were generally carried out in large environmental chambers and in many cases dilution had to be taken into account.[133,144] Since the OH radical concentrations were typically ~(2–5) × 10^6 molecule cm^{-3}, this dilution accounted for a significant portion of the observed organic loss rates, and the rate constant data obtained were accurate to only some ~±15–30%.[133,144]

Since 1978 the use of irradiated HONO–NO–air mixtures to generate higher OH radical levels [~(1–5) × 10^7 molecule cm^{-3}], coupled with in situ Fourier transform infrared (FT-IR) absorption spectroscopy or gas chromatography, has enabled more accurate relative rate constant[137,145] and product and mechanistic data[146] to be obtained. In the past four years Atkinson and co-workers[140,147] have used irradiated methyl nitrite–NO–air systems to generate OH radicals

$$CH_3ONO + h\nu \rightarrow CH_3O + NO$$

$$CH_3O + O_2 \rightarrow HCHO + HO_2$$

$$HO_2 + NO \rightarrow OH + NO_2$$

at concentrations up to ~(2–3) × 10^8 molecule cm^{-3}. As an example of this technique as routinely used,[140,147] CH_3ONO–NO–reactant organic–reference organic–air mixtures have been irradiated in a variety of chambers, ranging from all-Teflon chambers of ~60–6400-L volume to a 5800-L cylindrical evacuable Teflon-coated chamber with a 25-KW Xenon arc to provide irradiation.[140,147-150] Gas chromatography,[140,147,148] FT-IR absorption spectroscopy[149] and differential optical absorption spectroscopy (DOAS)[150] have been utilized to monitor the reactant and reference organics in these studies.

Recently, Ohta[142] has employed the photolysis of H_2O_2 at 253.7 nm to generate high concentrations of OH radicals and obtain highly precise relative rate constant ratios for a wide variety of alkenes and dialkenes. With both of these recent relative-rate techniques,[140,142,147,151-153] the precision of the derived rate constant ratios is generally ≲5% at the two least-squares standard deviation level. Furthermore, where the data of Ohta[142,152] and Atkinson and co-workers[151,153] overlap, the agreement has been found to be excellent[142,151-153] (see also the section below dealing with the alkenes).

In summary, it appears that these more recent experimental techniques can provide precise relative rate constant data for a wide variety of organics, including those of low volatility (down to <1 × 10^{-4} torr at room temperature[148,154]). The lower limit for the OH radical rate constants attainable with these techniques is set by the reproducibility and precision of the analytical monitoring techniques used and appears to be ~(1–3) × 10^{-13} cm^3 $molecule^{-1}$ s^{-1} under optimum conditions.[140,155,156]

Three nonphotolytic sources of OH radicals have been utilized to date.[135,141,143] Campbell and co-workers[135] have used the heterogeneous formation of OH radicals from the H_2O_2–NO_2 reaction system to determine rate constant ratios for, among other organics, a series of nitrites,[157,158] esters,[159] and aldehydes.[160] Tuazon et al.[143] have utilized the gas-phase reaction of N_2H_4 with O_3 in air (whose mechanism is not completely understood) to generate OH radicals in relatively high concentrations [$\sim(2–3) \times 10^7$ molecule cm^{-3} when averaged over a 25-min duration]. For methyl nitrite, the only organic which has been studied by both of these nonphotolytic OH radical generation techniques, the room-temperature rate constant obtained by Tuazon et al.[143] is a factor of ~7 lower than those reported by Campbell and co-workers.[157,158] Since relative rate constants obtained by using the N_2H_4–O_3 dark reaction and irradiated CH_3ONO–NO–air mixtures have been shown to be in good agreement for a variety of organics,[143] it is clear that the reliability of the heterogeneous H_2O_2–NO_2 reaction system needs to be demonstrated.

Finally, Barnes et al.[141] have used the well-understood thermal decomposition of HO_2NO_2 in the presence of NO in air to generate OH radicals.

$$HO_2NO_2 \rightleftarrows HO_2 + NO_2$$

$$HO_2 + NO \rightarrow OH + NO_2$$

This chemical system has been used, with analyses being carried out by using FT-IR absorption spectroscopy, to derive OH radical rate constants for a variety of organics at room temperature.[141]

The individual references cited above should be consulted for further details concerning these experimental techniques.

B. Mechanistic and Product Data

Although numerous mechanistic and product studies have been carried out during the past few years, there are still significant areas of uncertainty concerning the mechanisms and products of OH radical reactions with organic compounds. Two general techniques have been used, namely, static systems employing the photolytic generation of OH radicals combined with a quantitative analysis of the stable products formed,[146,161–169] and low-pressure molecular beam or discharge flow studies.[170–176]

In the static systems, OH radicals have been generated from the reaction of $O(^1D)$ atoms, produced from the photodissociation of N_2O or NO_2, with H_2, H_2O, or C_2H_6,[161–163] and from the photolysis of H_2O_2,[163] HONO,[146,164] and CH_3ONO[169,177] (and other alkyl nitrites[177–179]). Gas chromatography[162,165] (including combined gas chromatography–mass spectrometry[166]), FT-IR absorption spectroscopy,[146,164,178,179] and differential optical absorption spectroscopy[180] have been used for the quantitative determination of products. As an example of this general technique, Niki and co-workers[146,164,178] have used the irradiation of HONO–NO–organic–air mixtures with long path-length FT-IR absorption spectroscopic analysis of products to elucidate the mechanisms of the OH radical initiated oxidations of organic compounds under simulated atmospheric conditions. Similar studies have been carried out by other research groups.[177,180]

Related to this technique are the mechanistic and product data obtained from environmental chamber–computer modeling studies.[11–17] Although obviously in these studies the chemistry involved, even for a single organic, is exceedingly complex,[11] mechanistic conclusions can be obtained which are helpful in elucidating the reaction steps subsequent to the initial reaction with the OH radical under simulated atmospheric conditions.

Gutman and co-workers[170,171] and Sloane[172,174] have used photoionization–mass spectroscopy of crossed molecular beams of OH radicals and the reactant organic (alkenes,[171] alkynes,[170] and aromatics[172,174]) to detect the intermediate species and the final stable products. Unfortunately, from the viewpoint of interpreting these results in terms of atmospheric chemistry, because of the low pressures (at, or approaching, single-collision conditions), redissociation of the excited adducts can become dominant, especially for the alkenes and alkynes. Under these conditions the H atom abstraction reactions, which may be very minor processes at higher pressure where collisional deactivation of the adducts dominates, can become major reaction pathways.

Other studies utilizing discharge flow systems, operating at ~0.5–10 torr total pressure, with analyses of the intermediate species by mass spectrometry or photoionization–mass spectrometry have been carried out,[173,175,176] mainly with a view to determining the relative amounts of OH radical addition/H atom abstraction occurring during the reactions of OH radicals with alkenes. In these studies the total pressures were sufficiently high that the reactions were at, or close to, their limiting high-pressure regimes,[175] and hence the data obtained should be relevant to atmospheric conditions.

III. Kinetic, Mechanistic, and Product Data Obtained

In the following sections, the reactions of OH radicals with the various classes of organic compounds [alkanes (including cycloalkanes), haloalkanes, alkenes (including di- and trialkenes and cycloalkenes), haloalkenes, alkynes, oxygen-containing organics, sulfur-containing organics, nitrogen- and phosphorus-containing organics, aromatics, and organometallics] are discussed separately. As far as possible, the reaction mechanisms, including the subsequent reaction pathways under atmospheric conditions, are presented together with the compilations and evaluations of the available rate constant data. Data from relative rate constant studies have been reevaluated on the basis of the recommended rate constants for the reference reactions at the temperatures employed in these relative rate studies.

It should be noted that for those rate constant measurements where the rate constant for the reaction of OH radicals with an organic compound was determined relative to that for the reaction of OH radicals with CO, additional uncertainties in the derived rate constants arise because of the uncertainties in the value of this reference rate constant. Thus, as noted above, the rate constant at room temperature for the reaction of OH radicals with CO is pressure dependent up to at least atmospheric pressure,[92–101] with the rate constant at a given pressure also depending on the identity of the diluent gas.[92,96–98,101] At elevated temperatures, while there is general agreement from direct studies as to the magnitude of the rate constant, these studies[110,118,181–185] were carried out at low total pressures (≤100 torr)

TABLE I. Rate Constants k and Arrhenius Parameters for the Gas-Phase Reaction of OH Radicals with Alkanes

alkane	$10^{12}A$, cm^3 $molecule^{-1}$ s^{-1}	n	E, cal mol^{-1}	$10^{12}k$, cm^3 $molecule^{-1}$ s^{-1}	T, K	technique	ref	temp range covered, K
methane				0.0108 ± 0.0025	300	DF-EPR	Wilson and Westernberg[188]	
				0.00848 ± 0.00071	295	FP-KS	Greiner[21]	295–498
				0.00953 ± 0.00028	295			
				0.0106 ± 0.00025	296			
				0.0130 ± 0.00053	296			
				0.00804 ± 0.00020	301			
				0.00805 ± 0.00041	301			
				0.00903 ± 0.00088	302			
				0.0154 ± 0.0006	333			
				0.0352 ± 0.0007	370			
				0.0611 ± 0.0023	424			
				0.121 ± 0.004	492			
				0.121 ± 0.003	493			
				0.120 ± 0.003	493			
				0.113 ± 0.002	497			
	$5.5^{+0.8}_{-0.6}$		3772 ± 102	0.122 ± 0.003	498			
				0.00204 ± 0.00036^a	240	FP-RF	Davis et al.[182]	240–373
				0.00508 ± 0.00020^a	276			
				0.00775 ± 0.00063^a	298			
	2.36 ± 0.21		3400 ± 175	0.0242 ± 0.0037^a	373			
				0.00715 ± 0.00042	293	DF-RF	Margitan et al.[189]	293–427
				0.0212 ± 0.0004	359			
				0.0306 ± 0.0001	384			
				0.0422 ± 0.0018	407			
	3.83 ± 0.20		3660 ± 40	0.0521 ± 0.0016	427			
				0.0261 ± 0.0027	381	PR-RA	Gordon and Mulac[129]	381–416
				0.0548 ± 0.0017	416			
				0.00651 ± 0.00027	295 ± 2	FP-RA	Overend et al.[190]	
				0.0095 ± 0.0014	296	DF-LMR	Howard and Evenson[191]	
				0.0088 ± 0.0007	298	FP-RA	Zellner and Steinert[192]	298–892
				0.0148	330			
				0.020	358			
				0.028	381			
				0.061	444			
				0.070	453			
				0.113	498			
				0.174	525			
				0.257	564			
				0.251 ± 0.033	576			
				0.276 ± 0.033	584			
				0.335	622			
				0.551	629			
				0.822	671			
				0.830	680			
				1.12	738			
				1.21	756			
				1.51	776			
	5.76×10^{-9}	3.08	2007	2.71	892			
			3585 ± 240 (300–500 K)					
				0.0076 ± 0.0005	298	rel rate [rel to $k(OH + H_2) = 7.0 \times 10^{-15}$]^b	Cox et al.[93]	
				0.00750 ± 0.00060	298	FP-RF	Tully and Ravishankara[125]	298–1020

			0.0473 ± 0.0045	398			
			0.081 ± 0.011	448			
			0.145 ± 0.012	511			
			0.167 ± 0.006	529			
			0.314 ± 0.040	600			
			0.275 ± 0.044	619			
			0.578 ± 0.058	696			
			0.84 ± 0.15	772			
			1.50 ± 0.15	915			
1.32×10^{-5}	1.92	2692	2.00 ± 0.20	1020			
			0.00557 ± 0.00054	269	DF-RF	Jeong and Kaufman[186,193]	269–473
			0.00789 ± 0.00049	297			
			0.0178 ± 0.0012	339			
			0.0347 ± 0.023	389			
			0.0549 ± 0.0035	419			
1.28×10^{-12}	4.23	900 ± 1540	0.102 ± 0.007	473			
5.26 ± 0.88		3810 ± 120					
			0.0392 ± 0.0033	413	rel rate [rel to $k(OH + CO) = 1.12 \times 10^{-13}10^{3.94\times10^{-4}T}]^c$	Baulch et al.[194]	413–693
			0.0555 ± 0.0033	417			
			0.0369 ± 0.0030	422			
			0.0654 ± 0.0066	443			
			0.0792 ± 0.0073	471			
			0.0981 ± 0.0063	505			
			0.103 ± 0.018	517			
			0.0936 ± 0.0179	521			
			0.112 ± 0.006	546			
			0.165 ± 0.004	553			
			0.267 ± 0.015	603			
			0.349 ± 0.020	663			
			0.589 ± 0.060	693			
			0.00650	298	PR-RA	Jonah et al.[185]	298–1229
			0.00846	298			
			0.0189	348			
			0.0351	373			
			0.106	398			
			0.0938	415			
			0.175	424			
			0.124	450			
			0.209	483			
			0.174	483			
			0.336	543			
			0.584	571			
			0.545	613			
			0.760	667			
			0.893	709			
			0.991	712			
			1.04	769			
			1.52	858			
			2.48	873			
			2.27	974			
			2.01	974			
			4.50	1071			
			3.22	1125			
			4.19	1125			
			4.93	1229			

TABLE I (Continued)

alkane	$10^{12}A$, cm^3 molecule s^{-1}	n	E, cal mol^{-1}	$10^{12}k$, cm^3 molecule^{-1} s^{-1}	T, K	technique	ref	temp range covered, K
				0.0085 ± 0.0006	298 ± 3	FP-RF	Madronich and Felder[128]	298–1512
				0.0228 ± 0.0043	362 ± 10			
				0.0463 ± 0.0034	407 ± 5			
				0.0629 ± 0.009	410 ± 14			
				0.154 ± 0.014	510 ± 10			
				0.177 ± 0.017	525 ± 10			
				0.202 ± 0.010	546 ± 5			
				0.439 ± 0.038	626 ± 16			
				0.478 ± 0.07	698 ± 22			
				1.48 ± 0.08	900 ± 12			
				2.12 ± 0.23	967 ± 35			
				2.16 ± 0.11	1005 ± 15			
				2.72 ± 0.15	1103 ± 17			
				3.34 ± 0.20	1164 ± 17			
				2.41 ± 0.22	1174 ± 22			
				3.18 ± 0.17	1176 ± 17			
				3.89 ± 0.25	1196 ± 17			
				4.26 ± 0.39	1196 ± 37			
				3.77 ± 0.32	1238 ± 18			
				3.68 ± 0.23	1244 ± 17			
				3.58 ± 0.27	1261 ± 23			
				3.80 ± 0.37	1261 ± 18			
				4.74 ± 0.20	1300 ± 18			
				4.20 ± 0.21	1307 ± 18			
				4.84 ± 0.50	1314 ± 23			
				5.32 ± 0.31	1345 ± 18			
				5.61 ± 0.34	1365 ± 19			
				6.44 ± 0.53	1396 ± 19			
				5.98 ± 0.69	1455 ± 20			
				6.52 ± 1.15	1510 ± 20			
	$2.6^{+9.7}_{-2.1} \times 10^{-5}$	1.83 ± 0.17	2774 ± 266	6.74 ± 0.35	1512 ± 20			
methane-^{13}C				0.00850	d	rel rate [rel to $k(OH + CH_4)$ = 8.47×10^{-15}]^e	Rust and Stevens[195]	
methane-d_1				0.0365 ± 0.0017	416	PR-RA	Gordon and Mulac[129]	
methane-d_2				0.0299 ± 0.0017	416	PR-RA	Gordon and Mulac[129]	
methane-d_3				0.0111 ± 0.0005	416	PR-RA	Gordon and Mulac[129]	
methane-d_4				0.0050 ± 0.0002	416	PR-RA	Gordon and Mulac[129]	
ethane				0.310 ± 0.007	297	FP-KS	Greiner[21]	297–493
				0.340 ± 0.010	298			
				0.282 ± 0.007	299			
				0.239 ± 0.013	299			
				0.304 ± 0.035	300			
				0.224 ± 0.042	301			
				0.457 ± 0.010	335			
				0.750 ± 0.050	369			
				0.936 ± 0.058	424			
	$18.6^{+3.3}_{-2.7}$		2447 ± 106	1.55 ± 0.033	493			
				0.664 ± 0.033	381	PR-RA	Gordon and Mulac[129]	381–416
				0.797 ± 0.050	416			
				0.264 ± 0.017	295 ± 2	FP-RA	Overend et al.[190]	
				0.290 ± 0.060	296	DF-LMR	Howard and Evenson[196]	
				0.26 ± 0.04	298	DF-RF	Leu[197]	

				0.112 ± 0.018	250	DF-RF	Anderson and Stephens[198]	250–364
				0.176 ± 0.022	275			
				0.257 ± 0.031	298			
				0.349 ± 0.051	322			
	16.4 ± 2.6		2474 ± 91	0.526 ± 0.080	364			
				0.231 ± 0.040	295 ± 1	DF-RF	Lee and Tang[199]	
				0.080	238	LP-RF	Margitan and Watson[200]	
				0.259 ± 0.021	297	FP-RF	Tully et al.[201]	297–800
				0.771 ± 0.076	400			
				1.58 ± 0.10	499			
				2.61 ± 0.33	609			
				3.65 ± 0.25	697			
	1.43×10^{-2}	1.05	1810	5.07 ± 0.34	800			
				0.679 ± 0.048	403	rel rate [rel to $k(OH + CO) = 1.12 \times 10^{-13}] 10^{3.94 \times 10^{-4} T}]^c$	Baulch et al.[194]	403–683
				1.21 ± 0.12	443			
				1.30 ± 0.09	493			
				2.51 ± 0.18	561			
				2.26 ± 0.25	595			
				4.47 ± 0.51	683			
				0.196 ± 0.013	248	DF-RF	Jeong et al.[186]	248–472
				0.228 ± 0.014	273			
				0.310 ± 0.020	294			
				0.306 ± 0.021	298			
				0.426 ± 0.027	333			
				0.403 ± 0.027	333			
				0.538 ± 0.035	375			
				0.529 ± 0.034	375			
				0.799 ± 0.054	428			
				0.770 ± 0.048	429			
				0.993 ± 0.068	464			
	3.87×10^{-9}	3.09	−340 ± 680	1.03 ± 0.067	472			
	6.11 ± 0.60		1760 ± 70					
				0.105 ± 0.004	240	FP-RF	Smith et al.[202]	240–295
				0.137 ± 0.006	251			
				0.205 ± 0.009	273			
	18.0 ± 5.0		2464 ± 437	0.263 ± 0.010	295			
				0.239 ± 0.010	292.5	LP-LIF	Tully et al.[203]	293–705
				0.407 ± 0.017	340			
				0.651 ± 0.027	396			
				1.15 ± 0.048	478			
				1.23 ± 0.051	484			
				2.01 ± 0.083	577			
				2.11 ± 0.088	586			
				3.48 ± 0.144	705			
				0.22 ± 0.03	295	LP-LIF	Schmidt et al.[126]	
				0.267 ± 0.040	295	DF-RF	Baulch et al.[204]	
propane				1.21 ± 0.08	296	FP-KS	Greiner[21]	296–497
				1.26 ± 0.14	298			
				1.19 ± 0.04	298			
				1.01 ± 0.03	299			
				1.10 ± 0.05	299			
				1.30 ± 0.02	299			
				1.30 ± 0.13	299			
				1.44 ± 0.04	335			
				1.91 ± 0.05	375			
				2.19 ± 0.07	423			

TABLE I (Continued)

alkane	$10^{12}A$, cm^3 molecule s^{-1}	n	E, cal mol^{-1}	$10^{12}k$, cm^3 molecule^{-1} s^{-1}	T, K	technique	ref	temp range covered, K
				2.92 ± 0.12	497			
				3.19 ± 0.15	497			
				3.15 ± 0.07	497			
				2.97 ± 0.15	497			
	$12.0^{+1.5}_{-1.3}$		1349 ± 76	3.39 ± 0.15	497			
				0.83 ± 0.17	300	DF-EPR	Bradley et al.[205]	
				2.2 ± 0.6	298	rel rate [rel to k(OH + CO) = 1.52 × 10^{-13}][f]	Gorse and Volman[206]	
				2.16 ± 0.10	381	PR-RA	Gordon and Mulac[129]	381–416
				1.91 ± 0.08	416			
				2.02 ± 0.10	295 ± 2	FP-RA	Overend et al.[190]	
				1.98 ± 0.08	329 ± 5	MPS	Harker and Burton[130]	
				1.49 ± 0.21	300 ± 1	rel rate [rel to k(OH + n-butane) = 2.56 × 10^{-12}][g]	Darnall et al.[138]	
				2.0	300	rel rate [rel to k(OH + ethene) = 8.45 × 10^{-12}][g]	Cox et al.[139]	
				0.686 ± 0.107	253	DF-RF	Anderson and Stephens[198]	253–365
				0.879 ± 0.123	273			
				0.929 ± 0.121	297			
				0.113 ± 0.16	329			
	6.2 ± 2.4		1097 ± 225	0.141 ± 0.20	365			
				1.20 ± 0.05	299 ± 2	rel rate [rel to k(OH + n-butane) = 2.54 × 10^{-12}][g]	Atkinson et al.[207]	
				1.05 ± 0.04	297	FP-RF	Tully et al.[201]	297–690
				1.48 ± 0.06	326			
				2.51 ± 0.20	378			
				3.37 ± 0.23	469			
				4.78 ± 0.34	554			
	1.59 × 10^{-3}	1.40	850	8.78 ± 0.97	690			
				1.91 ± 0.15	428	rel rate [rel to k(OH + CO) = 1.12 × 10^{-13} $10^{3.94\times10^{-4}T}$][c]	Baulch et al.[194]	428–696
				2.81 ± 0.23	489			
				2.84 ± 0.08	538			
				4.02 ± 0.22	589			
				4.77 ± 0.51	641			
				7.11 ± 0.68	696			
				1.10 ± 0.04	293	LP-LIF	Tully et al.[208]	293–854
				1.52 ± 0.06	342			
				1.61 ± 0.07	351.5			
				2.14 ± 0.09	401			
				2.49 ± 0.10	428			
				3.24 ± 0.13	491			
				3.36 ± 0.14	501.5			
				3.34 ± 0.14	505			
				4.84 ± 0.20	602			
				4.84 ± 0.20	603			
				7.28 ± 0.30	732			
				9.31 ± 0.38	854			
				1.0 ± 0.2	295	LP-LIF	Schmidt et al.[126]	
				1.20 ± 0.18	295	DF-RF	Baulch et al.[204]	

n-butane			2.56 ± 0.08	298	FP-KS	Greiner[21]	298–495
			2.59 ± 0.22	301			
			2.79 ± 0.32	336			
			2.96 ± 0.10	373			
			4.85 ± 0.18	425			
			4.12 ± 0.15	428			
	$14.1^{+4.1}_{-3.1}$	1041 ± 185	4.90 ± 0.17	495			
			4.1	298	DF-MS	Morris and Niki[102]	
			2.35 ± 0.35	298	FP-RF	Stuhl[209]	
			2.9 ± 0.7	298	rel rate [rel to k(OH + CO) = 1.52 × 10^{-13}]^f	Gorse and Volman[206]	
			4.22 ± 0.17	298	PR-RA	Gordon and Mulac[129]	298–416
			4.15 ± 0.17	381			
			4.98 ± 0.17	416			
			2.37 ± 0.14	292 ± 2	rel rate [rel to k(OH + CO) = 1.60 × 10^{-13}]^f	Campbell et al.[135]	
			2.72 ± 0.27	297.7	FP-RF	Perry et al.[210]	298–420
			3.54 ± 0.35	351.0			
	17.6	1110 ± 300	4.69 ± 0.47	419.6			
			2.67 ± 0.22	297 ± 2	FP-RA	Paraskevopoulos and Nip[211]	
			2.52 ± 0.25	299 ± 2	rel rate [rel to k(OH + propene) = 2.62 × 10^{-11}]^g	Atkinson et al.[140]	
			1.46 ± 0.22	250	DF-RF	Anderson and Stephens[198]	250–365
			1.63 ± 0.21	274			
			1.68 ± 0.23	297			
			2.10 ± 0.34	329			
	8.2 ± 4.0	880 ± 284	2.57 ± 0.38	365			
			2.50 ± 0.24	302	rel rate [rel to k(OH + n-pentane) = 4.13 × 10^{-12}]^g	Behnke et al.[212]	
			2.71 ± 0.32	295 ± 1	rel rate [rel to k(OH + propene) = 2.68 × 10^{-11}]^g	Atkinson and Aschmann[153]	
			2.41 ± 0.10	294	LP-LIF	Tully et al.[208]	294–509
			2.95 ± 0.12	332			
			3.53 ± 0.15	377			
			4.56 ± 0.19	439			
			5.84 ± 0.25	509			
			2.3 ± 0.3	295	LP-LIF	Schmidt et al.[126]	
n-butane-d_{10}			0.697 ± 0.068	297 ± 2	FP-RA	Paraskevopoulos and Nip[211]	
2-methylpropane			2.14 ± 0.12	297	FP-KS	Greiner[21]	297–498
			2.22 ± 0.05	297			
			2.67 ± 0.17	298			
			2.56 ± 0.05	304			
			2.69 ± 0.15	305			
			3.01 ± 0.07	338			
			2.87 ± 0.07	371			
			3.04 ± 0.13	374			
			3.57 ± 0.15	425			

TABLE I (Continued)

alkane	$10^{12}A$, cm^3 molecule s^{-1}	n	E, cal mol^{-1}	$10^{12}k$, cm^3 molecule^{-1} s^{-1}	T, K	technique	ref	temp range covered, K
	$8.7^{+1.8}_{-1.5}$		769 ± 125	4.25 ± 0.22	498			
				3.6 ± 0.9	298	rel rate [rel to $k(OH + CO) = 1.52 \times 10^{-13}]^f$	Gorse and Volman[131,206]	
				2.2	303	rel rate [rel to k(OH + *cis*-2-butene) = $5.46 \times 10^{-11}]^g$	Wu et al.[136]	
				2.2^h	305	rel rate [rel to $k(OH + CO) = 1.60 \times 10^{-13}]^f$	Butler et al.[213]	
				2.36 ± 0.05	300 ± 1	rel rate [rel to k(OH + *n*-butane) = $2.56 \times 10^{-12}]^g$	Darnall et al.[138]	
				1.31 ± 0.19	251	DF-RF	Anderson and Stephens[198]	251–360
				1.46 ± 0.19	274			
				1.73 ± 0.25	299			
				1.95 ± 0.25	326			
	7.7 ± 1.1		890 ± 84	2.21 ± 0.39	360			
				2.22 ± 0.06	297 ± 2	rel rate [rel to k(OH + *n*-butane) = $2.51 \times 10^{-12}]^g$	Atkinson et al.[214]	
				2.19 ± 0.11	293	LP-LIF	Tully et al.[208]	293–864
				2.59 ± 0.13	342			
				3.21 ± 0.16	403			
				3.49 ± 0.17	424			
				4.03 ± 0.20	470			
				4.58 ± 0.23	509.5			
				5.49 ± 0.27	574			
				7.40 ± 0.37	705			
				10.13 ± 0.51	864			
				1.9 ± 0.3	295	LP-LIF	Schmidt et al.[126]	
2-methylpropane-d_9 [$(CD_3)_3CH$]				1.70 ± 0.09	293.5	LP-LIF	Tully et al.[208]	294–864
				1.91 ± 0.10	343			
				2.27 ± 0.11	403			
				2.81 ± 0.14	471			
				3.64 ± 0.18	574			
				5.28 ± 0.26	705			
				7.61 ± 0.38	864			
2-methylpropane-d_1 [$(CH_3)_3CD$]				1.36 ± 0.07	293.5	LP-LIF	Tully et al.[208]	294–864
				1.81 ± 0.09	344			
				2.44 ± 0.12	403			
				3.35 ± 0.17	473			
				4.84 ± 0.24	574			
				7.12 ± 0.36	705			
				9.90 ± 0.49	864			
2-methylpropane-d_{10} [$(CD_3)_3CD$]				0.956 ± 0.067	293.5	LP-LIF	Tully et al.[208]	294–864
				1.20 ± 0.08	340.5			
				1.58 ± 0.10	403			
				2.10 ± 0.12	473			
				3.09 ± 0.15	574			
				4.92 ± 0.25	705			
				7.30 ± 0.37	864			

n-pentane				6.55	303	rel rate [rel to $k(OH + cis\text{-}2\text{-butene}) = 5.46 \times 10^{-11}$]^g	Wu et al.[136]	
				3.51 ± 0.13	300 ± 1	rel rate [rel to $k(OH + n\text{-butane}) = 2.56 \times 10^{-12}$]^g	Darnall et al.[138]	
				5.3	300	rel rate [rel to $k(OH + \text{ethene}) = 8.45 \times 10^{-12}$]^g	Cox et al.[139]	
				4.1	~300	rel rate [rel to $k(OH + \text{ethene}) = 8.45 \times 10^{-12}$]^g	Barnes et al.[141]	
				4.06 ± 0.08	299 ± 2	rel rate [rel to $k(OH + n\text{-butane}) = 2.54 \times 10^{-12}$]^g	Atkinson et al.[207]	
2-methylbutane				2.9 ± 0.6	305 ± 2	rel rate [rel to $k(OH + n\text{-butane}) = 2.63 \times 10^{-12}$]^g	Lloyd et al.[144]	
				3.54 ± 0.07	300 ± 1	rel rate [rel to $k(OH + n\text{-butane}) = 2.56 \times 10^{-12}$]^g	Darnall et al.[138]	
				3.7	300	rel rate [rel to $k(OH + \text{ethene}) = 8.45 \times 10^{-12}$]^g	Cox et al.[139]	
				3.87 ± 0.10	297 ± 2	rel rate [rel to $k(OH + n\text{-butane}) = 2.51 \times 10^{-12}$]^g	Atkinson et al.[214]	
2,2-dimethylpropane				0.740 ± 0.020	292	FP-KS	Greiner[21]	292–493
				0.858 ± 0.038	292			
				0.875 ± 0.025	298			
				1.16 ± 0.08	335			
				1.41 ± 0.04	370			
				2.11 ± 0.10	424			
	$14.1^{+2.1}_{-1.8}$		1677 ± 88	2.54 ± 0.08	493			
				0.98 ± 0.16	300 ± 2	rel rate [rel to $k(OH + n\text{-butane}) = 2.56 \times 10^{-12}$]^g	Darnall et al.[138]	
				0.91 ± 0.10	297 ± 2	FP-RA	Paraskevopoulos and Nip[211]	
				0.76 ± 0.05	299 ± 2	rel rate [rel to $k(OH + n\text{-butane}) = 2.54 \times 10^{-12}$]^g	Atkinson et al.[147]	
				0.414 ± 0.071	249	DF-RF	Anderson and Stephens[198]	249–364
				0.460 ± 0.089	271			
				0.533 ± 0.098	296			
				0.772 ± 0.153	327			
	6.0 ± 4.1		1359 ± 372	0.987 ± 0.231	364			
				0.909 ± 0.115	287	LP-LIF	Tully et al.[203,215]	287–901
				1.27 ± 0.14	350			
				2.08 ± 0.19	431			
				3.17 ± 0.25	518			
				4.46 ± 0.38	600			
				7.02 ± 0.67	705			
				10.1 ± 1.1	812			
	8.60×10^{-9}	3.05	−676	12.5 ± 1.5	901			

TABLE I (Continued)

alkane	$10^{12}A$, cm^3 molecule s^{-1}	n	E, cal mol^{-1}	$10^{12}k$, cm^3 molecule^{-1} s^{-1}	T, K	technique	ref	temp range covered, K
2,2-dimethylpropane-d_{12}				0.180 ± 0.012	290	LP-LIF	Tully et al.[203,215]	290–903
				0.375 ± 0.025	352			
				0.728 ± 0.048	430			
				1.30 ± 0.09	508.5			
				2.19 ± 0.17	598			
				3.94 ± 0.34	705			
				5.62 ± 0.55	812			
	1.08×10^{-7}	2.71	610	8.09 ± 0.89	903			
n-hexane				5.5 ± 1.1	305 ± 2	rel rate [rel to k(OH + n-butane) = 2.63×10^{-12}]^g	Lloyd et al.[144]	
				6.0	303	rel rate [rel to k(OH + *cis*-2-butene) = 5.46×10^{-11}]^g	Wu et al.[136]	
				6.0 ± 0.9	292	rel rate [rel to k(OH + n-butane) = 2.44×10^{-12}]^g	Campbell et al.[216]	
				5.61 ± 0.09	299 ± 2	rel rate [rel to k(OH + n-butane) = 2.54×10^{-12}]^g	Atkinson et al.[147]	
				5.55 ± 0.20	298 ± 2	rel rate [rel to k(OH + propene) = 2.63×10^{-11}]^g	Atkinson et al.[217]	
				5.38 ± 0.11	302	rel rate [rel to k(OH + n-pentane) = 4.13×10^{-12}]^g	Behnke et al.[212]	
				5.31 ± 0.46	295 ± 1	rel rate [rel to k(OH + propene) = 2.68×10^{-11}]^g	Atkinson and Aschmann[153]	
				5.55 ± 0.55	295	rel rate [rel to k(OH + n-butane) = 2.49×10^{-12}]^g	Klein et al.[218]	
2-methylpentane				4.7 ± 1.0	305 ± 2	rel rate [rel to k(OH + n-butane) = 2.63×10^{-12}]^g	Lloyd et al.[144]	
				5.3	300	rel rate [rel to k(OH + ethene) = 8.45×10^{-12}]^g	Cox et al.[139]	
				5.52 ± 0.23	297 ± 2	rel rate [rel to k(OH + n-butane) = 2.51×10^{-12}]^g	Atkinson et al.[214]	
3-methylpentane				6.3 ± 1.3	305 ± 2	rel rate [rel to k(OH + n-butane) = 2.63×10^{-12}]^g	Lloyd et al.[144]	
				5.62 ± 0.10	297 ± 2	rel rate [rel to k(OH + n-butane) = 2.51×10^{-12}]^g	Atkinson et al.[214]	
2,2-dimethylbutane				2.59 ± 0.08	297 ± 2	rel rate [rel to k(OH + n-butane) = 2.51×10^{-12}]^g	Atkinson et al.[214]	

2,3-dimethylbutane			7.45 ± 0.22	300	FP-KS	Greiner[21]	300–498
			6.71 ± 0.22	336			
			6.81 ± 0.35	372			
			7.11 ± 0.65	424			
	$4.8^{+1.1}_{-0.9}$	−257 ± 133	5.94 ± 1.25	498			
			4.9 ± 1.0	305 ± 2	rel rate [rel to k(OH + 2-methylpropene) = 4.95 × 10^{-11}]^g	Darnall et al.[219]	
			5.32 ± 0.28	300 ± 1	rel rate [rel to k(OH + n-butane) = 2.56 × 10^{-12}]^g	Darnall et al.[138]	
			4.0	300	rel rate [rel to k(OH + ethene) = 8.45 × 10^{-12}]^g	Cox et al.[139]	
			6.16 ± 0.06	299 ± 2	rel rate [rel to k(OH + n-butane) = 2.54 × 10^{-12}]^g	Atkinson et al.[147]	
n-heptane			7.18 ± 0.17	299 ± 2	rel rate [rel to k(OH + n-butane) = 2.54 × 10^{-12}]^g	Atkinson et al.[207]	
			7.42 ± 0.09	302	rel rate [rel to k(OH + n-pentane) = 4.13 × 10^{-12}]^g	Behnke et al.[212]	
2,4-dimethylpentane			5.12 ± 0.10	297 ± 2	rel rate [rel to k(OH + n-butane) = 2.51 × 10^{-12}]^g	Atkinson et al.[214]	
2,2,3-trimethylbutane			5.23 ± 0.12	296	FP-KS	Greiner[21]	296–497
			4.86 ± 0.12	303			
			4.50 ± 0.33	371			
			4.60 ± 0.27	373			
	$7.9^{+2.1}_{-1.6}$	288 ± 145	6.33 ± 0.19	497			
			3.7 ± 0.8	305 ± 2	rel rate [rel to k(OH + 2-methylpropene) = 4.95 × 10^{-11}]^g	Darnall et al.[219]	
			4.09 ± 0.08	297 ± 2	rel rate [rel to k(OH + n-butane) = 2.51 × 10^{-12}]^g	Atkinson et al.[214]	
n-octane			8.42 ± 1.25	296	FP-KS	Greiner[21]	296–497
			12.0 ± 0.7	371			
			10.8 ± 0.5	371			
	$29.5^{+4.4}_{-3.8}$	724 ± 120	14.3 ± 0.4	497			
			8.86 ± 0.19	299 ± 2	rel rate [rel to k(OH + n-butane) = 2.54 × 10^{-12}]^g	Atkinson et al.[207]	
			8.80 ± 0.12	302	rel rate [rel to k(OH + n-pentane) = 4.13 × 10^{-12}]^g	Behnke et al.[212]	
2,2,4-trimethylpentane			3.90 ± 0.15	298	FP-KS	Geiner[21]	298–493
			3.55 ± 0.12	305			
			4.37 ± 0.23	339			
			5.25 ± 0.15	373			
			5.43 ± 0.13	423			
	$15.5^{+3.1}_{-2.6}$	847 ± 126	6.62 ± 0.42	493			
			3.56 ± 0.15	297 ± 2	rel rate [rel to k(OH + n-butane) = 2.51 × 10^{-12}]^g	Atkinson et al.[214]	

TABLE I (Continued)

alkane	$10^{12}A$, cm^3 molecule^{-1} s^{-1}	n	E, cal mol^{-1}	$10^{12}k$, cm^3 molecule^{-1} s^{-1}	T, K	technique	ref	temp range covered, K
2,2,3,3-tetramethylbutane				1.08 ± 0.02	294	FP-KS	Greiner[21]	294–495
				1.16 ± 0.10	301			
				1.42 ± 0.04	335			
				2.04 ± 0.08	370			
				2.21 ± 0.07	424			
	$16.2^{+3.3}_{-2.7}$		1593 ± 125	3.52 ± 0.12	495			
				1.03 ± 0.08	297 ± 2	rel rate [rel to k(OH + n-butane) = 2.51 × 10^{-12}][g]	Atkinson et al.[214]	
				0.948 ± 0.020	290	LP-LIF	Tully et al.[215]	290–738
				1.48 ± 0.04	348.5			
				2.38 ± 0.03	423.5			
				3.58 ± 0.05	506			
				5.27 ± 0.09	606			
	4.75 × 10^{-6}	2.20	136	9.36 ± 0.35	737.5			
n-nonane				10.5 ± 0.4	299 ± 2	rel rate [rel to k(OH + n-butane) = 2.54 × 10^{-12}][g]	Atkinson et al.[207]	
				9.7 ± 0.07	302	rel rate [rel to k(OH + n-pentane) = 4.13 × 10^{-12}][g]	Behnke et al.[212]	
n-decane				11.2 ± 0.6	299 ± 2	rel rate [rel to k(OH + n-butane) = 2.54 × 10^{-12}][g]	Atkinson et al.[207]	
				11.3 ± 0.2	302	rel rate [rel to k(OH + n-pentane) = 4.13 × 10^{-12}][g]	Behnke et al.[212]	
n-undecane				13.3 ± 0.2	302	rel rate [rel to k(OH + n-pentane) = 4.13 × 10^{-12}][g]	Behnke et al.[212]	
n-dodecane				13.9 ± 0.2	302	rel rate [rel to k(OH + n-pentane) = 4.13 × 10^{-12}][g]	Behnke et al.[212]	
n-tridecane				15.5 ± 0.2	302	rel rate [rel to k(OH + n-pentane) = 4.13 × 10^{-12}][g]	Behnke et al.[212]	

[a] Calculated by least-squares analyses of plots of the cited first-order OH radical decay rates against the CH_4 concentration. [b] From ref 93. [c] This rate constant expression used for k(OH + CO)[194] is in general agreement with the kinetic data of Greiner,[110] Westenberg and deHaas,[181] Davis et al.,[182] Smith and Zellner,[118] Vandooren et al.,[183] Ravishankara and Thompson,[184] and Jonah et al.[185] (see text). [d] Room temperature, not reported. [e] From present recommendations, at an assumed temperature of 298 K. [f] From the expression $k(\mathrm{OH} + \mathrm{CO}) = 1.50 \times 10^{-13} \times [(1 + 9.19 \times 10^{-4}P)/(1 + 2.24 \times 10^{-4}P)]$ cm^3 molecule^{-1} s^{-1} as recommended by Atkinson and Lloyd,[3] where P is the total pressure in torr. [g] From present recommendations, see text. [h] From the data obtained at 100-torr total pressure. Rate constants derived from the higher pressure data decrease monotonically with increasing pressure, for unknown reasons.

and/or with diluent gases (He, Ar) which have a low third-body efficiency in this reaction. Thus the magnitude of any pressure effect on this rate constant for the reaction of OH radicals with CO at elevated temperatures is presently not well understood. This introduces significant uncertainties into the derivation of rate constants from these relative rate studies, and accordingly the rate constants from relative rate studies utilizing CO as the reference compound are given a lower weight in the evaluations.

The most recent comprehensive review of OH radical reactions with organics was that of Atkinson et al.[1] in 1979, and this paper updates and substantially extends that review. The recent NASA[30] and CODATA[31] evaluations have dealt with the reactions of CH_4, C_2H_6, C_3H_8, a series of haloalkanes, and certain other C_2 alkenes and haloalkenes. For some of these organic compounds the latest NASA recommendations are used,[30] unless more recent data have become available. The mechanisms of OH radical reactions with a limited set of organics (formaldehyde, acetaldehyde, *n*-butane, 2,3-dimethylbutane, ethene, propene, 1-butene, *trans*-2-butene, toluene, and *m*-xylene and their atmospheric degradation products) have also been dealt with in detail in the recent review article of Atkinson and Lloyd.[3] In this paper the emphasis of discussions of products and mechanisms of OH radical reactions under atmospheric conditions is placed upon classes of organic compounds rather than on individual organics as was done by Atkinson and Lloyd.[3]

In the kinetic data tabulations, the experimental techniques used are denoted by abbreviations such as (for example) DF–RF, where the first letters denote the following: DF, discharge flow; FP, flash photolysis; LP, laser photolysis; MPS, modulation-phase shift; PR, pulsed radiolysis; and the second set of letters denote the detection technique; MS, mass spectroscopy (including photoionization–mass spectroscopy); EPR, electron paramagnetic resonance; KS, kinetic spectroscopy; LMR, laser magnetic resonance; RA, resonance absorption; RF, resonance fluorescence; and LIF, laser-induced fluorescence. The tables list, whenever available, the rate constants obtained at the various temperatures studied. The cited Arrhenius preexponential factors *A* and activation energies *E* are also listed.

In some studies covering wide temperature ranges, the simple Arrhenius expression has, as expected, been shown not to hold, with pronounced curvature in the Arrhenius plots being observed.[125,127,128] In these cases a three-parameter expression of the form

$$k = A'T^n e^{-E'/RT}$$

has been used and the reported values of A', E', and n are tabulated. Since to date most of the available OH radical rate constant data have been obtained over relatively limited temperature ranges ($\lesssim$500 K), the simple Arrhenius expression, although obviously too simplistic, is often totally adequate and convenient for expressing most of these experimental data over these limited temperature ranges. Thus in these cases recommendations are cast in the form of the Arrhenius equation

$$k = Ae^{-E/RT}$$

For organics for which reliable data exist covering large temperature ranges, e.g., $\lesssim$300 to $\gtrsim$1000 K (e.g., for methane, ethane, and propane) or for which their Arrhenius plots exhibit obvious curvature, a more realistic equation is used for the recommendations. The expression

$$k = A'T^2 e^{-E'/RT}$$

has been chosen in these evaluations, since this has been used in the recent NASA evaluation[30] and has been recommended by Jeong et al.[186] on theoretical grounds. Additionally, values of $n \approx 2$ in the above three-parameter expression have been derived from previous experimental studies[125,128] and theoretical evaluations[187] of these reactions over wide temperature ranges.

Since, as is evident from the discussion above, this review deals mainly with OH radical reactions with organic compounds under atmospheric conditions, kinetic and mechanistic data obtained at temperatures $\gtrsim$500 K are not specifically included, unless these data were obtained as an integral part of studies extending to lower temperatures. Furthermore, for the alkenes and haloalkenes the kinetic data obtained at low total pressures, where the rate constants are often well into the fall-off regime between second- and third-order kinetics, are not evaluated in detail, although citations to studies carried out in these fall-off regimes are given.

In the rate constant data tables, the error limits cited are those reported. In many cases these are two least-squares standard deviations and in others they are the estimated overall error limits. While for relative rate constant studies the use of two least-squares standard deviations may be a realistic estimation of the overall error limits with respect to the reference reaction rate constant, for the absolute rate constant determinations the overall error limits are expected to be of the order of ~10–15%, except for some of the most recent studies for which the overall error limits may have been reduced to ~6–10%.

A. Alkanes

1. *Kinetics*

The literature rate constant data for the reactions of OH radicals with the alkanes are listed in Table I (acyclic alkanes) and Table II (cycloalkanes). In addition the available rate constants for the reaction of OD radicals with alkanes are given in Table III. The OH radical reaction rate constants obtained by Horne and Norrish[105] for CH_4 and C_2H_6 have been omitted since the significantly higher rate constants obtained were probably due to the occurrence of secondary reactions at the high initial OH radical concentrations used.[21]

In general, the kinetic data obtained by the various experimental studies for a given alkane are in reasonable agreement, although it is obvious from Table I that for certain of these alkanes (for example, for propane, *n*-butane, 2-methylpropane, and 2,3-dimethylbutane) there are significant discrepancies in the reported rate constants and Arrhenius parameters.

The kinetic data for the individual alkanes are discussed as follows.

a. Methane, Methane-^{13}C, Methane-d_1, Methane-d_2, Methane-d_3, and Methane-d_4. The available rate constant data for methane are tabulated in Table

TABLE II. Rate Constants *k* and Arrhenius Parameters for the Gas-Phase Reaction of OH Radicals with Cycloalkanes

alkane	structure	$10^{12}A$, molecule^{-1} s^{-1}	E, cal, mol^{-1}	$10^{12}k$, cm^3 molecule^{-1} s^{-1}	T, K	technique	ref	temp range covered, K
cyclopropane				0.08 ± 0.02	295	FP-RF	Zetzsch[220]	
				0.062 ± 0.014	298 ± 2	FP-RA	Jolly et al.[221]	
cyclobutane				1.2 ± 0.3	298	rel rate [rel to k(OH + CO) = 1.52 × 10^{-13}][a]	Gorse and Volman[206]	
cyclopentane				6.2	298	rel rate [rel to k(OH + CO) = 1.52 × 10^{-13}][a]	Volman[222]	
				4.43 ± 0.27	300 ± 1	rel rate [rel to k(OH + n-butane) = 2.56 × 10^{-12}][b]	Darnall et al.[138]	
				5.24 ± 0.07	299 ± 2	rel rate [rel to k(OH + n-butane) = 2.54 × 10^{-12}][b]	Atkinson et al.[147]	
				5.18 ± 0.38	298 ± 2	FP-RA	Jolly et al.[221]	
cyclohexane				7.95 ± 0.43	295	FP-KS	Greiner[21]	295–497
				8.40 ± 0.55	338			
				7.70 ± 0.72	338			
				11.8 ± 0.6	370			
				9.93 ± 0.23	373			
				10.4 ± 0.6	425			
				10.1 ± 0.6	425			
		$23.5^{+4.7}_{-4.0}$	634 ± 145	12.4 ± 0.4	497			
				6.8 ± 1.7	298	rel rate [rel to k(OH + CO) = 1.52 × 10^{-13}][a]	Gorse and Volman[206]	
				6.5	303	rel rate [rel to k(OH + cis-2-butene) = 5.46 × 10^{-11}][b]	Wu et al.[136]	
				7.45 ± 0.05 }	299 ± 2	rel rate [rel to k(OH + n-butane) = 2.54 × 10^{-12}][b]	Atkinson et al.[147]	
				7.40 ± 0.25 }				
				7.07 ± 0.42	299 ± 2	rel rate [rel to k(OH + propene) = 2.62 × 10^{-11}][b]	Atkinson et al.[223]	
				7.38 ± 0.11	300 ± 3	rel rate [rel to k(OH + n-butane) = 2.56 × 10^{-12}][b]	Tuazon et al.[143]	
				7.14 ± 0.36	292	LP-LIF	Tully et al.[208]	292–491
				8.49 ± 0.42	342			
				10.13 ± 0.51	401			
				12.93 ± 0.65	491			
cycloheptane	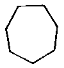			13.1 ± 2.1	298 ± 2	FP-RA	Jolly et al.[221]	
methylcyclohexane	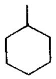			10.3 ± 0.3	297 ± 2	rel rate [rel to k(OH + n-butane = 2.51 × 10^{-12}][b]	Atkinson et al.[214]	
bicyclo[2.2.1]heptane				5.42 ± 0.14	299 ± 2	rel rate [rel to k(OH + cyclohexane) = 7.41 × 10^{-12}][b]	Atkinson et al.[224]	
bicyclo[2.2.2]octane				14.5 ± 1.0	299 ± 2	rel rate [rel to k(OH + cyclohexane) = 7.41 × 10^{-12}][b]	Atkinson et al.[224]	
bicyclo[3.3.0]octane	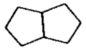			10.9 ± 0.6	299 ± 2	rel rate [rel to k(OH + cyclohexane) = 7.41 × 10^{-12}][b]	Atkinson et al.[224]	
cis-bicyclo[4.3.0]-nonane	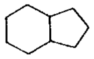			17.0 ± 1.2	299 ± 2	rel rate [rel to k(OH + cyclohexane) = 7.41 × 10^{-12}][b]	Atkinson et al.[224]	
$trans$-bicyclo[4.3.0]-nonane	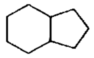			17.4 ± 1.3	299 ± 2	rel rate [rel to k(OH + cyclohexane) = 7.41 × 10^{-12}][b]	Atkinson et al.[224]	
cis-bicyclo[4.4.0]-decane	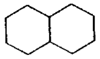			19.6 ± 1.4	299 ± 2	rel rate [rel to k(OH + cyclohexane) = 7.41 × 10^{-12}][b]	Atkinson et al.[224]	

trans-bicyclo[4.4.0]-decane	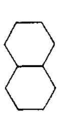	20.2 ± 1.2	299 ± 2	rel rate [rel to k(OH + cyclohexane) = 7.41×10^{-12}]^b	Atkinson et al.[224]
tricyclo[5.2.1.0^{2,6}]-decane		11.2 ± 0.4	299 ± 2	rel rate [rel to k(OH + cyclohexane) = 7.41×10^{-12}]^b	Atkinson et al.[224]
tricyclo[3.3.1.1^{3,7}]-decane		22.7 ± 2.0	299 ± 2	rel rate [rel to k(OH + cyclohexane) = 7.41×10^{-12}]^b	Atkinson et al.[224]

[a] From the expression $k(\mathrm{OH} + \mathrm{CO}) = 1.50 \times 10^{-13}\,[(1 + 9.19 \times 10^{-4}P)/(1 + 2.24 \times 10^{-4}P)]$ cm^3 molecule^{-1} s^{-1}, as recommended by Atkinson and Lloyd,[3] where P is the pressure of air in torr. [b] From present recommendations (see text).

TABLE III. Rate Constants *k* for the Gas-Phase Reactions of OD Radicals with Alkanes

alkane	$10^{12}k$, cm^3 molecule^{-1} s^{-1}	T, K	technique	ref
methane	0.0080 ± 0.0003	300	FP-KS	Greiner[108]
ethane	0.274 ± 0.027	300	FP-KS	Greiner[108]
n-butane	2.76 ± 0.22	297 ± 2	FP-RA	Paraskevopoulos and Nip[211]
n-butane-d_{10}	0.804 ± 0.063	297 ± 2	FP-RA	Paraskevopoulos and Nip[211]

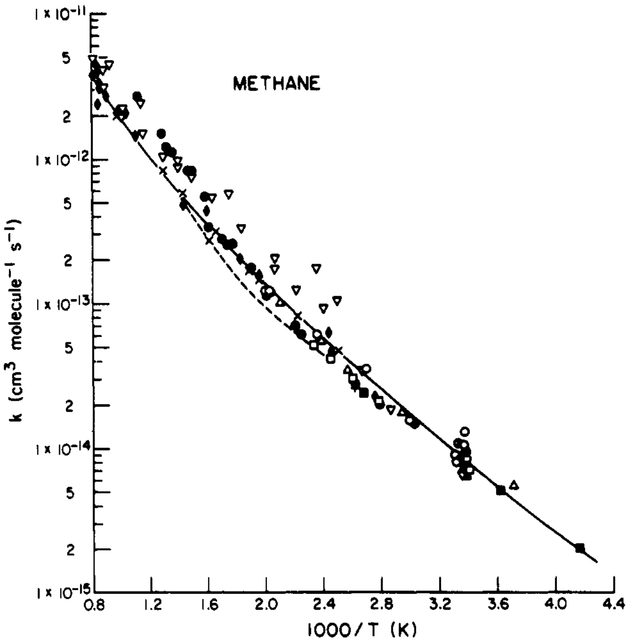

Figure 3. Arrhenius plot of the rate constants for the reaction of OH radicals with methane: (◑) Wilson and Westenberg;[188] (○) Greiner;[21] (■) Davis et al.;[182] (□) Margitan et al.;[189] (+) Gordon and Mulac;[129] (▲) Overend et al.;[190] (◒) Howard and Evenson;[191] (●) Zellner and Steiner;[192] (×) Tully and Ravishankara;[125] (△) Jeong and Kaufman;[186,193] (---) Baulch et al.;[194] (▽) Jonah et al.;[185] (♦) Madronich and Felder;[128] (—) recommendation (see text).

I, and the data of Wilson and Westenberg,[188] Greiner,[21] Davis et al.,[182] Margitan et al.,[189] Gordon and Mulac,[129] Overend et al.,[190] Howard and Evenson,[191] Zellner and Steinert,[192] Tully and Ravishankara,[125] Jeong and Kaufmann,[186,193] Baulch et al.,[194] Jonah et al.,[185] and Madronich and Felder[128] are plotted in Arrhenius form in Figure 3. As discussed above, the data of Baulch et al.[194] (obtained relative to the rate constant for the reaction of OH radicals with CO) are subject to significant uncertainties due to uncertainties in the rate constants for the reference reaction. Hence the individual rate constants from this study,[194] which are given in Table I, have not been plotted in Figure 3 but rather a curve has been drawn through these data points to indicate the magnitude and trend of these derived rate constant data.

It can be seen from Figure 3 that the data obtained from the absolute rate constant studies[21,125,128,129,182,185,186,188-193] are in general agreement, though there are certain areas of discrepancy. Thus the room-temperature rate constants show a spread of a factor of ~2 (though this is reduced to a factor of ~1.7, i.e., from ~6.5×10^{-15} cm^3 molecule^{-1} s^{-1} to ~1.1×10^{-14} cm^3 molecule^{-1} s^{-1} if the seven individual rate constant determinations of Greiner[21] at 295–302 K are averaged to a single value of ~9×10^{-15} cm^3 molecule^{-1} s^{-1}). In addition, there are discrepancies of up to a factor of ~2 between the data of Zellner and Steinert[192] and of Tully and Ravishankara[125] and Madronich and Felder[128] at temperatures ≳625 K, possibly because of the occurrence of secondary reactions, as discussed by Tully and Ravishankara.[125] At intermediate temperatures of ~ 300–625 K the rate constants of Greiner,[21] Davis et al.,[182] Margitan et al.,[189] Gordon and Mulac,[129] Zellner and Steinert,[192] Tully and Ravishankara,[125] Jeong and Kaufman,[186,193] and Madronich and Felder[128] are in good agreement. In particular, the rate constants recently determined by Tully and Ravishankara,[125] Jeong and Kaufman,[186,193] and Madronich and Felder[128] are in excellent agreement. It is apparent from these data that the Arrhenius plot of ln k vs. T^{-1} exhibits a significant degree of curvature, and such curvature is totally consistent with theoretical considerations.[187,225]

However, the most recent kinetic data of Jonah et al.,[185] obtained by using a pulsed radiolysis-resonance absorption technique, yield a linear Arrhenius plot over the entire temperature range studied (298–1229 K). These rate constants,[185] while in agreement with other literature data at ~300–380 and >600 K, are significantly higher in the intermediate temperature range of ~400–600 K. Unfortunately, the reasons for these discrepancies are not known.

With regard to the relative rate measurements, that of Cox et al.[93] at 298 K (not plotted in Figure 3) is in good agreement with the absolute rate constant data, while those of Baulch et al.[194] are in reasonable agreement with, though somewhat lower than, the absolute rate constants over the temperature range covered (413–693 K). With regard to these data of Baulch et al.,[194] this reasonable agreement indicates that the rate constant expression chosen for the reference reaction of OH radicals with CO must be essentially correct under the experimental conditions employed.

Consistent with the above discussion, the kinetic data of Greiner,[21] Davis et al.,[182] Margitan et al.,[189] Overend et al.,[190] Howard and Evenson,[191] Tully and Ravishankara,[125] Jeong and Kaufman,[186,193] and Madronich and Felder[128] have been used to evaluate the rate constant for the reaction of OH radicals with methane over the temperature range 240–1250 K. The rate constants obtained by Gordon and Mulac,[129] while in good agreement with the other literature data for methane over the temperature range covered (381–416 K), exhibit significant differences from the literature rate constants for certain of the other alkanes and alkenes studied (e.g., n-butane and propene) and are hence excluded from this recommendation. The datum of Wilson and Westenberg[188] has also been excluded from the evaluation since a stoichiometric factor was necessary to derive the rate constant for the elementary reaction from the observed rate coefficient.[188]

A unit-weighted least-squares fit of these data[21,125,128,182,186,189-191,193] to the expression $k = A'T^2e^{-E'/RT}$ yields the recommendation of

$$k(\text{methane}, T \leq 1250\text{ K}) = (6.95^{+0.68}_{-0.61}) \times 10^{-18}\, T^2 e^{-(1280\pm38)/T}\ \text{cm}^3\ \text{molecule}^{-1}\ \text{s}^{-1}$$

where the error limits are two least-squares standard deviations

$$k(\text{methane}) = 8.41 \times 10^{-15}\ \text{cm}^3\ \text{molecule}^{-1}\ \text{s}^{-1} \text{ at } 298\text{ K}$$

with an estimated overall uncertainty at 298 K of ±20%.

The limited data available show that there is no significant isotope effect for the reaction of OH radicals with $^{13}CH_4$, when compared to $^{12}CH_4$.[195] However, as expected because of the increased zero-point energy for C–D bonds vs. C–H bonds, the rate constants for the reaction of OH radicals with methane and the deuterated methanes decrease monotonically along the series $CH_4 > CH_3D > CH_2D_2 > CHD_3 > CD_4$ by a factor of ~1.8 per C–D vs. C–H bond at 416 K.[129]

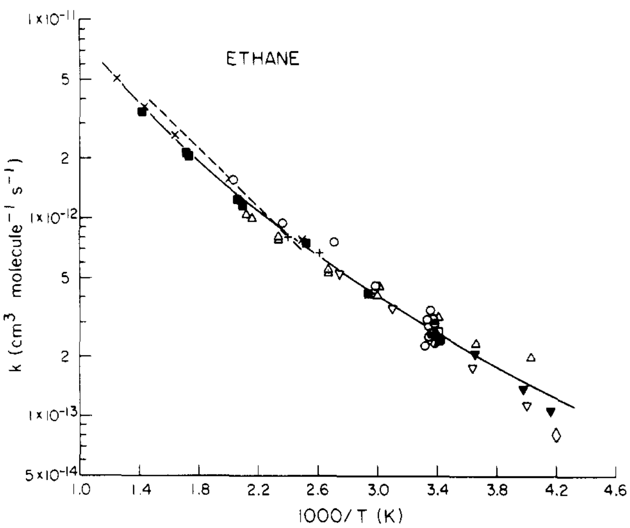

Figure 4. Arrhenius plot of the rate constants for the reaction of OH radicals with ethane: (○) Greiner;[21] (+) Gordon and Mulac;[129] (▲) Overend et al.;[190] (◐) Howard and Evenson;[196] (□) Leu;[197] (▽) Anderson and Stephens;[198] (◑) Lee and Tang;[199] (◇) Margitan and Watson,[200] (×) Tully et al.;[201] (- - -) Baulch et al.;[194] (△) Jeong et al.;[186] (▼) Smith et al.;[202] (■) Tully et al.;[203] (□) Baulch et al.;[204] (—) recommendation (see text).

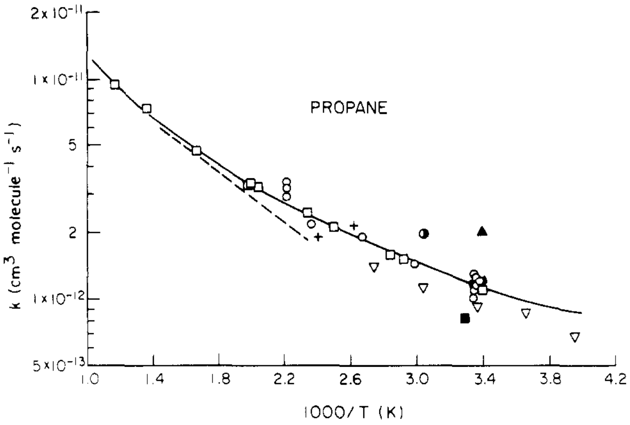

Figure 5. Arrhenius plot of the rate constants for the reaction of OH radicals with propane: (○) Greiner;[21] (■) Bradley et al.;[205] (+) Gordon and Mulac;[129] (▲) Overend et al.;[190] (◑) Harker and Burton;[130] (▽) Anderson and Stephens;[198] (●) Atkinson et al.;[207] (- - -) Baulch et al.;[194] (□) Tully et al.;[208] (♦) Baulch et al.;[204] (—) recommendation (see text).

b. Ethane. The available literature rate constants are listed in Table I, and are plotted in Arrhenius form in Figure 4. Perhaps surprisingly, a significant degree of scatter is observed, especially at temperatures ≲275 K. Especially disturbing is the marked disagreement at temperatures ≲250 between the rate constant determined by Jeong et al.[186] and those of Margitan and Watson,[200] Anderson and Stephens[198] (though it should be noted that for n-butane, 2-methylpropane, and 2,2-dimethylpropane and, to a lesser extent, for propane, the kinetic data of Anderson and Stephens[198] are significantly lower than other literature data) and Smith et al.[202] This discrepancy at low temperatures (i.e., ≲275 K) may suggest that erroneously high rate constants were measured in this temperature regime for methane, ethane, and a series of haloalkanes by Jeong and Kaufman[193] and Jeong et al.,[186] thus leading to an exaggerated curvature in their Arrhenius plots (see also the section below dealing with the reactions of OH radicals with the haloalkanes).

Again, it can be seen that the relative rate data for Baulch et al.[194] are in good agreement with the absolute rate constants of Greiner,[21] Gordon and Mulac,[129] Tully et al.,[201,203] and Jeong et al.,[186] thus further indicating that the rate constant chosen for the reference reaction of OH radicals with CO[194] was essentially correct for the conditions employed. In the absence of further information, the kinetic data of Greiner,[21] Overend et al.,[190] Howard and Evenson,[196] Leu,[197] Margitan and Watson,[200] Tully et al.,[201,203] Jeong et al.,[186] Smith et al.,[202] and Baulch et al.[204] have been utilized to derive a fit to the expression $k = A'T^2e^{-E'/RT}$. A unit-weighted least-squares fit of these data[21,186,190,196,197,200-204] to this expression yields the recommendation of

k(ethane) =

$$(1.37^{+0.23}_{-0.20}) \times 10^{-17}T^2e^{-(444\pm53)/T} \text{ cm}^3 \text{ molecule}^{-1} \text{ s}^{-1}$$

where the error limits are two least-squares standard deviations

$$k(\text{ethane}) = 2.74 \times 10^{-13} \text{ cm}^3 \text{ molecule}^{-1} \text{ s}^{-1} \text{ at 298 K}$$

with an estimated overall uncertainty at 298 K of ±20%.

From the above discussion it is obvious that further experimental data are urgently needed at temperatures ≤275 K.

c. Propane. The available kinetic data are listed in Table I, and the rate constants of Greiner,[21] Bradley et al.,[205] Gordon and Mulac,[129] Overend et al.,[190] Harker and Burton,[130] Anderson and Stephens,[198] Atkinson et al.,[207] Baulch et al.,[194] Tully et al.[208] (which supersede[208] the earlier data of Tully et al.[201]), and Baulch et al.[204] are plotted in Arrhenius form in Figure 5. Again, a significant amount of scatter is observed (up to a factor of ~1.8 at room temperature) for reasons which are not understood. The rate constants determined by Anderson and Stephens[198] at ≥298 K are consistently lower, by ~20%, than those of Greiner[21] and of Tully et al.[208] (This most recent study of Tully et al.[208] supersedes their earlier work,[201] which is believed to be in error due to a temperature calibration error.[208])

The rate constants of Greiner,[21] Atkinson et al.,[207] Tully et al.,[208] and Baulch et al.[204] are hence utilized for the evaluation of this reaction. While there is little or no evidence for curvature in the Arrhenius plot in Figure 5, a unit-weighted least-squares analysis of these data,[21,204,207,208] to the expression $k = A'T^2e^{-E'/RT}$ has been used to yield the recommended expression

k(propane) =

$$(1.27^{+0.11}_{-0.10}) \times 10^{-17}T^2e^{(14\pm31)/T} \text{ cm}^3 \text{ molecule}^{-1} \text{ s}^{-1}$$

where the error limits are two least-squares standard deviations

k(propane) =

$$1.18 \times 10^{-12} \text{ cm}^3 \text{ molecule}^{-1} \text{ s}^{-1} \text{ at 298 K}$$

with an estimated uncertainty at 298 K of ±30%.

As is the case for methane and ethane, the rate constants of Baulch et al.[194] are in reasonably good agreement with our recommendation, further confirming the consistency of the above recommendations and the choice of Baulch et al.[194] for the rate constant expression for the reference reaction of OH radicals with CO.

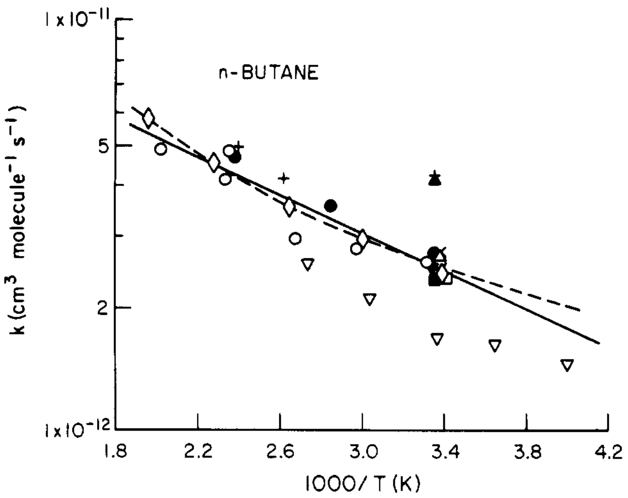

Figure 6. Arrhenius plot of the rate constants for the reaction of OH radicals with n-butane: (○) Greiner;[21] (▲) Morris and Niki;[102] (■) Stuhl;[209] (+) Gordon and Mulac;[129] (□) Campbell et al.;[135] (●) Perry et al.;[210] (△) Paraskevopoulos and Nip;[211] (▼) Atkinson et al.;[140] (▽) Anderson and Stephens;[198] (×) Atkinson and Aschmann;[153] (◇) Tully et al.;[208] (—) recommendation; (- - -) fit to modified Arrhenius expression (see text).

d. *n*-Butane and *n*-Butane-d_{10}. The available data for n-butane are listed in Table I, and the rate constants of Greiner,[21] Morris and Niki,[102] Stuhl,[209] Gordon and Mulac,[129] Campbell et al.,[135] Perry et al.,[210] Paraskevopoulos and Nip,[211] Atkinson et al.,[140,153] Anderson and Stephens,[198] and Tully et al.[208] are plotted in Figure 6. Unfortunately, the degree of scatter of these reported data is almost a factor of 2.5 at room temperature. The data of Gordon and Mulac[129] (which also show significant discrepancies with more recent data for propene), Anderson and Stephens[198] (which are also significantly lower than other reported data for 2-methylpropane and 2,2-dimethylpropane) and the less precise datum of Morris and Niki,[102] together with the relative rate constants of Gorse and Volman[206] and Campbell et al.,[135] have been neglected in the evaluation.

Thus, from the absolute rate constants of Greiner,[21] Stuhl,[209] Perry et al.,[210] Paraskevopoulos and Nip,[211] Atkinson et al.,[140,153] and Tully et al.,[208] a unit-weighted least-squares analysis yields the Arrhenius expression

k(n-butane) =

$$(1.55^{+0.38}_{-0.32}) \times 10^{-11}e^{-(540\pm79)/T} \text{ cm}^3 \text{ molecule}^{-1} \text{ s}^{-1}$$

where the error limits are two least-squares standard deviations

k(n-butane) =

$$2.53 \times 10^{-12} \text{ cm}^3 \text{ molecule}^{-1} \text{ s}^{-1} \text{ at 298 K}$$

with an estimated overall uncertainty at 298 K of ±20%. Using the expression $k = A'T^2e^{-E'/RT}$, these data yield

k(n-butane) =

$$(1.49^{+0.35}_{-0.29}) \times 10^{-17}T^2e^{(196\pm74)/T} \text{ cm}^3 \text{ molecule}^{-1} \text{ s}^{-1}$$

where the error limits are two least-squares standard deviations

k(n-butane) =

$$2.55 \times 10^{-12} \text{ cm}^3 \text{ molecule}^{-1} \text{ s}^{-1} \text{ at 298 K}$$

This expression is shown as the dashed line in Figure 6. Since the experimental data do not distinguish between these two alternative expressions, the simpler Arrhenius equation, shown as the solid line in Figure 6, is recommended over the temperature range ~300–500 K.

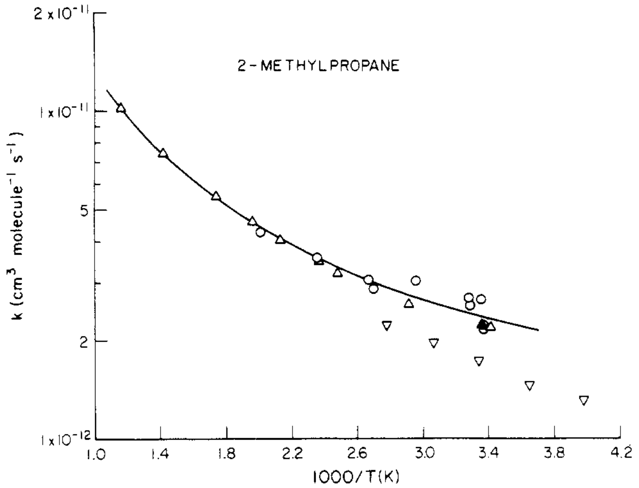

Figure 7. Arrhenius plot of the rate constants for the reaction of OH radicals with 2-methylpropane: (○) Greiner;[21] (▽) Anderson and Stephens;[198] (▲) Atkinson et al.;[214] (△) Tully et al.;[208] (—) recommendation (see text).

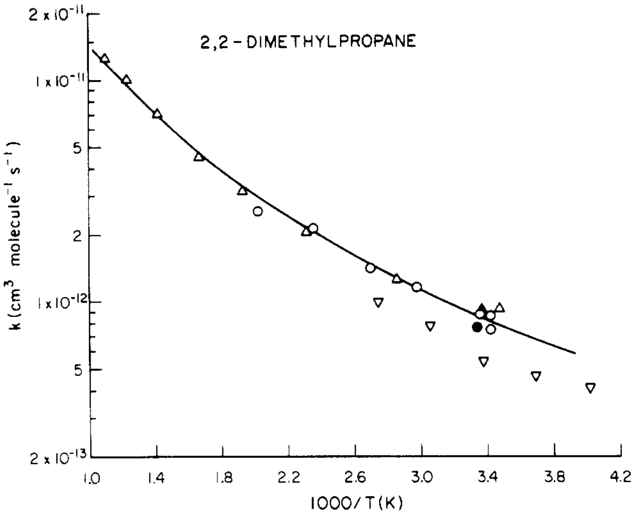

Figure 8. Arrhenius plot of the rate constants for the reaction of OH radicals with 2,2-dimethylpropane: (○) Greiner;[21] (▲) Paraskevopoulos and Nip;[211] (▽) Anderson and Stephens;[198] (●) Atkinson et al.;[147] (△) Tully et al.;[203,215] (—) recommendation (see text).

The relative rate constants of Gorse and Volman,[206] Campbell et al.,[135] and Behnke et al.[212] are in agreement within the error limits with this recommendation, as is the recent room temperature absolute rate constant determined by Schmidt et al.[126]

As expected, the room temperature rate constant for the reaction of OH radicals with n-butane-d_{10} is significantly lower than that for n-butane, by a factor of $\sim$3.5.[211]

e. 2-Methylpropane and 2-Methylpropane-d_1, -d_9, and -d_{10}. The available kinetic data are listed in Table I, and those of Greiner,[21] Anderson and Stephens,[198] Atkinson et al.[214] and Tully et al.[208] for 2-methylpropane are plotted in Figure 7. The relative rate constants of Wu et al.[136] and Butler et al.[213] are only of an approximate nature, and that of Darnall et al.[138] has been superseded by that of Atkinson et al.[214] Significant discrepancies still exist, however, with the data of Anderson and Stephens[198] being lower by a factor of $\sim$1.5 than those of Greiner,[21] Atkinson et al.,[214] and Tully et al.[208]

In view of the observations that the absolute rate constants of Greiner[21] and Tully and co-workers[203,208,215] are in excellent agreement and that the room temperature rate constants from these studies are in generally excellent agreement with the relative rate constant data of Atkinson and co-workers,[147,153,207,214] the data of Greiner,[21] Atkinson et al.,[214] and Tully et al.[208] have been used to derive the recommendation.

The Arrhenius plot (Figure 7) exhibits curvature, and a unit-weighted least-squares fit of these data[21,208,214] to the expression $k = A'T^2e^{-E'/RT}$ yields the recommended expression

$$k(\text{2-methylpropane}) = (9.58^{+1.10}_{-0.99}) \times 10^{-18}T^2e^{(305\pm40)/T}\ \text{cm}^3\ \text{molecule}^{-1}\ \text{s}^{-1}$$

where the error limits are two least-squares standard deviations

$$k(\text{2-methylpropane}) = 2.37 \times 10^{-12}\ \text{cm}^3\ \text{molecule}^{-1}\ \text{s}^{-1}$$

at 298 K, with an estimated uncertainty at 298 K of ±25%.

The room temperature relative rate constants of Wu et al.[136] and Darnall et al.[138] and the recent absolute rate constant of Schmidt et al.[126] are in reasonable agreement with this recommendation.

The rate constants for the reaction of OH radicals with $(CH_3)_3CD$, $(CD_3)_3CH$, and $(CD_3)_3CD$ are, as expected, significantly lower than those for $(CH_3)_3CH$.[208] Furthermore, Tully and co-workers[208] have shown that the rate constants for 2-methylpropane and 2-methylpropane-d_1, -d_9, and -d_{10} can be accurately expressed in the form

$$k_{\text{total}} = N_{\text{prim}}k_{\text{prim}} + N_{\text{tert}}k_{\text{tert}}$$

where N_{prim} and N_{tert} are the number of primary and tertiary C–H (or C–D) bonds, respectively, and k_{prim} and k_{tert} are the corresponding OH radical rate constants per primary and tertiary C–H (or C–D) bond, respectively. This finding is totally consistent with those of Greiner[21] and Darnall et al.[138] for the alkanes in general and shows that the principal of additive $-CH_3$, $-CH_2-$, and $>CH-$ (and $-CD_3$, $-CD_2-$, and $>CD-$) group rate constants[207,214] holds to a high degree of accuracy.

f. 2,2-Dimethylpropane and 2,2-Dimethylpropane-d_{12}. The available data are listed in Table I and those of Greiner,[21] Paraskevopoulos and Nip,[211] Anderson and Stephens,[198] Atkinson et al.,[147] and Tully et al.[203,215] for 2,2-dimethylpropane are plotted in Figure 8. The rate constant of Darnall et al.[138] has not been included since this work has been superseded by the more recent results of Atkinson et al.[147] using a more reliable and precise technique. As noted above for propane, n-butane, and 2-methylpropane, the rate constants obtained by Anderson and Stephens[198] for 2,2-dimethylpropane are consistently $\sim$30% lower than those of Greiner,[21] Paraskevopoulos and Nip,[211] Tully et al.,[203,215] and Atkinson et al.,[147] which are in excellent agreement.

Thus the rate constant for this reaction is evaluated from the data of Greiner,[21] Paraskevopoulos and Nip,[211] Atkinson et al.,[147] and Tully et al.[203,215] Since the Arrhenius expression clearly exhibits significant curvature (Figure 8), a unit-weighted least-squares analysis of these data[21,147,203,211,215] to the expression $k = A'T^2e^{-E'/RT}$ yields the recommendation of

$$k(\text{2,2-dimethylpropane}) = (1.75^{+0.25}_{-0.22}) \times 10^{-17}T^2e^{-(179\pm50)/T} \text{ cm}^3 \text{ molecule}^{-1} \text{ s}^{-1}$$

where the errors are two least-squares standard deviations

$$k(\text{2,2-dimethylpropane}) = 8.52 \times 10^{-13} \text{ cm}^3 \text{ molecule}^{-1} \text{ s}^{-1} \text{ at 298 K}$$

with an estimated overall uncertainty at 298 K of ±20%.

As expected on the basis of the higher bond dissociation energy for C–D vs. C–H bonds, the rate constants for the reaction of OH radicals with 2,2-dimethylpropane-d_{12} are significantly lower than those for 2,2-dimethylpropane[203,215] and, as discussed by Tully et al.,[203,215] are in accord with theoretical predictions.

g. 2,3-Dimethylbutane. The available data are listed in Table I and are plotted in Arrhenius form in Figure 9. The sole absolute rate constant study is that of Greiner,[21] while four relative rate determinations have been carried out by Darnall et al.,[138,219] Cox et al.,[139] and Atkinson et al.[147] The room-temperature rate constant determined by Greiner[21] is 20% higher than that derived by Atkinson et al.,[147] the most recent and precise of the relative rate studies. Furthermore, these rate constants of Greiner[21] lead to a negative Arrhenius activation energy of –0.26 kcal mol^{-1}.[21] Since the relative rate constant data of Atkinson and co-workers[147,207,214] generally agree very well with the absolute values obtained by Greiner[21] and Tully et al.,[203,208,215] and since the earlier relative rate constant measurements for 2,3-dimethylbutane[138,139,219] lead to a still lower room-temperature rate constant of ~(4–5) × 10^{-12} cm^3 molecule^{-1} s^{-1}, the recent room-temperature rate constant obtained by Atkinson et al.[147] is recommended. Taken in conjunction with the rate constants obtained by Greiner[21] at elevated temperatures, it is recommended for the temperature range ~300–500 K that

$$k(\text{2,3-dimethylbutane}) = 6.2 \times 10^{-12} \text{ cm}^3 \text{ molecule}^{-1} \text{ s}^{-1}$$

independent of temperature, with an estimated uncertainty at 298 K of ±30%.

h. 2,2,3-Trimethylbutane. The available rate constants[21,214,219] are listed in Table I and plotted in Arrhenius form in Figure 10. There is seen to be a significant degree of scatter in the reported data. Analogous to the situation for 2,3-dimethylbutane, the recent relative rate constant of Atkinson et al.[214] is weighted heavily in recommending that

$$k(\text{2,2,3-trimethylbutane}) = 4.1 \times 10^{-12} \text{ cm}^3 \text{ molecule}^{-1} \text{ s}^{-1} \text{ at 298 K}$$

with an estimated uncertainty of ±30%. While no firm recommendation concerning the Arrhenius parameters can be made, an Arrhenius activation energy of ~0.6 kcal mol^{-1} yields an Arrhenius preexponential factor of 1.1 × 10^{-11} cm^3 molecule^{-1} s^{-1}, a value in the range expected by analogy with other alkanes (Table I). A tentative recommendation of

$$k(\text{2,2,3-trimethylbutane}) = 1.12 \times 10^{-11}e^{-300/T} \text{ cm}^3 \text{ molecule}^{-1} \text{ s}^{-1}$$

is shown as the dashed line in Figure 10 and is likely to be applicable only over the temperature range ~ 290–500 K.

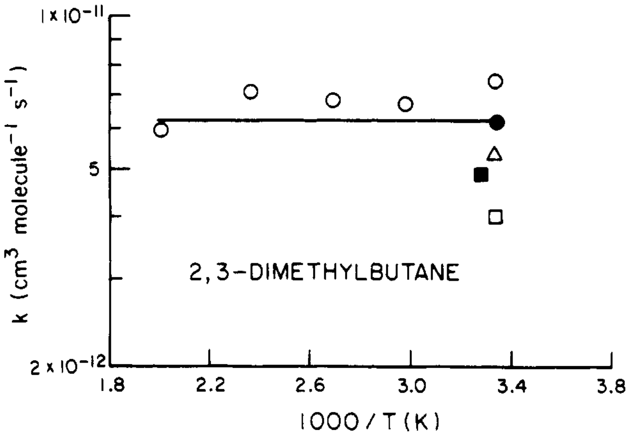

Figure 9. Arrhenius plot of the rate constants for the reaction of OH radicals with 2,3-dimethylbutane: (○) Greiner;[21] (■) Darnall et al.;[219] (△) Darnall et al.;[138] (□) Cox et al.;[139] (●) Atkinson et al.;[147] (—) recommendation (see text).

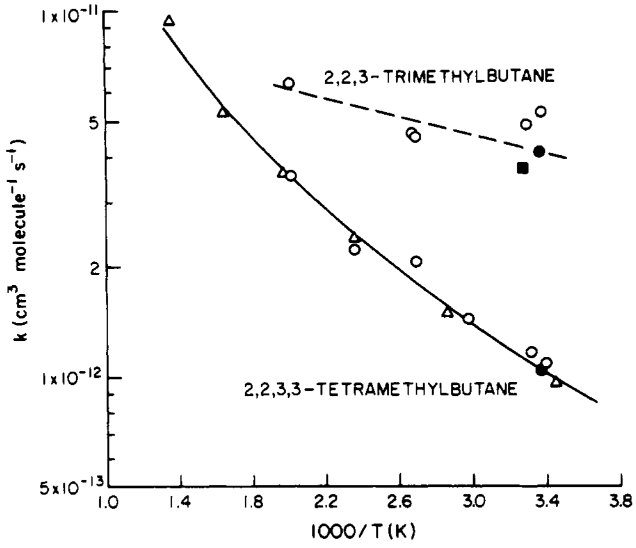

Figure 10. Arrhenius plot of the rate constants for the reaction of OH radicals with 2,2,3-trimethylbutane and 2,2,3,3-tetramethylbutane: (○) Greiner;[21] (■) Darnall et al.;[219] (●) Atkinson et al.;[214] (△) Tully et al.;[215] (- - -) tentative recommendation for 2,2,3-trimethylbutane (see text); (—) recommendation for 2,2,3,3-tetramethylbutane (see text).

i. *n*-Octane. The available kinetic data are listed in Table I, and those of Greiner[21] and Atkinson et al.[207] are plotted in Arrhenius form in Figure 11. The rate constant derived by Behnke et al.[212] at 302 K is in excellent agreement with those of Greiner[21] and Atkinson et al.[207] Since there is no evidence of curvature in the Arrhenius plot (Figure 11), a unit-weighted least-squares analysis of the data of Greiner[21] and Atkinson et al.[207] yields the recommended Arrhenius expression of

$$k(n\text{-octane}) = (3.12^{+0.88}_{-0.69}) \times 10^{-11}e^{-(380\pm87)/T}$$

where the error limits are two least-squares standard deviations

$$k(n\text{-octane}) = 8.72 \times 10^{-12} \text{ cm}^3 \text{ molecule}^{-1} \text{ s}^{-1} \text{ at 298 K}$$

with an estimated overall uncertainty at 298 K of ±20%.

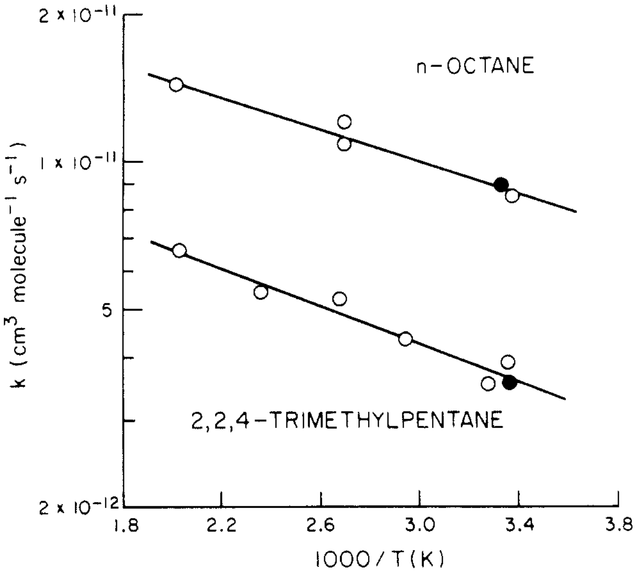

Figure 11. Arrhenius plots of the rate constants for the reactions of OH radicals with *n*-octane and 2,2,4-trimethylpentane: (○) Greiner;[21] (●) Atkinson et al.[207] (*n*-octane), Atkinson et al.[214] (2,2,4-trimethylpentane); (—) recommendations (see text).

j. 2,2,4-Trimethylpentane. The available rate constants[21,214] are given in Table I and plotted in Arrhenius form in Figure 11. The relative rate measurement of Atkinson et al.[214] at room temperature is in excellent agreement with that determined by Greiner[21] using flash photolysis–kinetic spectroscopy. A unit-weighted least-squares analysis of these data yields the recommended Arrhenius expression

k(2,2,4-trimethylpentane) =

$$(1.62^{+0.44}_{-0.35}) \times 10^{-11} e^{-(443\pm84)/T} \text{ cm}^3 \text{ molecule}^{-1} \text{ s}^{-1}$$

where the error limits are two least-squares standard deviations

k(2,2,4-trimethylpentane) =

$$3.66 \times 10^{-12} \text{ cm}^3 \text{ molecule}^{-1} \text{ s}^{-1} \text{ at } 298 \text{ K}$$

with an estimated overall uncertainty at 298 K of ±20%.

k. 2,2,3,3-Tetramethylbutane. The available data of Greiner,[21] Atkinson et al.,[214] and Tully et al.[215] are listed in Table I and plotted in Figure 10. Again, the agreement at room temperature between the relative rate constant obtained by Atkinson et al.[214] and the absolute rate constants of Greiner[21] and Tully et al.[215] is excellent. The Arrhenius plot clearly exhibits curvature (Figure 10) and hence a unit-weighted least-squares fit of these data[21,214,215] to the expression $k = A''T^2e^{-E'/RT}$ yields the recommendation

k(2,2,3,3-tetramethylbutane) =

$$(1.87^{+0.31}_{-0.26}) \times 10^{-17} T^2 e^{-(133\pm57)/T} \text{ cm}^3 \text{ molecule}^{-1} \text{ s}^{-1}$$

where the error limits are two least-squares standard deviations

k(2,2,3,3-tetramethylbutane) =

$$1.06 \times 10^{-12} \text{ cm}^3 \text{ molecule}^{-1} \text{ s}^{-1} \text{ at } 298 \text{ K}$$

with an estimated overall uncertainty at 298 K of ±20%.

l. Cyclohexane. The available rate constants[21,136,143,147,206,208,223] are given in Table II and plotted in Arrhenius form in Figure 12. These data are seen to be in generally good agreement. The relative rate constants of Gorse and Volman[206] and Wu et al.[136] are subject to large uncertainties (of the order of ~±25%), and hence the rate constants of Greiner,[21] Atkinson et al.,[147,223] Tuazon et al.,[143] and Tully et al.[208] have been used in the evaluation of this rate constant. No unambiguous evidence for curvature in the Arrhenius plot over this relatively limited temperature range (292–497 K) is evident from Figure 12, and hence a unit-weighted least-squares analysis of these rate constant data[21,143,147,208,223] yields the recommended Arrhenius expression

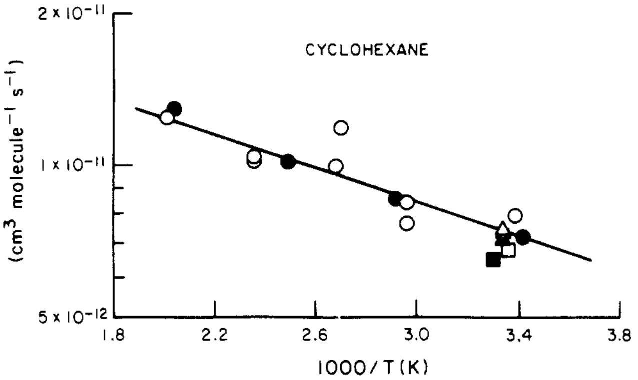

Figure 12. Arrhenius plot of the rate constants for the reaction of OH radicals with cyclohexane: (○) Greiner;[21] (□) Gorse and Volman;[206] (■) Wu et al.;[136] (△) Atkinson et al.[147] and Tuazon et al.;[143] (▲) Atkinson et al.;[223] (●) Tully et al.;[208] (—) recommendation (see text).

k(cyclohexane) =

$$(2.73^{+1.03}_{-0.74}) \times 10^{-11} e^{-(390\pm81)/T} \text{ cm}^3 \text{ molecule}^{-1} \text{ s}^{-1}$$

where the error limits are two least-squares standard deviations

k(cyclohexane) =

$$7.38 \times 10^{-12} \text{ cm}^3 \text{ molecule}^{-1} \text{ s}^{-1} \text{ at } 298 \text{ K}$$

with an estimated overall uncertainty at 298 K of ±20%.

m. Other Acyclic and Cycloalkanes. For the remaining acyclic alkanes and cycloalkanes for which rate constants are available (Tables I and II), data are available only at room temperature. Apart from the absolute rate constants determined for cyclopropane, cyclopentane, and cycloheptane by Jolly et al.[221] and for cyclopropane by Zetzsch,[220] the available data for these acyclic alkanes and cycloalkanes have been obtained from relative rate studies.

For these acyclic alkanes, the most recent and precise data are from the relative rate studies of Atkinson and co-workers[143,207,214] and Behnke et al.[212] For the alkanes which have been studied by both of these groups (i.e., *n*-butane, *n*-hexane, *n*-heptane, *n*-octane, *n*-nonane, and *n*-decane), the agreement is excellent. Hence the room-temperature recommendations are based on these studies.

n. *n*-Pentane. There is a significant degree of scatter in the available rate constant data. However, on the basis of the rate constant obtained by Atkinson et al.,[207] it is recommended that

k(n-pentane) =

$$4.06 \times 10^{-12} \text{ cm}^3 \text{ molecule}^{-1} \text{ s}^{-1} \text{ at } 299 \text{ K}$$

with an estimated uncertainty of ±30%. An estimated

Arrhenius activation energy of 1.0 kcal mol^{-1} has been used to derive rate constants for this reaction at other temperatures.

o. 2-Methylbutane. The available rate constants (Table I) are in reasonable agreement, and on the basis of that obtained by Atkinson et al.,[214] it is recommended that

$$k(\text{2-methylbutane}) = 3.9 \times 10^{-12}\ \text{cm}^3\ \text{molecule}^{-1}\ \text{s}^{-1} \text{ at } 298\ \text{K}$$

with an estimated uncertainty of ±30%.

p. *n*-Hexane. The available rate constants[136,144,147,153,212,216-218] (Table I) are in excellent agreement. In the recommendation the rate constant of Atkinson et al.,[147] corrected to 298 K by using an estimated Arrhenius activation energy of 0.80 kcal mol^{-1}, is used to obtain

$$k(n\text{-hexane}) = 5.58 \times 10^{-12}\ \text{cm}^3\ \text{molecule}^{-1}\ \text{s}^{-1} \text{ at } 298\ \text{K}$$

with an estimated uncertainty of ±20%.

q. 2-Methylpentane. The available rate constants[139,144,214] (Table I) are in good agreement, and it is recommended, on the basis of the datum of Atkinson et al.,[214] that

$$k(\text{2-methylpentane}) = 5.5 \times 10^{-12}\ \text{cm}^3\ \text{molecule}^{-1}\ \text{s}^{-1} \text{ at } 298\ \text{K}$$

with an estimated uncertainty of ±25%.

r. 3-Methylpentane. The two relative rate studies[144,214] are in agreement within the experimental errors, and it is recommended, on the basis of the recent rate constant derived by Atkinson et al.,[214] that

$$k(\text{3-methylpentane}) = 5.6 \times 10^{-12}\ \text{cm}^3\ \text{molecule}^{-1}\ \text{s}^{-1} \text{ at } 298\ \text{K}$$

with an estimated uncertainty of ±25%.

For *n*-heptane through *n*-tridecane, the sole data available are those of Atkinson et al.[214] and Behnke et al.[212] Tentative recommendations at room temperature are as follows:

$$k(n\text{-heptane}) = 7.2 \times 10^{-12}\ \text{cm}^3\ \text{molecule}^{-1}\ \text{s}^{-1} \text{ at } 298\ \text{K}$$

$$k(n\text{-nonane}) = 1.00 \times 10^{-11}\ \text{cm}^3\ \text{molecule}^{-1}\ \text{s}^{-1} \text{ at } 298\ \text{K}$$

$$k(n\text{-decane}) = 1.12 \times 10^{-11}\ \text{cm}^3\ \text{molecule}^{-1}\ \text{s}^{-1} \text{ at } 298\ \text{K}$$

all with estimated uncertainties of ±25%.

For *n*-undecane, *n*-dodecane, and *n*-tridecane the values obtained by Behnke et al.[212] are recommended, with estimated uncertainties of ±30%.

s. Cyclopentane. The available data[138,147,221,222] (Table II) show significant discrepancies. However, the rate constant obtained by Jolly et al.[221] using a flash photolysis–resonance absorption technique is in excellent agreement with the relative rate constant derived by Atkinson et al.[147] It is thus recommended that

$$k(\text{cyclopentane}) = 5.2 \times 10^{-12}\ \text{cm}^3\ \text{molecule}^{-1}\ \text{s}^{-1} \text{ at } 298\ \text{K}$$

with an estimated uncertainty of ±25%.

For the remaining cycloalkanes, until further data become available, only the single determinations available for each cycloalkane can be used. Obviously, confirming data are necessary before any firm recommendations can be made.

t. Reactions of OD Radicals with Alkanes. To date, kinetic data are available (Table III) for only four alkanes and then only at room temperature. By comparison with the data given in Table I, it is evident that the rate constants at room temperature for the reactions of OD radicals with methane, ethane, and *n*-butane are essentially identical with those for the reactions of OH radicals with these alkanes. This is to be expected, since the thermochemistries of these OD radical reactions are essentially identical with those for the corresponding OH radical reactions.[226] However, as with the OH radical reactions, the rate constant for the reaction of OD radicals with *n*-butane-d_{10}[211] is lower by a factor of ~3 than that for the reaction of OD radicals with *n*-butane and is essentially identical with that for the reaction of OH radicals with *n*-butane-d_{10}. This is again expected on thermochemical grounds, since the abstraction of D atoms from C–D bonds by OH or OD radicals are less exothermic by ~0.9 kcal mol^{-1} than are the corresponding abstractions of H atoms from C–H bonds.[226]

2. Mechanism

These reactions obviously proceed via H atom abstraction from the C–H bonds, with the room-temperature rate constants increasing with decreasing C–H bond dissociation energy.[227] These reactions are all exothermic, with reaction exothermicities of 15 kcal mol^{-1} for methane,[226] 21 kcal mol^{-1} for ethane and primary C–H bonds,[226] 25 kcal mol^{-1} for secondary C–H bonds,[226] and 27 kcal mol^{-1} for tertiary C–H bonds.[226] This is consistent with the low Arrhenius activation energies encountered, and for alkanes containing tertiary C–H bonds the temperature dependencies are small. For the $\geq C_3$ alkanes it is obvious that more than one alkyl radical is formed from the reaction of OH radicals with the parent alkane, and estimation techniques are available for calculating the distribution of the individual alkyl radicals formed. The simplest of these techniques is that of Greiner,[21] who derived rate constants per primary, secondary, and tertiary C–H bond of

$$k(\text{primary}) = 1.02 \times 10^{-12} e^{-823/T}\ \text{cm}^3\ \text{molecule}^{-1}\ \text{s}^{-1}$$

$$k(\text{secondary}) = 2.34 \times 10^{-12} e^{-428/T}\ \text{cm}^3\ \text{molecule}^{-1}\ \text{s}^{-1}$$

$$k(\text{tertiary}) = 2.09 \times 10^{-12} e^{96/T}\ \text{cm}^3\ \text{molecule}^{-1}\ \text{s}^{-1}$$

More recently, Darnall et al.[138] derived modified values of

$$k(\text{primary}) = 1.01 \times 10^{-12} e^{-823/T}\ \text{cm}^3\ \text{molecule}^{-1}\ \text{s}^{-1}$$

$$k(\text{secondary}) = 2.41 \times 10^{-12} e^{-428/T}\ \text{cm}^3\ \text{molecule}^{-1}\ \text{s}^{-1}$$

$$k(\text{tertiary}) = 2.10 \times 10^{-12}\ \text{cm}^3\ \text{molecule}^{-1}\ \text{s}^{-1}$$

independent of temperature. These later expressions of Darnall et al.[138] are applicable over the temperature range ~300–500 K and, from a knowledge of the overall OH radical rate constant, the distribution of individual alkyl radicals formed from $\geq C_3$ alkanes (except cyclopropane and cyclobutane and other strained cycloalkanes) can be readily estimated. More recently, Atkinson and co-workers[207,214,224] have shown that the above estimation techniques are too simplistic since they neglect the effects of differing neighboring groups[207,214] and, for cycloalkanes, of ring strain[224] (see section IV for a more detailed discussion of these topics). Based upon the most recent study[214] and taking into account the slightly lower recommended rate constant for the reaction of OH radicals with *n*-butane

$$k(\text{primary}) = 2.79 \times 10^{-12}e^{-823/T}\ \text{cm}^3\ \text{molecule}^{-1}\ \text{s}^{-1}$$

$$k(\text{secondary}) = 5.31 \times 10^{-12}e^{-(528-70n\beta)/T}\ \text{cm}^3\ \text{molecule}^{-1}\ \text{s}^{-1}$$

[a typographical error exists in ref 214 for the preexponential factor for k(secondary)] and

$$k(\text{tertiary}) = 1.7 \times 10^{-12}e^{70n\beta/T}\ \text{cm}^3\ \text{molecule}^{-1}\ \text{s}^{-1}$$

where $n\beta$ is the number of next nearest neighbors.[214]

These expressions are applicable to the acyclic alkanes and nonstrained cycloalkanes. For cycloalkanes with ring strain, at room temperature the above three expressions are reduced in accordance with the equation[214,224]

$$\frac{k^{\text{strained}}}{k^{\text{unstrained}}} = 1.31\text{e}^{-(0.062E_{\text{strain}})}$$

for values of $E_{\text{strain}} \geq 5$ kcal mol^{-1}, where E_{strain} is the overall ring strain energy.[224] As an example, use of the above expressions yield the following distribution of alkyl radicals from the reaction of OH radicals with 2-methylpentane at room temperature:

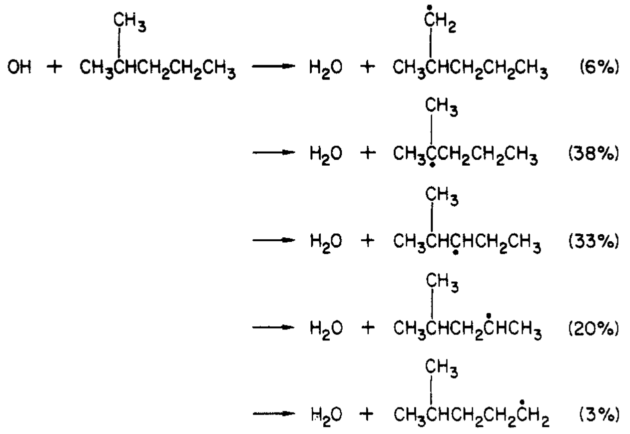

$$\begin{aligned}\text{OH} + \text{CH}_3\overset{\text{CH}_3}{\text{C}}\text{HCH}_2\text{CH}_2\text{CH}_3 &\rightarrow \text{H}_2\text{O} + \text{CH}_3\overset{\dot{\text{C}}\text{H}_2}{\text{C}}\text{HCH}_2\text{CH}_2\text{CH}_3 \quad (6\%)\\ &\rightarrow \text{H}_2\text{O} + \text{CH}_3\overset{\text{CH}_3}{\dot{\text{C}}}\text{CH}_2\text{CH}_2\text{CH}_3 \quad (38\%)\\ &\rightarrow \text{H}_2\text{O} + \text{CH}_3\overset{\text{CH}_3}{\text{C}}\text{H}\dot{\text{C}}\text{HCH}_2\text{CH}_3 \quad (33\%)\\ &\rightarrow \text{H}_2\text{O} + \text{CH}_3\overset{\text{CH}_3}{\text{C}}\text{HCH}_2\dot{\text{C}}\text{HCH}_3 \quad (20\%)\\ &\rightarrow \text{H}_2\text{O} + \text{CH}_3\overset{\text{CH}_3}{\text{C}}\text{HCH}_2\text{CH}_2\dot{\text{C}}\text{H}_2 \quad (3\%)\end{aligned}$$

The detailed discussion in section IV concerning the a priori estimation of OH radical rate constants leads to slightly different expressions for k_{primary}, $k_{\text{secondary}}$, and k_{tertiary} and hence to slightly differing alkyl radical distributions. For example, use of the estimation procedures discussed in section IV (applicable only at 298 K) leads to a distribution of the hexyl radicals shown above of 7, 44, 26, 20, and 3%, respectively. These minor differences from the differing estimation techniques illustrate the likely uncertainties in these alkyl radical distributions.

3. Atmospheric Reactions

Reaction with the OH radical is the almost exclusive loss process for the alkanes in the troposphere (nighttime reaction with the NO_3 radical can contribute a small portion, <10%, of the overall loss processes[228]) and is a major loss process in the stratosphere. In the troposphere the alkyl radicals initially formed from OH radical reaction react rapidly with O_2

$$\text{R} + \text{O}_2 \xrightarrow{\text{M}} \text{RO}_2$$

with rate constants at atmospheric pressure and room temperature of $\gtrsim 1 \times 10^{-12}$ cm^3 molecule^{-1} s^{-1}.[3,30,229–232]

The subsequent reactions of these alkylperoxy (RO_2) radicals in the troposphere depend on the NO to HO_2 radical concentration ratio. If the NO concentration is sufficiently high [≳30 parts per trillion (ppt)],[2] then the RO_2 radicals will react with NO:

$$\text{RO}_2 + \text{NO} \rightarrow \text{products}$$

However, at lower NO concentrations, RO_2 radicals will react primarily with HO_2

$$\text{RO}_2 + \text{HO}_2 \rightarrow \text{ROOH} + \text{O}_2$$

and other RO_2 radicals. Present ambient atmospheric data indicate that the tropospheric NO concentrations are ≲200 ppt in clean continental air,[233–238] with values of ~4 ppt having been measured in maritime equatorial Pacific regions.[239] Hence both loss processes for RO_2 radicals are expected to occur in the troposphere.

The alkylperoxy radicals derived from methane and ethane react with NO with rate constants of $\sim 4.2 \times 10^{-12}e^{180/T}$ cm^3 molecule^{-1} s^{-1},[3,30] to yield the corresponding alkoxy radical and NO_2,[3] as, for example

$$\text{C}_2\text{H}_5\text{O}_2 + \text{NO} \rightarrow \text{C}_2\text{H}_5\text{O} + \text{NO}_2$$

Under tropospheric conditions the resulting methoxy and ethoxy radicals react solely with O_2 to yield formaldehyde and acetaldehyde, respectively, together with an HO_2 radical,[3] for example

$$\text{C}_2\text{H}_5\text{O} + \text{O}_2 \rightarrow \text{CH}_3\text{CHO} + \text{HO}_2$$

The reaction of the HO_2 radical with NO

$$\text{HO}_2 + \text{NO} \rightarrow \text{OH} + \text{NO}_2$$

completes the chain regeneration of OH radicals, and the overall reaction can be written, taking ethane as an example, as

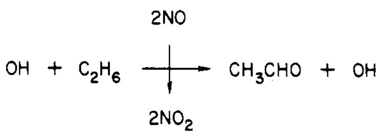

$$\text{OH} + \text{C}_2\text{H}_6 \xrightarrow[\text{2NO}_2]{\text{2NO}} \text{CH}_3\text{CHO} + \text{OH}$$

For the larger ($\geq C_3$) alkylperoxy radicals it has been shown[28,29,240,241] that the reaction with NO also proceeds via the direct formation of alkyl nitrates (pathway b)

$$\text{RO}_2 + \text{NO} \rightarrow \text{RO} + \text{NO}_2 \quad \text{(a)}$$

$$\text{RO}_2 + \text{NO} \xrightarrow{\text{M}} \text{RONO}_2 \quad \text{(b)}$$

For the *n*-alkane series the alkyl nitrate yield at 735 torr total pressure of air and 299 ± 2 K increases monotonically from ≤0.014 for ethane to ~0.33 for *n*-octane.[28] Furthermore, as expected for an overall addition reaction, the alkyl nitrate yields for *n*-pentane and *n*-heptane have been shown to be a function of the temperature and pressure, increasing with increasing pressure and with decreasing temperature.[241] The most recent study of Atkinson et al.[29] concerning the alkyl nitrate yields from a series of branched and cyclic al-

TABLE IV. Rate Constant Ratios $k_b/(k_a + k_b)$ for Primary, Secondary, and Tertiary Alkyl Peroxy (RO_2) Radicals at 299 ± 2 K and 735-740-Torr Total Pressure of Air[242]

	primary		secondary		tertiary	
alkane	RO_2	$k_b/(k_a + k_b)$	RO_2	$k_b/(k_a + k_b)$	RO_2	$k_b/(k_a + k_b)$
ethane	ethyl	≤0.014				
propane	1-propyl	0.020 ± 0.009[a]	2-propyl	0.042 ± 0.003[a]		
n-butane	1-butyl	≤0.041[a]	2-butyl	0.090 ± 0.008[a]		
n-pentane			2-pentyl	0.129 ± 0.016[a]		
				0.134 ± 0.002[b]		
			3-pentyl	0.131 ± 0.016[a]		
				0.146 ± 0.009[b]		
2,2-dimethylpropane	neopentyl	0.051 ± 0.005[c]				
2-methylbutane			2-methyl-3-butyl	0.141 ± 0.003[c]	2-methyl-2-butyl	0.047 ± 0.002[c]
n-hexane			2-hexyl	0.209 ± 0.032[a]		
			3-hexyl	0.230 ± 0.031[a]		
cyclohexane			cyclohexyl	0.160 ± 0.015[c]		
2-methylpentane			2-methyl-3-pentyl + 2-methyl-4-pentyl	0.190 ± 0.018[c]	2-methyl-2-pentyl	0.031 ± 0.008[c]
3-methylpentane			3-methyl-2-pentyl	0.178 ± 0.017[c]		
n-heptane			2-heptyl	0.301 ± 0.049[a]		
				0.291 ± 0.022[b]		
			3-heptyl	0.323 ± 0.048[a]		
				0.325 ± 0.014[b]		
			4-heptyl	0.301 ± 0.045[a]		
				0.285 ± 0.015[b]		
n-octane			2-octyl	0.323 ± 0.024[a]		
			3-octyl	0.348 ± 0.032[a]		
			4-octyl	0.329 ± 0.032[a]		

[a] From Atkinson et al.,[28] 299 K, 735-torr total pressure. [b] From Atkinson et al.,[29] 300 K, 740-torr total pressure. [c] From Atkinson et al.,[241] 298 K, 735-torr total pressure.

kylperoxy radicals shows that, to a first approximation, the alkyl nitrate yields for secondary alkylperoxy radicals are a function of the carbon number of the RO_2 radical.[242] Furthermore, the available data show that the alkyl nitrate yields from primary and tertiary alkylperoxy radicals are significantly lower than those from secondary alkylperoxy radicals of the same carbon number,[29,242] by factors of ~2.5 and 4, respectively, at room temperature and ~735–740 torr total pressure of air.[29,242] Table IV gives the rate constant ratios $k_b/(k_a + k_b)$ obtained[28,29,241] at room temperature and atmospheric pressure for the alkylperoxy radicals studied to date, as reanalyzed[242] to be consistent with the CH_3–, $-CH_2$–, and >CH– group rate constants presented in section IV below.

The yields of secondary alkyl nitrates, Y_s, from the corresponding alkylperoxy radicals, i.e., the rate constant ratios $k_b/(k_a + k_b)$, as a function of temperature, pressure, and the size of the molecule, are fit by the following expression[29]

$$Y_s = \left\{ \frac{Y_0^{300}[M](T/300)^{-m_0}}{1 + \dfrac{Y_0^{300}[M](T/300)^{-m_0}}{Y_\infty^{300}(T/300)^{-m_\infty}}} \right\} F^Z$$

where

$$Z = \left[1 + \left\{ \log_{10} \left[\frac{Y_0^{300}[M](T/300)^{-m_0}}{Y_\infty^{300}(T/300)^{-m_\infty}} \right] \right\}^2 \right]^{-1}$$

Y_s is the secondary alkyl nitrate yield at a concentration [M] (molecule cm^{-3}) of air and a temperature $T(K)$, n is the number of carbons in the alkane, and $Y_0^{300} = \alpha e^{\beta n}$. From a nonlinear least-squares fit of this equation to the data of Atkinson et al.,[28,29,241] Carter and Atkinson[242] derived the following values of these parameters

$$Y_\infty^{300} = 0.435 \qquad \alpha = 1.95 \times 10^{-22}\ \text{cm}^3\ \text{molecule}^{-1}$$
$$\beta = 0.947 \qquad m_0 = 2.99 \qquad m_\infty = 4.69 \qquad F = 0.556$$

For the $\geq C_3$ alkanes, reaction pathways for the alkoxy radicals produced from the reaction of RO_2 radicals with NO, other than that with O_2 discussed above, become significant. As discussed by Atkinson and Lloyd,[3,243] these $\geq C_3$ alkoxy radicals can react with O_2,[3,242,244-247] unimolecularly decompose[3,242,244,245,248,249] or unimolecularly isomerize via a 1,5-H atom shift.[3,145,242,244,250,251] These reactions are shown, for example, for the 2-pentoxy radical

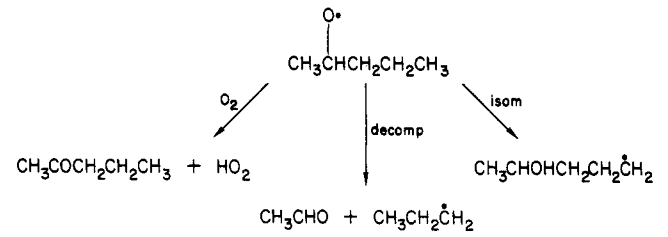

and methods for estimating the absolute and relative rates of these processes are available.[3,242,244-246,248-250]

The reaction pathways subsequent to the initial isomerization process have not been experimentally delineated but are expected to include, at least part of the time, a second isomerization. As an example, the expected isomerization reaction sequence for the 2-pentoxy radical is shown (alkyl nitrate formation from the reaction of the $CH_3CHOHCH_2CH_2CH_2O\dot{O}$ radical with NO has been neglected for simplicity)

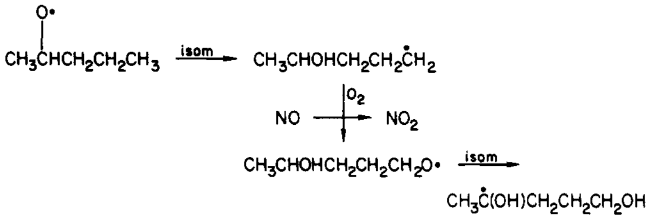

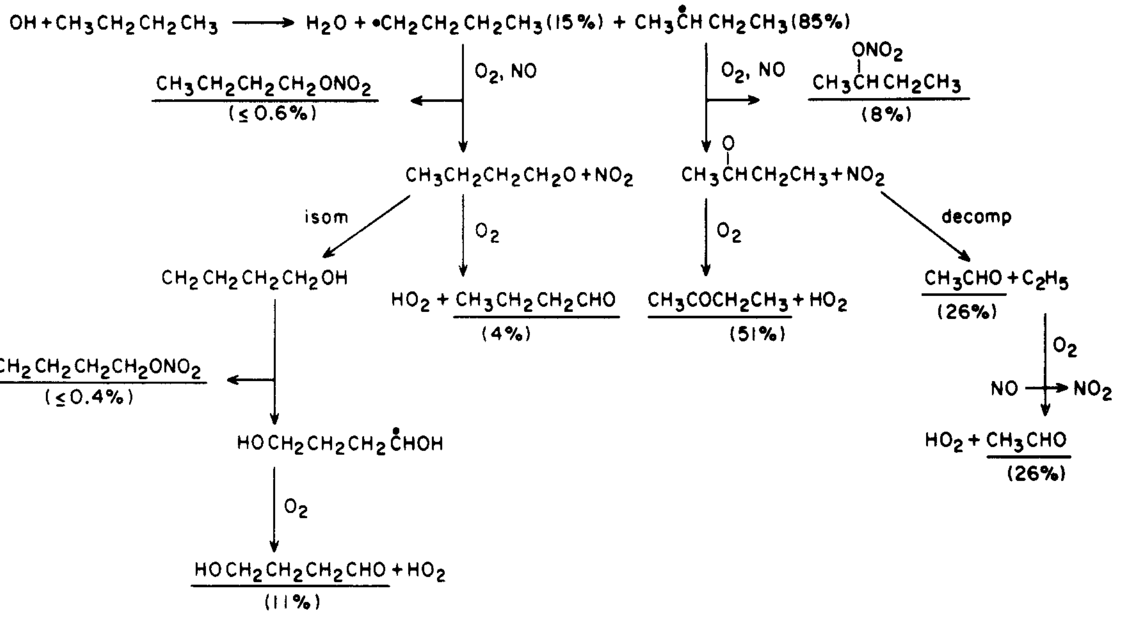

Figure 13. The major reaction pathways occurring during the tropospheric degradation resulting from the reaction of *n*-butane with OH radicals.[3]

The resulting α-hydroxy radicals have been shown to react rapidly with O_2 to yield the carbonyl and an HO_2 radical,[3,146,252-256] as, for example

$$CH_3\dot{C}(OH)CH_2CH_2CH_2OH + O_2 \rightarrow HO_2 + CH_3COCH_2CH_2CH_2OH$$

As an example of the reaction degradation pathways of alkanes under atmospheric conditions, Figure 13 shows those for the reaction of OH radicals with *n*-butane.

B. Haloalkanes

1. *Kinetics*

The available rate constant data are listed in Table V. The relative rate constants obtained by Cox et al.[274] and Butler et al.[275] are not included, since the rate constants derived in the study of Cox et al.[274] have a stated accuracy of approximately a factor of 2, due to uncertainties in the number of molecules of NO oxidized per OH radical reacted,[274] and the rate constants obtained by Butler et al.[275] were derived from a complex expression which cannot be reevaluated in the light of more recent rate constant data for the reference reactions. It can then be seen that these data listed in Table V for the C_1 and C_2 haloalkanes all arise from absolute rate constant studies.

As discussed below for the individual haloalkanes, apart from CH_3CCl_3 for which significant discrepancies appear to have arisen in all but the most recent studies[71,72,186] due to problems associated with the presence of reactive impurities, these data are in general agreement, apart from those from the study of Clyne and Holt.[261] As noted in previous evaluations,[1,30] for several of the haloalkanes studied by Clyne and Holt[261] the room-temperature rate constants and the Arrhenius activation energies are significantly higher than the other absolute literature values given in Table V. Furthermore, the derived Arrhenius preexponential factors (Table V) appear in many cases to be unreasonably high. Thus these data of Clyne and Holt[261] are not included in the evaluations and recommendations for the individual haloalkanes given below.

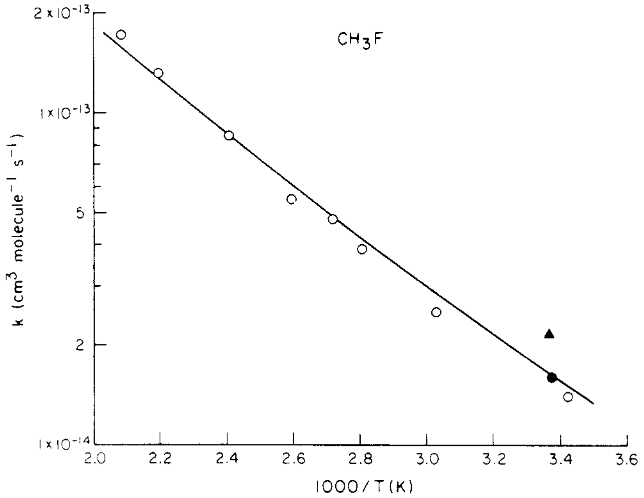

Figure 14. Arrhenius plot of the rate constants for the reaction of OH radicals with CH_3F: (●) Howard and Evenson;[191] (▲) Nip et al.;[257] (○) Jeong and Kaufman;[186,193] (—) recommendation (see text).

In the evaluations and recommendations, it is apparent that for most of these haloalkanes the Arrhenius plots exhibit distinct curvature. In accordance with the NASA evaluation,[30] in most cases least-squares analyses of the data for these haloalkanes have been carried out by using the expression $k = A'T^2e^{-E'/RT}$ and the recommendations are generally in this form. The use of this expression is consistent with previous evaluations[187] and theoretical expectations[193] and yields good fits to the experimental data over the temperature ranges studied (i.e., ~240–500 K). Furthermore, the use of this expression is generally consistent with nonlinear least-squares analyses of the kinetic data for several of these haloalkanes. It should be noted that the recommended expressions are strictly applicable only over the temperature ranges for which data are available.

The kinetic data for the individual haloalkanes are discussed below.

a. CH_3F. The available rate constants[186,191,193,257] are listed in Table V and plotted in Arrhenius form in

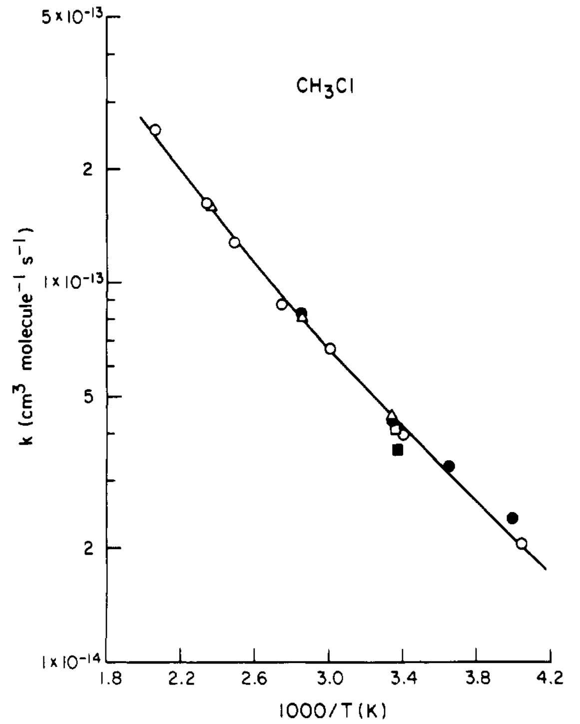

Figure 15. Arrhenius plot of the rate constants for the reaction of OH radicals with CH_3Cl: (■) Howard and Evenson;[191] (△) Perry et al.;[258] (●) Davis et al.;[259] (□) Paraskevopoulos et al.;[260] (○) Jeong and Kaufman;[193] (—) recommendation (see text).

Figure 14. These rate constants of Howard and Evenson,[191] Nip et al.,[257] and Jeong and Kaufman[186,193] are in reasonably good agreement at room temperature. A unit-weighted least-squares analysis of these data yields the recommended expression

$$k(CH_3F) = (5.51^{+3.36}_{-2.08}) \times 10^{-18} T^2 e^{-(1005\pm168)/T} \text{ cm}^3 \text{ molecule}^{-1} \text{ s}^{-1}$$

where the error limits are two least-squares standard deviations

$$k(CH_3F) = 1.68 \times 10^{-14} \text{ cm}^3 \text{ molecule}^{-1} \text{ s}^{-1} \text{ at } 298 \text{ K}$$

with an estimated uncertainty at 298 K of ±30%.

b. CH_3Cl. The available rate constants[191,193,258-260] are listed in Table V and plotted in Arrhenius form in Figure 15. It can be seen that these rate constants of Howard and Evenson,[191] Perry et al.,[258] Davis et al.,[259] Paraskevopoulos et al.,[260] and Jeong and Kaufman[193] are in excellent agreement. A unit-weighted least-squares analysis yields the recommended expression

$$k(CH_3Cl) = (3.50^{+0.71}_{-0.58}) \times 10^{-18} T^2 e^{-(585\pm59)/T} \text{ cm}^3 \text{ molecule}^{-1} \text{ s}^{-1}$$

where the error limits are two least-squares standard deviations

$$k(CH_3Cl) = 4.36 \times 10^{-14} \text{ cm}^3 \text{ molecule}^{-1} \text{ s}^{-1} \text{ at } 298 \text{ K}$$

with an estimated uncertainty at 298 K of ±20%. This recommendation is essentially identical with that recommended by the recent NASA evaluation.[30]

c. CH_3Br. The available rate constants[191,259] are listed in Table V and plotted in Arrhenius form in Figure 16. The only two absolute studies carried out[191,259] are in good agreement. The Arrhenius plot does not show any evidence of curvature over the relatively small temperature range (244–350 K) studied, and hence a unit-weighted least-squares analysis yields

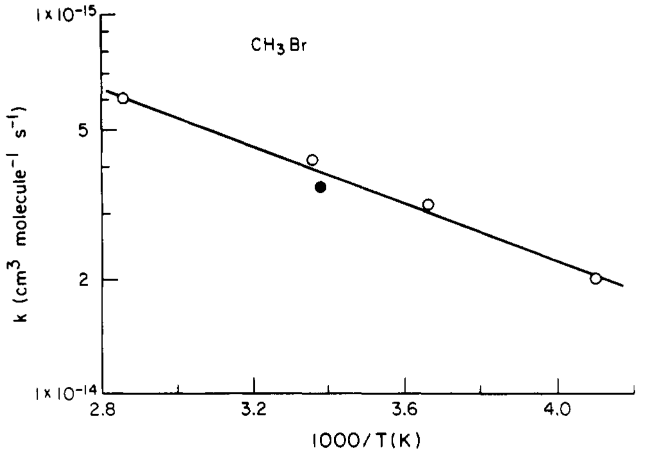

Figure 16. Arrhenius plot of the rate constants for the reaction of OH radicals with CH_3Br: (●) Howard and Evenson;[191] (○) Davis et al.;[259] (—) recommendation (see text).

the recommended Arrhenius expression

$$k(CH_3Br) = (7.40^{+5.31}_{-3.09}) \times 10^{-13} e^{-(875\pm155)/T} \text{ cm}^3 \text{ molecule}^{-1} \text{ s}^{-1}$$

where the error limits are two least-squares standard deviations

$$k(CH_3Br) = 3.93 \times 10^{-14} \text{ cm}^3 \text{ molecule}^{-1} \text{ s}^{-1} \text{ at } 298 \text{ K}$$

with an estimated uncertainty at 298 K of ±20%.

Alternatively, using the expression $k = A'T^2e^{-E'/RT}$, a unit-weighted least-squares analysis yields

$$k(CH_3Br) = (1.17^{+0.91}_{-0.51}) \times 10^{-18} T^2 e^{-(296\pm164)/T} \text{ cm}^3 \text{ molecule}^{-1} \text{ s}^{-1}$$

where the error limits are two least-squares standard deviations

$$k(CH_3Br) = 3.85 \times 10^{-14} \text{ cm}^3 \text{ molecule}^{-1} \text{ s}^{-1} \text{ at } 298 \text{ K}$$

with an estimated uncertainty at 298 K of ±20%. This is essentially identical with the recent NASA recommendation.[30]

Since these two- and three-parameter expressions are almost indistinguishable (within 2–3%) over the temperature range studied (244–350 K), we recommend the use of either expression. The recommended Arrhenius line is plotted in Figure 16.

d. CH_2F_2. The available rate constants[191,193,257,261] are listed in Table V and plotted in Arrhenius form in Figure 17. In this case the rate constants of Clyne and Holt[261] are in reasonably good agreement with those of Howard and Evenson,[191] Nip et al.,[257] and Jeong and Kaufman,[193] although their room-temperature rate constant[261] is the lowest of those measured. In accordance with the discussion above, a unit-weighted least-squares analysis, using the expression $k = A'T^2e^{-E'/RT}$, of the data of Howard and Evenson,[191] Nip et al.,[257] and Jeong and Kaufman[193] yields the recommended expression of

$$k(CH_2F_2) = (5.06^{+2.66}_{-1.74}) \times 10^{-18} T^2 e^{-(1107\pm142)/T} \text{ cm}^3 \text{ molecule}^{-1} \text{ s}^{-1}$$

where the errors are two least-squares standard deviations

$$k(CH_2F_2) = 1.09 \times 10^{-14} \text{ cm}^3 \text{ molecule}^{-1} \text{ s}^{-1} \text{ at } 298 \text{ K}$$

with an estimated uncertainty at 298 K of ±30%.

TABLE V. Rate Constants k and Arrhenius Parameters for the Gas-Phase Reaction of OH Radicals with Haloalkanes

haloalkane	$10^{12}A$, cm^3 molecule^{-1} s^{-1}	n	E, cal mol^{-1}	$10^{14}k$, cm^3 molecule^{-1} s^{-1}	T, K	technique	ref	temp range, covered, K
CH_3F				1.6 ± 0.35	296 ± 2	DF-LMR	Howard and Evenson[191]	
				2.17 ± 0.18	297 ± 2	FP-RA	Nip et al.[257]	
				1.40 ± 0.09	292	DF-RF	Jeong and Kaufman[186,193]	292–480
				2.50 ± 0.18	330			
				3.86 ± 0.33	356			
				4.76 ± 0.31	368			
				5.48 ± 0.66	385			
				8.56 ± 0.66	416			
				13.1 ± 1.1	455			
	7.96×10^{-13}	4.32 ± 1.95	550 ± 1450	17.1 ± 1.1	480			
	8.11 ± 1.35		3750 ± 120					
CH_3Cl				3.6 ± 0.8	296 ± 2	DF-LMR	Howard and Evenson[191]	
				4.4 ± 0.5	298.4	FP-RF	Perry et al.[258]	298–423
				8.1 ± 0.8	349.3			
	4.1		2700 ± 300	16.8 ± 1.7	422.6			
				2.38 ± 0.14	250	FP-RF	Davis et al.[259]	250–350
				3.26 ± 0.06	273			
				4.29 ± 0.21	298			
	1.84 ± 0.18		2181 ± 70	8.28 ± 0.28	350			
				4.10 ± 0.68	297	FP-RA	Paraskevoupoulos et al.[260]	
				2.03 ± 0.15	247	DF-RF	Jeong and Kaufman[186,193]	247–483
				3.95 ± 0.26	293			
				6.68 ± 0.46	332			
				8.74 ± 0.58	363			
				12.8 ± 0.9	401			
				16.3 ± 1.3	426			
	2.21×10^{-9}	3.08 ± 1.26	460 ± 840	25.4 ± 2.0	483			
	3.04 ± 0.43		2510 ± 90					
CH_3Br				3.5 ± 0.8	296 ± 2	DF-LMR	Howard and Evenson[191]	
				2.01 ± 0.12	244	FP-RF	Davis et al.[259]	244–350
				3.16 ± 0.15	273			
				4.14 ± 0.43	298			
	0.793 ± 0.079		1766 ± 116	6.08 ± 0.40	350			
CH_2F_2				0.78 ± 0.12	296 ± 2	DF-LMR	Howard and Evenson[191]	
				0.58 ± 0.03	293	DF-RF	Clyne and Holt[261]	293–429
				1.61 ± 0.50	327			
				2.41 ± 0.35	368			
	$7.4^{+7.4}_{-3.7}$		4173 ± 397	6.03 ± 0.40	429			
				1.17 ± 0.14	297 ± 2	FP-RA	Nip et al.[257]	
				0.429 ± 0.038	250	DF-RF	Jeong and Kaufman[186,193]	250–492
				1.12 ± 0.075	298			
				2.10 ± 0.14	336			
				4.34 ± 0.27	384			
				7.27 ± 0.46	432			
				9.51 ± 0.66	464			
	2.52×10^{-9}	3.09 ± 1.32	1350 ± 910	14.1 ± 1.2	492			
	4.37 ± 0.58		3510 ± 100					
CH_2FCl				3.7 ± 0.6	296 ± 2	DF-LMR	Howard and Evenson[191]	
				1.65 ± 0.36	245	FP-RF	Watson et al.[262]	245–375
				4.21 ± 0.41	298			
	2.84 × 0.3		2502 ± 99	9.80 ± 0.34	375			
				2.8 ± 0.5	273	FP-RA	Handwerk and Zellner[263]	273–373

				3.5 ± 0.7	293			
	3.1 ± 0.9		2623 ± 199	11 ± 2	373			
				4.45 ± 0.66	297	FP-RA	Paraskevopoulos et al.[260]	
				2.76 ± 0.18	250	DF-RF	Jeong and Kaufman[186,193]	250–486
				4.94 ± 0.30	295			
				6.60 ± 0.40	323			
				8.85 ± 0.55	348			
				14.0 ± 0.9	399			
				17.2 ± 1.1	438			
	1.57×10^{-7}	2.41 ± 1.11	610 ± 760	25.4 ± 1.7	486			
	2.37 ± 0.29		2260 ± 80					
CH_2Cl_2				15.5 ± 3.4	296 ± 2	DF-LMR	Howard and Evenson[191]	
				14.5 ± 2.0	298.5	FP-RF	Perry et al.[258]	
				4.75 ± 0.57	245	FP-RF	Davis et al.[259]	245–375
				11.6 ± 0.5	298			
	4.27 ± 0.63		2174 ± 161	22.3 ± 0.5	375			
				9.59 ± 0.69	251	DF-RF	Jeong and Kaufman[186,193]	251–455
				15.3 ± 0.95	292			
				20.8 ± 1.4	323			
				27.6 ± 1.9	342			
				35.2 ± 2.4	384			
				45.0 ± 2.9	415			
	1.61×10^{-7}	2.54 ± 1.40	370 ± 980	60.9 ± 3.8	455			
	5.57 ± 0.77		2070 ± 90					
CHF_3				$0.02^{+0.02}_{-0.015}$	296 ± 2	DF-LMR	Howard and Evenson[191]	
				0.13 ± 0.04	296	DF-RF	Clyne and Holt[261]	296–430
				0.14 ± 0.06	430			
				0.035 ± 0.017	297 ± 2	FP-RA	Nip et al.[257]	
				0.169 ± 0.011	387	DF-RF	Jeong and Kaufman[186,193]	387–480
				0.237 ± 0.017	410			
				0.331 ± 0.027	428			
				0.448 ± 0.029	447			
				0.564 ± 0.036	465			
	2.98 ± 1.07		5780 ± 310	0.719 ± 0.045	480			
CHF_2Cl				0.475 ± 0.048	296.9	FP-RF	Atkinson et al.[264]	297–434
				1.15 ± 0.12	348.0			
	1.21		3250 ± 300	2.71 ± 0.27	433.7			
				0.34 ± 0.07	296 ± 2	DF-LMR	Howard and Evenson[191]	
				0.170 ± 0.040	250	FP-RF	Watson et al.[262]	250–350
				0.277 ± 0.038	273			
				0.48 ± 0.046	298			
	0.925 ± 0.10		3130 ± 141	1.01 ± 0.08	350			
				0.177 ± 0.002	253	DF-RF	Chang and Kaufman[265]	253–427
				0.425 ± 0.028	296			
				1.20 ± 0.03	358			
	1.20 ± 0.16		3292 ± 77	2.49 ± 0.10	427			
				0.20	263	FP-RA	Handwerk and Zellner[263]	263–373
				0.27	273			
				0.51	283			
				0.46 ± 0.08	293			
	2.1 ± 0.6		3537 ± 298	1.7 ± 0.3	373			
				0.33 ± 0.07	294	DF-RF	Clyne and Holt[261]	294–426
				0.77 ± 0.12	321			
				1.28 ± 0.11	343			
				1.97 ± 0.07	376			
				2.77 ± 0.17	391			

TABLE V (Continued)

haloalkane	$10^{12}A$, cm^3 molecule^{-1} s^{-1}	n	E, cal mol^{-1}	$10^{14}k$, cm^3 molecule^{-1} s^{-1}	T, K	technique	ref	temp range, covered, K
	$9.5^{+1.7}_{-1.4}$		4570 ± 397	3.90 ± 0.07	426			
				0.458 ± 0.058	297	FP-RA	Paraskevopoulos et al.[260]	
				0.483 ± 0.032	293	DF-RF	Jeong and Kaufman[186,193]	293–482
				0.768 ± 0.048	327			
				1.08 ± 0.075	360			
				1.79 ± 0.14	391			
				2.75 ± 0.18	436			
	5.03×10^{-16}	5.11 ± 2.09	−500 ± 1550	4.39 ± 0.27	482			
	1.27 ± 0.21		3300 ± 120					
$CHFCl_2$				2.6 ± 0.4	296 ± 2	DF-LMR	Howard and Evenson[191]	
				2.7 ± 0.3	298.4	FP-RF	Perry et al.[258]	298–422
				4.8 ± 0.5	349.5			
	1.75		2490 ± 300	9.1 ± 0.9	421.7			
				1.12 ± 0.12	245	FP-RF	Watson et al.[262]	245–375
				2.09 ± 0.18	273			
				2.88 ± 0.24	298			
	1.87 ± 0.2		2474 ± 52	6.68 ± 0.82	375			
				1.28 ± 0.25	241	DF-RF	Chang and Kaufman[265]	241–396
				1.73 ± 0.13	250			
				2.70 ± 0.20	288			
				3.04 ± 0.11	296			
				7.17 ± 0.16	380			
	1.16 ± 0.17		2132 ± 79	7.52 ± 0.29	396			
				3.54 ± 0.26	293	DF-RF	Clyne and Holt[261]	293–413
				6.57 ± 0.22	330			
				9.77 ± 0.38	373			
	$4.8^{+1.0}_{-0.8}$		2782 ± 199	15.2 ± 1.0	413			
				3.39 ± 0.86	297	FP-RA	Paraskevopoulos et al.[260]	
				1.88 ± 0.14	250	DF-RF	Jeong and Kaufman[186,193]	250–483
				3.37 ± 0.22	295			
				4.25 ± 0.27	315			
				5.85 ± 0.36	354			
				7.86 ± 0.48	392			
				10.5 ± 0.65	433			
	1.97×10^{-6}	1.94 ± 1.20	760 ± 820	14.8 ± 1.0	483			
	1.19 ± 0.15		2090 ± 90					
$CHCl_3$				10.1 ± 1.5	296 ± 2	DF-LMR	Howard and Evenson[191]	
				4.39 ± 0.28	245	FP-RF	Davis et al.[259]	245–375
				11.4 ± 0.7	298			
	4.69 ± 0.71		2254 ± 214	21.8 ± 1.4	375			
				5.51 ± 0.41	249	DF-RF	Jeong and Kaufman[186,193]	249–487
				10.1 ± 0.65	298			
				16.0 ± 1.0	339			
				23.2 ± 1.6	370			
				30.8 ± 2.0	411			
				44.8 ± 2.7	466			
	6.91×10^{-8}	2.65 ± 1.13	520 ± 790	55.0 ± 3.9	487			
	5.63 ± 0.68		2350 ± 90					

CF_4			<0.04	296 ± 2	DF-LMR	Howard and Evenson[191]	
			<0.1	293	DF-RF	Clyne and Holt[266]	
CF_3Cl			<0.07	296 ± 2	DF-LMR	Howard and Evenson[191]	
CF_3Br			<0.1	298	DF-EPR	Le Bras and Combourieu[267]	
CF_3I			12 ± 2	295	FP-RA	Garraway and Donovan[268]	
CF_2Cl_2			<0.1	297.3	FP-RF	Atkinson et al.[264]	297–424
			<0.1	342.9			
			<0.1	423.8			
			<0.04	296 ± 2	DF-LMR	Howard and Evenson[191]	
			<0.06	478	DF-RF	Chang and Kaufman[269]	298–478
			<0.1	293	DF-RF	Clyne and Holt[266]	
CF_2ClBr			<0.1	293	DF-RF	Clyne and Holt[266]	
$CFCl_3$			<0.1	296.8	FP-RF	Atkinson et al.[264]	297–424
			<0.1	347.7			
			<0.1	423.8			
			<0.05	296 ± 2	DF-LMR	Howard and Evenson[191]	
			<0.05	480	DF-RF	Chang and Kaufman[269]	381–480
			<0.1	293	DF-RF	Clyne and Holt[266]	
CCl_4			<0.4	296 ± 2	DF-LMR	Howard and Evenson[191]	
			<0.1	293	DF-RF	Clyne and Holt[266]	
CH_3CH_2F			23.2 ± 3.7	297 ± 2	FP-RA	Nip et al.[257]	
CH_3CH_2Cl			39.0 ± 7.0	296	DF-LMR	Howard and Evenson[196]	
			39.3 ± 5.3	297	FP-RA	Paraskevopoulos et al.[260]	
CH_3CHF_2			3.1 ± 0.7	296	DF-LMR	Howard and Evenson[196]	
			3.5 ± 0.5	293	FP-RA	Handwerk and Zellner[263]	
			4.66 ± 0.16	293	DF-RF	Clyne and Holt[261]	293–417
			7.16 ± 0.26	323			
			10.1 ± 0.8	363			
	$3.0^{+1.0}_{-0.8}$	2384 ± 199	16.4 ± 0.5	417			
			3.70 ± 0.37	297 ± 2	DF-RA	Nip et al.[257]	
CH_2FCH_2F			11.2 ± 1.2	298	FF-RA	Martin and Paraskevopoulos[270]	
CH_3CHCl_2			26.0 ± 6.0	296	DF-LMR	Howard and Evenson[196]	
CH_2ClCH_2Cl			22.0 ± 5.0	296	DF-LMR	Howard and Evenson[196]	
CH_2BrCH_2Br			25.0 ± 5.5	296	DF-LMR	Howard and Evenson[196]	
CH_3CF_3			<0.1	293	DF-RF	Clyne and Holt[261]	293–425
			0.47 ± 0.15	333			
			1.29 ± 0.35	378			
	69^{+105}_{-42}	6358 ± 994	3.84 ± 1.23	425			
			0.17 ± 0.04	298	FP-RA	Martin and Paraskevopoulos[270]	
CH_2FCHF_2			4.98 ± 0.82	293	DF-RF	Clyne and Holt[261]	293–441
			4.68 ± 0.40	294			
			6.74 ± 0.43	335			
			9.09 ± 0.42	383			
	$1.5^{+0.5}_{-0.4}$	1987 ± 199	18.9 ± 0.6	441			
			1.83 ± 0.18	298	FP-RA	Martin and Paraskevopoulos[270]	
CH_3CF_2Cl			0.283 ± 0.042	296	DF-LMR	Howard and Evenson[196]	
			0.192 ± 0.048	273	FP-RF	Watson et al.[262]	273–375
			0.322 ± 0.048	298			
	1.15 ± 0.15	3473 ± 60	1.09 ± 0.14	375			
			0.37 ± 0.07	293	FP-RA	Handwerk and Zellner[263]	293–373

TABLE V (Continued)

haloalkane	$10^{12}A$, cm^3 molecule^{-1} s^{-1}	n	E, cal mol^{-1}	$10^{14}k$, cm^3 molecule^{-1} s^{-1}	T, K	technique	ref	temp range, covered, K
	1.8 ± 0.5		3557 ± 298	1.4 ± 0.3	373			
				0.84 ± 0.18	293	DF-RF	Clyne and Holt[261]	293–417
				0.60 ± 0.07	293			
				1.20 ± 0.11	323			
				1.44 ± 0.37	363			
				3.09 ± 0.15	380			
	$3.3^{+4.3}_{-1.9}$		3577 ± 596	4.06 ± 0.27	417			
				0.463 ± 0.173	297	FP-RA	Paraskevopoulos et al.[260]	
CH_3CCl_3				1.5 ± 0.3	296	DF-LMR	Howard and Evenson[196]	
				0.712 ± 0.094	260	FP-RF	Watson et al.[262]	260–375
				1.59 ± 0.16	298			
	3.72 ± 0.4		3233 ± 99	4.85 ± 0.58	375			
				1.55 ± 0.22	275	DF-RF	Chang and Kaufman[265]	275–405
				2.19 ± 0.26	298			
				3.03 ± 0.30	320			
				4.94 ± 0.48	355			
	1.95 ± 0.24		2645 ± 74	6.87 ± 0.40	405			
				1.81 ± 0.16	293	DF-RF	Clyne and Holt[266]	293–430
				2.78 ± 0.74	310			
				4.59 ± 0.56	338			
				5.73 ± 0.51	371			
				7.29 ± 0.44	399			
	$2.4^{+0.9}_{-0.7}$		2770 ± 225	8.63 ± 0.40	430			
				0.83 ± 0.07	278	DF-RF	Jeong and Kaufman[71] and Jeong et al.[186]	278–457
				1.06 ± 0.11	293			
				2.93 ± 0.19	352			
				5.52 ± 0.41	400			
	5.95 × 10^{-8}	2.65 ± 2.44	1705 ± 1720	10.2 ± 0.65	457			
	5.04 ± 0.96		3570 ± 130					
				0.318 ± 0.095	222	FP-RF	Kurylo et al.[72]	222–363
				0.447 ± 0.135	253			
				0.540 ± 0.145	263			
				1.08 ± 0.20	296			
	5.4 ± 1.8		3596 ± 199 (253–363 K)	3.85 ± 0.75	363			
$CH_2ClCHCl_2$				28.4 ± 2.1	277	DF-RF	Jeong and Kaufman[71] and Jeong et al.[186]	277–461
				31.8 ± 2.0	295			
				37.6 ± 2.3	322			
				43.6 ± 2.8	346			
				46.8 ± 2.9	386			
				49.2 ± 3.1	400			
				52.7 ± 3.5	424			
	6.84 × 10^{-3}	1.21 ± 1.91	1800 ± 1340	57.6 ± 3.7	461			
	1.65 ± 0.27		960 ± 110					
CH_2FCF_3				0.55 ± 0.07	294	DF-RF	Clyne and Holt[261]	294–429
				1.32 ± 0.10	327			
				1.64 ± 0.31	344			
				1.92 ± 0.08	358			
				3.83 ± 0.49	393			
				4.20 ± 0.47	424			

	$3.2^{+2.3}_{-1.3}$		3577 ± 397	3.64 ± 0.38	429			
				0.515 ± 0.058	298	FP-RA	Martin and Paraskevopoulos[270]	
				0.393 ± 0.024	249	DF-RF	Jeong et al.[186]	249–473
				0.441 ± 0.040	250			
				0.552 ± 0.035	268			
				0.773 ± 0.071	291			
				0.823 ± 0.055	295			
				0.844 ± 0.073	298			
				1.54 ± 0.12	342			
				2.54 ± 0.17	380			
				3.94 ± 0.26	430			
				4.56 ± 0.29	447			
	1.22×10^{-13}	4.36 ± 1.14	−90 ± 770	6.44 ± 0.40	473			
	1.10 ± 0.11		2830 ± 70					
CHF_2CHF_2				0.53 ± 0.15	294	DF-RF	Clyne and Holt[261]	294–434
				1.88 ± 0.27	333			
				2.12 ± 0.41	389			
	$2.8^{+6.5}_{-2.0}$		3577 ± 795	4.82 ± 0.36	434			
CH_2ClCF_3				1.05 ± 0.23	296	DF-LMR	Howard and Evenson[196]	
				1.1 ± 0.2	263	FP-RA	Handwerk and Zellner[263]	263–373
				1.2 ± 0.2	268			
				1.2 ± 0.2	273			
				1.5 ± 0.3	283			
				1.5 ± 0.3	293			
				2.8	337			
	1.1 ± 0.3		2504 ± 119	3.6 ± 0.8	373			
				1.03 ± 0.30	294	DF-RF	Clyne and Holt[261]	294–427
				3.83 ± 0.57	322			
				3.86 ± 0.31	344			
				6.94 ± 0.33	358			
				6.58 ± 0.25	385			
				13.0 ± 1.2	407			
	39^{+46}_{-21}		4570 ± 596	15.4 ± 1.3	427			
CH_2ClCF_2Cl				0.839 ± 0.037	250	FP-RF	Watson et al.[271]	250–350
				1.9 ± 0.2	298			
	1.87 ± 0.27		2684 ± 155	3.95 ± 0.10	350			
	3^{+6}_{-1}		3135^{+795}_{-457}[a]					
				1.42 ± 0.11	249	DF-RF	Jeong et al.[186]	249–473
				1.60 ± 0.10	253			
				1.91 ± 0.16	267			
				2.72 ± 0.18	295			
				2.42 ± 0.16	297			
				4.31 ± 0.28	333			
				5.95 ± 0.37	365			
				8.06 ± 0.51	383			
				10.4 ± 0.65	418			
	2.97×10^{-13}	4.58 ± 1.13	−500 ± 750	16.0 ± 1.15	473			
	2.02 ± 0.24		2510 ± 70					

TABLE V (Continued)

haloalkane	$10^{12}A$, cm^3 molecule^{-1} s^{-1}	n	E, cal mol^{-1}	$10^{14}k$, cm^3 molecule^{-1} s^{-1}	T, K	technique	ref	temp range, covered, K
CHF_2CF_3				0.50 ± 0.22	294	DF-RF	Clyne and Holt[261]	294–441
				0.49 ± 0.14	294			
				0.62 ± 0.18	336			
				1.13 ± 0.33	378			
	$0.17^{+0.10}_{-0.06}$		2186 ± 199	1.58 ± 0.29	441			
				0.249 ± 0.028	298	FP-RA	Martin and Paraskevopoulos[270]	
$CHFClCF_3$				1.24 ± 0.19	296	DF-LMR	Howard and Evenson[196]	
				0.433 ± 0.019	250	FP-RF	Watson et al.[271]	250–375
				0.94 ± 0.03	301			
	0.613 ± 0.04		2472 ± 179	2.28 ± 0.16	375			
$CHCl_2CF_3$				2.84 ± 0.43	296	DF-LMR	Howard and Evenson[196]	
				1.62 ± 0.05	245	FP-RF	Watson et al.[271]	245–375
				3.6 ± 0.4	298			
	1.24 ± 0.3		2098 ± 139	7.2 ± 0.35	375			
	(1.4 ± 0.4)		2190^{+312}_{-211} [a]					
				3.86 ± 0.19	293	DF-RF	Clyne and Holt[261]	293–429
				5.86 ± 0.15	329			
				8.01 ± 0.33	366			
	1.12 ± 0.05		1987 ± 199	11.1 ± 0.4	429			
CF_2ClCF_2Cl				<0.05	296	DF-LMR	Howard and Evenson[196]	
$CF_2ClCFCl_2$				<0.03	296	DF-LMR	Howard and Evenson[196]	
				<0.03	298	FP-RF	Watson et al.[262]	
$CH_2ClCHClCH_3$				≤44	~296	rel rate [rel to k(OH + dimethyl ether = 2.96×10^{-12}][b]	Tuazon et al.[272]	
$CH_2BrCHBrCH_2Cl$				44 ± 6	296 ± 2	rel rate [rel to k(OH + dimethyl ether = 2.96×10^{-12}][b]	Tuazon et al.[273]	

[a] Arrhenius expression estimated after allowance for possible contributions to the observed OH radical decay rates from the observed impurity levels present[271] (see text). [b] From the recommendation.

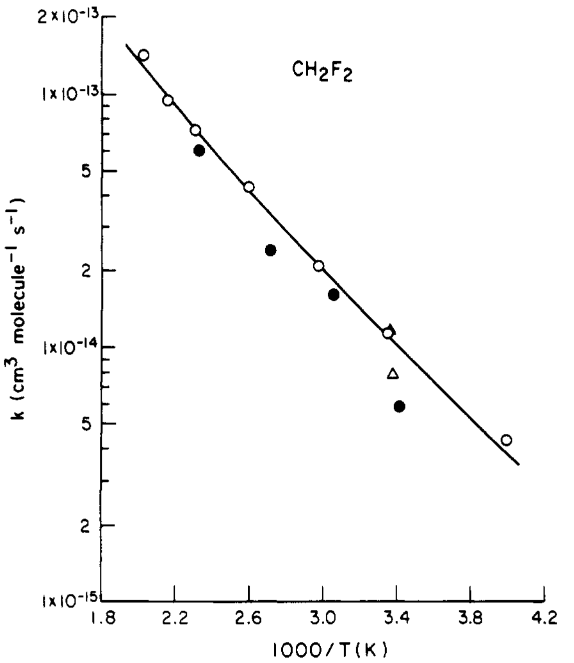

Figure 17. Arrhenius plot of the rate constants for the reaction of OH radicals with CH_2F_2: (△) Howard and Evenson;[191] (●) Clyne and Holt;[261] (▲) Nip et al.;[257] (○) Jeong and Kaufman;[193] (—) recommendation (see text).

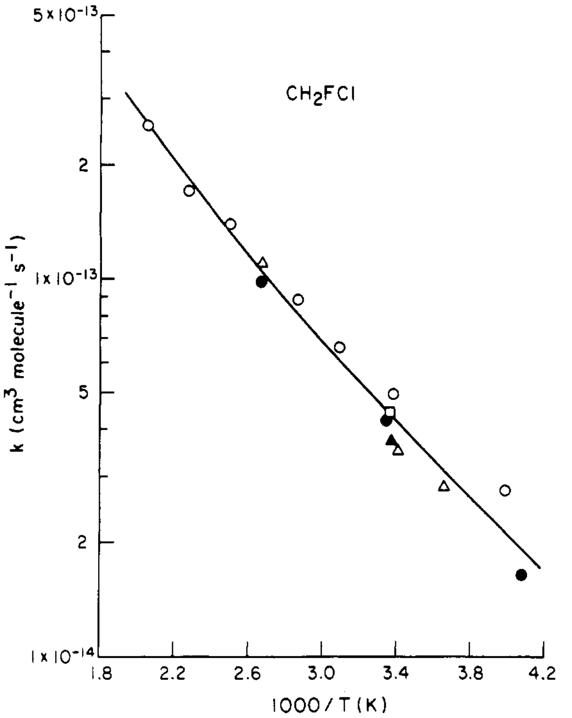

Figure 18. Arrhenius plot of the rate constants for the reaction of OH radicals with CH_2FCl: (▲) Howard and Evenson;[191] (●) Watson et al.;[262] (△) Handwerk and Zellner;[263] (□) Paraskevopoulos et al.;[260] (○) Jeong and Kaufman;[193] (—) recommendation (see text).

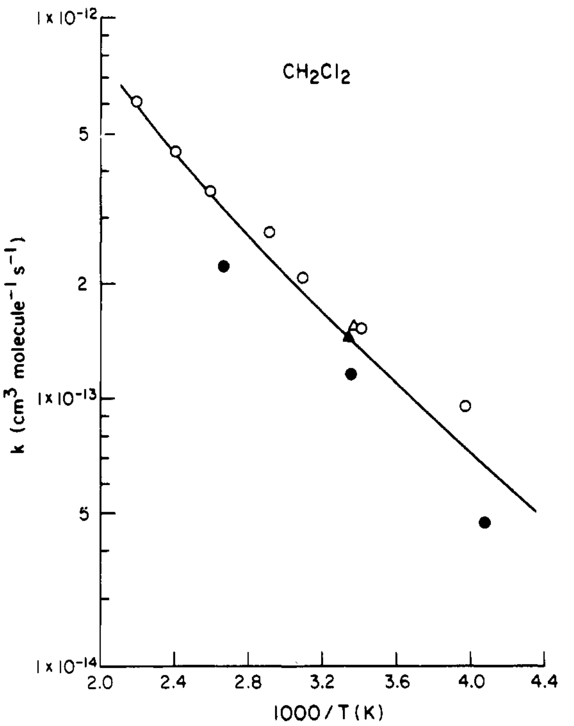

Figure 19. Arrhenius plot of the rate constants for the reaction of OH radicals with CH_2Cl_2: (△) Howard and Evenson;[191] (▲) Perry et al.;[258] (●) Davis et al.;[259] (○) Jeong and Kaufman;[193] (—) recommendation (see text).

e. CH_2FCl. The available rate constants[191,193,260,262,263] are listed in Table V and plotted in Arrhenius form in Figure 18. The rate constants from the studies of Howard and Evenson,[191] Watson et al.,[262] Handwerk and Zellner,[263] Paraskevopoulos et al.,[260] and Jeong and Kaufman[193] are in reasonably good agreement, though there is a significant discrepancy between the rate constants obtained by Watson et al.[262] and by Jeong and Kaufman[193] at ~250 K. Although it is not obvious from Figure 18 whether or not the Arrhenius plot exhibits curvature, a unit-weighted least-squares analysis of these data has been carried out, using the equation $k = A'T^2e^{-E'/RT}$, to yield the recommended expression

$$k(CH_2FCl) =$$

$$(3.77^{+1.65}_{-1.15}) \times 10^{-18}T^2e^{-(604\pm115)/T}\ \text{cm}^3\ \text{molecule}^{-1}\ \text{s}^{-1}$$

where the error limits are two least-squares standard deviations

$$k(CH_2FCl) =$$

$$4.41 \times 10^{-14}\ \text{cm}^3\ \text{molecule}^{-1}\ \text{s}^{-1}\ \text{at 298 K}$$

with an estimated uncertainty at 298 K of ±20%. This recommendation is identical with that of the recent NASA evaluation.[30]

f. CH_2Cl_2. The available kinetic data[191,193,258,259] are listed in Table V and plotted in Arrhenius form in Figure 19. While the room-temperature rate constants of Howard and Evenson,[191] Perry et al.,[258] and Jeong and Kaufman[193] are in excellent agreement, the rate constants obtained by Davis et al.[259] are uniformly lower than those of Jeong and Kaufman[193] by ~20–40% over the temperature range common to both studies. However, a unit-weighted least-squares analysis of the data from all four of these studies[191,193,258,259] was carried out, using the equation $k = A'T^2e^{-E'/RT}$, to derive the recommended expression

$$k(CH_2Cl_2) =$$

$$(8.54^{+8.18}_{-4.18}) \times 10^{-18}T^2e^{-(500\pm212)/T}\ \text{cm}^3\ \text{molecule}^{-1}\ \text{s}^{-1}$$

where the error limits are two least-squares standard deviations

$$k(CH_2Cl_2) =$$

$$1.42 \times 10^{-13}\ \text{cm}^3\ \text{molecule}^{-1}\ \text{s}^{-1}\ \text{at 298 K}$$

with an estimated uncertainty at 298 K of ±25%. This recommendation is virtually identical with that of the

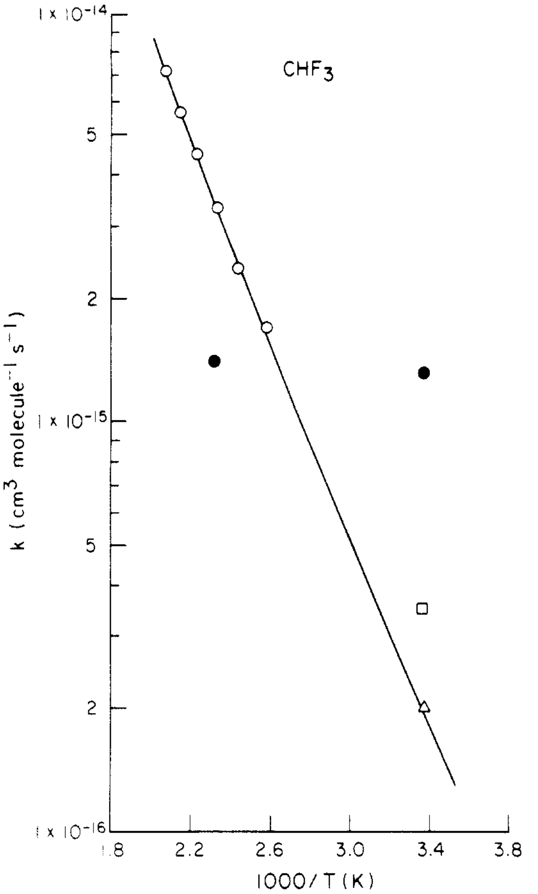

Figure 20. Arrhenius plot of the rate constants for the reaction of OH radicals with CHF_3: (△) Howard and Evenson;[191] (●) Clyne and Holt;[261] (□) Nip et al.;[257] (○) Jeong and Kaufman;[186,193] (—) recommendation (see text).

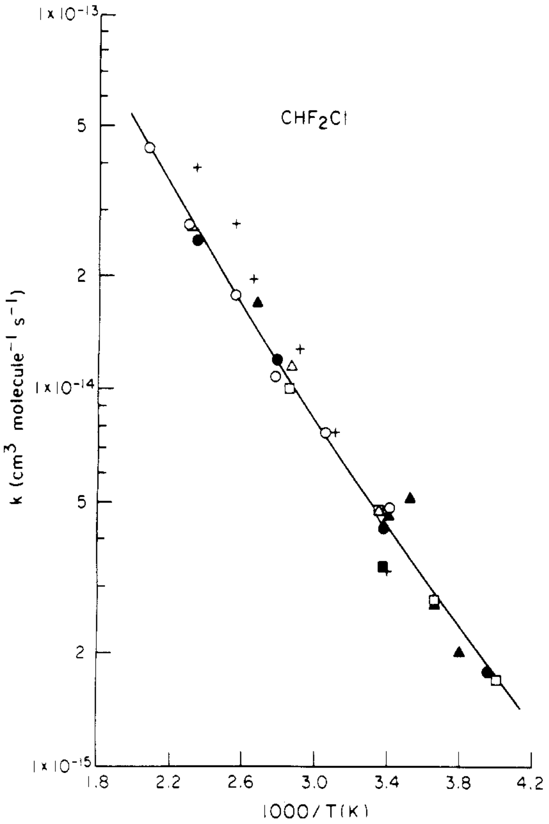

Figure 21. Arrhenius plot of the rate constants for the reaction of OH radicals with CHF_2Cl: (△) Atkinson et al.;[264] (■) Howard and Evenson;[191] (□) Watson et al.;[262] (●) Chang and Kaufman;[265] (▲) Handwerk and Zellner;[263] (+) Clyne and Holt;[261] (▽) Paraskevopoulos et al.;[260] (○) Jeong and Kaufman;[193] (—) recommendation (see text).

recent NASA evaluation,[30] but with slightly higher estimated uncertainty limits at 298 K.

g. CHF_3. The available rate constants[186,191,193,257,261] are listed in Table V and plotted in Arrhenius form in Figure 20. The reaction of OH radicals with CHF_3 is seen to be very slow at room temperature, and the rate constants determined by Howard and Evenson[191] and Nip et al.[257] are subject to large uncertainties. This appears to be also true for the rate constants reported by Clyne and Holt,[261] since their data show no significant effect of temperature and differ by factors of >2 from the other literature data. In view of the significant uncertainties associated with the rate constants measured by Howard and Evenson[191] and Nip et al.,[257] a unit-weighted least-squares analysis of the data of Jeong and Kaufman[186,193] has been carried out, using the equation $k = A'T^2e^{-E'/RT}$, to yield the recommended expression

$$k(CHF_3) =$$
$$(2.1^{+0.88}_{-0.62}) \times 10^{-18}T^2e^{-(2048\pm148)/T} \text{ cm}^3 \text{ molecule}^{-1} \text{ s}^{-1}$$

where the errors are two least-squares standatd deviations

$k(CHF_3) = 2.0 \times 10^{-16}$ cm^3 molecule^{-1} s^{-1} at 298 K with an estimated uncertainty at 298 K of ±50%. This recommended expression yields a rate constant at 296 K in excellent (though no doubt fortuitous) agreement with that measured by Howard and Evenson[191] and in agreement, within the error limits, with that of Nip et al.[257] Since this recommendation is based upon data obtained over the limited temperature range 387–480 K, it should be used with caution for temperatures $\lesssim$300 K.

h. CHF_2Cl. The available rate constants[191,193,260–265] are listed in Table V and plotted in Figure 21. It can be seen that the rate constants of Atkinson et al.,[264] Howard and Evenson,[191] Watson et al.,[262] Chang and Kaufman,[265] Handwerk and Zellner,[263] Paraskevopoulos et al.,[260] and Jeong and Kaufman[193] are in good agreement. While the rate constants measured by Clyne and Holt[261] agree well with those studies at ~294–321 K, their rate constants at higher temperatures are increasingly higher than the consensus values from these other studies.[191,193,260,262–265] A unit-weighted least-squares analysis of the rate constant data of Atkinson et al.,[264] Howard and Evenson,[191] Watson et al.,[262] Chang and Kautman,[265] Handwerk and Zellner,[263] Paraskevopoulos et al.,[260] and Jeong and Kaufman[193] yields the recommended expression

$$k(CHF_2Cl) =$$
$$(1.51^{+0.51}_{-0.39}) \times 10^{-18}T^2e^{-(1000\pm94)/T} \text{ cm}^3 \text{ molecule}^{-1} \text{ s}^{-1}$$

where the error limits are two least-squares standard deviations

$$k(CHF_2Cl) =$$
$$4.68 \times 10^{-15} \text{ cm}^3 \text{ molecule}^{-1} \text{ s}^{-1} \text{ at 298 K}$$

with an estimated uncertainty at 298 K of ±20%.

i. $CHFCl_2$. The available rate constants[191,193,258,260–262,265] are listed in Table V and plotted in Arrhenius form in Figure 22. Analogous to CHF_2Cl,

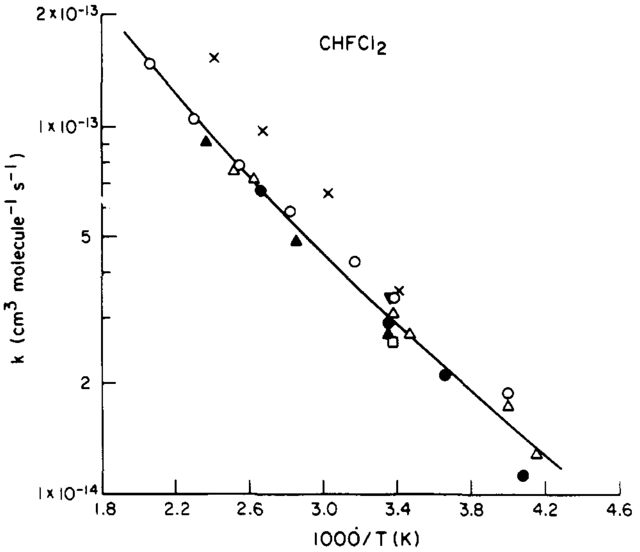

Figure 22. Arrhenius plot of the rate constants for the reaction of OH radicals with $CHFCl_2$: (□) Howard and Evenson;[191] (▲) Perry et al.;[258] (●) Watson et al.;[262] (△) Chang and Kaufman,[265] (×) Clyne and Holt;[261] (▼) Paraskevopoulos et al.;[260] (○) Jeong and Kaufman;[193] (—) recommendation (see text).

the rate constants measured by Clyne and Holt[261] at elevated temperatures are significantly higher than those of Howard and Evenson,[191] Perry et al.,[258] Watson et al.,[262] Chang and Kaufman,[265] Paraskevopoulos et al.,[260] and Jeong and Kaufman,[193] all of which are in reasonably good agreement. A unit-weighted least-squares analysis of these latter data[191,193,258,260,262,265] yields the recommended expression

$$k(CHFCl_2) = (1.70^{+0.47}_{-0.37}) \times 10^{-18}T^2e^{-(479\pm76)/T}\ \mathrm{cm^3\ molecule^{-1}\ s^{-1}}$$

where the error limits are two least-squares standard deviations

$$k(CHFCl_2) = 3.03 \times 10^{-14}\ \mathrm{cm^3\ molecule^{-1}\ s^{-1}\ at\ 298\ K}$$

with an estimated uncertainty at 298 K of ±20%. This recommendation is essentially identical with that of the recent NASA evaluation.[30]

j. $CHCl_3$. The available kinetic data[191,193,259] are listed in Table V and plotted in Arrhenius form in Figure 23. It can be seen that these rate constants of Howard and Evenson,[191] Davis et al.,[259] and Jeong and Kaufman[193] are in excellent agreement, and a unit-weighted least-squares analysis of these data yields the recommended expression

$$k(CHCl_3) = (6.30^{+1.17}_{-1.00}) \times 10^{-18}T^2e^{-(504\pm56)/T}\ \mathrm{cm^3\ molecule^{-1}\ s^{-1}}$$

where the error limits are two least-squares standard deviations

$$k(CHCl_3) = 1.03 \times 10^{-13}\ \mathrm{cm^3\ molecule^{-1}\ s^{-1}\ at\ 298\ K}$$

with an estimated uncertainty at 298 K of ±20%.

This recommendation is identical with that of the recent NASA evaluation.[30]

k. CH_3CH_2Cl. The rate constants obtained by Howard and Evenson[196] and Paraskevopoulos et al.[260] at room temperature are in excellent agreement, and it is recommended that

$$k(CH_3CH_2Cl) = 4.0 \times 10^{-13}\ \mathrm{cm^3\ molecule^{-1}\ s^{-1}\ at\ 298\ K}$$

with an estimated uncertainty of ±30%. No temperature dependence is available.

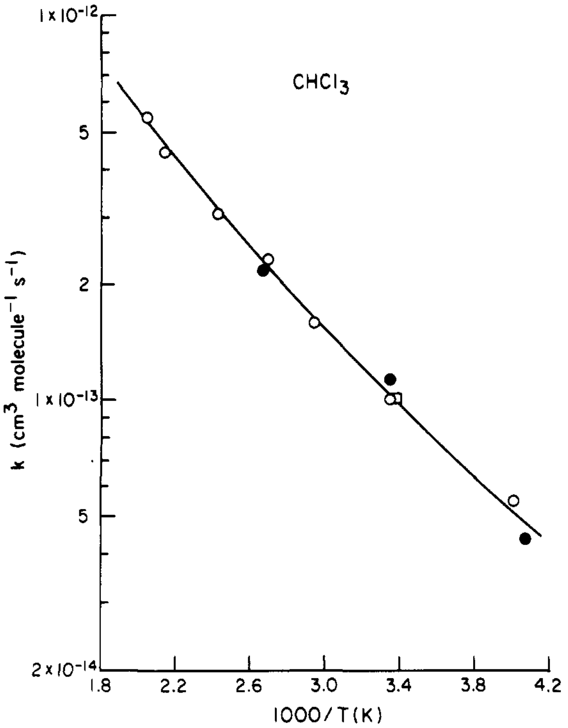

Figure 23. Arrhenius plot of the rate constants for the reaction of OH radicals with $CHCl_3$: (□) Howard and Evenson;[191] (●) Davis et al.;[259] (○) Jeong and Kaufman;[193] (—) recommendation (see text).

l. CH_3CHF_2. Rate constants have been determined for the reaction of OH radicals with CH_3CHF_2 by Howard and Evenson,[196] Handwerk and Zellner,[263] Clyne and Holt,[261] and Nip et al.[257] The rate constants of Howard and Evenson,[196] Handwerk and Zellner,[263] and Nip et al.[257] are in reasonable agreement but are significantly lower than the room-temperature rate constant of Clyne and Holt.[261] Since the data of Clyne and Holt[261] are neglected in these evaluations, it is recommended that

$$k(CH_3CHF_2) = 3.4 \times 10^{-14}\ \mathrm{cm^3\ molecule^{-1}\ s^{-1}\ at\ {\sim}295\ K}$$

with an estimated uncertainty of ±30%.

m. CH_3CF_2Cl. The available rate constants[196,260-263] are listed in Table V and plotted in Arrhenius form in Figure 24. It is evident that the rate constants of Howard and Evenson,[196] Watson et al.,[262] Handwerk and Zellner,[263] and Paraskevopoulos et al.[260] are in reasonably good agreement, though significantly lower than those measured by Clyne and Holt.[261] A unit-weighted least-squares analysis of these data of Howard and Evenson,[196] Watson et al.,[262] Handwerk and Zellner,[263] and Paraskevopoulos et al.[260] yields the recommended expression

$$k(CH_3CF_2Cl) = (2.05^{+5.75}_{-1.51}) \times 10^{-18}T^2e^{-(1171\pm413)/T}\ \mathrm{cm^3\ molecule^{-1}\ s^{-1}}$$

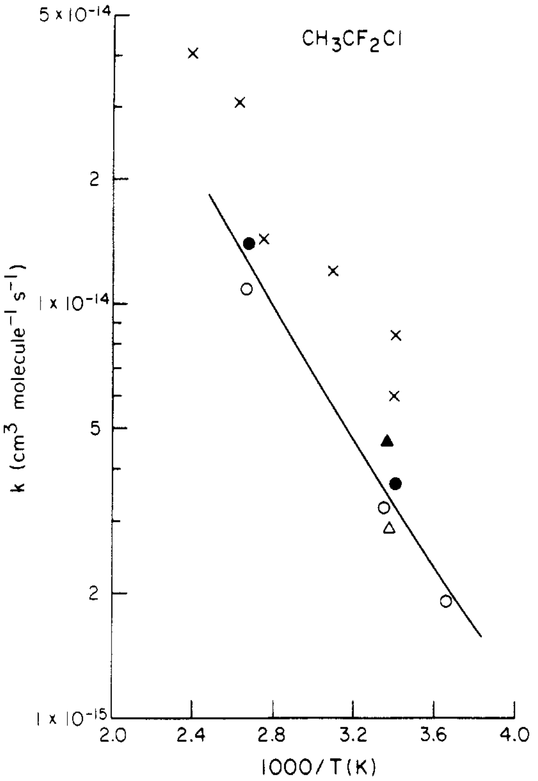

Figure 24. Arrhenius plot of the rate constants for the reaction of OH radicals with CH_3CF_2Cl: (△) Howard and Evenson;[196] (○) Watson et al.;[262] (●) Handwerk and Zellner;[263] (×) Clyne and Holt;[261] (▲) Paraskevopoulos et al.;[260] (—) recommendation (see text).

where the errors are two least-squares standard deviations

$$k(CH_3CF_2Cl) = 3.58 \times 10^{-15} \text{ cm}^3 \text{ molecule}^{-1} \text{ s}^{-1} \text{ at } 298 \text{ K}$$

with an estimated uncertainty at 298 K of ±50%.

n. CH_3CCl_3. The available kinetic data are listed in Table V. As discussed previously,[30,71,72] it now appears that the earlier rate constants determined by Howard and Evenson,[196] Watson et al.,[262] Chang and Kaufman,[265] and Clyne and Holt,[266] which yield a room-temperature rate constant of ~(1.5–2.2) × 10^{-14} cm^3 $molecule^{-1}$ s^{-1} and an Arrhenius activation energy of ~2.6–3.2 kcal mol^{-1}, were erroneously high due to contamination by small amounts of highly reactive (relative to CH_3CCl_3) $CH_2{=}CCl_2$ impurity. The most recent studies of Jeong and Kaufman[71,186] and Kurylo et al.,[72] in which the CH_3CCl_3 samples were extensively purified, are in excellent agreement and yield significantly lower rate constants than did these previous studies.[196,262,265,266] The rate constant measured by Kurylo et al.[72] at 222 K, which is significantly higher than expected by extrapolation of the higher temperature data,[71,72,186] may still have been affected by $CH_2{=}CCl_2$ impurity problems.[72]

Thus, only the data of Jeong and Kaufman[71,186] and those of Kurylo et al.[72] at ≥253 K (which are plotted in Figure 25) are used in the evaluation. A unit-weighted least-squares analysis of these data yields the recommended expression

$$k(CH_3CCl_3) = (5.92^{+1.28}_{-1.05}) \times 10^{-18}T^2e^{-(1129\pm71)/T} \text{ cm}^3 \text{ molecule}^{-1} \text{ s}^{-1}$$

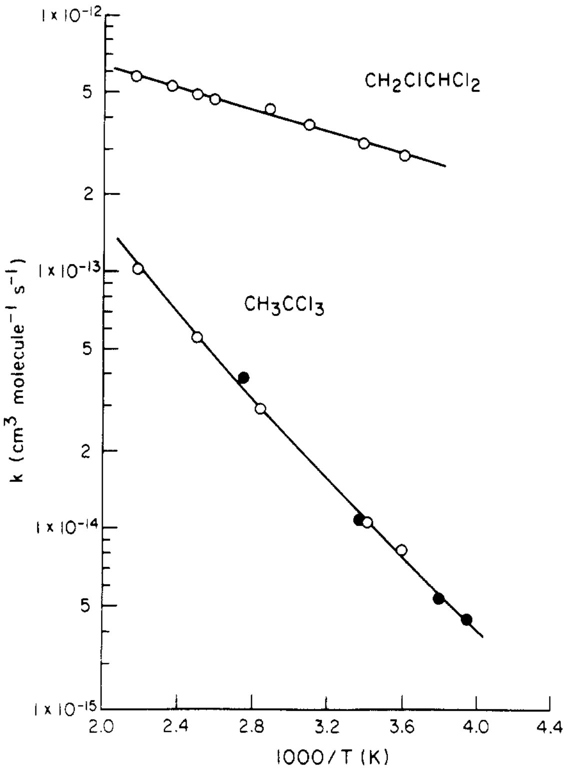

Figure 25. Arrhenius plot of the rate constants for the reaction of OH radicals with CH_3CCl_3 and $CH_2ClCHCl_2$: (○) Jeong and Kaufman;[71,186] (●) Kurylo et al.[72] (the rate constant at 222 K has been neglected[72]); (—) recommendations (see text).

where the errors are two least-squares standard deviations

$$k(CH_3CCl_3) = 1.19 \times 10^{-14} \text{ cm}^3 \text{ molecule}^{-1} \text{ s}^{-1} \text{ at } 298 \text{ K}$$

with an estimated uncertainty at 298 K of ±20%. This recommendation, though using the same data set as the recent NASA evaluation,[30] utilizes the equation $k = A'T^2e^{-E'/RT}$ rather than the simple Arrhenius expression.[30]

o. $CH_2ClCHCl_2$. The sole reported rate constants for this reaction are those of Jeong and Kaufman,[71,186] and these are plotted in Arrhenius form in Figure 25. These data yield an excellent straight line Arrhenius plot of

$$k(CH_2ClCHCl_2) = (1.66^{+0.21}_{-0.19}) \times 10^{-12}e^{-(483\pm43)/T} \text{ cm}^3 \text{ molecule}^{-1} \text{ s}^{-1}$$

where the errors are two least-squares standard deviations

$$k(CH_2ClCHCl_2) = 3.28 \times 10^{-13} \text{ cm}^3 \text{ molecule}^{-1} \text{ s}^{-1} \text{ at } 298 \text{ K}$$

with an estimated uncertainty at 298 K of ±25%. With use of the alternative equation $k = A'T^2e^{-E'/RT}$, a unit-weighted least-squares analysis yields

$$k(CH_2ClCHCl_2) = (1.77^{+0.42}_{-0.34}) \times 10^{-18}T^2e^{(219\pm74)/T} \text{ cm}^3 \text{ molecule}^{-1} \text{ s}^{-1}$$

where the errors are two least-squares standard deviations, and

$$k(CH_2ClCHCl_2) = 3.28 \times 10^{-13} \text{ cm}^3 \text{ molecule}^{-1} \text{ s}^{-1} \text{ at } 298 \text{ K}$$

identical with that derived from the simple Arrhenius

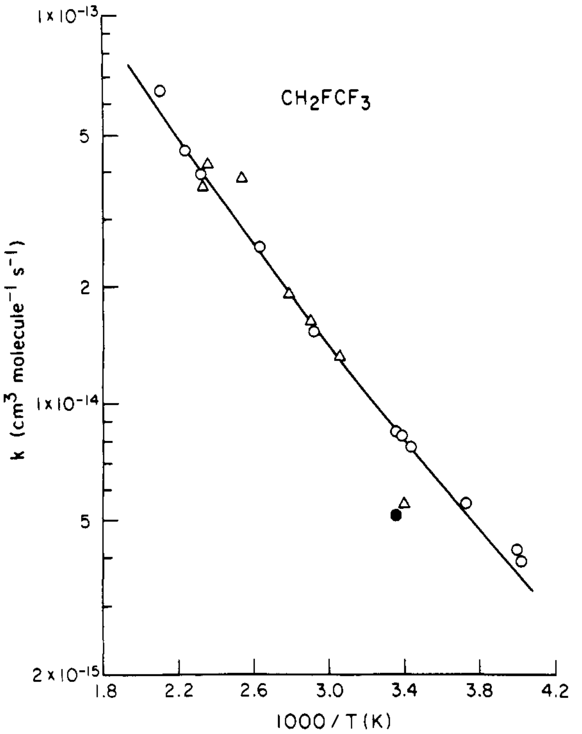

Figure 26. Arrhenius plot of the rate constants for the reaction of OH radicals with CH_2FCF_3: (△) Clyne and Holt;[261] (●) Martin and Paraskevopoulos;[270] (○) Jeong and Kaufman;[186] (—) recommendation (see text).

expression. Since this more complex equation yields a worse fit to the experimental data, the simple Arrhenius expression given above is recommended for use over the limited temperature range studied (277–461 K). This Arrhenius line is plotted in Figure 25.

p. CH_2FCF_3. The available kinetic data[186,261,270] are listed in Table V and plotted in Arrhenius form in Figure 26. The rate constant of Martin and Paraskevopoulos[270] at 298 K is significantly lower than that of Jeong et al.[186] (though it is in agreement with that of Clyne and Holt[261]). However, in view of the above discussion regarding the criteria for evaluating these reactions, the rate constants determined by Clyne and Holt[261] are neglected. A unit-weighted least-squares fit of the data of Martin and Paraskevopoulos[270] and Jeong et al.,[186] to the expression $k = A'T^2e^{-E'/RT}$, yields the recommendation

$$k(CH_2FCF_3) = (1.27^{+1.07}_{-0.51}) \times 10^{-18}T^2e^{-(769\pm163)/T} \text{ cm}^3 \text{ molecule}^{-1} \text{ s}^{-1}$$

where the errors are two least-squares standard deviations

$$k(CH_2FCF_3) = 8.54 \times 10^{-15} \text{ cm}^3 \text{ molecule}^{-1} \text{ s}^{-1} \text{ at } 298 \text{ K}$$

with an estimated uncertainty at 298 K of +20%, −40%.

q. CH_2ClCF_3. The available rate constants[196,261,263] are listed in Table V and plotted in Arrhenius form in Figure 27. Again, the rate constants of Clyne and Holt[261] exhibit a much higher temperature dependence than do those of Handwerk and Zellner.[263] Hence, from a unit-weighted least-squares analysis of the rate constant data of Howard and Evenson[196] and Handwerk and Zellner,[263] the recommended expression

$$k(CH_2ClCF_3) = (8.50^{+20.74}_{-6.03}) \times 10^{-19}T^2e^{-(458\pm326)/T} \text{ cm}^3 \text{ molecule}^{-1} \text{ s}^{-1}$$

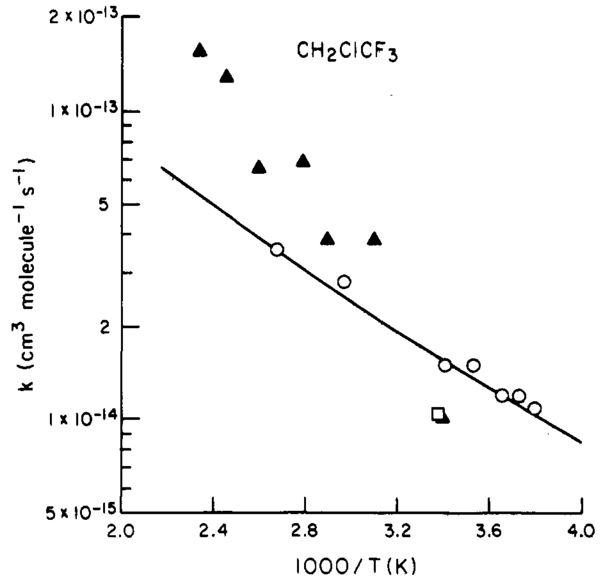

Figure 27. Arrhenius plot of the rate constants for the reaction of OH radicals with CH_2ClCF_3: (□) Howard and Evenson;[196] (○) Handwerk and Zellner;[263] (▲) Clyne and Holt;[261] (—) recommendation (see text).

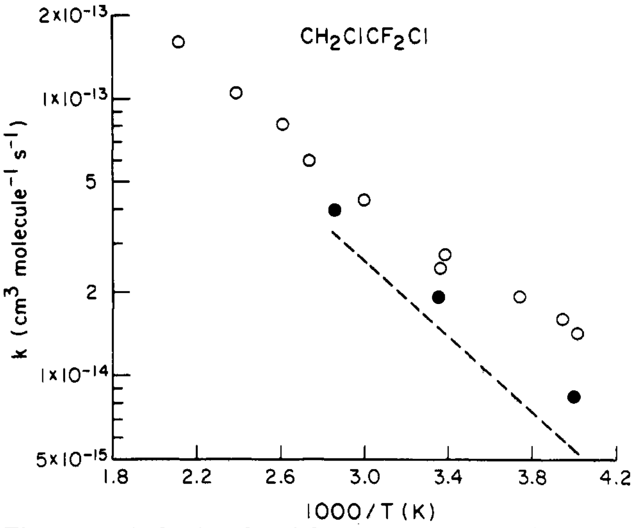

Figure 28. Arrhenius plot of the rate constants for the reaction of OH radicals with CH_2ClCF_2Cl: (●) Observed rate constants of Watson et al.;[271] (- - -) rate constants of Watson et al.[271] after correction for presence of observed impurities[271] (see text); (○) Jeong et al.[186]

is obtained, where the errors are two least-squares standard deviations,

$$k(CH_2ClCF_3) = 1.62 \times 10^{-14} \text{ cm}^3 \text{ molecule}^{-1} \text{ s}^{-1} \text{ at } 298 \text{ K}$$

with an estimated uncertainty at 298 K of ± a factor of 2.

r. CH_2ClCF_2Cl. The available rate constants[186,271] are listed in Table V and plotted in Arrhenius form in Figure 28. It can be seen that the measured rate constants of Watson et al.[271] are consistently lower than those of Jeong et al.,[186] especially at lower temperatures. Furthermore, Watson et al.,[271] from an analysis of the purity of the CH_2ClCF_2Cl sample used, concluded that the true rate constants for this reaction were lower than those measured, and their estimated Arrhenius expression, after correction for the presence of these impurities, is shown in Figure 28 as the dashed line.

In view of the discrepancies between these data sets,

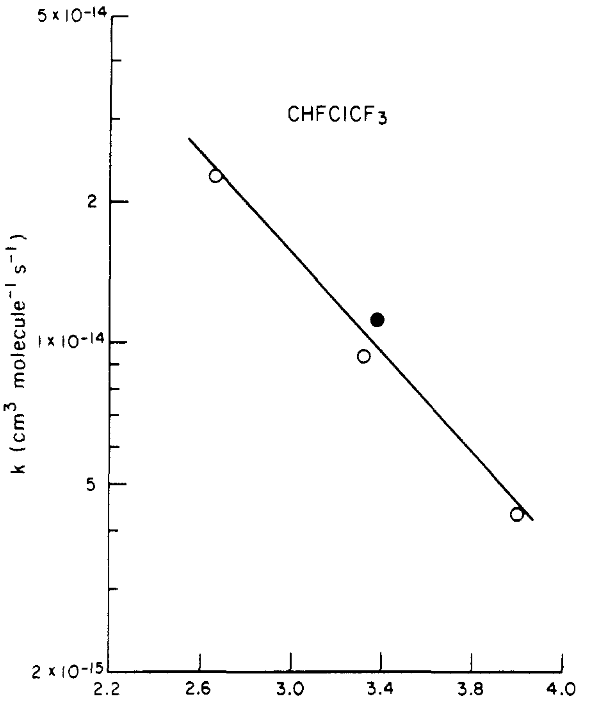

Figure 29. Arrhenius plot of the rate constants for the reaction of OH radicals with $CHFClCF_3$: (●) Howard and Evenson;[196] (○) Watson et al.;[271] (—) recommendation (see text).

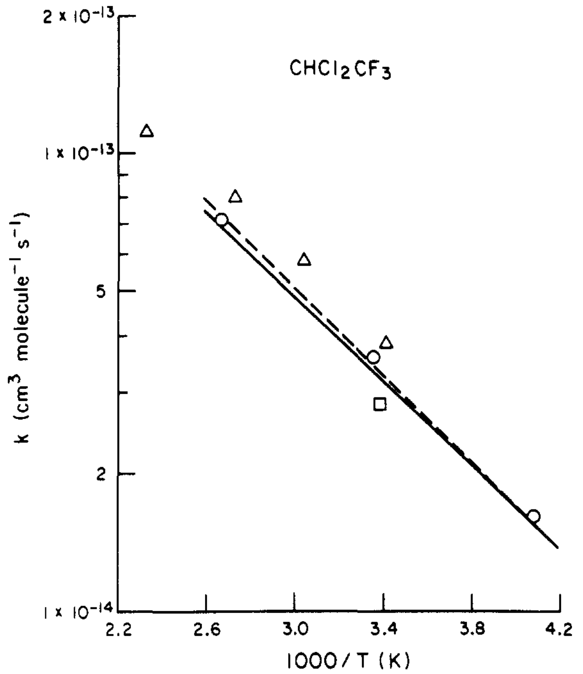

Figure 30. Arrhenius plot of the rate constants for the reaction of OH radicals with $CHCl_2CF_3$: (□) Howard and Evenson;[196] (○) observed rate constants of Watson et al.;[271] (- - -) rate constants of Watson et al.[271] after correction for presence of observed impurities[271] (see text); (△) Clyne and Holt;[261] (—) recommendation (see text).

no recommendation for the rate constants for this reaction is made, except to recommend that further experimental work be carried out.

s. $CHFClCF_3$. The rate constants of Howard and Evenson[196] and Watson et al.[271] are listed in Table V and plotted in Arrhenius form in Figure 29. These two studies are in good agreement, and a unit-weighted least-squares analysis of these data yields the recommended Arrhenius expression

$$k(CHFClCF_3) = (6.38^{+18.14}_{-4.72}) \times 10^{-13} e^{-(1233\pm399)/T} \text{ cm}^3 \text{ molecule}^{-1} \text{ s}^{-1}$$

where the errors are two least-squares standard deviations

$$k(CHFClCF_3) = 1.02 \times 10^{-14} \text{ cm}^3 \text{ molecule}^{-1} \text{ s}^{-1} \text{ at } 298 \text{ K}$$

with an estimated uncertainty at 298 K of ±30%. Using the expression $k = A'T^2e^{-E'/RT}$, a unit-weighted least-squares analysis of these data yields

$$k(CHFClCF_3) = (9.12^{+29.26}_{-6.95}) \times 10^{-19} T^2 e^{-(624\pm416)/T} \text{ cm}^3 \text{ molecule}^{-1} \text{ s}^{-1}$$

where the errors are two least-squares standard deviations

$$k(CHFClCF_3) = 1.00 \times 10^{-14} \text{ cm}^3 \text{ molecule}^{-1} \text{ s}^{-1} \text{ at } 298 \text{ K}$$

In view of the small temperature range covered (250–375 K), the use of the simple Arrhenius expression (the recommended line in Figure 29) is recommended over this temperature range, with an estimated uncertainty of the rate constant at 298 K of ±30%.

t. $CHCl_2CF_3$. The rate constants of Howard and Evenson,[196] Watson et al.,[271] and Clyne and Holt[261] are listed in Table V and plotted in Arrhenius form in Figure 30. Watson et al.[271] estimated that impurity contributions could have led to their observed rate constants being somewhat high and estimated the Arrhenius expression shown as the dashed line in Figure 30. These estimated rate constants of Watson et al.,[271] taking into account the presence of reactive impurities, are only slightly different from the measured rate constants (which exhibit no unambiguous curvature in the Arrhenius plot). Hence a unit-weighted least-squares analysis of the rate constant data of Howard and Evenson[196] and Watson et al.[271] has been carried out to yield the tentatively recommended Arrhenius expression of

$$k(CHCl_2CF_3) = (1.16^{+1.44}_{-0.64}) \times 10^{-12} e^{-(1056\pm237)/T} \text{ cm}^3 \text{ molecule}^{-1} \text{ s}^{-1}$$

where the errors are two least-squares standard deviations

$$k(CHCl_2CF_3) = 3.35 \times 10^{-14} \text{ cm}^3 \text{ molecule}^{-1} \text{ s}^{-1} \text{ at } 298 \text{ K}$$

with an estimated uncertainty at 298 K of +20%, −40%.

u. CF_4, CF_3Cl, CF_3Br, CF_2Cl_2, CF_2ClBr, $CFCl_3$, CCl_4, CF_2ClCF_2Cl, and $CF_2ClCFCl_2$. For these haloalkanes only upper limit rate constants are available (Table V) with room-temperature rate constants $<1 \times 10^{-15}$ cm³ molecule⁻¹ s⁻¹. For CF_2Cl_2 and $CFCl_3$, Chang and Kaufman[269] have obtained upper limit rate constants of $<6 \times 10^{-16}$ cm³ molecule^{-1} s^{-1} at 478 K and $<5 \times 10^{-16}$ cm³ molecule^{-1} s^{-1} at 480 K, respectively, indicating that these two OH radical reactions have Arrhenius activation energies ≥7 kcal mol^{-1}.[269]

For the remaining haloalkanes listed in Table V, only single reliable studies have been carried out (although two studies were carried out for CH_3CF_3, CH_2FCHF_2, and CHF_2CF_3, the rate constant data of Clyne and Holt[261] are discounted), and no firm recommendations are made.

The rate constant data discussed above show that Cl and Br atom substitution for H atoms in methane lead to enhancement of the room-temperature rate constants, while F atom substitution initially enhances the room-temperature rate constant (in CH_3F), but in more highly substituted halomethanes (CHF_3 and CHF_2Cl) F atom substitution diminishes them. Similar trends are seen in the haloethanes. These substituent effects are discussed in more detail in section IV below.

2. *Mechanism*

Analogous to the alkanes, for haloalkanes with F, Cl, and Br substituents these reactions must proceed via H atom abstraction.[226] However, Garraway and Donovan[268] have reported a room-temperature rate constant of 1.2×10^{-13} cm^3 molecule^{-1} s^{-1} for the reaction of OH radicals with CF_3I and further report that reaction occurs for other, non-hydrogen-containing, iodine-substituted alkanes such as C_2F_5I and C_3F_7I. If these observations are correct, then these reactions must then occur via I atom abstraction to yield HOI and the corresponding C_nF_{2n+1} radical.

3. *Mechanism under Atmospheric Conditions*

The radicals initially formed after H atom abstraction (or, for CF_3I and its homologues, after I atom abstraction)[268] react rapidly under atmospheric conditions with O_2

$$R + O_2 \xrightarrow{M} RO_2$$

with limiting high-pressure rate constants of $>1 \times 10^{-12}$ cm^3 molecule^{-1} s^{-1} for R = CF_3,[276] $CFCl_2$,[277,278] and CCl_3.[279,280] These halogen-substituted RO_2 radicals then appear to react with NO or NO_2

$$RO_2 + NO \rightarrow RO + NO_2$$

$$RO_2 + NO_2 \rightleftarrows RO_2NO_2$$

with the haloalkyl peroxynitrates being thermally unstable.[281,282] The reactions with NO proceed with room-temperature rate constants of $\sim(1.6\text{–}1.9) \times 10^{-11}$ cm^3 molecule^{-1} s^{-1} for R = CF_3,[278] CF_2Cl,[278] $CFCl_2$,[278,283] and CCl_3,[278,280] these being approximately a factor of 2 higher than the corresponding rate constants for reaction of NO with CH_3O_2 radicals.[3]

The subsequent reactions of the haloalkoxy radicals are less well understood. For those haloalkoxy radicals containing a hydrogen atom, i.e., CHX_2O where X = F, Cl, or Br, it is expected that, analogous to the methoxy and ethoxy radicals,[3] H atom abstraction by O_2 will occur

$$CHX_2O + O_2 \rightarrow HO_2 + CX_2O$$

thus leading to products such as $COCl_2$, COFCl, and COF_2 from $CHCl_2O$, CHFClO, and CHF_2O radicals, respectively. For the haloalkoxy radicals which do not contain a hydrogen atom, elimination of a halogen atom appears to occur[278,284–286]

$$CX_3O \rightarrow CX_2O + X$$

where X = F or Cl (and presumably also Br).

C. Alkenes

1. *Kinetics*

The rate constants obtained in the limiting high-pressure second-order kinetic regime are listed in Tables VI (acyclic monoalkenes), VII (acyclic di- and trialkenes), and VIII (cyclic mono-, di-, and trialkenes). The data reported by Cox[307] from the photolysis of HONO–alkene–air mixtures at 300 K and atmospheric pressure of air have not been included, since the stoichiometric factors were not specified (though, as discussed below, they are expected to be 2) and these rate coefficients are based upon a not accurately known rate constant for the reaction of OH radicals with CO under the experimental conditions employed. However, on the basis of our present knowledge of the rate constant for this reference reaction and the reaction stoichiometries for these OH–alkene reactions, these data[307] are consistent with the elementary rate constants recommended below. Simonaitis and Heicklen[132] obtained rate constants for propene at 373 and 473 K, relative to that for the reaction of OH radicals with CO at total pressures of ~400–800 torr (mainly H_2O). Rate constant ratios of $k(\text{OH + propene})/k(\text{OH + CO}) = 75 \pm 8$ at 373 K and 55 ± 6 at 473 K were determined.[132] As discussed previously,[1] while subject to significant uncertainties, mainly concerning the rate constant of the reference reaction under the experimental conditions employed, these data are generally consistent with the recommendation.

In addition, a set of rate constants for isoprene and a series of monoterpenes can be derived from the experimental NO–photooxidation rates of Grimsrud et al.[308] at 301 ± 1 K. These data[308] must be viewed as semiquantitative only,[292,304] since their use assumes that the OH radical concentrations were identical in the separate NO–organic–air irradiations and that O_3 reactions were negligible.

As noted above, the rate constants listed in Tables VI, VII, and VIII are, in most cases, in the limiting high pressure second-order kinetic regime. However, the rate constants determined for the lower (C_3–C_4) alkenes using discharge flow techniques at total pressures of ~1 torr may still be in the fall-off regime between second- and third-order kinetics. These data are thus not used in the evaluation of the recommended rate constants, and the most reliable rate constant data in the fall-off regions are indicated for the individual alkenes studied.

a. Ethene and Ethene-*d*$_4$. The limiting high-pressure second-order rate constants obtained (other than that of Cox,[307] as noted above) are listed in Table VI. At room temperature this limiting second-order high-pressure kinetic regime for ethene is attained at total diluent pressures of helium, ≳400 torr,[122,309,310] argon, ≳225 torr,[218,287,288] and CF_4 and SF_6, ≳200 torr,[119] while Tully[305] has shown that for helium diluent the limiting high-pressure second-order kinetic regime appears to be attained at total pressures of ≳600–700 torr at 425 K. Since Atkinson et al.[287] observed that the total pressure at which this limiting second-order high-pressure limit is attained for argon diluent does not depend markedly on the temperature over the range 299–425 K, these data indicate (making the reasonable assumption that N_2 has as good, or better, a third-body efficiency as Ar[218]) that the reaction of OH radicals with

TABLE VI. Rate Constants *k* and Arrhenius Parameters for the Gas-Phase Reaction of OH Radicals with Acyclic Monoalkenes at the High-Pressure Limit

alkene	$10^{12}A$, cm^3 molecule^{-1} s^{-1}	E, cal mol^{-1}	$10^{12}k$, cm^3 molecule^{-1} s^{-1}	T, K	technique	ref	temp range covered, K
ethene			6.23 ± 0.33	381	PR-RA	Gordon and Mulac[129]	381–416
			7.31 ± 0.33	416			
			7.6 ± 1.5	305 ± 2	rel rate [rel to k(OH + n-butane) = 2.63×10^{-12}]^a	Lloyd et al.[144]	
			7.85 ± 0.79	299.2	FP-RF	Atkinson et al.[287]	299–425
			6.76 ± 0.68	351.3			
	2.18	−770 ± 300	5.35 ± 0.54	425.1			
			10.0 ± 1.7	296	FP-RA	Overend and Paraskevopoulos[119]	
			8.34 ± 0.39	299 ± 2	rel rate [rel to k(OH + n-butane) = 2.54×10^{-12}]^a	Atkinson et al.[147]	
			8.47 ± 0.24	291	LP-LIF	Tully[122]	291–591
			6.15 ± 0.35	361.5			
	1.36	−1063 ± 82	4.55 ± 0.27^b	438			
			8.8 ± 2.0	296	LP-RF	Zellner and Lorenz[288]	296–524
			$5.5^{+3.3}_{-1.7}$	524			
			7.3 ± 1.0	295	LP-LIF	Schmidt et al.[126]	
			8.66 ± 0.40	295 ± 1	rel rate [rel to k(OH + propene) = 2.68×10^{-11}]^a	Atkinson and Aschmann[153]	
			8.3 ± 0.6	295	rel rate [rel to k(OH + n-hexane) = 5.51×10^{-12}]^a	Klein et al.[218]	
ethene-d_4			8.80 ± 0.51	298 ± 2	rel rate [rel to k(OH + ethene) = 8.54×10^{-12}]^a	Niki et al.[137]	
propene			17 ± 4	300	DF-MS	Morris et al.[85]	
			5.0 ± 1.7	300	DF-EPR	Bradley et al.[205]	
			14.5 ± 2.2	298	FP-RF	Stuhl[289]	
			13.6 ± 2.7	298	rel rate [rel to k(OH + CO) = 1.52×10^{-13}]^c	Gorse and Volman[206]	
			14.3 ± 0.7	381	PR-RA	Gordon and Mulac[129]	381–416
			20.0 ± 1.0	416			
			5 ± 1	300	DF-RA	Pastrana and Carr[290]	
			25.1 ± 2.5	297.6	FP-RF	Atkinson and Pitts[291]	298–424
			20.4 ± 2.1	345.5			
			16.4 ± 1.6	390.3			
	4.1	−1080 ± 300	14.7 ± 1.5	423 .6			
			25.5 ± 5.1	305 ± 2	rel rate [rel to k(OH + n-butane) = 2.63×10^{-12}]^a	Lloyd et al.[144]	
			21.8	303	rel rate [rel to k(OH + *cis*-2-butene) = 5.46×10^{-11}]^a	Wu et al.[136]	
			24.2 ± 3.6	305 ± 2	rel rate [rel to k(OH + 2-methylpropene) = 4.95×10^{-11}]^a	Winer et al.[292]	
			24.2 ± 4.9	305 ± 2	rel rate [rel to k(OH + 2-methylpropene) = 4.95×10^{-11}]^a	Winer et al.[293]	

			26.0 ± 1.7	298	FP-RF	Ravishankara et al.[294]	
			24.6 ± 2.8	297 ± 2	FP-RA	Nip and Paraskevopoulos[295]	
			25.2	300	rel rate [rel to $k(OH + ethene) = 8.45 \times 10^{-12}]^{a}$	Cox et al.[139]	
			26.2	~300	rel rate [rel to $k(OH + ethene) = 8.45 \times 10^{-12}]^{a}$	Barnes et al.[141]	
			19 ± 3	298	DF-RF	Smith[296]	
			30 ± 5	297	LP-RF	Zellner and Lorenz[288]	
			22 ± 4	295	LP-LIF	Schmidt et al.[126]	
			27.1 ± 0.3	293	LP-LIF	Tully and Goldsmith[297]	293–896
			21.7 ± 0.2	338.5			
			17.5 ± 0.2	400			
			15.9 ± 0.2	422			
			14.9 ± 0.3	440.5			
	4.58 ± 0.46	−1042 ± 76 (293–467 K)	13.9 ± 0.2	467			
			3.79 ± 0.17	701			
			3.60 ± 0.11	705			
			4.57 ± 0.12	782			
			4.74 ± 0.08	785			
			5.44 ± 0.11	857			
	33.1 ± 7.6	3062 ± 354 (701–896 K)	5.95 ± 0.16	896			
			29.3 ± 2.0	295	rel rate [rel to $k(OH + n\text{-hexane}) = 5.51 \times 10^{-12}]^{a}$	Klein et al.[218]	
propene-d_6			18.7	298	DF-MS	Morris and Niki[102]	
			16.8	298	FP-RF	Stuhl[289]	
			27.9 ± 0.2	293	LP-LIF	Tully and Goldsmith[297]	293–896
			22.3 ± 0.3	338			
			18.4 ± 0.3	392			
			15.7 ± 0.2	440.5			
	4.79 ± 0.51	−1030 ± 78 (293–481 K)	13.7 ± 0.1	481			
			2.65 ± 0.10	701			
			2.35 ± 0.09	705			
			3.21 ± 0.16	781			
			3.29 ± 0.15	785			
			3.56 ± 0.13	857			
	18.7 ± 9.7	2787 ± 803 (701–896 K)	3.85 ± 0.12	896			
1-butene			40.8	298	DF-MS	Morris and Niki[102]	
			15 ± 1	300	DF-RA	Pastrana and Carr[290]	
			35.3 ± 3.6	297.7	FP-RF	Atkinson and Pitts[291]	298–424
			30.0 ± 3.0	344.1			
	7.6	−930 ± 300	22.2 ± 2.2	423.7			
			28.4	303	rel rate [rel to $k(OH + cis\text{-2-butene}) = 5.46 \times 10^{-11}]^{a}$	Wu et al.[136]	
			29.5 ± 2.1	298	FP-RF	Ravishankara et al.[294]	
			33.4 ± 2.5	297 ± 2	FP-RA	Nip and Paraskevopoulos[295]	
			32.1	~300	rel rate [rel to $k(OH + ethene) = 8.45 \times 10^{-12}]^{a}$	Barnes et al.[141]	
			30 ± 4	298	DF-MS	Biermann et al.[175]	
			31.3 ± 0.8	298 ± 2	rel rate [rel to $k(OH + propene) = 2.63 \times 10^{-11}]^{a}$	Ohta[152]	

TABLE VI (Continued)

alkene	$10^{12}A$, cm^3 molecule^{-1} s^{-1}	E, cal mol^{-1}	$10^{12}k$, cm^3 molecule^{-1} s^{-1}	T, K	technique	ref	temp range covered, K
2-methylpropene			31.9 ± 1.6	295 ± 1	rel rate [rel to k(OH + propene) = 2.68×10^{-11}]^a	Atkinson and Aschmann[153]	
			64.6	298	DF-MS	Morris and Niki[102]	
			50.7 ± 5.1	297.2	FP-RF	Atkinson and Pitts[291]	297–424
			39.0 ± 3.9	345.5			
	9.2	-1000 ± 300	30.5 ± 3.1	423.9			
			50.2	303	rel rate [rel to k(OH + *cis*-2-butene) = 5.46×10^{-11}]^a	Wu et al.[136]	
			61.7	~300	rel rate [rel to k(OH + ethene) = 8.45×10^{-12}]^a	Barnes et al.[141]	
			54.7 ± 0.9	298 ± 2	rel rate [rel to k(OH + 2-methyl-2-butene) = 8.69×10^{-11}]^a	Ohta[152]	
cis-2-butene			52.3 ± 2.4	295 ± 1	rel rate [rel to k(OH + propene) = 2.68×10^{-11}]^a	Atkinson and Aschmann[153]	
			61.2	298	DF-MS	Morris and Niki[102]	
			53.7 ± 5.4	297.6	FP-RF	Atkinson and Pitts[291]	298–425
			43.0 ± 4.3	345.7			
	10.4	-970 ± 300	32.9 ± 3.3	424.9			
			57.3 ± 11.5	305 ± 2	rel rate [rel to k(OH + n-butane) = 2.63×10^{-12}]^a	Lloyd et al.[144]	
			60.4 ± 9.0	305 ± 2	rel rate [rel to k(OH + 2-methylpropene) = 4.95×10^{-11}]^a	Winer et al.[292]	
			42.2 ± 1.9	298	FP-RF	Ravishankara et al.[294]	
			54.7 ± 1.8	298 ± 2	rel rate [rel to k(OH + 2-methyl-2-butene) = 8.69×10^{-11}]^a	Ohta[152]	
trans-2-butene			57.1 ± 1.4	295 ± 1	rel rate [rel to k(OH + propene) = 2.68×10^{-11}]^a	Atkinson and Aschmann[153]	
			71.4	298	DF-MS	Morris and Niki[102]	
			12 ± 10	300	DF-RA	Pastrana and Carr[290]	
			69.9 ± 7.0	297.8	FP-RF	Atkinson and Pitts[291]	298–425
			57.0 ± 5.7	346.1			
	11.2	-1090 ± 300	40.3 ± 4.1	425.0			
			71.0	303	rel rate [rel to k(OH + *cis*-2-butene) = 5.46×10^{-11}]^a	Wu et al.[136]	
			59.9 ± 3.1	297 ± 2	rel rate [rel to k(OH + *cis*-1,3-pentadiene) = 1.01×10^{-10}]^d	Ohta[142]	
1-pentene			65.1 ± 1.4	295 ± 1	rel rate [rel to k(OH + propene) = 2.68×10^{-11}]^a	Atkinson and Aschmann[153]	
			42.5	298	DF-MS	Morris and Niki[102]	
			30.6	303	rel rate [rel to	Wu et al.[136]	

					k(OH + *cis*-2-butene) = 5.46×10^{-11}]^{a}		
			39.7 ± 3.8	297 ± 2	FP-RA	Nip and Paraskevopoulos[295]	
			29 ± 4	298	DF-MS	Biermann et al.[175]	
			28.7 ± 1.3	298	FP-RF	Biermann et al.[175]	
			31.9 ± 1.4	295 ± 1	rel rate [rel to k(OH + propene) = 2.68×10^{-11}]^{a}	Atkinson and Aschmann[153]	
cis-2-pentene			65.5	303	rel rate [rel to k(OH + *cis*-2-butene) = 5.46×10^{-11}]^{a}	Wu et al.[136]	
			65.1 ± 1.7	298 ± 2	rel rate [rel to k(OH + *cis*-2-butene) = 5.61×10^{-11}]^{a}	Ohta[152]	
trans-2-pentene			67.2 ± 2.0	297 ± 2	rel rate [rel to k(OH + 1,3-butadiene) = 6.72×10^{-11}]^{a}	Ohta[142]	
2-pentene (*cis* + *trans* mixture)			90.1	298	DF-MS	Morris and Niki[102]	
2-methyl-1-butene			90.1	298	DF-MS	Morris and Niki[102]	
			60.1	303	rel rate [rel to k(OH + *cis*-2-butene) = 5.46×10^{-11}]^{a}	Wu et al.[136]	
			60.7 ± 1.1	298 ± 2	rel rate [rel to k(OH + 2-methylpropene) = 5.14×10^{-11}]^{a}	Ohta[152]	
3-methyl-1-butene			31.0 ± 3.1	299.2	FP-RF	Atkinson et al.[298]	299–423
			24.0 ± 2.4	349.9			
	5.23	−1060 ± 300	18.4 ± 1.9	423.2			
			32.4 ± 1.1	295 ± 1	rel rate [rel to k(OH + propene) = 2.68×10^{-11}]^{a}	Atkinson and Aschmann[153]	
2-methyl-2-butene			119	298	DF-MS	Morris and Niki[102]	
			78 ± 8	297.7	FP-RF	Atkinson et al.[299]	298–425
			77 ± 8	298.0			
			67 ± 7	345.2			
			62 ± 9	421.6			
	36	−450 ± 400	62 ± 9	424.5			
			87.3 ± 8.8	299.5	FP-RF	Atkinson and Pitts[300]	299–426
			65.4 ± 6.6	356.2			
	19.1	−895 ± 300	56.0 ± 5.6	426.1			
			91 ± 6	300 ± 1	rel rate [rel to k(OH + *cis*-2-butene) = 5.54×10^{-11}]^{a}	Atkinson et al.[301]	
			89.9 ± 3.4	299 ± 2	rel rate [rel to k(OH + propene) = 2.62×10^{-11}]^{a}	Atkinson et al.[147]	
			85.3 ± 2.7	297 ± 2	rel rate [rel to k(OH + 1,3-butadiene) = 6.72×10^{-11}]^{a}	Ohta[142]	
			88.4 ± 3.5	295 ± 1	rel rate [rel to k(OH + propene) = 2.68×10^{-11}]^{a}	Atkinson and Aschmann[153]	
1-hexene			32.8	303	rel rate [rel to k(OH + *cis*-2-butene) = 5.46×10^{-11}]^{a}	Wu et al.[136]	

TABLE VI (Continued)

alkene	$10^{12}A$, cm^3 molecule^{-1} s^{-1}	E, cal mol^{-1}	$10^{12}k$, cm^3 molecule^{-1} s^{-1}	T, K	technique	ref	temp range covered, K
			37.5 ± 1.1	295 ± 1	rel rate [rel to k(OH + propene) = 2.68×10^{-11}]^a	Atkinson and Aschmann[153]	
2-methyl-1-pentene			62.6 ± 0.9	298 ± 2	rel rate [rel to k(OH + 2-methyl-2-butene) = 8.69×10^{-11}]^a	Ohta[152]	
2-methyl-2-pentene			87.8 ± 1.8	298 ± 2	rel rate [rel to k(OH + 2-methyl-2-butene) = 8.69×10^{-11}]^a	Ohta[152]	
			89.8 ± 1.3	298 ± 2	rel rate [rel to k(OH + *cis*-2-pentene) = 6.51×10^{-11}]^e	Ohta[152]	
trans-4-methyl-2-pentene			60.8 ± 0.7	298 ± 2	rel rate [rel to k(OH + *trans*-2-pentene) = 6.68×10^{-11}]^f	Ohta[152]	
3,3-dimethyl-1-butene			28.4	303	rel rate [rel to k(OH + *cis*-2-butene) = 5.46×10^{-11}]^a	Wu et al.[136]	
2,3-dimethyl-2-butene			153	298	DF-MS	Morris and Niki[102]	
			110 ± 22	298	FP-RF	Perry[302]	
			56.7 ± 1.9	298	FP-RF	Ravishankara et al.[294]	
			128 ± 9	300 ± 1	rel rate [rel to k(OH + *cis*-2-butene) = 5.54×10^{-11}]^a	Atkinson et al.[301]	
			112 ± 6	299 ± 2	rel rate [rel to k(OH + propene) = 2.62×10^{-11}]^a	Atkinson et al.[147]	
			115 ± 4	298 ± 2	rel rate [rel to k(OH + 2-methyl-1,3-butadiene) = 1.01×10^{-10}]^a	Atkinson et al.[151]	
			111 ± 2	294 ± 2	rel rate [rel to k(OH + 2-methyl-1,3-butadiene) = 1.02×10^{-10}]^a	Atkinson et al.[303]	
			112 ± 5	295 ± 1	rel rate [rel to k(OH + propene) = 2.68×10^{-11}]^a	Atkinson and Aschmann[153]	
			103 ± 1	298 ± 2	rel rate [rel to k(OH + 2-methyl-2-butene) = 8.69×10^{-11}]^a	Ohta[152]	
			111 ± 3	294	rel rate [rel to k(OH + 2-methyl-1,3-butadiene) = 1.02×10^{-10}]^a	Atkinson et al.[304]	
1-heptene			36.1 ± 7.2	305 ± 2	rel rate [rel to k(OH + 2-methylpropene) = 4.95×10^{-11}]^a	Darnall et al.[219]	
			40.5 ± 1.6	295 ± 1	rel rate [rel to k(OH + propene) = 2.68×10^{-11}]^a	Atkinson and Aschmann[153]	
2,3-dimethyl-2-pentene			98.2 ± 0.9	298 ± 2	rel rate [rel to k(OH + 2-methyl-2-butene) =	Ohta[152]	

					8.69×10^{-11}][a]		
			108 ± 1	298 ± 2	rel rate [rel to *k*(OH + 2,3-dimethyl-2-butene) = 1.10×10^{-10}][a]	Ohta[152]	
trans-4,4-dimethyl-2-pentene			54.8 ± 0.7	298 ± 2	rel rate [rel to *k*(OH + *trans*-2-pentene) = 6.68×10^{-11}][f]	Ohta[152]	

[a] From present recommendations (see text). [b] Probably still in the fall-off regime between second- and third-order kinetics.[305] [c] From the expression $k(\mathrm{OH} + \mathrm{CO}) = 1.50 \times 10^{-13}[(1 + 9.19 \times 10^{-4}P)/(1 + 2.24 \times 10^{-4}P)]$ cm³ molecule⁻¹ s⁻¹,[3] where *P* is the total pressure in torr. [d] From the rate constant determined by Ohta[142] (Table VII). [e] From the rate constant determined by Ohta.[152] [f] From the rate constant determined by Ohta,[142] using an assumed Arrhenius activation energy of −1.0 kcal mol⁻¹.

TABLE VII. Rate Constants *k* and Arrhenius Parameters for the Gas-Phase Reaction of OH Radicals with Acyclic Di- and Trialkenes at the High-Pressure Limit

alkene	$10^{12}A$, cm³ molecule⁻¹ s⁻¹	*E*, cal mol⁻¹	$10^{12}k$, cm³ molecule⁻¹ s⁻¹	*T*, K	technique	ref	temp range covered, K
propadiene			4.5 ± 2.5[a]	300	DF-EPR	Bradley et al.[205]	
			9.30 ± 0.93	299.0	FP-RF	Atkinson et al.[298]	299–421
			8.70 ± 0.87	349.7			
	5.59	−305 ± 300	8.02 ± 0.80	420.8			
			10.1 ± 1.4	297 ± 2	rel rate [rel to *k*(OH + 1,3-butadiene) = 6.72×10^{-11}][b]	Ohta[142]	
			9.84 ± 0.97	295 ± 1	rel rate [rel to *k*(OH + propene) = 2.68 $\times 10^{-11}$][b]	Atkinson and Aschmann[153]	
1,2-butadiene			26.2 ± 2.0	297 ± 2	rel rate [rel to *k*(OH + 1,3-butadiene) = 6.72×10^{-11}][b]	Ohta[142]	
1,3-butadiene			67.9 ± 13.6	305 ± 2	rel rate [rel to *k*(OH + *n*-butane) = 2.63 $\times 10^{-12}$][b]	Lloyd et al.[144]	
			68.5 ± 6.9	299.5	FP-RF	Atkinson et al.[298]	299–424
			57.2 ± 5.7	347.2			
	14.5	−930 ± 300	43.3 ± 4.4	424.0			
			65.1	~300	rel rate [rel to *k*(OH + ethene) = 8.45 × 10^{-12}][b]	Barnes et al.[141]	
			61.6 ± 1.5	297 ± 2	rel rate [rel to *k*(OH + propene) = 2.65 $\times 10^{-11}$][b]	Ohta[142]	
			68.8 ± 2.2	297 ± 2	rel rate [rel to *k*(OH + 2-methyl-2-butene) = 8.72×10^{-11}][b]	Ohta[142]	
			67.8 ± 2.2	295 ± 1	rel rate [rel to *k*(OH + propene) = 2.68 $\times 10^{-11}$][b]	Atkinson and Aschmann[153]	
1,2-pentadiene			35.6 ± 1.4	297 ± 2	rel rate [rel to *k*(OH + 1,3-butadiene) = 6.72×10^{-11}][b]	Ohta[142]	
cis-1,3-pentadiene			101 ± 4	297 ± 2	rel rate [rel to *k*(OH + 1,3-butadiene) = 6.72×10^{-11}][b]	Ohta[142]	
1,4-pentadiene			53.3 ± 1.4	297 ± 2	rel rate [rel to *k*(OH + propene) = 2.65 $\times 10^{-11}$][b]	Ohta[142]	
3-methyl-1,2-butadiene			57.1 ± 2.0	297 ± 2	rel rate [rel to *k*(OH + 1,3-butadiene) = 6.72×10^{-11}][b]	Ohta[142]	
2-methyl-1,3-butadiene			78	300	rel rate [rel to *k*(OH + ethene) = 8.45 × 10^{-12}][b]	Cox et al.[139]	
			99.8 ± 4.5	299 ± 2	rel rate [rel to *k*(OH + propene = 2.62 $\times 10^{-11}$][b]	Atkinson et al.[147]	

			92.6 ± 15	299	FP-RF	Kleindienst et al.[306]	299–422
			76.4 ± 12	349			
	23.6	−813 ± 55	62.1 ± 8.2	422			
			99.5 ± 2.7	297 ± 2	rel rate [rel to *k*(OH + 1,3-butadiene) = 6.72 × 10^{-11}][b]	Ohta[142]	
			102.1 ± 4.0	295 ± 1	rel rate [rel to *k*(OH + propene) = 2.68 × 10^{-11}][b]	Atkinson and Aschmann[153]	
trans-1,3-hexadiene			113 ± 4	297 ± 2	rel rate [rel to *k*(OH + 1,3-butadiene) = 6.72 × 10^{-11}][b]	Ohta[142]	
trans-1,4-hexadiene			90.7 ± 5.4	297 ± 2	rel rate [rel to *k*(OH + 1,3-butadiene) = 6.72 × 10^{-11}][b]	Ohta[142]	
			90.9 ± 4.3	297 ± 2	rel rate [rel to *k*(OH + propene) = 2.65 × 10^{-11}][b]	Ohta[142]	
1,5-hexadiene			62.5 ± 1.4	297 ± 2	rel rate [rel to *k*(OH + 1,3-butadiene) = 6.72 × 10^{-11}][b]	Ohta[142]	
			61.7 ± 3.5	297 ± 2	rel rate [rel to *k*(OH + propene) = 2.65 × 10^{-11}][b]	Ohta[142]	
2,4-hexadiene (cis + trans mixture)			135 ± 6	297 ± 2	rel rate [rel to *k*(OH + 1,3-butadiene) = 6.72 × 10^{-11}][b]	Ohta[142]	
2-methyl-1,4-pentadiene			79.2 ± 8.1	297 ± 2	rel rate [rel to *k*(OH + *cis*-1,3-pentadiene) = 1.01 × 10^{-10}][c]	Ohta[142]	
3-methyl-1,3-pentadiene			137 ± 8	297 ± 2	rel rate [rel to *k*(OH + *cis*-1,3-pentadiene) = 1.01 × 10^{-10}][c]	Ohta[142]	
4-methyl-1,3-pentadiene			132 ± 4	297 ± 2	rel rate [rel to *k*(OH + *cis*-1,3-pentadiene) = 1.01 × 10^{-10}][c]	Ohta[142]	
2,3-dimethyl-1,3-butadiene			122 ± 6	297 ± 2	rel rate [rel to *k*(OH + 1,3-butadiene) = 6.72 × 10^{-11}][b]	Ohta[142]	
2-methyl-1,5-hexadiene			96.3 ± 4.4	297 ± 2	rel rate [rel to *k*(OH + 1,5-hexadiene) = 6.21 × 10^{-11}][c]	Ohta[142]	
2,5-dimethyl-1,5-hexadiene			120 ± 2	297 ± 2	rel rate [rel to *k*(OH + 1,5-hexadiene) = 6.21 × 10^{-11}][c]	Ohta[142]	
2,5-dimethyl-2,4-hexadiene			211 ± 10	297 ± 2	rel rate [rel to *k*(OH + 2-methyl-1,5-hexadiene) = 9.63 × 10^{-11}][c]	Ohta[142]	
cis-1,3,5-hexatriene			111 ± 8	294 ± 2	rel rate [rel to *k*(OH + 2-methyl-1,3-butadiene) = 1.02 × 10^{-10}][b]	Atkinson et al.[303]	
trans-1,3,5-hexatriene			112 ± 18	294 ± 2	rel rate [rel to *k*(OH + 2-methyl-1,3-butadiene) = 1.02 × 10^{-10}][b]	Atkinson et al.[303]	
3-methylene-7-methyl-1,6-octadiene (myrcene)			213 ± 16	294 ± 1	rel rate [rel to *k*(OH + 2,3-dimethyl-2-butene) = 1.12 × 10^{-10}][b]	Atkinson et al.[304]	
3,7-dimethyl-1,3,6-octatriene (*cis*- and *trans*-ocimene)			250 ± 19[d]	294 ± 1	rel rate [rel to *k*(OH + 2,3-dimethyl-2-butene) = 1.12 × 10^{-10}][b]	Atkinson et al.[304]	

[a] May not be at the high pressure limit.[1,298] [b] From the present recommendations (see text). [c] From the rate constants determined by Ohta.[142] [d] *cis*- and *trans*-isomers have identical rate constants within ±20%.[304]

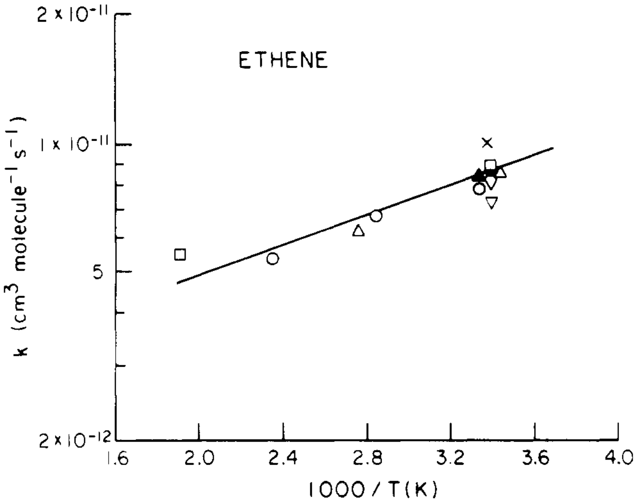

Figure 31. Arrhenius plot of the limiting high-pressure second-order rate constants for the reaction of OH radicals with ethene: (○) Atkinson et al.;[287] (×) Overend and Paraskevopoulos;[119] (▲) Atkinson et al.;[147] (△) Tully;[122] (□) Zellner and Lorenz;[288] (▽) Schmidt et al.;[126] (●) Atkinson and Aschmann;[153] (◇) Klein et al.;[218] (—) recommendation (see text).

ethene will be at, or close to, the limiting high-pressure second-order kinetic limit throughout the troposphere.

In the fall-off region, rate constants have been obtained by Greiner,[111] Morris et al.,[85] Smith and Zellner,[118] Klein et al.,[218] Pastrana and Carr,[290] Davis et al.,[309] Howard,[78] Atkinson et al.,[287] Overend and Paraskevopoulos,[119] Farquharson and Smith,[311] Tully,[122,305] and Zellner and Lorenz,[288] and these references should be consulted for kinetic data in the fall-off regime.

In the limiting high pressure regime, the available kinetic data for ethene (Table VI) are in reasonable agreement. The most definitive studies are judged to be the absolute rate constant determinations carried out by Atkinson et al.[287] and Tully[122] and the relative rate studies of Atkinson et al.[147] and Atkinson and Aschmann.[153] These data, together with those of Overend and Paraskevopoulos,[119] Zellner and Lorenz,[288] Schmidt et al.,[126] and Klein et al.[218] are plotted in Arrhenius form in Figure 31. The remaining limiting high-pressure rate constants listed in Table VI[129,144] are in agreement, within the experimental errors, with these data. Tully[122] has observed that for temperatures ≥438 K (in general agreement with earlier predictions[1,312] based upon analogy with OH radical reactions with the aromatic hydrocarbons[1,312,313]) the OH–ethene adduct thermally back-decomposes to the reactants on a time scale of ≲10 ms. At lower temperatures, i.e., ≤438 K, the rate constants obtained by Atkinson et al.[287] and Tully[122] are in excellent agreement (Figure 31). Thus, from a least-squares analysis of these data[122,287] (but neglecting the rate constant of Tully[122] at 438 K, which was almost certainly not at the high-pressure limit[305])

$$k(\text{ethene}) = (2.03^{+0.44}_{-0.36}) \times 10^{-12} e^{(411\pm67)/T} \text{ cm}^3 \text{ molecule}^{-1} \text{ s}^{-1}$$

where the indicated error limits are two least-squares standard deviations

$$k(\text{ethene}) = 8.06 \times 10^{-12} \text{ cm}^3 \text{ molecule}^{-1} \text{ s}^{-1} \text{ at } 298 \text{ K}$$

From a recent precise relative rate constant determination, Atkinson et al.[147] derived a value of k(ethene) = (8.34 ± 0.39) × 10^{-12} cm^3 molecule^{-1} s^{-1} at 299 ± 2 K relative to the recommendation for n-butane, while Atkinson and Aschmann[153] have derived a value of k(ethene) = 8.66 × 10^{-12} cm^3 molecule^{-1} s^{-1} at 295 ± 1 K, relative to the recommendation for propene (see the discussion below concerning propene). Since this latter rate constant was derived from a least-squares analysis of the relative rate constants for a series of alkenes and dialkenes with the corresponding absolute rate constant data (see below), this rate constant at 295 K and the temperature dependence obtained from the studies of Atkinson et al.[287] and Tully[122] have been used to recommend

$$k(\text{ethene}) = (2.15^{+0.47}_{-0.38}) \times 10^{-12} e^{(411\pm67)/T} \text{ cm}^3 \text{ molecule}^{-1} \text{ s}^{-1}$$

where the indicated error limits are equivalent to two standard deviations, and

$$k(\text{ethene}) = 8.54 \times 10^{-12} \text{ cm}^3 \text{ molecule}^{-1} \text{ s}^{-1} \text{ at } 298 \text{ K}$$

with an estimated uncertainty at 298 K of ±15%.

The sole rate constant obtained for ethane-d_4 at room temperature and approximately atmospheric pressure of air,[137] which will be the limiting high-pressure value, is essentially identical to that for ethene-h_4.[137] Thus, as expected for an addition reaction (see below), this reaction of the OH radical with ethene-d_4 exhibits a negligible kinetic isotope effect.

b. Propene and Propene-d_6. The limiting high-pressure second-order rate constants obtained (other than that of Cox,[307] as noted above) are listed in Table VI. At room temperature this limiting second-order high-pressure kinetic regime is attained at total diluent pressures of helium, ≲20 torr,[294] argon, ≳10 torr,[218,288,291] and air, ≳10 torr.[218]

While there is a significant degree of scatter in the reported, supposedly high-pressure data (ref 126, 129, 136, 139, 141, 144, 206, 218, 288, 289, 291–295, 297), the most definitive limiting high-pressure studies are judged to be the absolute rate constant determinations carried out by Atkinson and Pitts,[291] Ravishankara et al.,[294] Nip and Paraskevopoulos,[295] and Tully and Goldsmith[297] and the relative rate constant study of Atkinson and Aschmann.[153] The data of Atkinson and Pitts,[291] Ravishankara et al.,[294] Nip and Paraskevopoulos,[295] Zellner and Lorenz,[288] Schmidt et al.,[126] and Tully and Goldsmith[297] are plotted in Arrhenius form in Figure 32. In the rate constant evaluation the absolute rate constants determined by Atkinson and Pitts,[291] Ravishankara et al.,[294] Nip and Paraskevopoulos,[295] and Tully and Goldsmith,[297] together with the relative rate constants determined for a series of alkenes by Atkinson and Aschmann,[153] are used. The less precise room temperature data of Lloyd et al.,[144] Wu et al.,[136] Winer et al.,[292,293] Cox et al.,[139] Barnes et al.,[141] Zellner and Lorenz,[288] Schmidt et al.,[126] and Klein et al.[218] are in good agreement with these rate constants.

From a unit-weighted least-squares analysis of the rate constants of Atkinson and Pitts,[291] Ravishankara et al.,[294] Nip and Paraskevopoulos,[295] and Tully and Goldsmith[297] for temperatures ≤467 K, the Arrhenius expression

$$k(\text{propene}, T \leq 467 \text{ K}) = (4.72^{+0.63}_{-0.56}) \times 10^{-12} e^{(504\pm45)/T} \text{ cm}^3 \text{ molecule}^{-1} \text{ s}^{-1}$$

is obtained, where the errors are two least-squares

TABLE VIII. Rate Constants k and Arrhenius Parameters for the Gas-Phase Reaction of OH Radicals with Cyclic Mono-, Di-, and Trialkenes

cycloalkene	structure	$10^{12}A$, cm^3 molecule^{-1} s^{-1}	E, cal mol^{-1}	$10^{12}k$, cm^3 molecule^{-1} s^{-1}	T, K	technique	ref	temp range covered, K
cyclopentene				67.0 ± 2.4	298 ± 2	rel rate [rel to k(OH + 2-methyl-1,3-butadiene) = 1.01×10^{-10}]^a	Atkinson et al.[151]	
cyclohexene	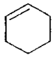			65.5	303	rel rate [rel to k(OH + *cis*-2-butene) = 5.46×10^{-11}]^a	Wu et al.[136]	
				75.7 ± 15.1	305 ± 2	rel rate [rel to k(OH + 2-methylpropene) = 4.95×10^{-11}]^a	Darnall et al.[219]	
				65.5	300	rel rate [rel to k(OH + ethene) = 8.45×10^{-12}]^a	Cox et al.[139]	
				67.6	~300	rel rate [rel to k(OH + ethene) = 8.45×10^{-12}]^a	Barnes et al.[141]	
				64.6 ± 2.5	297 ± 2	rel rate [rel to k(OH + 1,5-hexadiene) = 6.21×10^{-11}]^b	Ohta[142]	
				67.4 ± 1.7	298 ± 2	rel rate [rel to k(OH + 2-methyl-1,3-butadiene) = 1.01×10^{-10}]^a	Atkinson et al.[151]	
1,3-cyclohexadiene				163 ± 5	298 ± 2	rel rate [rel to k(OH + 2-methyl-1,3-butadiene) = 1.01×10^{-10}]^a	Atkinson et al.[151]	
1,4-cyclohexadiene	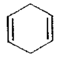			99.4 ± 3.1	297 ± 2	rel rate [rel to k(OH + 1,5-hexadiene = 6.21×10^{-11}]^b	Ohta[142]	
				99.4 ± 4.1	298 ± 2	rel rate [rel to k(OH + 2-methyl-1,3-butadiene) = 1.01×10^{-10}]^a	Atkinson et al.[151]	
cycloheptene	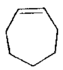			74.1 ± 2.3	298 ± 2	rel rate [rel to k(OH + 2-methyl-1,3-butadiene) = 1.01×10^{-10}]^a	Atkinson et al.[151]	
1,3-cycloheptadiene	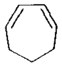			139 ± 4	294 ± 2	rel rate [rel to k(OH + 2-methyl-1,3-butadiene) = 1.02×10^{-10}]^a	Atkinson et al.[303]	
1,3,5-cycloheptatriene	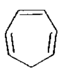			97.4 ± 2.5	294 ± 2	rel rate [rel to k(OH + 2-methyl-1,3-butadiene) = 1.02×10^{-10}]^a	Atkinson et al.[303]	
1-methylcyclohexene	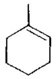			94.5 ± 18.9	305 ± 2	rel rate [rel to k(OH + 2-methylpropene) = 4.95×10^{-11}]^a	Darnall et al.[219]	
bicyclo[2.2.1]-2-heptene				49.1 ± 4.0	298 ± 2	rel rate [rel to k(OH + 2-methyl-1,3-butadiene) = 1.01×10^{-10}]^a	Atkinson et al.[151]	
bicyclo[2.2.1]-2,5-heptadiene				120 ± 10	298 ± 2	rel rate [rel to k(OH + 2-methyl-1,3-butadiene) = 1.01×10^{-10}]^a	Atkinson et al.[151]	
bicyclo[2.2.2]-2-octene				40.6 ± 1.9	298 ± 2	rel rate [rel to k(OH + 2-methyl-1,3-butadiene) = 1.01×10^{-10}]^a	Atkinson et al.[151]	
α-pinene	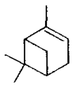			56.4 ± 8.5	305 ± 2	rel rate [rel to k(OH + 2-methylpropene) = 4.95×10^{-11}]^a	Winer et al.[292]	
				60.1 ± 8.2	298	FP-RF	Kleindienst et al.[306]	298–422
				51.0 ± 6.9	349			
		13.7	−887 ± 150	38.8 ± 5.7	422			
				54.5 ± 3.2	294 ± 1	rel rate [rel to k(OH + 2,3-dimethyl-2-butene) = 1.12×10^{-10}]^a	Atkinson et al.[304]	
β-pinene	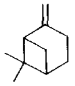			65.8 ± 9.9	305 ± 2	rel rate [rel to k(OH + 2-methylpropene) = 4.95×10^{-11}]^a	Winer et al.[292]	
				77.6 ± 11	297	FP-RF	Kleindienst et al.[306]	297–423
				67.8 ± 11	350			
		23.6	−712 ± 115	54.2 ± 10	423			
				79.5 ± 5.2	294 ± 1	rel rate [rel to k(OH + 2,3-dimethyl-2-butene) = 1.12×10^{-10}]^a	Atkinson et al.[304]	

d-limonene	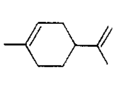	146 ± 22	305 ± 2	rel rate [rel to *k*(OH + 2-methylpropene) = 4.95 × 10^{-11}]^a	Winer et al.[292]
		169 ± 5	294 ± 1	rel rate [rel to *k*(OH + 2,3-dimethyl-2-butene) = 1.12 × 10^{-10}]^a	Atkinson et al.[304]
Δ^3-carene	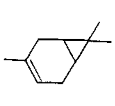	87.0 ± 4.3	294 ± 1	rel rate [rel to *k*(OH + 2,3-dimethyl-2-butene) = 1.12 × 10^{-10}]^a	Atkinson et al.[304]
γ-terpinene	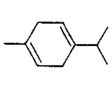	176 ± 18	294 ± 1	rel rate [rel to *k*(OH + 2,3-dimethyl-2-butene) = 1.12 × 10^{-10}]^a	Atkinson et al.[304]
α-phellandrene	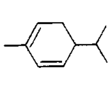	310 ± 71	294 ± 1	rel rate [rel to *k*(OH + 2,3-dimethyl-2-butene) = 1.12 × 10^{-10}]^a	Atkinson et al.[304]
α-terpinene	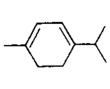	360 ± 40	294 ± 1	rel rate [rel to *k*(OH + 2,3-dimethyl-2-butene) = 1.12 × 10^{-10}]^a	Atkinson et al.[304]

---

[a] From the present recommendations (see text). [b] From the rate constant determined by Ohta.[142]

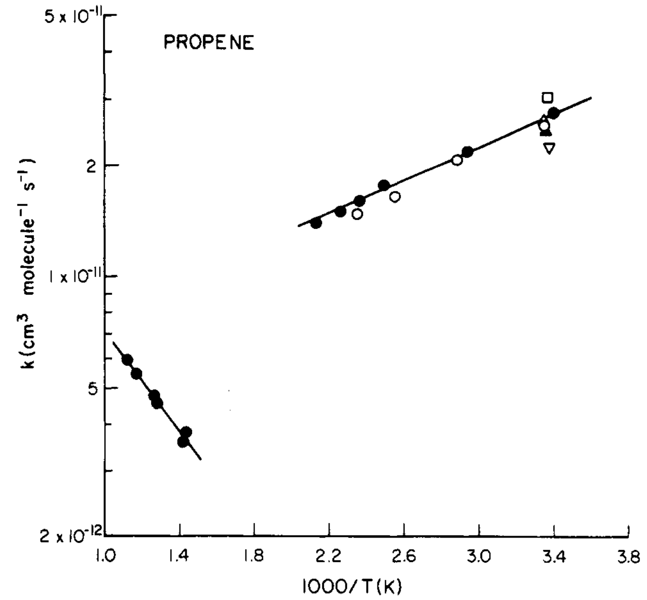

Figure 32. Arrhenius plot of the limiting high-pressure second-order rate constants for the reaction of OH radicals with propene: (○) Atkinson and Pitts;[291] (△) Ravishankara et al.;[294] (▲) Nip and Paraskevopoulos;[295] (□) Zellner and Lorenz;[288] (▽) Schmidt et al.;[126] (●) Tully and Goldsmith;[297] (—) recommendation (see text).

standard deviations. However, in the extensive and precise relative rate constant study of Atkinson and Aschmann,[153] relative rate constants for a series of alkenes (and *n*-butane and *n*-hexane) were obtained at 295 ± 1 K. Following the procedure of Atkinson and Aschmann,[153] a least-squares fit of these relative rate constants at 295 ± 1 K[153] to the absolute rate constants at 295 K for ethene,[122,287] propene,[291,294,295,297] 1-butene,[291,294,295] 1-pentene,[295] 3-methyl-1-butene,[298] 2-methylpropene,[291] *cis*-2-butene,[291] *trans*-2-butene,[291] 2-methyl-2-butene,[300] propadiene,[298] 1,3-butadiene,[298] and 2-methyl-1,3-butadiene[306] (using the observed temperature dependencies or an estimated Arrhenius activation energy of −1.0 kcal mol^{-1} to extrapolate or interpolate these observed absolute rate constants to 295 K) has been used to obtain a value of

$$k(\text{propene}) = 2.68 \times 10^{-11}\ \text{cm}^3\ \text{molecule}^{-1}\ \text{s}^{-1} \text{ at } 295\ \text{K}$$

with an estimated overall uncertainty of ~±15%.

Use of this 295 K rate constant, together with the temperature dependence derived above, yields the recommended Arrhenius expression of

$$k(\text{propene}, T \leq 467\ \text{K}) = (4.85^{+0.65}_{-0.58}) \times 10^{-12} e^{(504 \pm 45)/T}\ \text{cm}^3\ \text{molecule}^{-1}\ \text{s}^{-1}$$

where the error limits are two least-squares standard deviations

$$k(\text{propene}) = 2.63 \times 10^{-11}\ \text{cm}^3\ \text{molecule}^{-1}\ \text{s}^{-1} \text{ at } 298\ \text{K}$$

with an estimated uncertainty at 298 K of ±15%.

In the discussions below this Arrhenius expression, together with the 295 K relative rate constants derived by Atkinson and Aschmann,[153] is used to derive the rate constants at 295 K for the other alkenes and dialkenes studied by Atkinson and Aschmann.[153]

For temperatures ≥700 K, Tully and Goldsmith[297] have observed that the rate constant for the reaction of OH radicals with propene increases with increasing temperature (Figure 32), with an Arrhenius expression in this temperature regime ($896 < T < 701$ K) of

$$k(\text{propene}, 896 < T < 701\ \text{K}) = (3.30^{+0.86}_{-0.68}) \times 10^{-11} e^{-(1539\pm180)/T}\ \text{cm}^3\ \text{molecule}^{-1}\ \text{s}^{-1}$$

Recently, Smith et al.[314] have determined, using multiphoton infrared laser absorption to heat the reactant mixture and thermally dissociate H_2O_2, with LIF detection, rate constants for this reaction over the temperature range 960–1210 K [and for the reactions of OH radicals with methane (830–1412 K) and propane (1074 K)]. Over this limited temperature range, the rate constants were independent of the total pressure and fitted the Arrhenius expression

$$k(\text{propene}, 960 < T < 1210\ \text{K}) = (8.4 \pm 5.0) \times 10^{-11} e^{-(2870\pm600)/T}\ \text{cm}^3\ \text{molecule}^{-1}\ \text{s}^{-1}$$

These rate constants exhibit a significantly higher temperature dependence than reported by Tully and Goldsmith[297] for temperatures >701 K and are up to a factor of 2 lower than those calculated from the Arrhenius expression of Tully and Goldsmith.[297]

As discussed in the section below dealing with the mechanism of these reactions, these kinetic data suggest that at temperatures $\lesssim$467 K the reaction proceeds via OH radical addition to the olefinic double bond while for temperatures $\gtrsim$700 K the reaction proceeds via H atom abstraction from the $-CH_3$ substituent group. The rate constants of Tully and Goldsmith[297] for propene-d_6 are totally consistent with this scenario. Thus for temperatures $\lesssim$480 K, the rate constants for propene-h_6 and propene-d_6 are essentially identical, while for temperatures $\gtrsim$701 K the OH radical rate constants for reaction with propene-d_6 are ~35% lower than those for propene-h_6.[297] However, it should be noted that these propene-d_6 rate constants for temperatures ≥701 K also include other reaction processes, such as OD radical formation, in addition to H atom abstraction.[297]

c. 1-Butene. The available rate constants are listed in Table VI. As for propene, the limiting high-pressure second-order rate constants are obtained at total pressures of helium of $\gtrsim$20 torr.[294] The most recent kinetic data of Atkinson and Pitts,[291] Wu et al.,[136] Ravishankara et al.,[294] Nip and Paraskevopoulos,[295] Barnes et al.,[141] Biermann et al.[175] (which is possibly still in the fall-off region between second- and third-order kinetics), Ohta,[152] and Atkinson and Aschmann[153] are in good agreement. The rate constants of Atkinson and Pitts,[291] Ravishankara et al.,[294] Nip and Paraskevopoulos,[295] Ohta,[152] and Atkinson and Aschmann[153] are plotted in Arrhenius form in Figure 33. Since the sole reported temperature dependence is that of Atkinson and Pitts,[291] this temperature dependence is recommended. As for ethene and propene, the rate constant derived from the best fit analysis of the relative rate constant data of Atkinson and Aschmann[153] for a series of alkenes and dialkenes with the available absolute data (as described above) is recommended. This analysis yields

$$k(\text{1-butene}) = 3.19 \times 10^{-11}\ \text{cm}^3\ \text{molecule}^{-1}\ \text{s}^{-1}\ \text{at 295 K}$$

This rate constant, when combined with the temperature dependence reported by Atkinson and Pitts,[291] leads to the recommendation of

$$k(\text{1-butene}) = 6.53 \times 10^{-12} e^{468/T}\ \text{cm}^3\ \text{molecule}^{-1}\ \text{s}^{-1}$$

$$k(\text{1-butene}) = 3.14 \times 10^{-11}\ \text{cm}^3\ \text{molecule}^{-1}\ \text{s}^{-1}\ \text{at 298 K}$$

with an estimated uncertainty at 298 K of ±20%.

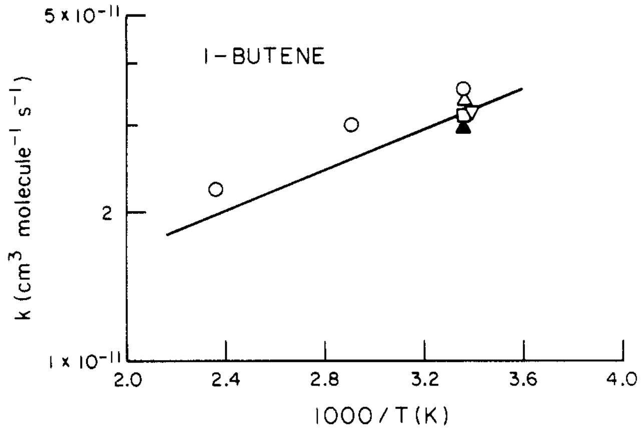

Figure 33. Arrhenius plot of the limiting second-order high-pressure rate constants for the reaction of OH radicals with 1-butene: (○) Atkinson and Pitts;[291] (▲) Ravishankara et al.;[294] (△) Nip and Paraskevopoulos;[295] (□) Ohta;[152] (▽) Atkinson and

The kinetic data of Barnes et al.,[141] Biermann et al.,[175] and Ohta,[152] which were not used in the evaluation, are in good[141,175] or excellent[152] agreement with this recommended rate constant.

d. 2-Methylpropene. The available kinetic data are listed in Table VI. The sole absolute study carried out is that of Atkinson and Pitts,[291] who also carried out the only temperature dependence study. Thus this temperature dependence,[291] equivalent to an Arrhenius activation energy of −1.00 kcal mol^{-1}, is used in combination with the best-fit rate constant from the relative rate constant data of Atkinson and Aschmann[153] of

$$k(\text{2-methylpropene}) = 5.23 \times 10^{-11}\ \text{cm}^3\ \text{molecule}^{-1}\ \text{s}^{-1}\ \text{at 295 K}$$

to yield the recommendation of

$$k(\text{2-methylpropene}) = 9.51 \times 10^{-12} e^{503/T}\ \text{cm}^3\ \text{molecule}^{-1}\ \text{s}^{-1}$$

$$k(\text{2-methylpropene}) = 5.14 \times 10^{-11}\ \text{cm}^3\ \text{molecule}^{-1}\ \text{s}^{-1}\ \text{at 298 K}$$

with an estimated uncertainty at 298 K of ±20%.

The relative rate constants at room temperature obtained by Wu et al.,[136] Barnes et al.,[141] and (especially) Ohta[152] are in good agreement with this recommendation.

e. *cis*-2-Butene. The available rate constants are listed in Table VI, from which it can be seen that the absolute rate constant study of Atkinson and Pitts[291] is in excellent agreement with the relative rate constants derived by Lloyd et al.,[144] Ohta,[152] and Atkinson and Aschmann.[153] As for the simpler alkenes discussed above, the Arrhenius activation energy determined by Atkinson and Pitts[291] is used, together with the best-fit rate constant at 295 K derived from the relative rate constant data of Atkinson and Aschmann[153] and the available absolute rate data for a series of alkenes and dialkenes (see above), to recommend

$$k(cis\text{-2-butene}) = 5.71 \times 10^{-11}\ \text{cm}^3\ \text{molecule}^{-1}\ \text{s}^{-1}\ \text{at } 295\ \text{K}$$

$$k(cis\text{-2-butene}) = 1.09 \times 10^{-11} e^{488/T}\ \text{cm}^3\ \text{molecule}^{-1}\ \text{s}^{-1}$$

$$k(cis\text{-2-butene}) = 5.61 \times 10^{-11}\ \text{cm}^3\ \text{molecule}^{-1}\ \text{s}^{-1}\ \text{at } 298\ \text{K}$$

with an estimated overall uncertainty at 298 K of ±20%.

The relative rate constant of Ohta[152] is in excellent agreement with this recommendation. However, as discussed previously,[1,153] the rate constant of Ravishankara et al.[294] at 298 K appears to be ~20% low, possibly because of wall losses in the static system used.

f. *trans*-2-Butene. The available kinetic data (apart from that of Cox,[307] as noted above) are listed in Table VI. The apparently reliable rate constant data of Atkinson and Pitts,[291] Wu et al.,[136] Ohta,[142] and Atkinson and Aschmann[153] are in reasonable agreement. Consistent with the previous criteria, the temperature dependence determined by Atkinson and Pitts[291] of an Arrhenius activation energy of −1.09 kcal mol^{-1} is used, together with the best fit of the relative rate constants of Atkinson and Aschmann[153] to the absolute rate constant data for a series of alkenes and dialkenes (see above), to yield

$$k(trans\text{-2-butene}) = 6.51 \times 10^{-11}\ \text{cm}^3\ \text{molecule}^{-1}\ \text{s}^{-1}\ \text{at } 295\ \text{K}$$

$$k(trans\text{-2-butene}) = 1.01 \times 10^{-11} e^{549/T}\ \text{cm}^3\ \text{molecule}^{-1}\ \text{s}^{-1}$$

$$k(trans\text{-2-butene}) = 6.37 \times 10^{-11}\ \text{cm}^3\ \text{molecule}^{-1}\ \text{s}^{-1}\ \text{at } 298\ \text{K}$$

with an estimated uncertainty at 298 K of ±20%.

g. 3-Methyl-1-butene. The sole data available for this alkene are (Table VI) from the absolute rate constant study of Atkinson et al.[298] and the relative rate constant study of Atkinson and Aschmann.[153] These data are in excellent agreement, and, consistent with the above discussions, lead to the recommendation of

$$k(\text{3-methyl-1-butene}) = 5.32 \times 10^{-12} e^{533/T}\ \text{cm}^3\ \text{molecule}^{-1}\ \text{s}^{-1}$$

$$k(\text{3-methyl-1-butene}) = 3.18 \times 10^{-11}\ \text{cm}^3\ \text{molecule}^{-1}\ \text{s}^{-1}\ \text{at } 298\ \text{K}$$

with an estimated uncertainty at 298 K of ±20%.

h. 2-Methyl-2-butene. The available kinetic data are listed in Table VI, and it can be seen that the more recent absolute and relative rate constants of Atkinson and Pitts,[300] Atkinson et al.,[147,301] Ohta,[142] and Atkinson and Aschmann[153] are in excellent agreement [the absolute rate constant study of Atkinson et al.[299] has been superseded by that of Atkinson and Pitts,[300] although it is in agreement with this later study[300] within the experimental error limits].

Again, consistent with the above recommendations for the alkenes, the temperature dependence of Atkinson and Pitts,[300] equivalent to an Arrhenius activation energy of −0.895 kcal mol^{-1}, is used together with the best-fit rate constant of

$$k(\text{2-methyl-2-butene}) = 8.84 \times 10^{-11}\ \text{cm}^3\ \text{molecule}^{-1}\ \text{s}^{-1}\ \text{at } 295\ \text{K}$$

to recommend

$$k(\text{2-methyl-2-butene}) = 1.92 \times 10^{-11} e^{450/T}\ \text{cm}^3\ \text{molecule}^{-1}\ \text{s}^{-1}$$

$$k(\text{2-methyl-2-butene}) = 8.69 \times 10^{-11}\ \text{cm}^3\ \text{molecule}^{-1}\ \text{s}^{-1}$$

at 298 K, with an estimated uncertainty at 298 K of ±20%.

i. 2,3-Dimethyl-2-butene. The available rate constants (all obtained at around room temperature) are listed in Table VI. The most recent rate constants of Atkinson et al.,[147,151,303,304] Atkinson and Aschmann,[153] and Ohta[152] are in good agreement, and, using an assumed Arrhenius activation energy of −1.0 kcal mol^{-1} for this reaction, a unit-weighted least-squares analysis of these data yields

$$k(\text{2,3-dimethyl-2-butene}) = 1.10 \times 10^{-10}\ \text{cm}^3\ \text{molecule}^{-1}\ \text{s}^{-1}\ \text{at } 298\ \text{K}$$

with an estimated uncertainty of ±20%.

Again, as discussed previously[1,147,153] the room-temperature rate constant obtained by Ravishankara et al.[294] is low, by a factor of ~2, presumably due to wall losses in the static reaction system used.

j. Propadiene. The available rate constants are listed in Table VII, and those of Atkinson et al.,[298] Ohta,[142] and Atkinson and Aschmann[153] are in good agreement. Atkinson et al.[298] showed that at room temperature the rate constant for this reaction is in the fall-off region between second- and third-order kinetics below ~25 torr total pressure of argon.

Consistent with the above recommendations for the alkenes, the observed temperature dependence, equivalent to an Arrhenius activation energy of −0.305 kcal mol^{-1},[298] is used together with the best-fit rate constant of

$$k(\text{propadiene}) = 9.84 \times 10^{-12}\ \text{cm}^3\ \text{molecule}^{-1}\ \text{s}^{-1}\ \text{at } 295\ \text{K}$$

to recommend

$$k(\text{propadiene}) = 5.86 \times 10^{-12} e^{153/T}\ \text{cm}^3\ \text{molecule}^{-1}\ \text{s}^{-1}$$

$$k(\text{propadiene}) = 9.79 \times 10^{-12}\ \text{cm}^3\ \text{molecule}^{-1}\ \text{s}^{-1}\ \text{at } 298\ \text{K}$$

with an estimated uncertainty at 298 K of ±25%.

The rate constant reported by Bradley et al.,[205] obtained at a total pressure of ~1 torr, is almost certainly in the fall-off region.

k. 1,3-Butadiene. The available kinetic data are listed in Table VII. It can be seen from this table that the room-temperature rate constants of Lloyd et al.,[144] Atkinson et al.,[298] Barnes et al.,[141] Ohta,[142] and Atkinson and Aschmann[153] are in very good agreement. As in the above recommendations for the alkenes, the sole temperature dependence of Atkinson et al.,[298] equivalent to an Arrhenius activation energy of −0.93 kcal mol^{-1}, is used together with the least-squares fit of the rate constants at 295 K of Atkinson and Aschmann[153] to the available absolute rate constant data (see above) to recommend

k(1,3-butadiene) =

$$1.39 \times 10^{-11} e^{468/T} \text{ cm}^3 \text{ molecule}^{-1} \text{ s}^{-1}$$

k(1,3-butadiene) =

$$6.68 \times 10^{-11} \text{ cm}^3 \text{ molecule}^{-1} \text{ s}^{-1} \text{ at } 298 \text{ K}$$

with an estimated uncertainty at 298 K of ±20%.

The relative rate constants of Lloyd et al.,[144] Barnes et al.,[141] and Ohta[142] are in very good agreement with this recommendation.

l. 2-Methyl-1,3-butadiene. The available rate constants are listed in Table VII. The most recent data of Atkinson et al.,[147] Atkinson and Aschmann,[153] Kleindienst et al.,[306] and Ohta[142] are in good agreement. Consistent with the above recommendations, the temperature dependence reported by Keindienst et al.,[306] equivalent to an Arrhenius activation energy of −0.813 kcal mol^{-1}, is used, together with the rate constant resulting from a best fit of the relative rate constants of Atkinson and Aschmann[195] to the available rate constant data of

k(2-methyl-1,3-butadiene) =

$$1.02 \times 10^{-10} \text{ cm}^3 \text{ molecule}^{-1} \text{ s}^{-1} \text{ at } 295 \text{ K}$$

to recommend

k(2-methyl-1,3-butadiene) =

$$2.55 \times 10^{-11} e^{409/T} \text{ cm}^3 \text{ molecule}^{-1} \text{ s}^{-1}$$

k(2-methyl-1,3-butadiene) =

$$1.01 \times 10^{-10} \text{ cm}^3 \text{ molecule}^{-1} \text{ s}^{-1} \text{ at } 298 \text{ K}$$

with an estimated uncertainty at 298 K of ±20%.

m. Cyclohexene. While no temperature-dependent data are available, the reported room-temperature rate constants[136,139,141,142,151,219] (Table VIII) are in good agreement. Using the above recommendation for 2-methyl-1,3-butadiene, it is recommended, based upon the recent study of Atkinson et al.,[151] that

k(cyclohexene) =

$$6.74 \times 10^{-11} \text{ cm}^3 \text{ molecule}^{-1} \text{ s}^{-1} \text{ at } 298 \text{ K}$$

with an estimated uncertainty of ±20%.

n. α-Pinene. The available kinetic data are listed in Table VIII and plotted in Arrhenius form in Figure 34. The room-temperature rate constants of Winer et al.,[292] Kleindienst et al.,[306] and Atkinson et al.[304] are in reasonable agreement. The temperature dependence determined by Kleindienst et al.[306] is used together with the 294 K rate constant of Atkinson et al.[304] to recommend

k(α-pinene) =

$$(1.20^{+0.52}_{-0.37}) \times 10^{-11} e^{(444 \pm 125)/T} \text{ cm}^3 \text{ molecule}^{-1} \text{ s}^{-1}$$

where the indicated error limits are two least-squares standard deviations

k(α-pinene) =

$$5.32 \times 10^{-11} \text{ cm}^3 \text{ molecule}^{-1} \text{ s}^{-1} \text{ at } 298 \text{ K}$$

with an estimated uncertainty at 298 K of ±25%.

o. β-Pinene. The available kinetic data are listed in Table VIII and plotted in Arrhenius form in Figure 35. The relative rate constant of Atkinson et al.[304] is in excellent agreement with the absolute rate constants of Kleindienst et al.[306] and in reasonable agreement with that of Winer et al.[292] As for α-pinene, the recommendation uses the temperature dependence determined by Kleindienst et al.,[306] in conjunction with the 294 K rate constant of Atkinson et al.,[304] to derive

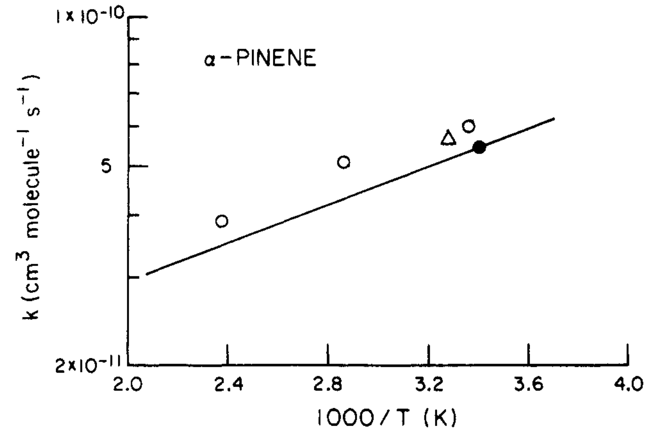

Figure 34. Arrhenius plot of the rate constants for the reaction of OH radicals with α-pinene: (△) Winer et al.;[292] (○) Kleindienst et al.;[306] (●) Atkinson et al.;[304] (—) recommendation (see text).

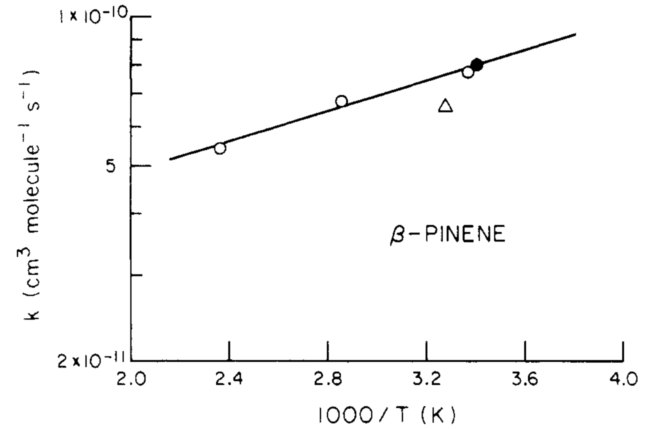

Figure 35. Arrhenius plot of the rate constants for the reaction of OH radicals with β-pinene: (△) Winer et al.;[292] (○) Kleindienst et al.;[306] (●) Atkinson et al.;[304] (—) recommendation (see text).

k(β-pinene) =

$$(2.36^{+0.88}_{-0.64}) \times 10^{-11} e^{(357 \pm 110)/T} \text{ cm}^3 \text{ molecule}^{-1} \text{ s}^{-1}$$

where the error limits are two least-squares standard deviations

k(β-pinene) =

$$7.82 \times 10^{-11} \text{ cm}^3 \text{ molecule}^{-1} \text{ s}^{-1} \text{ at } 298 \text{ K}$$

with an estimated uncertainty at 298 K of ±25%.

For the other alkenes, dialkenes, trialkenes, cycloalkenes, cyclodialkenes, and cyclotrialkenes listed in Tables VI through VIII, no specific recommendations are made. However, in general it is recommended that the room-temperature rate constants in Tables VI through VIII derived from the relative rate constant studies of Ohta,[142,152] Atkinson and Aschmann,[153] and Atkinson et al.[151,303,304] be used. Thus, as seen from these tables, these data of Ohta[142,152] and Atkinson and co-workers[151,153,303] are totally self-consistent, with virtually identical, to within typically ~5%, rate constants for a given alkene being derived from a variety of reference organics.

Apart from propadiene, it appears that these OH radical reactions exhibit temperature dependencies equivalent to a negative Arrhenius activation energy of very close to -1.0 kcal mol^{-1} (equivalent to a temperature dependence of $T^{-1.5}$ for the temperature ranges studied).

Two explanations for these negative temperature dependencies have been discussed,[1,291,315] these involving either (a) the initial formation of a weakly bound complex which can either decompose back to reactants or evolve to the OH–alkene adduct or (b) a bimolecular process with the negative temperature dependencies arising from a zero or near-zero activation energy combined with a temperature-dependent preexponential factor. In case (a), the presently favored explanation, the mechanism is then

$$A + B \underset{b}{\overset{a}{\rightleftharpoons}} (AB) \xrightarrow{c} AB^*$$

where (AB) is the weakly bound complex and AB* is the OH–alkene adduct. Hence $k_{obsd} = k_a k_c/(k_b + k_c)$ and negative temperature dependencies will arise, when, as expected to be generally the case, $k_b > k_c$ for $E_b > E_c$ and E_a being zero or near-zero.

In case (b), the preexponential factor A is given from transition state theory by[1,291]

$$A = \tau\left(\frac{kT}{h}\right)\frac{Q^{\ddagger}_{\text{OH-alkene}}}{Q_{\text{alkene}}Q_{\text{OH}}}$$

where τ is the transmission factor, kT/h is the frequency factor, and Q_{OH}, Q_{alkene}, and $Q^{\ddagger}_{\text{OH-alkene}}$ are the partition functions for the OH radical, the alkene, and the OH–alkene transition state, respectively. For temperature ranges below ~500 K, this reduces to[1,291]

$$A \;\alpha\; \tau\left(\frac{Q^{\ddagger}_{\text{OH-alkene}}}{Q_{\text{alkene}}}\right)T^{-1.5}$$

Hence if $\tau(Q^{\ddagger}_{\text{OH-alkene}}/Q_{\text{alkene}})$ is temperature independent, then the preexponential factor A will vary as $T^{-1.5}$ and so, for zero activation energy, will the rate constant. While at present nothing can be stated with any certainty about the vibrational partition function for the OH–alkene transition state, or its temperature dependence, this $T^{-1.5}$ dependence is essentially identical with the experimentally observed temperature dependencies for the reaction of OH radicals with unsaturated carbon–carbon bonds.

The room-temperature rate constants for the monoalkenes increase monotonically with the number of substituents around the double bond, and, as discussed by Atkinson et al.[151] for the acyclic and cyclic monoalkenes and the nonconjugated di- and trialkenes, the rate constants can be estimated to a high degree of accuracy (±30%) from the degree and position of alkyl substituents around the double bond(s).[151] Similarly, for alkenes containing conjugated double-bond systems, reasonably accurate predictions of the room temperature rate constants can be made from the rate constants for $>C{=}C{-}C{=}C<$ systems with the varying numbers of substituents around this double bond system. As an example, the OH radical rate constant for 3-methylene-7-methyl-1,6-octadiene (myrcene) can be estimated by addition of the rate constants for the $>C{=}CH-$ group (2-methyl-2-butene) to that for the $CH_2{=}CHC{=}CH_2$ group (2-methyl-1,3-butadiene).[151] This estimation technique is discussed below in section IV in more detail.

2. Mechanism

The available kinetic and mechanistic data show that at ≲500 K the reaction of OH radicals to the alkenes proceeds predominantly via addition of the OH radical to the carbon–carbon double bond(s). Thus in the discharge flow–mass spectrometric study of Morris et al.,[85] mass peaks corresponding to the OH–alkene adducts were observed for ethene and propene. These adduct peaks increased in intensity as the total pressure was increased from 1 to 4 torr,[85] showing that OH radical addition was occurring and that these addition adducts were being collisionally stabilized.

As noted above, numerous kinetic studies[78,119,218,287,288,297,309,311] have shown for ethene[78,119,218,287,288,309,311] and propene[218,288] that the rate constants are in the fall-off region between second-order and third-order kinetics at total pressures of argon below ~225 torr for ethene[218,287,288] and below ~10 torr for propene.[218,288] These observations show that these reactions proceed via initial addition of OH radicals to the alkene to form an initially energy-rich OH–alkene adduct, which can decompose back to the reactants or be collisionally stabilized, e.g., for ethene

$$OH + C_2H_4 \rightleftarrows HOC_2H_4^*$$

$$HOC_2H_4^* + M \rightarrow HOC_2H_4 + M$$

For ethene, Howard[78] has shown from a kinetic study over the total pressure range 0.7–7 torr of helium that the rate constant extrapolates to essentially zero at zero pressure. Thus, as expected from the high C–H bond energy of ~108 kcal mol^{-1} in ethene,[226] H atom abstraction from ethene is essentially negligible at room temperature.

This prediction from kinetic studies is confirmed by the recent discharge flow–mass spectrometric study of Bartels et al.,[316] in which the abstraction channel was shown to account for <2.5% of the overall reaction channels at ~2-torr total pressure and 295 K. These investigations[78,316] thus show, in contradiction to the earlier product study of Meagher and Heicklen[163] (involving a difficult to interpret final product analysis which can be reinterpreted as indicating an ~10% H atom abstraction route at the high-pressure limit), that H atom abstraction from ethene under atmospheric conditions is totally negligible.

For propene and the butenes, Hoyermann and Sievert[173,176] have shown from discharge flow–mass spectroscopy studies that H atom abstraction from these alkenes is also insignificant, being <5% for propene and 2-methylpropene and <10% for 1-butene and *cis* and *trans*-2-butene. That H atom abstraction from propene is negligible is totally consistent with the product study of Cvetanovic,[162] who, from a comprehensive investigation of the products formed and their formation reactions (mainly via radical-radical processes), concluded that the OH radical addition pathway was the major, if not exclusive reaction pathway, and that addition to the terminal carbon atom

$$OH + CH_2CH{=}CH_2 \rightarrow CH_3\dot{C}HCH_2OH$$

occurs ~65% of the time at room temperature.[162]

While it has been apparent for some time that H atom abstraction from ethene and the methyl-substituted alkenes is negligible at room temperature,[1] there have been questions concerning the importance of H atom abstraction from acyclic alkenes with $\geq C_2$ side chains containing weak allylic hydrogens. Thus Atkinson et al.[298] postulated from a correlation between the $O(^3P)$ atom and OH radical rate constants for a series of alkenes that H atom abstraction from 1-butene accounted for ~30% (19 ± 6% using the more recent rate constant data[152,153]) of the overall OH radical reaction at room temperature, and this postulate appeared to be confirmed by the photoionization–mass spectroscopy study of Biermann et al.[175] However, the recent definitive discharge flow–mass spectroscopic and final product studies of Hoyermann and Sievert[176] and Atkinson et al.[317] show that H atom abstraction from 1-butene accounts for <10% of the overall OH radical reaction at room temperature. In the recent study of Atkinson et al.,[317] a complete product balance was obtained, within the experimental error limits.

Hence it now appears that H atom abstraction from acyclic alkenes containing $\geq C_2$ side chains is also of minimal importance and that at room temperature the reactions of OH radicals with these alkenes can be considered to proceed almost totally via OH radical addition to the olefinic double bonds. Of course, for the 1-alkenes and other alkenes with long side chains it must be expected that H atom abstraction from the >CH–, $-CH_2-$, and $-CH_3$ groups will occur, but with rate constants for H abstraction from these groups approximately similar to those for the corresponding alkane groups.

However, Ohta[318] has shown that benzene is a minor, but significant, product formed during irradiations of CH_3ONO–NO–cyclohexadiene–air mixtures, accounting for 8.9% and 15.3% of the overall reaction pathways for 1,3-cyclohexadiene and 1,4-cyclohexadiene, respectively. These data show that H atom abstraction from the allylic C–H bonds (of bond dissociation energy 73 ± 5 kcal mol^{-1} [319]) in these cyclohexadienes does occur, with a rate constant per allylic C–H bond of $\sim 3.7 \times 10^{-12}$ cm^3 $molecule^{-1}$ s^{-1} for both 1,3- and 1,4-cyclohexadiene.

The formation of the OH–ethene adduct is calculated to be ~32 kcal mol^{-1} exothermic[226] (formation of the other OH–alkene adducts have similar calculated exothermicities) and formation of an H atom together with $HOCH{=}CH_2$ is endothermic from the reactants by ~7 kcal mol^{-1}.[226] Melius et al.[320] have calculated that the thermochemically most favorable decomposition pathway for the OH–ethene adduct involves redissociation back to the reactants. Indeed, at elevated temperatures decomposition of the thermalized OH–ethene adduct, and the thermalized OH–alkene adducts in general, is expected to occur, with a calculated lifetime at 660 K of ~1 ms.[1,312] This situation is analogous to that for the OH radical reactions with the aromatic hydrocarbons[312,313] and has been experimentally observed by Tully[122] and Tully and Goldsmith.[297] Thus in the recent flash photolysis studies of Tully[122] and Tully and Goldsmith[297] for ethene[122] and propene,[297] nonexponential OH radical decays were observed to occur for temperatures ≳438–481 K, and the derived rate constants decreased rapidly with increasing temperature over the temperature range ~450–700 K.

This is totally consistent with the increasing importance of thermal decomposition of the thermalized OH–alkene adducts at elevated temperature, with the adduct decomposing within the time scale of the experimental observations for temperatures ≳435–480 K. At still higher temperatures the addition pathway becomes unimportant due to the extremely rapid decomposition rate of the OH–alkene adduct back to reactants, and for ethene the reaction is then expected to proceed via H atom abstraction,[320] with a positive temperature dependence.

For the higher alkenes, as noted above, other decomposition pathways of the OH–alkene adducts (e.g., CH_3 radical elimination and isomerization followed by decomposition reactions) may also become of importance in this temperature regime, and the situation at elevated temperatures where thermal decomposition of the OH–alkene adduct becomes important may be more complex.[297,320]

Furthermore, at low total pressures other reactions of the chemically activated OH–alkene adducts can occur. Thus, for example, Bartels et al.[316] have observed the formation of HCHO + CH_3 and CH_3CHO + H as decomposition products of the OH–ethene adduct at total pressures of ~2 torr. Under these low-pressure conditions the reaction sequence appears to be[316]

$$\begin{tikzcd}
OH + C_2H_4 \arrow[r, shift left] & {[\dot{C}H_2CH_2OH]^*} \arrow[l, shift left] \arrow[r, "M"] \arrow[d, "isom"] & HO CH_2\dot{C}H_2 \\
 & {[CH_3CH_2O]^*} \arrow[r] \arrow[dr] & CH_3 + HCHO \\
 & & CH_3CHO + H
\end{tikzcd}$$

Clearly, at low total pressures and/or high temperatures, the reaction dynamics of these reactions, even for ethene, are complex, and further experimental and theoretical studies are required.

3. Mechanism under Atmospheric Conditions

As discussed above, the initial reaction of OH radicals with the alkenes at around room temperature leads to the formation of a rapidly thermalized OH–alkene adduct

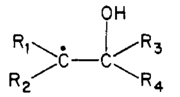

Analogous to alkyl radicals, this β-hydroxyalkyl radical is expected to react rapidly with O_2 under atmospheric conditions[3] to yield a (β-hydroxyalkyl)peroxy radical

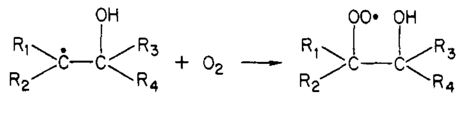

As discussed above for the alkylperoxy radicals, in the presence of NO these (β-hydroxyalkyl)peroxy radicals react to form the corresponding β-hydroxyalkoxy radicals, together with the formation of NO_2

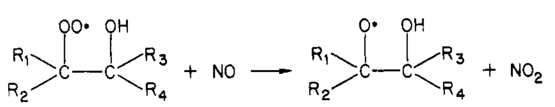

While formation of the hydroxyalkyl nitrates

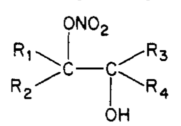

is also expected to occur from the $\geq C_3$ (β-hydroxyalkyl)peroxy radicals, no unambiguous evidence has been presented for this reaction pathway (partly because few, if any, data concerning such products have been reported for these $\geq C_3$ alkene reactions). As for the alkoxy radicals formed from the alkanes, these β-hydroxyalkoxy radicals can in principal react via three routes, i.e., reaction with O_2 (if an α-H atom is present), decomposition, and isomerization via a 1,5-H atom shift.[3]

Taking the $CH_3CH_2CH(OH)CH_2O\cdot$ radical formed subsequent to the internal addition of an OH radical to 1-butene as an example, these reactions are

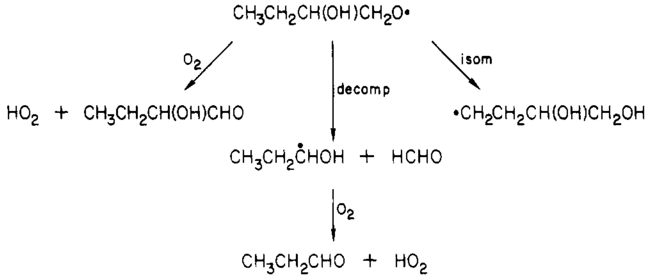

Obviously isomerization can only occur for alkenes with $\geq C_2$ side chains, and, at least for the $CH_3CH_2CH(OH)CH_2\dot{O}$ radical formed from 1-butene, isomerization does not appear to be of importance.[317] This experimental observation is in accord with the arguments of Atkinson and Lloyd[3] that decomposition should dominate over isomerization for the β-hydroxyalkoxy radicals formed from the reaction of OH radicals with the alkenes.

Despite earlier theoretical thermochemical estimates,[244,245,248,321] the experimental data show that under atmospheric conditions decomposition of these β-hydroxyalkoxy radicals dominates over reaction with O_2.[3,146,164,317] For the β-hydroxyalkoxy radical formed from ethene, Niki and co-workers[164] have shown that both reaction with O_2 and decomposition occur

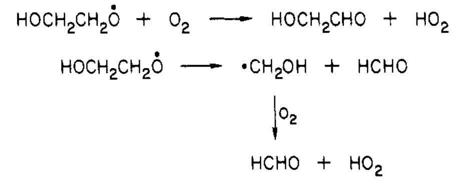

with the reaction with O_2 occurring 22 ± 5% of the time at 760 torr total pressure of air and 298 K.[164] For the β-hydroxyalkoxy radicals formed from the higher alkenes, Niki and co-workers[146] and Atkinson and co-workers[317] have shown that decomposition predominates, ultimately forming aldehydes and HO_2 (see also Atkinson and Lloyd[3]). As an example, the reaction sequence following OH radical addition to propene is shown in Figure 36.

D. Haloalkenes

1. Kinetics

The available limiting high-pressure second-order rate constants are listed in Table IX. In addition, Howard[78] has determined, using a discharge flow laser magnetic resonance (DF-LMR) technique, rate constants for the reactions of OH radicals with $CH_2{=}CHCl$, $CH_2{=}CF_2$, and $CF_2{=}CFCl$ at 296 K over the total pressure range of 0.7–7 torr of helium. For these haloalkenes the rate constants are in the fall-off region between second- and third-order kinetics,[78] with limiting high-pressure second-order rate constants at 296 K of $\gtrsim 2 \times 10^{-12}$ cm^3 molecule^{-1} s^{-1} for $CH_2{=}CF_2$ and $\gtrsim 7 \times 10^{-12}$ cm^3 molecule^{-1} s^{-1} for $CF_2{=}CFCl$.[78] For $CHCl{=}CCl_2$ the reaction at 296 K is in the fall-off region below ~2 torr total pressure of helium.[78]

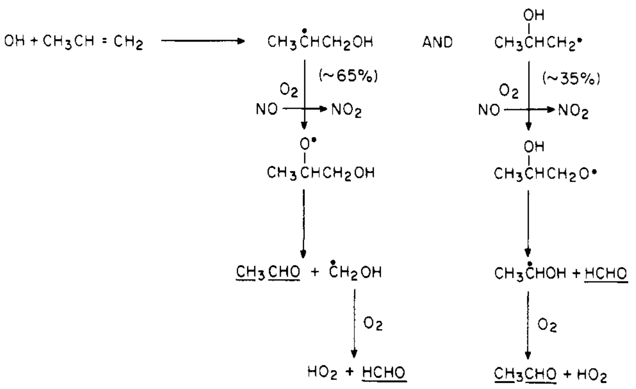

Figure 36. The reaction sequence under atmospheric conditions (in the presence of NO) following OH radical reaction with propene (stable products are underlined and the possible formation of minor amounts of hydroxyalkyl nitrates has been neglected).

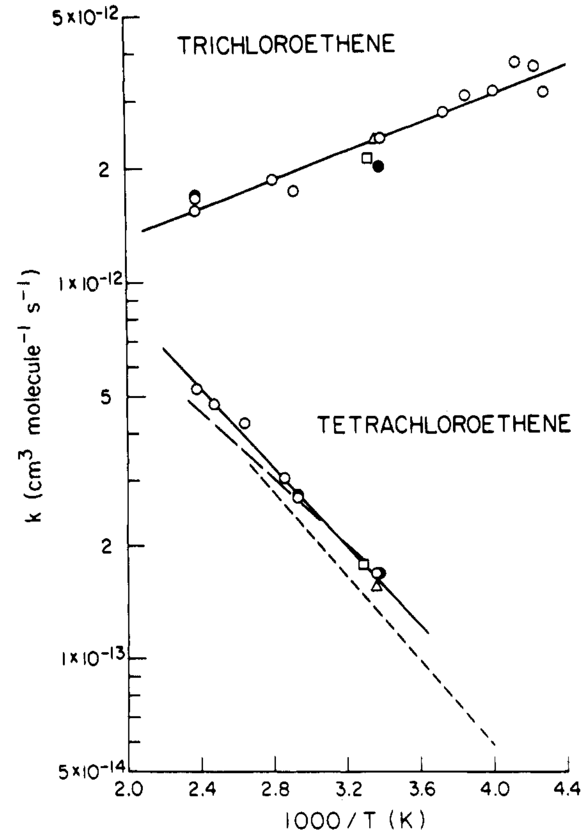

Figure 37. Arrhenius plot of the limiting high-pressure rate constants for the reaction of OH radicals with trichloroethene and tetrachloroethene: (●) Howard;[78] (○) Chang and Kaufman;[265] (△) Davis et al.;[323] (- - -) Arrhenius line of Davis et al.[323] for tetrachloroethene; (□) Kirchner;[324] (— — —) Arrhenius line of Kirchner[324] for tetrachloroethene; (—) recommendations (see text).

Rate constant data for the individual haloalkenes are discussed below.

a. Trichloroethene. The available rate constants[78,265,292,323,324] are listed in Table IX, and those of

TABLE IX. Rate Constants and Arrhenius Parameters for the Gas-Phase Reaction of OH Radicals with Haloalkenes at the High-Pressure Limit

haloalkene	$10^{12}A$, cm^3 molecule^{-1} s^{-1}	E, cal mol^{-1}	$10^{12}k$, cm^3 molecule^{-1} s^{-1}	T, K	technique	ref	temp range covered, K
$CH_2{=}CHF$			5.56 ± 0.56	299.2	FP-RF	Perry et al.[322]	299–426
			4.44 ± 0.45	346.8			
	1.48	−775 ± 300	3.76 ± 0.38	426.1			
$CH_2{=}CHCl$			6.60 ± 0.66	299.2	FP-RF	Perry et al.[322]	299–423
			5.01 ± 0.51	357.8			
	1.14	−1045 ± 300	3.95 ± 0.40	422.5			
$CH_2{=}CHBr$			6.81 ± 0.69	298.6	FP-RF	Perry et al.[322]	299–424
			6.00 ± 0.60	350.0			
	1.79	−805 ± 300	4.56 ± 0.46	423.7			
$CHCl{=}CCl_2$			4.4 ± 1.3	305 ± 2	rel rate [rel to k(OH + 2-methylpropene) = 4.95×10^{-11}]^a	Winer et al.[292]	
			2.0 ± 0.4	296	DF-LMR	Howard[78]	
			2.35 ± 0.25	298	FP-RF	Davis et al.[323]	
			3.12 ± 0.24	234	DF-RF	Chang and Kaufman[265]	234–420
			3.65 ± 0.21	237			
			3.73 ± 0.18	243			
			3.14 ± 0.16	250			
			3.06 ± 0.07	260			
			2.78 ± 0.17	268			
			2.37 ± 0.10	296			
			1.74 ± 0.04	343			
			1.86 ± 0.13	357			
			1.67 ± 0.03	420			
			1.55 ± 0.06	420			
	0.532 ± 0.071	−884 ± 81	1.68 ± 0.04	420			
			2.11	305	DF-MS	Kirchner[324]	
$CCl_2{=}CCl_2$			2.2 ± 0.7	305 ± 2	rel rate [rel to k(OH + 2-methylpropene) = 4.95×10^{-11}]^a	Winer et al.[292]	
			0.170 ± 0.034	296	DF-LMR	Howard[78]	
	10.5 ± 5.0	2573 ± 298	0.155 ± 0.015	298	FP-RF	Davis et al.[323]	250–375
			0.169 ± 0.007	297	DF-RF	Chang and Kaufman[265]	297–420
			0.270 ± 0.009	341			
			0.276 ± 0.010	341			
			0.303 ± 0.034	350			
			0.424 ± 0.016	378			
			0.477 ± 0.014	403			
	9.44 ± 1.34	2382 ± 109	0.526 ± 0.061	420			
	5.53	2055	0.179	305	DF-MS	Kirchner[324]	~305–430^b
Z-$CH_2ClCH{=}CHCl$			7.48 ± 0.12	295 ± 2	rel rate [rel to k(OH + n-octane) = 8.71×10^{-12}]^a	Tuazon et al.[272]	
E-$CH_2ClCH{=}CHCl$			12.6 ± 0.4	295 ± 2	rel rate [rel to k(OH + n-octane) = 8.71×10^{-12}]^a	Tuazon et al.[272]	
$(CH_2Cl)_2C{=}CH_2$			40.2 ± 5.4	295 ± 2	rel rate [rel to k(OH + 2-methyl-1,3-butadiene) = 1.02×10^{-10}]^a	Tuazon et al.[272]	

[a] From the present recommendations (see text). [b] Temperature range covered estimated from the graphical presentation.[324]

Howard,[78] Davis et al.,[323] Chang and Kaufman,[265] and Kirchner,[324] which are in good agreement, are plotted in Arrhenius form in Figure 37. The relative rate constant of Winer et al.[292] was at, or close to, the lower limit of values able to be derived by their technique and has hence been neglected in the evaluation. The rate constant recently reported by Kirchner[324] at 305 K has not been used in the evaluation because of the general lack of details available.

From a unit-weighted least-squares analysis of the data of Howard,[78] Davis et al.,[323] and Chang and Kaufman,[265] the recommended Arrhenius expression

$$k(\text{trichloroethene}) = (5.63^{+1.54}_{-1.20}) \times 10^{-13} e^{(427\pm70)/T} \text{ cm}^3 \text{ molecule}^{-1} \text{ s}^{-1}$$

is obtained, where the errors are two least-squares standard deviations

$$k(\text{trichloroethene}) = 2.36 \times 10^{-12} \text{ cm}^3 \text{ molecule}^{-1} \text{ s}^{-1} \text{ at } 298 \text{ K}$$

with an estimated uncertainty at 298 K of ±30%.

b. Tetrachloroethene. The kinetic data[78,265,292,323,324] are listed in Table IX, and those of Howard,[78] Davis et al.,[323] Chang and Kaufman,[265] and Kirchner,[324] which are in good agreement, are plotted in Arrhenius form in Figure 37. (Only the reported rate constants at 298 K and 305 K for the studies of Davis et al.[323] and Kirchner,[324] respectively, can be plotted, together with the reported Arrhenius expressions.[323,324]) Analogous to the case for trichloroethene, the relative rate constant obtained by Winer et al.[292] has been neglected and the kinetic data of Kirchner[324] have not been used in the evaluation.

From a unit-weighted least-squares analysis of the data of Howard,[78] Chang, and Kaufman[265] and the 298 K rate constant of Davis et al.,[323] it is recommended that

$$k(\text{tetrachloroethene}) = (9.64^{+2.85}_{-2.20}) \times 10^{-12} e^{-(1209\pm88)/T} \text{ cm}^3 \text{ molecule}^{-1} \text{ s}^{-1}$$

where the indicated errors are two least-squares standard deviations

$$k(\text{tetrachloroethene}) = 1.67 \times 10^{-13} \text{ cm}^3 \text{ molecule}^{-1} \text{ s}^{-1} \text{ at } 298 \text{ K}$$

with an estimated uncertainty at 298 K of ±30%.

For the remaining haloalkenes, no recommendations are made. It is of interest to note that for vinyl fluoride, vinyl chloride, vinyl bromide, and trichloroethene, the reported temperature dependencies are negative, with Arrhenius activation energies of ~−1 kcal mol^{-1} (similar to those for the alkenes), while tetrachloroethene has a positive Arrhenius activation energy of ~2.4 kcal mol^{-1}.

2. Mechanism

The available kinetic and product data show that, analogous to the alkenes, these reactions proceed via OH radical addition to the carbon–carbon double bonds. This is totally consistent with the observed fall-off dependence of several of these rate constants,[78] and hence, taking the vinyl halides as an example, these reactions proceed via addition of the OH radical to the haloalkenes to form an initially energy-rich OH–haloalkene adduct. This adduct can decompose back to the reactants or be collisionally stabilized, as shown, for example, for the vinyl halides (X = F, Cl, or Br).

$$\text{OH} + \text{CH}_2\text{=CHX} \rightleftarrows \text{HOC}_2\text{H}_3\text{X}^*$$

$$\text{HOC}_2\text{H}_3\text{X}^* + \text{M} \rightarrow \text{HOC}_2\text{H}_3\text{X} + \text{M}$$

This reaction to form the OH–haloalkene adduct is ~35 kcal mol^{-1} exothermic for all three halogen substituents[226] (similar to the situation for the alkenes). The elimination of an F atom from the OH–vinyl fluoride adduct

$$\text{HOC}_2\text{H}_3\text{F}^* \rightarrow \text{CH}_2\text{=CHOH} + \text{F}$$

is endothermic by ~19 kcal mol^{-1}.[322] Hence for the reactions of OH radicals with vinyl fluoride, and for other haloalkenes containing no Cl or Br atoms attached to the double bond, the rate constant will exhibit similar behavior to that for ethene, showing fall-off behavior from second- to third-order kinetics as the total pressure decreases.

For the reaction of OH radicals with vinyl chloride and vinyl bromide (any by analogy, probably also for other haloalkenes with Cl or Br atoms attached to the olefinic double bond) the elimination of Cl or Br atoms from the OH–haloalkene adducts are thermochemically favorable,[78] with the overall reactions being exothermic by ~11 and ~24 kcal mol^{-1} for X = Cl and Br, respectively.[322] In order for these Cl or Br atom eliminations to occur, the OH radical must add at the carbon atom to which the halogen substituent is located (the α-carbon atom) or, after OH radical addition to the β-carbon atom, a rapid 1,2-migration of OH must occur. If these elimination reactions occur, then the observed rate constants will exhibit second-order kinetics, even at low total pressures where collisional stabilization of the OH–haloalkene adducts is not effective. At higher total pressures collisional stabilization of the adducts will become competitive with Cl or Br atom elimination, although the observed rate constant will remain pressure independent and still be that for the initial reaction to form the adduct.

However, Howard[78] has shown that for the reaction of OH radicals with vinyl chloride at 296 K the rate constant approaches a limiting low-pressure value of ~1 × 10^{-12} cm^3 molecule^{-1} s^{-1}, a factor of ~7 lower than the limiting high-pressure rate constant.[322] Thus the elimination of a Cl atom is a relatively minor reaction pathway. This then implies that for the reaction of OH radicals with vinyl chloride (and presumably for other haloalkenes with Cl or Br atoms attached to the double bond) the two extreme reaction pathways involve either (a) OH radical addition only to the β-carbon atom and that a 1,2-migration of OH has an activation energy of $\gtrsim$35 kcal mol^{-1}, so that this 1,2-migration becomes rate determining, or (b) OH radical addition occurs at both the α- and β-positions, but mainly at the β-position, the 1,2-migration of OH is negligible slow, and hence the elimination reaction occurs only after OH radical addition at the α-position. While this latter situation is the most likely,[322] further work concerning both the pressure dependencies of the overall rate constants and the amount of reaction proceeding via halogen atom elimination is required for this class of organic compounds.

3. Mechanism under Atmospheric Conditions

Little information is available concerning the products and mechanisms of these reactions under atmospheric conditions. By analogy with the alkenes, the OH–haloalkene adducts are expected to rapidly add O_2 and then react with NO to yield the alkoxy radical, as shown, for example, for vinyl chloride

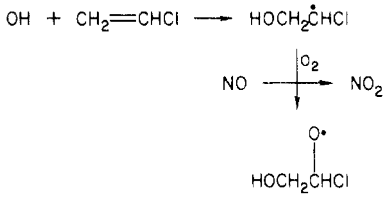

However, the subsequent reactions of these alkoxy radicals under atmospheric conditions are not known. A recent product study[325] has shown the formation of HC(O)Cl from vinyl chloride and trichloroethene and of phosgene ($COCl_2$) from trichloroethene and tetrachloroethene, though in less than unit yields (especially so for $COCl_2$ from tetrachloroethene).[325] Thus, although decomposition of these hydroxyhaloalkoxy radicals does occur, other reaction pathways also appear to be operative, e.g.

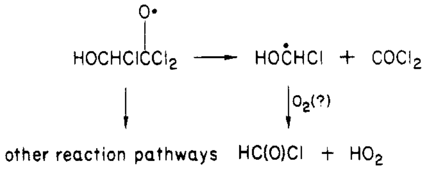

Further work concerning the products and mechanisms, subsequent to the initial OH radical addition, of the haloalkenes under atmospheric conditions is clearly necessary.

E. Alkynes

1. Kinetics

The available kinetic data, reported to be at the high-pressure limit, are listed in Table X. Wilson and Westenberg[188] also measured an effective rate constant for the reaction of OH radicals with acetylene of $nk = 1.0 \times 10^{-12}$ cm^3 molecule^{-1} s^{-1} at 300 K and ~1-torr total pressure of argon and helium, where n is the stoichiometry number, which was not measured. The data for the individual reactions are discussed below.

a. Acetylene. Despite earlier evidence that the rate constant for the reaction of OH radicals with acetylene did not exhibit a pressure dependence,[118,309,333,334] the more recent flash or laser photolysis studies of Perry et al.,[96] Michael et al.,[326] Perry and Williamson,[327] Schmidt et al.,[126] and Wahner and Zetzsch[329] show conclusively that this rate constant exhibits fall-off behavior below ~200-torr (and probably below ~1000-torr[126,329]) total pressure of argon or nitrogen at around room temperature.

The reported limiting second-order high-pressure rate constants are listed in Table X and those of Perry et al.,[96] Michael et al.,[326] Perry and Williamson,[327] Atkinson and Aschmann,[328] Schmidt et al.,[126] and Wahner and Zetzsch[329] are plotted in Arrhenius form in Figure 38. It can be seen that the room-temperature limiting high-pressure rate constants show a spread of ~30% and that the temperature dependence reported by Michael et al.[326] of ~1.3 kcal mol^{-1} is significantly higher than those determined by Perry et al.[96] and Perry and Williamson[327] of ~0.3–0.6 kcal mol^{-1}.

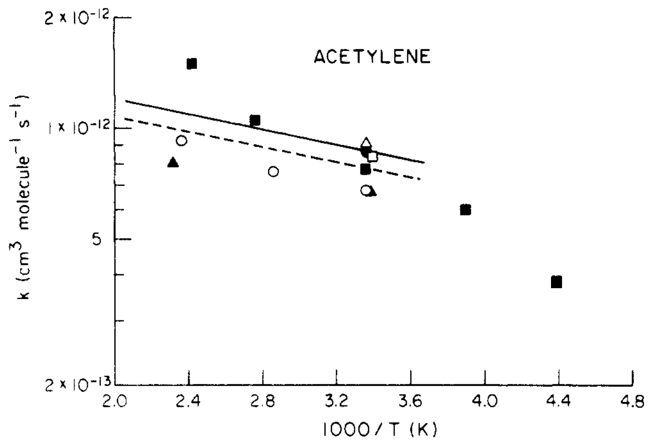

Figure 38. Arrhenius plot of the limiting high-pressure rate constants for the reaction of OH radicals with acetylene: (○) Perry et al.;[96] (■) Michael et al.;[326] (▲) Perry and Williamson;[327] (●) Atkinson and Aschmann;[328] (□) Schmidt et al.;[126] (△) Wahner and Zetzsch;[329] (—) limting high-pressure recommendation; (- - -) 760-torr total pressure of air recommendation (see text).

On the basis of the more recent studies of Schmidt et al.[126] and Wahner and Zetzsch,[329] which extended to higher total pressures, it is likely that the rate constants reported by Perry et al.[96] and Perry and Williamson[327] were not completely at the high-pressure limit. The recommended limiting high-pressure rate constant for this reaction utilizes the temperature dependence obtained by Perry et al.[96] and Perry and Williamson,[327] together with the mean of the room-temperature limiting high-pressure rate constants of Schmidt et al.[126] and Wahner and Zetzsch,[329] yielding

$$k(\text{acetylene, limiting high pressure}) = 1.90 \times 10^{-12} e^{-(233\pm127)/T} \text{ cm}^3 \text{ molecule}^{-1} \text{ s}^{-1}$$

where the indicated error limit in the Arrhenius activation energy is two least-squares standard deviations

$$k(\text{acetylene, limiting high pressure}) = 8.7 \times 10^{-13} \text{ cm}^3 \text{ molecule}^{-1} \text{ s}^{-1} \text{ at } 298 \text{ K}$$

with an estimated uncertainty at 298 K of ±30%.

At atmospheric pressure (i.e., 760-torr total pressure of air), the recommended rate constants are ~10% lower, based upon the kinetic studies of Schmidt et al.[126] and Wahner and Zetzsch,[329] i.e.

$$k(\text{acetylene, 760 torr of air}) = 1.7 \times 10^{-12} e^{-(233\pm127)/T} \text{ cm}^3 \text{ molecule}^{-1} \text{ s}^{-1}$$

where the indicated error limit in the Arrhenius activation energy is again two least-squares standard deviations and

$$k(\text{acetylene, 760 torr of air}) = 7.8 \times 10^{-13} \text{ cm}^3 \text{ molecule}^{-1} \text{ s}^{-1}$$

at 298 K, with an estimated overall uncertainty at 298 K of ±25%.

In the fall-off region, rate constants have been obtained by Perry et al.,[96] Michael et al.,[326] Perry and Williamson,[327] Schmidt et al.,[126] and Wahner and Zetzsch.[329] The data of Perry et al.,[96] Perry and Wil-

TABLE X. Rate Constants *k* and Arrhenius Parameters for the Gas-Phase Reaction of OH Radicals with Alkynes at the High-Pressure Limit

alkyne	$10^{12}A$, cm^3 molecule^{-1} s^{-1}	*E*, cal mol^{-1}	$10^{12}k$, cm^3 molecule^{-1} s^{-1}	*T*, K	technique	ref	temp range covered, K
acetylene			0.165 ± 0.015	300	FP-RF	Davis et al.[309]	
			0.679 ± 0.070	298.1	FP-RF	Perry et al.[96]	298–422
			0.763 ± 0.100	350.2			
	1.91	620 ± 400	0.926 ± 0.120	422.4			
			0.384 ± 0.025	228	FP-RF	Michael et al.[326]	228–413
			0.597 ± 0.050	257			
			0.776 ± 0.073	298			
			1.06 ± 0.16	362			
	6.83 ± 1.19	1284 ± 93	1.50 ± 0.16	413			
			0.675 ± 0.70	297	FP-RF	Perry and Williamson[327]	297–429
			0.798 ± 0.90	429			
			0.86 ± 0.14	298 ± 2	rel rate [rel to $k(OH + cyclohexane) = 7.38 \times 10^{-12}$]^a	Atkinson and Aschmann[328]	
			0.83 ± 0.08	295	LP-LIP	Schmidt et al.[126]	
			0.9^b	298 ± 3	LP-RA	Wahner and Zetzsch[329]	
propyne			0.95 ± 0.17^c	300	DF-EPR	Bradley et al.[205]	
			6.06 ± 0.30	298 ± 2	rel rate [rel to $k(OH + cyclohexane) = 7.38 \times 10^{-12}$]^a	Atkinson and Aschmann[328]	
1-butyne			8.04 ± 0.23	298 ± 2	rel rate [rel to $k(OH + cyclohexane) = 7.38 \times 10^{-12}$]^a	Atkinson and Aschmann[328]	
butadiyne (diacetylene)			50	*d*	DF-RF	Homann et al.[330]	
			15.7 ± 0.6	297 ± 2	rel rate [rel to $k(OH + cyclohexane) = 7.34 \times 10^{-12}$]^a	Atkinson and Aschmann[331]	
			15.6 ± 0.2	297 ± 2	rel rate [rel to $k(OH + n\text{-octane}) = 8.68 \times 10^{-12}$]^a	Atkinson and Aschmann[331]	
			22.0 ± 1.1	296	FP-RF	Perry[332]	296–688
			19.5 ± 1.4	365			
			18.2 ± 2.0	475			
	11.1	−410 ± 300	14.5 ± 0.9	688			

[a] From the present recommendations (see text). [b] Rate constants of (8.3 ± 0.6) × 10^{-13} cm^3 molecule^{-1} s^{-1} and (8.1 ± 0.7) × 10^{-13} cm^3 molecule^{-1} s^{-1} were determined at total pressures of N_2 diluent of 749 and 771 torr, respectively.[329] [c] Probably in the fall-off region between second- and third-order kinetics.[1] [d] Room temperature, not reported.

liamson,[327] Schmidt et al.,[126] and Wahner and Zetzsch[329] are in reasonably good agreement and show that the limiting low-pressure second-order rate constant at room temperature is $\lesssim 3 \times 10^{-13}$ cm^3 molecule^{-1} s^{-1} and may in fact be much lower [Schmidt et al.[126] estimate a limiting low-pressure second-order rate constant at room temperature of $\sim(5 \pm 3) \times 10^{-14}$ cm^3 molecule^{-1} s^{-1}]. This is in contrast to the data of Michael et al.,[326] which indicate a limiting low-pressure second-order rate constant of $\sim 4 \times 10^{-13}$ cm^3 molecule^{-1} s^{-1}, independent of temperature over the range 228–413 K. Consistent with the high-pressure rate constant recommendations, the data of Perry et al.,[96] Perry and Williamson,[327] Schmidt et al.,[126] and Wahner and Zetzsch[329] in the fall-off regime are recommended. These room-temperature rate constants of Schmidt et al.[126] and Wahner and Zetzsch[329] for M = N_2 or air can be reasonably well fit by the equation

$$k(\text{acetylene, 298 K}) = \left(\frac{k_0[\mathrm{M}]}{1 + \dfrac{k_0[\mathrm{M}]}{k_\infty}}\right) 0.6^{\{1+ [\log k_0[\mathrm{M}]/k_\infty]^2\}^{-1}}$$

with

$$k_0 = 4 \times 10^{-30} \text{ cm}^6 \text{ molecule}^{-2} \text{ s}^{-1}$$

$$k_\infty = 8.7 \times 10^{-13} \text{ cm}^3 \text{ molecule}^{-1} \text{ s}^{-1}$$

For the remaining alkynes studied to date (propyne, 1-butyne, and butadiyne), no firm recommendations are made. The rate constant obtained by Bradley et al.[205] for propyne at $\sim$1-torr total pressure is almost certainly in the fall-off kinetic regime.[1] The room-temperature rate constants increase markedly from acetylene to propyne, with a further small increase to 1-butyne,[328] totally consistent with these reactions proceeding via OH radical addition to the $-C{\equiv}C-$ bond.[96,328]

For butadiyne, the most recent studies of Atkinson and Aschmann[331] and Perry[332] indicate that the room-temperature rate constant is $\sim 2 \times 10^{-11}$ cm^3 molecule^{-1} s^{-1}. The sole temperature dependence reported[332] yields a negative Arrhenius activation energy of -0.4 kcal mol^{-1}, consistent with the temperature dependencies observed for the alkenes which have similar room temperature rate constants.

2. Mechanism

As discussed above, the observations of a fall-off in the rate constants for acetylene below $\sim$200–1000-torr total pressure of argon or nitrogen[96,126,326,327,329] show that the initial reaction of OH radicals with acetylene proceeds via OH radical addition to the $-C{\equiv}C-$ bond to form an initially energy-rich adduct

$$OH + C_2H_2 \rightarrow [HOCH{=}\dot{C}H]^*$$

This addition reaction to form the adduct is estimated to be exothermic by $\sim$30 kcal mol^{-1}.[226] Hence, analogous to the situation for the alkenes and haloalkenes, this energy-rich HOC_2H_2 radical adduct can then back-decompose to reactants or be collisionally stabilized

$$[HOCH{=}\dot{C}H]^* \rightarrow OH + C_2H_2$$

$$[HOCH{=}\dot{C}H]^* + M \rightarrow HOCH{=}\dot{C}H + M$$

A further possible decomposition pathway for the adduct is via the elimination of an H atom[1,96,335]

$$[HOCH{=}\dot{C}H]^* \rightarrow \rightarrow H + C_2H_2O$$

The overall reaction

$$OH + C_2H_2 \rightarrow H + C_2H_2O$$

is exothermic by $\sim$26 kcal mol^{-1} if the C_2H_2O product is ketene, but if the initial product formed after H atom elimination is $HOC{\equiv}CH$, then the elimination reaction will be much less exothermic.[1,96]

The formation of C_2H_2O and C_2DHO from the reaction of OH radicals with C_2H_2 and C_2D_2, respectively, has been observed by Gutman and co-workers[170] using crossed molecular beams with photoionization mass spectrometric detection. These observations indicate that this elimination reaction does occur, with the H (or D) atom eliminated originating from the acetylene.[170] More recently, the C_2H_2O product has been identified as ketene by Hack et al.[336] from a discharge flow–mass spectrometry study of this reaction at a total pressure of $\sim$2 torr. The low-pressure room temperature rate constant estimated by Schmidt et al.[126] may then be associated with that for the overall elimination reaction, although further work is obviously necessary concerning this issue. Under these low-pressure conditions, the initially formed, energy-rich, OH–C_2H_2 adduct can thus either be stabilized or isomerize (presumably to the vinoxy radical) with subsequent decomposition.[336] This reaction sequence explains the observed formation of CHDCO from the reactions of OH radicals with C_2D_2[170] and OD radicals with C_2H_2.[336]

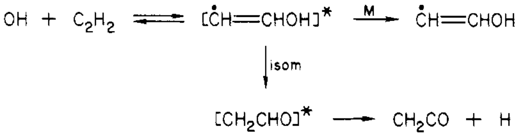

Recent product data at higher pressure and room temperature[126] (see below) indicates that the thermalized OH–C_2H_2 adduct can also isomerize to the vinoxy radical, followed by secondary reactions of this vinoxy radical.

However, at elevated temperatures, where back-decomposition of the thermalized OH–C_2H_2 adduct becomes rapid, the reaction will then be expected to switch over from predominant initial formation of the thermalized OH–C_2H_2 adduct to formation of CH_2CO + H via a direct reaction involving initial OH radical addition followed by isomerization and H atom elimination.[335,337] (It should be noted that no direct reaction not involving the formation of an OH–C_2H_2 adduct is postulated to occur.) In the transition region between these two temperature regimes, nonexponential OH radical decays may be observed (as for the alkenes[122,297] and the aromatic hydrocarbons[312,313]). The expected kinetic and mechanistic behavior of this OH radical reaction with acetylene has been recently discussed in detail from a theoretical viewpoint by Lin and Lin[335] and Smith et al.,[337] and this latter study[337] has also provided important experimental kinetic data over the temperature range 900–1300 K. Clearly, the products and their distributions arising from this reaction (and from OH radical reactions with the alkynes and alkenes in general) are highly dependent upon the pressure and temperature regimes encountered.

For the higher alkynes, the reactions are also expected to proceed via initial OH radical addition,[328] although at elevated temperatures elimination processes will probably become more complex.[332]

3. Mechanism under Atmospheric Conditions

The only information concerning the reaction mechanism and products formed under atmospheric conditions for this class of organics arises from the recent study of the reaction of OH radicals with acetylene carried out by Schmidt et al.[126] In this study, with argon or air as the diluent gas, it was evident that OH radicals were regenerated from the reaction of OH radicals with C_2H_2 (in the presence of O_2), and the vinoxy (CH_2CHO) radical was directly observed by laser-induced fluorescence.[126] Glyoxal was the major stable product observed.

The observation that vinoxy radicals were formed in the absence and presence of O_2 shows that the initial $OH-C_2H_2$ adduct must rearrange to yield the vinoxy radical.[126] This formation of glyoxal and OH radicals suggests that the reaction of the vinoxy radical with O_2 proceeds via[126]

$$CH_2CHO + O_2 \rightarrow (CHO)_2 + OH$$

Gutman and Nelson[338] have recently shown that the reaction of CH_2CHO with O_2 probably proceeds via initial addition to form a O_2CH_2CHO complex, with a rate constant of $\sim 2.5 \times 10^{-13}$ cm^3 molecule^{-1} s^{-1} at 100-torr total pressure of N_2. They further postulated that this O_2CH_2CHO adduct could decompose to formaldehyde, CO and OH radicals, in addition to being collisionally stabilized.[338] Their postulate of OH radical formation[338] is hence in agreement with the observations of Schmidt et al.[126]

However, Schmidt et al.[126] concluded that a variety of reaction pathways subsequent to the initial reaction of OH radicals with C_2H_2 were necessary to explain their results, and this reference should be consulted for further details. Clearly, further experimental work is necessary concerning the mechanistic details of, and the products formed from, the OH radical reactions with C_2H_2 and the higher alkynes under atmospheric conditions.

F. Oxygen-Containing Organics

1. Kinetics

The available kinetic data are listed in Table XI. The rate constants for the reaction of OH radicals with formaldehyde reported by Smith,[372] relative to those for the self-reaction of the OH radical, have not been included since their derivation from more recent OH radical self-reaction rate constants[30] cannot be undertaken with the available information. The kinetic data listed in Table XI for the individual reactions are discussed below, by class of oxygen-containing organics.

a. Aldehydes. i. Formaldehyde, Formaldehyde-^{13}*C*, and Formaldehyde-*d*$_1$. The available data (except those of Smith,[372] as noted above) are listed in Table XI. The rate constants obtained by Morris and Niki,[103] Niki et al.,[137] Atkinson and Pitts,[340] Stief et al.,[341] and Temps and Wagner[342] for $^{12}CH_2O$ and of Niki et al.[343] for $^{13}CH_2O$ are plotted in Figure 39. A significant amount of scatter in these data at room temperature is evident. The room-temperature rate constants of Atkinson and Pitts,[340] Stief et al.,[341] Temps and Wagner,[342] and Niki et al.[343] are in good agreement (making the reasonable assumption that the kinetic isotope effect for formaldehyde-^{13}*C* is negligible[343]), with a mean value of 8.94×10^{-12} cm^3 molecule^{-1} s^{-1} at 298 ± 2 K. However, the earlier room-temperature rate constants of Morris and Niki[102,103] and Niki et al.[137] are ~50% higher, for reasons which are not presently known. From the rate constant data of Atkinson and Pitts[340] and Stief et al.,[341] it is clear that the temperature dependence is essentially zero, within the experimental errors, although it is possible that the Arrhenius plot exhibits curvature with a shallow minimum at room temperature.

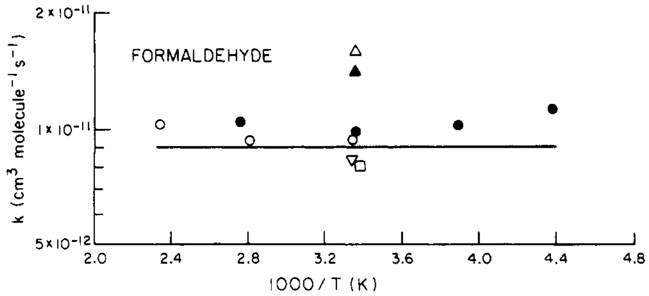

Figure 39. Arrhenius plot of the rate constants for the reaction of OH radicals with formaldehyde and formaldehyde-^{13}*C*: (▲) Morris and Niki;[103] (△) Niki et al.;[137] (○) Atkinson and Pitts;[340] (●) Stief et al.;[341] (□) Temps and Wagner;[342] (▽) Niki et al.[343] (for formaldehyde-^{13}*C*); (—) recommendation (see text).

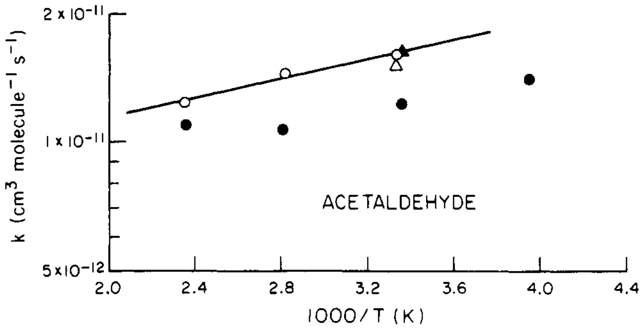

Figure 40. Arrhenius plot of the rate constants for the reaction of OH radicals with acetaldehyde: (△) Morris et al.;[85] (▲) Niki et al.;[137] (○) Atkinson and Pitts;[340] (●) Semmes et al.;[346] (—) recommendation (see text).

On the basis of the rate constants obtained by Atkinson and Pitts,[340] Stief et al.,[341] Temps and Wagner,[342] and Niki et al.[343] and with the assumption of no temperature dependence, it is recommended that

$$k(\text{formaldehyde}) = 9.0 \times 10^{-12} \text{ cm}^3 \text{ molecule}^{-1} \text{ s}^{-1}$$

independent of temperature over the range ~228–426 K. In view of the somewhat higher reported rate constants at both higher and lower temperatures, an overall uncertainty of ±15% at 298 K and ±30% at other temperatures over this limited temperature range is estimated.

At higher temperatures, i.e., ≥700 K, the available data indicate that an Arrhenius plot of this reaction rate constant must exhibit significant curvature,[340] with the rate constant at ~700–1800 K being in the range ~(4–8) × 10^{-11} cm^3 molecule^{-1} s^{-1}.[373–377]

As expected, the rate constant for the reaction of OH radicals with formaldehyde-^{13}*C* is, within the likely

TABLE XI. Rate Constants k and Arrhenius Parameters for the Gas-Phase Reaction of OH Radicals with Oxygen-Containing Organics

oxygenate	$10^{12}A$, cm^3 molecule^{-1} s^{-1}	E, cal mol^{-1}	$10^{12}k$, cm^3 molecule^{-1} s^{-1}	T, K	technique	ref	temp range covered, K
				Aldehydes			
formaldehyde			≥6.6	300	DF-MS	Herron and Penzhorn[339]	
			14 ± 3.5	298	DF-MS	Morris and Niki[103]	
			15.3	298	DF-MS	Morris and Niki[102]	
			15.8 ± 0.9	298 ± 2	rel rate [rel to k(OH + ethane-d_4) = 8.80 × 10^{-12}][a]	Niki et al.[137]	
			9.4 ± 1.0	299.3	FP-RF	Atkinson and Pitts[340]	299–426
			9.4 ± 1.0	356.5			
	12.5	175 ± 300	10.3 ± 1.1	426.4			
			11.22 ± 0.98	228	FP-RF	Stief et al.[341]	228–362
			10.28 ± 0.90	257			
			9.86 ± 1.13	298			
	10.5 ± 1.1	0	10.46 ± 1.50	362			
			8.1 ± 0.5	296	DF-LMR	Temps and Wagner[342]	
formaldehyde-^{13}C			8.41 ± 0.51	299 ± 2	rel rate [rel to k(OH + ethene) = 8.49 × 10^{-12}][b]	Niki et al.[343]	
formaldehyde-d_1			~14	298	DF-MS	Morris and Niki[103]	
acetaldehyde			15 ± 3.8	300	DF-MS	Morris et al.[85]	
			15.3	300	DF-MS	Morris and Niki[102]	
			≤20	295 ± 2	rel rate [rel to k(OH + HONO) = 6.6 × 10^{-12}][c]	Cox et al.[344]	
			16.2 ± 1.7	298 ± 2	rel rate [rel to k(OH + ethene) = 8.54 × 10^{-12}][b]	Niki et al.[137]	
			16.0 ± 1.6	299.4	FP-RF	Atkinson and Pitts[340]	299–426
			14.4 ± 1.5	355.0			
	6.87	−510 ± 300	12.4 ± 1.3	426.1			
			12.8 ± 4.3	298	rel rate [rel to k(OH + ethene) = 8.54 × 10^{-12}][b]	Kerr and Sheppard[345]	
			14.0 ± 3.1	253	FP-RF	Semmes et al.[346]	253–424
			12.2 ± 2.7	298			
			10.7 ± 2.3	356			
	7.1 ± 0.2	−328 ± 181	11.0 ± 2.3	424			
1-propanal			30.6	298	DF-MS	Morris and Niki[102]	
			22.2 ± 0.9	298 ± 2	rel rate [rel to k(OH + ethene) = 8.54 × 10^{-12}][b]	Niki et al.[137]	
			19.5 ± 1.5	298	rel rate [rel to k(OH + ethene) = 8.54 × 10^{-12}][b]	Kerr and Sheppard[345]	
			18.5 ± 2.1	298	rel rate [rel to k(OH + acetaldehyde) = 1.62 × 10^{-11}][b]	Audley et al.[160]	
			17.1 ± 2.4	298	FP-RF	Semmes et al.[346]	
1-butanal [($CH_3(CH_2)_2CHO$)]			25.3 ± 0.6	298	rel rate [rel to k(OH + ethene) = 8.54 × 10^{-12}][b]	Kerr and Sheppard[345]	
			26.2 ± 3.3	298	rel rate [rel to k(OH + acetaldehyde) = 1.62 × 10^{-11}][b]	Audley et al.[160]	
			30.8 ± 4.2	258	FP-RF	Semmes et al.[346]	258–422
			20.6 ± 3.0	298			
			18.2 ± 2.6	361			
	5.7 ± 0.3	−817 ± 326	15.4 ± 2.3	422			
2-methyl-1-propanal			29.0 ± 5.7	298	rel rate [rel to k(OH + ethene) =	Kerr and Sheppard[345]	

$[(CH_3)_2CHCHO]$					8.54×10^{-12}]^b		
			18.1 ± 2.1	298	rel rate [rel to k(OH + acetaldehyde) = 1.62×10^{-11}]^b	Audley et al.[160]	
			33.4 ± 4.5	255	FP-RF	Semmes et al.[346]	255–423
			24.2 ± 3.3	298			
			19.7 ± 2.7	354			
	6.8 ± 0.3	−781 ± 248	18.2 ± 2.7	423			
1-pentanal $[CH_3(CH_2)_3CHO]$			27.7 ± 4.2	298	rel rate [rel to k(OH + ethene) = 8.54×10^{-12}]^b	Kerr and Sheppard[345]	
			14.3 ± 1.8	298	rel rate [rel to k(OH + acetaldehyde) = 1.62×10^{-11}]^b	Audley et al.[160]	
			38.9 ± 5.7	253	FP-RF	Semmes et al.[346]	253–410
			26.9 ± 3.9	298			
			23.3 ± 3.4	355			
	6.3 ± 0.2	−896 ± 215	19.0 ± 2.8	410			
3-methyl-1-butanal $[(CH_3)_2CHCH_2CHO]$			29.0 ± 0.9	298	rel rate [rel to k(OH + ethene) = 8.54×10^{-12}]^b	Kerr and Sheppard[345]	
			19.1 ± 2.1	298	rel rate [rel to k(OH + acetaldehyde) = 1.62×10^{-11}]^b	Audley et al.[160]	
			25.8 ± 4.0	298	FP-RF	Semmes et al.[346]	
2,2-dimethyl-1-propanal $[(CH_3)_3CCHO]$			22.5 ± 6.2	298	rel rate [rel to k(OH + ethene) = 8.54×10^{-12}]^b	Kerr and Sheppard[345]	
			8.75 ± 0.97	298	rel rate [rel to k(OH + acetaldehyde) = 1.62×10^{-11}]^b	Audley et al.[160]	
			33.9 ± 6.4	254	FP-RF	Semmes et al.[346]	254–425
			30.6 ± 4.4	298			
			21.8 ± 3.1	354			
	6.7 ± 0.3	−841 ± 306	17.6 ± 2.9	425			
benzaldehyde $[C_6H_5CHO]$			14.1 ± 0.9	298 ± 2	rel rate [rel to k(OH + ethene-d_4) = 8.80×10^{-12}]^a	Niki et al.[137]	
			11.9 ± 2.3	298	rel rate [rel to k(OH + ethene) = 8.54×10^{-12}]^b	Kerr and Sheppard[345]	
				Ketones			
acetone			≤0.53	300	rel rate [rel to k(OH + ethene) = 8.45×10^{-12}]^b	Cox et al.[139]	
			0.23 ± 0.03	300	FP-RF	Zetzsch[347]	
			0.62 ± 0.09	298	rel rate [rel to k(OH + n-hexane) = 5.58×10^{-12}]^b	Chiorboli et al.[348]	
2-butanone			3.5 ± 1.0	305 ± 2	rel rate [rel to k(OH + 2-methylpropene) = 4.95×10^{-11}]^b	Winer et al.[292]	
			2.75	300	rel rate [rel to k(OH + ethene) = 8.45×10^{-12}]^b	Cox et al.[139]	
			0.95 ± 0.09	295 ± 2	rel rate [rel to k(OH + ethene) = 8.68×10^{-12}]^b	Cox et al.[145]	
			1.2 ± 0.2	300	FP-RF	Zetzsch[347]	
2-pentanone			4.64 ± 0.14	299 ± 2	rel rate [rel to k(OH + cyclohexane) = 7.41×10^{-12}]^b	Atkinson et al.[349]	
3-pentanone			1.82 ± 0.33	299 ± 2	rel rate [rel to k(OH + cyclohexane) = 7.41×10^{-12}]^b	Atkinson et al.[349]	
2-hexanone			8.97 ± 0.60	299 ± 2	rel rate [rel to k(OH + cyclohexane) = 7.41×10^{-12}]^b	Atkinson et al.[349]	
3-hexanone			6.81 ± 0.29	299 ± 2	rel rate [rel to k(OH + cyclohexane) = 7.41×10^{-12}]^b	Atkinson et al.[349]	
2,4-dimethyl-3-pentanone			5.31 ± 0.40	299 ± 2	rel rate [rel to k(OH + cyclohexane) = 7.41×10^{-12}]^b	Atkinson et al.[349]	
4-methyl-2-pentanone			15 ± 5	305 ± 2	rel rate [rel to k(OH + 2-methylpropene) = 4.95×10^{-11}]^b	Winer et al.[292]	

TABLE XI (Continued)

oxygenate	$10^{12}A$, cm^3 molecule^{-1} s^{-1}	E, cal mol^{-1}	$10^{12}k$, cm^3 molecule^{-1} s^{-1}	T, K	technique	ref	temp range covered, K
			13.1	300	rel rate [rel to k(OH + ethene) = 8.45×10^{-12}][b]	Cox et al.[139]	
			14.9 ± 0.4	295 ± 2	rel rate [rel to k(OH + ethene) = 8.68×10^{-12}][b]	Cox et al.[145]	
			14.2 ± 0.7	299 ± 2	rel rate [rel to k(OH + cyclohexane) = 7.41×10^{-12}][b]	Atkinson et al.[349]	
2,6-dimethyl-4-heptanone			25 ± 8	305 ± 2	rel rate [rel to k(OH + 2-methylpropene) = 4.95×10^{-11}][b]	Winer et al.[292]	
			27.1 ± 1.4	299 ± 2	rel rate [rel to k(OH + cyclohexane) = 7.41×10^{-12}][b]	Atkinson et al.[349]	
α,β-Unsaturated Carbonyls							
acrolein ($CH_2{=}CHCHO$)			25.3 ± 3.2	298 ± 2	rel rate [rel to k(OH + n-butane) = 2.53×10^{-12}][b]	Maldotti et al.[350]	
			20.3 ± 2.4	298 ± 2	rel rate [rel to k(OH + ethene) = 8.54×10^{-12}][b]	Kerr and Sheppard[345]	
			19.0 ± 1.3	299 ± 2	rel rate [rel to k(OH + propene) = 2.62×10^{-11}][b]	Atkinson et al.[223]	
crotonaldehyde (*trans*-$CH_3CH{=}CHCHO$)			35.2 ± 6.9	298	rel rate [rel to k(OH + ethene) = 8.54×10^{-12}][b]	Kerr and Sheppard[345]	
			36.4 ± 4.2	299 ± 2	rel rate [rel to k(OH + propene) = 2.62×10^{-11}][b]	Atkinson et al.[223]	
methacrolein [$CH_2{=}C(CH_3)CHO$]			31.4 ± 4.9	300	FP-RF	Kleindienst et al.[306]	300–423
			29.9 ± 4.8	350			
	17.7	-347 ± 103	26.5 ± 3.9	423			
			29.6 ± 2.4	299 ± 2	rel rate [rel to k(OH + propene) = 2.62×10^{-11}][b]	Atkinson et al.[223]	
methyl vinyl ketone ($CH_2{=}CHCOCH_3$)			14.8	300	rel rate [rel to k(OH + ethene) = 8.45×10^{-12}][b]	Cox et al.[139]	
			17.9 ± 2.8	298	FP-RF	Kleindienst et al.[306]	298–424
			13.5 ± 2.4	350			
	3.85	-906 ± 145	11.4 ± 2.1	424			
			19.6 ± 1.5	299 ± 2	rel rate [rel to k(OH + propene) = 2.62×10^{-11}][b]	Atkinson et al.[223]	
Ketenes							
ketene ($CH_2{=}CO$)			>1.7	295	rel rate [rel to k(OH + C_3O_2) = 1.4×10^{-12}][d]	Faubel et al.[351]	
α-Dicarbonyls							
glyoxal [$(CHO)_2$]			11.2 ± 0.4	298 ± 2	rel rate [rel to k(OH + cyclohexane) = 7.38×10^{-12}][b]	Plum et al.[150]	
methylglyoxal (CH_3COCHO)			7.1 ± 1.6	297	FP-RF	Kleindienst et al.[306]	
			16.9 ± 1.2	298 ± 2	rel rate [rel to k(OH + cyclohexane) = 7.38×10^{-12}][b]	Plum et al.[150]	
biacetyl ($CH_3COCOCH_3$)			$0.24^{+0.08}_{-0.06}$	298	FP-RF	Darnall et al.[165]	
Unsaturated 1,4-Dicarbonyls							
cis-3-hexene-2,5-dione			63 ± 6	298 ± 2	rel rate [rel to k(OH + propene) = 2.63×10^{-11}][b]	Tuazon et al.[352]	

trans-3-hexene-2,5-dione			53 ± 3	298 ± 2	rel rate [rel to k(OH + propene) = 2.63×10^{-11}]^b	Tuazon et al.[352]	
				Alcohols			
methanol			1.02 ± 0.16	292	rel rate [rel to k(OH + n-butane) = 2.44×10^{-12}]^b	Campbell et al.[216]	
			1.06 ± 0.10	296 ± 2	FP-RA	Overend and Paraskevopoulos[353]	
			1.00 ± 0.10	298	FP-RF	Ravishankara and Davis[354]	
			1.10	~300	rel rate [rel to k(OH + ethene) = 8.45×10^{-12}]^b	Barnes et al.[141]	
			0.75 ± 0.15	293	LP-RF	Hägele et al.[355]	295–420
			0.94 ± 0.19	294			
			0.71 ± 0.15	295			
			0.97 ± 0.20	324			
			1.33 ± 0.27	372			
	12 ± 3	1609 ± 99	1.74 ± 0.35	420			
			0.945 ± 0.072	300 ± 3	rel rate [rel to k(OH + dimethyl ether) = 3.01×10^{-12}]^b	Tuazon et al.[143]	
	11 ± 3	1586 ± 90	0.76	298	DF-LIF	Meier et al.[87,356]	300–1020
			0.71 ± 0.08	296	FP-RF	Zetzsch[357]	
ethanol			3.25 ± 0.51	292	rel rate [rel to k(OH + n-butane) = 2.44×10^{-12}]^b	Campbell et al.[216]	
			3.74 ± 0.37	296 ± 2	FP-RA	Overend and Paraskevopoulos[353]	
			2.62 ± 0.36	298	FP-RF	Ravishankara and Davis[354]	
			3.5 ± 0.6	295 ± 2	rel rate [rel to k(OH + propene) = 2.68×10^{-11}]^b	Cox and Goldstone[358]	
	4.4 ± 1.0	544 ± 179	1.75^e	298	DF-LIF	Meier et al.[356,359]	300–1000
			3.0 ± 0.6	296	LP-RF	Lorenz et al.[360]	296–609
			2.9 ± 0.6	296			
			3.0 ± 0.6	298			
			2.5 ± 0.5	339			
			3.3 ± 0.6	386			
			3.1 ± 0.6	386			
			3.6 ± 0.7	452			
			4.3 ± 0.8	524			
			4.0 ± 0.8	525			
	5.6 ± 0.6	397 ± 99	3.7 ± 0.8	609			
1-propanol			4.07 ± 0.65	292	rel rate [rel to k(OH + n-butane) = 2.44×10^{-12}]^b	Campbell et al.[216]	
			5.33 ± 0.53	296 ± 2	FP-RA	Overend and Paraskevopoulos[353]	
2-propanol			6.9 ± 2.1	305 ± 2	rel rate [rel to k(OH + 2-methylpropene) = 4.95×10^{-11}]^b	Lloyd et al.[361]	
			5.48 ± 0.55	296 ± 2	FP-RA	Overend and Paraskevopoulos[353]	
1-butanol			7.32 ± 1.37	292	rel rate [rel to k(OH + n-butane) = 2.44×10^{-12}]^b	Campbell et al.[216]	
2-methyl-2-propanol			1.09 ± 0.13	295 ± 2	rel rate [rel to k(OH + ethene) = 8.68×10^{-12}]^b	Cox and Goldstone[358]	
allyl alcohol ($CH_2{=}CHCH_2OH$)			25.9 ± 3.3	440	PR-RA	Gordon and Mulac[129]	
2-chloroethanol			1.4 ± 0.1	295	FP-RF	Wiedelmann and Zetzsch[362]	
				Glycols			
1,2-ethanediol ($HOCH_2CH_2OH$)			7.7 ± 1.1	295	FP-RF	Wiedelmann and Zetzsch[362]	
1,2-propanediol ($HOCH_2CHOHCH_3$)			12 ± 1	295	FP-RF	Wiedelmann and Zetzsch[362]	
2-hydroxyethyl ether ($HOCH_2CHOCH_2CH_2OH$)			30 ± 2	295	FP-RF	Wiedelmann and Zetzsch[362]	

TABLE XI (Continued)

oxygenate	$10^{12}A$, cm^3 molecule^{-1} s^{-1}	E, cal mol^{-1}	$10^{12}k$, cm^3 molecule^{-1} s^{-1}	T, K	technique	ref	temp range covered, K
				Ethers			
dimethyl ether			3.50 ± 0.35	298.9	FP-RF	Perry et al.[363]	299–424
			4.31 ± 0.43	350.5			
	12.9	770 ± 300	5.13 ± 0.51	423.9			
			2.95 ± 0.12	295	LP-LIF	Tully et al.[364]	295–442
			3.40 ± 0.14	332			
			3.81 ± 0.16	377.5			
			4.52 ± 0.19	442			
diethyl ether			9.2 ± 1.8	305 ± 2	rel rate [rel to k(OH + 2-methylpropene) = 4.95×10^{-11}]^b	Lloyd et al.[361]	
			13.4 ± 0.6	295	LP-LIF	Tully et al.[364]	295–442
			12.9 ± 0.6	332			
			12.4 ± 0.5	377.5			
			11.8 ± 0.5	442			
di-*n*-propyl ether			16.8 ± 3.4	305 ± 2	rel rate [rel to k(OH + 2-methylpropene) = 4.95×10^{-11}]^b	Lloyd et al.[361]	
methyl *tert*-butyl ether			2.86 ± 0.52	295 ± 2	rel rate [rel to k(OH + ethene) = 8.68×10^{-12}]^b	Cox and Goldstone[358]	
			2.42 ± 0.39	295 ± 2	rel rate [rel to k(OH + n-hexane) = 5.51×10^{-12}]^b	Cox and Goldstone[358]	
tetrahydrofuran			14.4 ± 2.9	305 ± 2	rel rate [rel to k(OH + 2-methylpropene) = 4.95×10^{-11}]^b	Winer et al.[293]	
			16.2 ± 2.2	298	FP-RF	Ravishankara and Davis[354]	
vinyl methyl ether ($CH_2{=}CHOCH_3$)			33.5 ± 3.4	299.1	FP-RF	Perry et al.[363]	299–427
			26.0 ± 2.6	352.4			
	6.10	−1015 ± 300	20.1 ± 2.0	427.0			
furan			105 ± 8	295 ± 1	DF-RF	Lee and Tang[199]	
			39.3 ± 2.8	298 ± 2	rel rate [rel to k(OH + n-hexane) = 5.58×10^{-12}]^b	Atkinson et al.[217]	
			49.6 ± 3.3	254	FP-RF	Wine and Thompson[365]	254–424
			40.8 ± 1.8	297			
			43.1 ± 1.2	297			
			38.7 ± 2.2	299			
			41.6 ± 3.5	299			
			38.3 ± 4.5	300			
			31.9 ± 1.6	365			
	13.2 ± 2.9	−662 ± 133	29.9 ± 2.0	424			
			42.3 ± 3.2	295 ± 2	rel rate [rel to k(OH + 2-methyl-1,3-butadiene = 1.02×10^{-10}]^b	Tuazon et al.[272]	
				Esters			
methyl acetate			0.17 ± 0.05	292	rel rate [rel to k(OH + n-butane) = 2.44×10^{-12}]^b	Campbell and Parkinson[159]	
ethyl acetate			1.82 ± 0.36	292	rel rate [rel to k(OH + n-butane) = 2.44×10^{-12}]^b	Campbell and Parkinson[159]	

			1.7 ± 0.2	296	FP-RF	Zetzsch[357]	
n-propyl acetate			4.2 ± 0.9	305 ± 2	rel rate [rel to k(OH + 2-methylpropene) = 4.95×10^{-11}]^b	Winer et al.[293]	
sec-butyl acetate			5.4 ± 1.1	305 ± 2	rel rate [rel to k(OH + 2-methylpropene) = 4.95×10^{-11}]^b	Winer et al.[293]	
methyl propionate			0.27 ± 0.10	292	rel rate [rel to k(OH + *n*-butane) = 2.44×10^{-12}]^b	Campbell and Parkinson[159]	
ethyl propionate			1.66 ± 0.35	292	rel rate [rel to k(OH + *n*-butane) = 2.44×10^{-12}]^b	Campbell and Parkinson[159]	
			Carboxylic Acids				
formic acid			0.32 ± 0.10	298	FP-RF	Zetzsch and Stuhl[366]	
			0.461 ± 0.051	298	FP-RF	Wine et al.[367]	298–430
			0.405 ± 0.047	298			
			0.545 ± 0.012	298			
			0.448 ± 0.032	298			
			0.432 ± 0.065	298			
			0.446 ± 0.011	298			
			0.449 ± 0.026	298			
			0.428 ± 0.049	298			
			0.481 ± 0.059	298			
			0.482 ± 0.042	298			
			0.523 ± 0.030	299			
			0.466 ± 0.007	299			
			0.480 ± 0.075	299			
			0.464 ± 0.037	299			
			0.495 ± 0.081	299			
			0.490 ± 0.094	300			
			0.539 ± 0.076	300			
			0.446 ± 0.033	300			
			0.443 ± 0.053	300			
			0.495 ± 0.050	320			
			0.406 ± 0.024	337			
			0.433 ± 0.037	374			
			0.505 ± 0.002	378			
			0.479 ± 0.068	402			
			0.407 ± 0.034	428			
			0.409 ± 0.051	428			
			0.439 ± 0.072	430			
	0.363 ± 0.086 [0.462 ± 0.078	−153 ± 149 0]	0.434 ± 0.053	430			
formic acid-d_1 (DCOOH)			0.435 ± 0.038	298	FP-RF	Wine et al.[367]	
			0.498 ± 0.099	298			
			0.456 ± 0.028	298			
acetic acid			0.6 ± 0.2	298	FP-RF	Zetzsch and Stuhl[366]	
propionic acid			1.6 ± 0.5	298	FP-RF	Zetzsch and Stuhl[366]	
butyric acid			2.4 ± 0.7	298	FP-RF	Zetzsch and Stuhl[366]	
			Oxides				
ethene oxide	11 ± 4	2901 ± 298 (T = 297–435 K)	0.081 ± 0.016	298	LP-RF	Lorenz and Zellner[368]	297–515
			0.053 ± 0.01	295	FP-RF	Zetzsch[220]	
propene oxide			1.2 ± 0.7	300 ± 1	rel rate [rel to k(*n*-butane)-k(neopentane) = 1.68×10^{-12}]^b	Winer et al.[369]	
			0.52 ± 0.1	295	FP-RF	Zetzsch[220]	

TABLE XI (Continued)

oxygenate	$10^{12}A$, cm^3 molecule^{-1} s^{-1}	E, cal mol^{-1}	$10^{12}k$, cm^3 molecule^{-1} s^{-1}	T, K	technique	ref	temp range covered, K
1,2-butene oxide			2.1 ± 0.7	300 ± 1	rel rate [rel to k(n-butane)-k(neopentane) = 1.68 × 10^{-12}]^b	Winer et al.[369]	
1-chloro-2,3-epoxypropane			0.44 ± 0.05	295	FP-RF	Zetzsch[220]	
			Hydroperoxides				
methyl hydroperoxide			10.2 ± 0.8	f	rel rate [rel to k(OH + ethene) = 8.54 × 10^{-12}]^b	Niki et al.[370]	
			11.0 ± 1.2	f	rel rate [rel to k(OH + acetaldehyde) = 1.62 × 10^{-11}]^b	Niki et al.[370]	
tert-butyl hydroperoxide			3.0 ± 0.8	298	FP-RA	Anastasi et al.[371]	

[a] From the rate constant ratio k(OH + ethene-d_4)/k(OH + ethene)[137] and the recommendation for ethene (see text). [b] From the recommendations (see text). [c] From ref 93. [d] From ref 351. [e] Calculated at 298 K from the cited Arrhenius expression. [f] Room temperature, not reported. 298 K has been assumed, based on previous studies carried out by Niki and co-workers.[137,146,164]

experimental errors, essentially identical with that for formaldehyde-^{12}C.[343] Similarly, Morris and Niki[103] determined that the room-temperature rate constant for the reaction of formaldehyde-d_1 with OH radicals is essentially identical with that for the reaction of OH radicals with formaldehyde, showing that any primary deuterium isotope effect is small. This is consistent with the lack of a temperature dependence for the reaction of OH radicals with formaldehyde (see above).

ii. Acetaldehyde. The available data are listed in Table XI, and those of Morris et al.,[85] Niki et al.,[137] Atkinson and Pitts,[340] and Semmes et al.[346] are plotted in Arrhenius form in Figure 40. Within the cited experimental errors, these data are in reasonably good agreement. From a unit-weighted least-squares analysis of the rate constants determined by Atkinson and Pitts[340] (which are in excellent agreement with that of Niki et al.[137] at 298 K) it is recommended that

$$k(\text{acetaldehyde}) = (6.87^{+1.46}_{-1.20}) \times 10^{-12} e^{(256\pm68)/T} \text{ cm}^3 \text{ molecule}^{-1} \text{ s}^{-1}$$

where the errors are two least squares standard deviations

$$k(\text{acetaldehyde}) = 1.62 \times 10^{-11} \text{ cm}^3 \text{ molecule}^{-1} \text{ s}^{-1}$$

at 298 K, with an estimated uncertainty at 298 K of ±20%.

The recent rate constant data of Semmes et al.[346] were not included in this analysis since they reported difficulties in adequately determining the acetaldehyde concentrations in their reactant mixtures.

For the higher aldehydes, recommendations are made only for propionaldehyde (1-propanal) and benzaldehyde at room temperature.

iii. 1-Propanal. From the recent room-temperature rate constants of Niki et al.,[137] Kerr and Sheppard,[345] and Semmes et al.,[346] a mean value of

$$k(\text{1-propanal}) = 1.96 \times 10^{-11} \text{ cm}^3 \text{ molecule}^{-1} \text{ s}^{-1} \text{ at 298 K}$$

is recommended, with an estimated overall uncertainty of ±25%.

iv. Benzaldehyde. From the same room temperature rate constant studies of Niki et al.[137] and Kerr and Sheppard,[345] it is recommended that

$$k(\text{benzaldehyde}) = 1.30 \times 10^{-11} \text{ cm}^3 \text{ molecule}^{-1} \text{ s}^{-1} \text{ at 298 K}$$

with an estimated overall uncertainty of ±25%.

Benzaldehyde is included in the aldehydes rather than with the aromatics since it is apparent[1,3,137] that the reaction proceeds predominantly via interaction with the –CHO group, and not with the aromatic ring.

For the other aldehydes listed in Table XI, it is evident that in several instances significant discrepancies exist between the data of Kerr and Sheppard[345] and Semmes et al.[346] and those of Audley et al.;[160] for example, for 1-pentanal, 2,2-dimethyl-1-propanal, 2-methyl-1-propanal, and 3-methyl-1-butanal (Table XI). Thus no firm recommendations for these aldehydes are made. However, in view of the fact that for 1-propanal and benzaldehyde the experimental data of Kerr and Sheppard[345] also agree well with those of Niki et al.,[137] it is recommended that further studies of the heterogeneous reaction system used by Campbell and co-workers[160] be carried out. In the meantime, the room-temperature rate constants obtained by Kerr and Sheppard[345] and Semmes et al.[346] for 1-butanal, 2-methyl-1-propanal, 1-pentanal, 3-methyl-1-butanal and 2,2-dimethyl-1-propanal are tentatively recommended, combined with the temperature dependencies (all of which are negative, equivalent to an Arrhenius activation energy of −0.8 kcal mol^{-1}) obtained by Semmes et al.[346]

b. Ketones. The available kinetic data are listed in Table XI. No temperature dependencies have been determined, and only for acetone, 2-butanone, 4-methyl-2-pentanone, and 2,6-dimethyl-4-heptanone have more than a single study been carried out. The recommendations for these ketones are as follows.

i. Acetone. The room-temperature rate constant determined by Zetzsch,[347] using a flash photolysis–resonance fluorescence technique, is recommended, i.e.

$$k(\text{acetone}) = 2.3 \times 10^{-13} \text{ cm}^3 \text{ molecule}^{-1} \text{ s}^{-1} \text{ at } 300 \text{ K}$$

with an estimated uncertainty of ±40%.

This rate constant is consistent with the upper limit derived by Cox et al.[139] from photolysis of HONO–NO–organic–air mixtures and is of the magnitude expected from the fact that the C–H bond dissociation energies in acetone (98.3 ± 1.8 kcal mol^{-1} [319]) are essentially identical with those in ethane.[226,319] The reasons for the higher rate constant reported by Chiorboli et al.[348] are not known.

ii. 2-Butanone. The reported room-temperature rate constants (Table XI) vary by a factor of ~4. However, the two most recent values of Cox et al.[145] and Zetzsch[347] are in reasonable agreement and are totally consistent with the rate constants reported by Atkinson et al.[349] for the higher ketones. Thus it is recommended that

$$k(\text{2-butanone}) = 1.0 \times 10^{-12} \text{ cm}^3 \text{ molecule}^{-1} \text{ s}^{-1} \text{ at } 300 \text{ K}$$

with an estimated uncertainty of ±30%.

iii. 4-Methyl-2-pentanone. The four reported room-temperature rate constants are in good agreement, and the average of the two most recent (and supposedly accurate) determinations of Cox et al.[145] and Atkinson et al.[349] of

$$k(\text{4-methyl-2-pentanone}) = 1.41 \times 10^{-11} \text{ cm}^3 \text{ molecule}^{-1} \text{ s}^{-1} \text{ at } 297 \pm 4 \text{ K}$$

is recommended, with an estimated uncertainty of ±20%.

iv. 2,6-Dimethyl-4-heptanone. The two reported room-temperature rate constants of Winer et al.[292] and Atkinson et al.[349] are in good agreement, and the most recent and precise rate constant of Atkinson et al.[349] of

$$k(\text{2,6-dimethyl-4-heptanone}) = 2.71 \times 10^{-11} \text{ cm}^3 \text{ molecule}^{-1} \text{ s}^{-1} \text{ at } 299 \pm 2 \text{ K}$$

is recommended, with an estimated uncertainty of ±25%.

For the remaining ketones no firm recommendations are made.

c. α,β-Unsaturated Carbonyls. The available rate constant data of Cox et al.,[139] Maldotti et al.,[350] Kerr and Sheppard,[345] Kleindienst et al.,[306] and Atkinson et al.[223] are listed in Table XI. For all four of the α,β-unsaturated carbonyls investigated, two or more studies have been carried out. The recommendations are as follows.

i. Acrolein. The three room-temperature studies[223,345,350] are in reasonable agreement. The mean of the two most recent studies of Kerr and Sheppard[345] and Atkinson et al.[223] of

$$k(\text{acrolein}) = 1.96 \times 10^{-11} \text{ cm}^3 \text{ molecule}^{-1} \text{ s}^{-1} \text{ at } 298 \text{ K}$$

is recommended, with an estimated uncertainty of ±25%.

By analogy with the saturated aldehydes, with which this recommended rate constant is in good agreement, it is expected that this reaction will have a negative temperature dependence equivalent to an Arrhenius activation energy of $-(0.5^{+0.5}_{-0.3})$ kcal mol^{-1}.

ii. Crotonaldehyde. The two room-temperature rate constants of Kerr and Sheppard[345] and Atkinson et al.[223] are in excellent agreement, and a rate constant of

$$k(\text{crotonaldehyde}) = 3.6 \times 10^{-11} \text{ cm}^3 \text{ molecule}^{-1} \text{ s}^{-1} \text{ at } 298 \text{ K}$$

is recommended, with an estimated uncertainty of ±25%.

By analogy with methacrolein (see below) a negative temperature dependence equivalent to an Arrhenius activation energy of −(0.3 ± 0.2) kcal mol^{-1} is expected.

iii. Methacrolein. The rate constants of Kleindienst et al.[306] and Atkinson et al.[223] are in excellent agreement (Table XI) and are plotted in Arrhenius form in Figure 41. From a unit-weighted least-squares analysis of these data, the Arrhenius expression

$$k(\text{methacrolein}) = (1.96^{+0.74}_{-0.53}) \times 10^{-11} e^{(134 \pm 106)/T} \text{ cm}^3 \text{ molecule}^{-1} \text{ s}^{-1}$$

is recommended, where the errors are two least-squares standard deviations and

$$k(\text{methacrolein}) = 3.07 \times 10^{-11} \text{ cm}^3 \text{ molecule}^{-1} \text{ s}^{-1} \text{ at } 298 \text{ K}$$

with an estimated overall uncertainty at 298 K of ±25%.

iv. Methyl Vinyl Ketone. The reported rate constants[139,223,306] are plotted in Figure 41 and show an ~35% spread at room temperature. As above for methacrolein, from a unit-weighted least-squares analysis of the data of Kleindienst et al.[306] and Atkinson et al.[223] the Arrhenius expression

$$k(\text{methyl vinyl ketone}) = (3.29^{+2.15}_{-1.30}) \times 10^{-12} e^{(514 \pm 167)/T} \text{ cm}^3 \text{ molecule}^{-1} \text{ s}^{-1}$$

is recommended, where the indicated errors are two least-squares standard deviations, and

$$k(\text{methyl vinyl ketone}) = 1.85 \times 10^{-11} \text{ cm}^3 \text{ molecule}^{-1} \text{ s}^{-1} \text{ at } 298 \text{ K}$$

with an estimated overall uncertainty at 298 K of ±30%.

d. Ketenes, α-Dicarbonyls, and Unsaturated 1,4-Dicarbonyls. No recommendations are made for these compounds.

e. Alcohols and Glycols. Again the relevant kinetic data are listed in Table XI. Only for methanol and ethanol have temperature dependence studies been carried out, while for 1- and 2-propanol two room-tem-

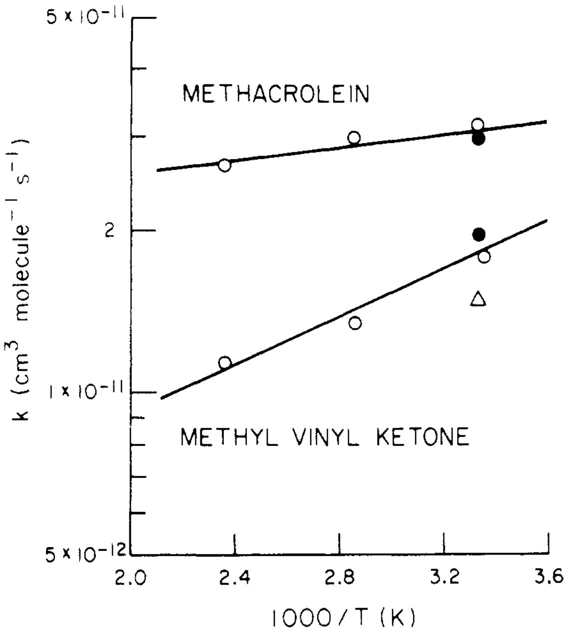

Figure 41. Arrhenius plot of the rate constants for the reaction of the OH radical with methacrolein and methyl vinyl ketone: (△) Cox et al.;[139] (○) Kleindienst et al.;[306] (●) Atkinson et al.;[223] (—) recommendations (see text).

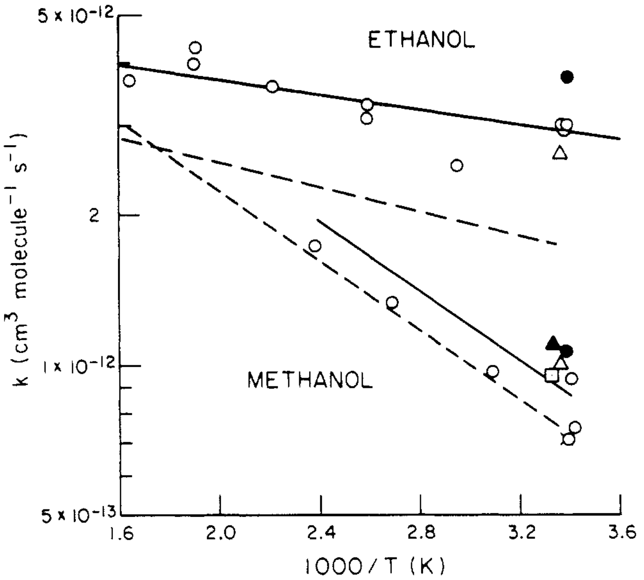

Figure 42. Arrhenius plot of the rate constants (≤625 K) for the reaction of OH radicals with methanol and ethanol: (●) Overend and Paraskevopoulos;[353] (△) Ravishankara and Davis;[354] (▲) Barnes et al.;[141] (□) Tuazon et al.;[143] (×) Zetzsch;[357] (○) Hägele et al.[355] (for methanol), Lorenz et al.[360] (for ethanol); (- - -) Meier et al.;[87,356,359] (—) recommendations (see text).

perature rate constants have been obtained for each of these alcohols. The recommendations are as follows.

i. **Methanol.** The available rate constant data[87,141,143,216,353-357] are listed in Table XI, and those of Overend and Paraskevopoulos,[353] Ravishankara and Davis,[354] Barnes et al.,[141] Tuazon et al.,[143] Hägele et al.,[355] Meier et al.,[87,356] and Zetzsch[357] are plotted in Arrhenius form in Figure 42. In addition to these rate constants, Osif et al.[378] also determined rate constants at 298 and 345 K, relative to those for the reaction of OH radicals with CO, at total pressure of 28–203 torr of $CH_3OH + N_2O + CO$. While no quantitative estimate of this reference reaction rate constant can be made, a lower limit of 1.5×10^{-13} cm³ molecule⁻¹ s⁻¹ at 298 K is applicable, and hence

$$k(CH_3OH) \geq (9.5 \pm 1.5) \times 10^{-14} \text{ cm}^3 \text{ molecule}^{-1} \text{ s}^{-1} \text{ at } 298 \text{ K}$$

is obtained, with an upper limit at this temperature of $\lesssim 2 \times 10^{-13}$ cm^3 molecule^{-1} s^{-1}.[92-101] This is lower by a factor of ~4–10 than the room-temperature rate constants listed in Table XI and is hence neglected in the evaluation.

At room temperature the rate constants of Overend and Paraskevopoulos,[353] Ravishankara and Davis,[354] Barnes et al.,[141] Tuazon et al.,[143] Hägele et al.,[355] Meier et al.,[87,356] and Zetzsch[357] show a spread of ~50%, and on the basis of this divergent data set, it can only be recommended that

$$k(\text{methanol}) = (9 \pm 3) \times 10^{-13} \text{ cm}^3 \text{ molecule}^{-1} \text{ s}^{-1}$$

at 298 K, with a temperature dependence equivalent to an Arrhenius activation energy of ~1.6 kcal mol^{-1}.[87,355,356] This then yields the provisionally recommended Arrhenius expression of

$$k(\text{methanol}) = 1.34 \times 10^{-11} e^{-805/T} \text{ cm}^3 \text{ molecule}^{-1} \text{ s}^{-1}$$

with the rate constant at any temperature over the range 298–420 K being uncertain by ± a factor of ~1.5. This Arrhenius preexponential factor appears somewhat large, by a factor of ~2–5, and further work concerning the kinetics of this reaction is obviously necessary.

ii. **Ethanol.** The available data are listed in Table XI, and those of Overend and Paraskevopoulos,[353] Ravishankara and Davis,[354] Lorenz et al.,[360] and Meier et al.[356,359] are plotted in Arrhenius form in Figure 42. A significant degree of scatter, in excess of a factor of 2 at room temperature, is evident. The rate constant at room temperature reported by Meier et al.[356,359] is significantly lower than the remaining absolute[353,354,360] and relative[358] rate constants, and until further information becomes available, these rate constants[356,359] have been neglected in the evaluation.

On the basis of a unit-weighted least-squares analysis of the data of Overend and Paraskevopoulos,[353] Ravishankara and Davis,[354] and Lorenz et al.,[360] the Arrhenius expression

$$k(\text{ethanol}) = (5.27^{+1.97}_{-1.43}) \times 10^{-12} e^{-(176 \pm 114)/T} \text{ cm}^3 \text{ molecule}^{-1} \text{ s}^{-1}$$

is provisionally recommended, where the indicated errors are two least-squares standard deviations, and

$$k(\text{ethanol}) = 2.9 \times 10^{-12} \text{ cm}^3 \text{ molecule}^{-1} \text{ s}^{-1} \text{ at } 298 \text{ K}$$

with an estimated uncertainty at 298 K of ±40%.

For the remaining alcohols and for the glycols no recommendations are made.

f. **Ethers.** The available kinetic data are listed in Table XI, and it can be seen that only for dimethyl ether, diethyl ether, tetrahydrofuran, and furan have studies been carried out by more than one research group. The data for dimethyl ether, diethyl ether, tetrahydrofuran, and furan are discussed as follows.

i. **Dimethyl Ether.** Two studies have been carried out by Perry et al.[363] and Tully and co-workers,[364] both using flash or laser photolysis techniques. However, the rate constants determined by Perry et al.[363] are uniformly 15% higher than the recent values of Tully and

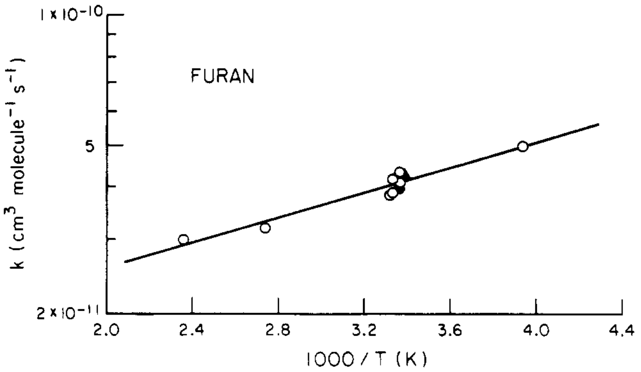

Figure 43. Arrhenius plot of the rate constants for the reaction of OH radicals with furan: (●) Atkinson et al.;[217] (▲) Tuazon et al.;[272] (○) Wine and Thompson;[365] (—) recommendation (see text).

co-workers[364] over the entire temperature range studied. This implies the existence of a systematic error in the earlier work,[363] possibly associated with the presence of a reactive impurity. Although further studies are necessary, the most recent rate constants of Tully and co-workers[364] are used to recommend, from a unit-weighted least-squares analysis, that

$$k(\text{dimethyl ether}) = (1.04^{+0.11}_{-0.10}) \times 10^{-11} e^{-(372\pm35)/T} \text{ cm}^3 \text{ molecule}^{-1} \text{ s}^{-1}$$

where the indicated error limits are two least-squares standard deviations

$$k(\text{dimethyl ether}) = 2.98 \times 10^{-12} \text{ cm}^3 \text{ molecule}^{-1} \text{ s}^{-1} \text{ at } 298 \text{ K}$$

with an estimated overall uncertainty at 298 K of ±20%.

ii. Diethyl Ether. Rate constants have been obtained by Lloyd et al.[361] using a relative rate method and recently by Tully and co-workers[364] using a LP–LIF technique. The room-temperature rate constant of Tully and co-workers[364] is significantly higher (by ~45%) than that of Lloyd et al.[361] In the absence of further data, no firm recommendations are made. However, it is noteworthy that the data of Tully and co-workers[364] indicate a small negative temperature dependence equivalent to an Arrhenius activation energy of −230 cal mol^{-1}. If confirmed, this finding is of interest with regards to the reaction dynamics of this apparently H atom abstraction process.

iii. Tetrahydrofuran. The room-temperature rate constants of Winer et al.[293] and Ravishankara and Davis[354] are in good agreement. The mean of these rate constants

$$k(\text{tetrahydrofuran}) = 1.5 \times 10^{-11} \text{ cm}^3 \text{ molecule}^{-1} \text{ s}^{-1} \text{ at } \sim 300 \text{ K}$$

is recommended, with an estimated uncertainty of ±30%. The temperature dependence of this reaction is expected, a priori, to be small.

iv. Furan. Rate constants for the reaction of OH radicals with furan have been determined by Lee and Tang,[199] Atkinson et al.,[217] Wine and Thompson,[365] and Tuazon et al.[272] The room-temperature rate constants from the latter three studies[217,272,365] are in excellent agreement but are a factor of ~2.5 lower than that of Lee and Tang.[199] It should be noted that a similar discrepancy occurs for the analogous reaction of OH radicals with thiophene (see Table XII below), suggesting the occurrence of a systematic error in this discharge flow system study of Lee and Tang,[199] at least for these two heterocycles [their room-temperature rate constant for ethane[199] is consistent with other literature data (Table I)].

The rate constants of Atkinson et al.,[217] Wine and Thompson,[365] and Tuazon et al.[272] are plotted in Arrhenius form in Figure 43, and a unit-weighted least-squares analysis of these data yields the recommended Arrhenius expression of

$$k(\text{furan}) = (1.32^{+0.30}_{-0.24}) \times 10^{-11} e^{(334\pm62)/T} \text{ cm}^3 \text{ molecule}^{-1} \text{ s}^{-1}$$

where the errors are two least-squares standard deviations

$$k(\text{furan}) = 4.05 \times 10^{-11} \text{ cm}^3 \text{ molecule}^{-1} \text{ s}^{-1} \text{ at } 298 \text{ K}$$

with an estimated uncertainty at 298 K of ±20%.

For the remaining ethers no recommendations are made. The reported room-temperature rate constants for the saturated ethers are analogous to the alkanes in that they increase with the number of primary and secondary (especially the latter) C–H bonds. Comparison of the rate constants for these ethers with those for the corresponding alkanes containing the same numbers of primary and secondary C–H bonds shows that the rate constants per C–H bond are enhanced in the ethers. This implies that the C–H bonds are weakened due to proximity to the oxygen atom, and this is consistent with the reported bond dissociation energies of 93 ± 1 kcal mol^{-1} for $H-CH_2OCH_3$[319] and 91.7 ± 0.4 kcal mol^{-1} for $H-CH(CH_3)OC_2H_5$,[379] which are significantly lower than typical primary and secondary C–H bond energies in the alkane series of ~98 and ~95 kcal mol^{-1}, respectively.[226,319]

For vinyl methyl ether and furan, the reactions almost certainly proceed via initial OH radical addition to the >C=C< double bond (see below), and this is consistent with the magnitude of the room-temperature rate constants and the negative temperature dependencies (equivalent to Arrhenius activation energies of ~−0.6 to −1.0 kcal mol^{-1} [363,365]).

g. Esters. The available data are listed in Table XI. Since, apart from ethyl acetate, only single studies have been carried out for each of these esters, no recommendations are made. With the assumption that these data are correct, the observation that the rate constants for methyl acetate and methyl propionate are similar, as are those for ethyl acetate and ethyl propionate, indicates that the reaction with $R_1C(O)OR_2$ occurs mainly at the $-OR_2$ entity rather than at the R_1CO entity. The magnitude of the rate constants for the acetate series further shows that they increase with the number of secondary and tertiary C–H bonds, as expected for H atom abstraction reactions. Furthermore, analogous to the ethers, the rate constants per C–H bond for the $-OR_2$ entities are higher than those for the corresponding alkanes.

h. Carboxylic Acids. The available data are listed in Table XI. While the first four members of this homologous series have been studied, only for formic acid has more than one study been carried out. The extensive investigation of Wine et al.[367] yields a room-temperature rate constant ~50% higher than that of Zetzsch and Stuhl.[366] However, considering the difficulties involved with measuring the concentrations of formic acid (which is prone to dimerization) in the reactant mixtures, this may be considered to be reasonable agreement.

The data of Wine et al.[367] show that the reaction of OH radicals with formic acid has an essentially zero temperature dependence and, when compared with the corresponding data for DCOOH at 298 K,[367] that there is no significant deuterium isotope effect.

From the study of Zetzsch and Stuhl[366] it can be seen that the room-temperature rate constants increase along the homologous series.

i. Oxides and Hydroperoxides. The available kinetic data are listed in Table XI. Apart from ethene oxide and propene oxide, for which the data are not in good agreement (Table XI), only single studies have been carried out for each of these organics and thus no recommendations are made. The available mechanistic[368,370] data are discussed in the following section.

2. Mechanisms and Subsequent Reactions under Atmospheric Conditions

a. Aldehydes. The available mechanistic and product data show that these reactions proceed via overall H atom abstraction. Thus for formaldehyde, the reaction can proceed via the pathways

$$\mathrm{OH + HCHO \rightarrow HCO + H_2O} \qquad \text{(a)}$$

$$\mathrm{OH + HCHO \rightarrow HCOOH + H} \qquad \text{(b)}$$

$$\mathrm{OH + HCHO \rightarrow H + CO + H_2O} \qquad \text{(c)}$$

and Morrison and Heicklen,[380] Temps and Wagner,[342] and Niki et al.[343] have shown that reaction pathway b is negligible, accounting for $\lesssim 2\%$ of the overall reaction.[343] Morrison and Heicklen[380] did not observe HCOOH formation (<10%) but concluded that reaction pathways a and c occurred with approximately equal probability. More recently Temps and Wagner,[342] using a discharge flow technique with LMR detection to monitor both OH and HCO radicals, have shown that reaction pathway a accounts for 100 ± 5% of the overall reaction.

While such definite evidence is not available for the higher aldehydes, the observation of peroxyacetyl nitrate (PAN) from the reaction of OH radicals with CH_3CHO in air in the presence of NO_x,[3] i.e.

$$\mathrm{OH + CH_3CHO \rightarrow H_2O + CH_3\dot{C}O}$$

$$\mathrm{CH_3\dot{C}O + O_2 \rightarrow CH_3C(O)OO\cdot}$$

$$\mathrm{CH_3C(O)OO\cdot + NO_2 \rightleftarrows \underset{PAN}{CH_3C(O)OONO_2}}$$

shows that this reaction must also proceed via overall H atom abstraction from the -CHO group. This is consistent with the observation that the room-temperature rate constants for the $\geq C_2$ aldehydes are reasonably similar, increasing only slightly with the length of the alkyl side chain[345,346] (showing that the alkyl substituent group has only a minimal effect on the OH radical rate constant) and with the fact that the H-CO bond dissociation energy is also essentially invariant for the aldehyde series.[319,381]

Thus the reactions of the OH radical with the aliphatic aldehydes, including benzaldehyde for which OH radical addition to the aromatic ring is expected to occur less rapidly than for benzene (i.e., $<1.2 \times 10^{-12}$ cm^3 molecule^{-1} s^{-1} at 298 K),[3] proceed essentially totally via H atom abstraction from the -CHO group. For the $\geq C_2$ aldehydes, these reactions exhibit negative temperature dependencies equivalent to Arrhenius activation energies of -(0.3-0.8) kcal mol^{-1}.[340,346] It is possible that this indicates that, although the overall reactions proceed via H atom abstraction, the initial reaction involves the formation of a complex[346] which rapidly decomposes to the observed products.

Subsequent to the initial OH radical reaction, the resulting $R\dot{C}O$ radicals react further with O_2. The reaction of HCO with O_2 is unique for these RCO radicals in that a metathesis reaction to yield HO_2 radicals and CO occurs:[3]

$$\mathrm{HCO + O_2 \rightarrow HO_2 + CO}$$

For the higher RCO radicals, O_2 addition occurs to form the acyl radical[3]

$$\mathrm{R\dot{C}O + O_2 \rightarrow RC(O)OO\cdot}$$

These acyl radicals can then react with NO_2, to form the thermally unstable (with a lifetime at 298 K of ~45 min)[3] acyl peroxynitrates

$$\mathrm{RC(O)OO\cdot + NO_2 \rightleftarrows RC(O)OONO_2}$$

or with NO

$$\mathrm{RC(O)OO\cdot + NO \rightarrow RC(O)O\cdot + NO_2}$$

The RC(O)O· radicals rapidly decompose to yield the alkyl radical and CO_2

$$\mathrm{RC(O)O\cdot \rightarrow R\cdot + CO_2}$$

followed by the reactions of the alkyl radicals, as discussed above under the section dealing with the alkanes.

b. Ketones. The available kinetic[3,349] and product[139,145] data show that the ketones not containing unsaturated carbon-carbon bonds react with OH radicals via H atom abstraction from the C-H bonds. The most recent and extensive kinetic study of Atkinson et al.[349] shows that the >C=O group decreases the reactivity of C—H bonds on the α-carbon atom toward attack by the OH radical, relative to those in the analogous alkane, but increases the reactivity of the C—H bonds on the β-carbon atom. This effect is somewhat unexpected, since the available thermochemical data[319] for the primary C-H bond strengths in acetone and the secondary C-H bond strengths in 2-butanone do not indicate any increase in C-H bond strengths on the α-carbon; in fact for 2-butanone the reverse has been observed.[319,382]

An a priori predictive technique has been developed from the available, but rather limited, data base,[349] which allows the estimation of the distribution of initially formed radicals, and this topic is discussed in further detail in section IV below.

Under atmospheric conditions, the radicals initially formed will rapidly add O_2;[3] e.g., for the $CH_3\dot{C}HCOCH_3$ radical formed from 2-butanone

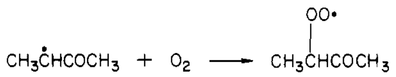

$$\mathrm{CH_3\dot{C}HCOCH_3 + O_2 \rightarrow CH_3\overset{OO\cdot}{\overset{|}{C}}HCOCH_3}$$

Reaction with NO will lead mainly to the formation of the corresponding alkoxy radical (though nitrate formation may occur to a small, presently unknown, but still possibly significant extent[3])

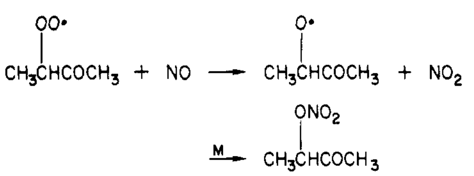

$$CH_3\overset{OO\cdot}{C}HCOCH_3 + NO \longrightarrow CH_3\overset{O\cdot}{C}HCOCH_3 + NO_2$$
$$\xrightarrow{M} CH_3\overset{ONO_2}{C}HCOCH_3$$

As for alkoxy radicals in general, the alkoxy radicals resulting from such reaction sequences can react with O_2, decompose, or isomerize. The available information regarding these processes for the alkoxy radicals generated from the ketones is limited, though estimation techniques are available.[244,248] For example, for the $CH_3CH(O\cdot)COCH_3$ radical discussed above, the dominant reaction under atmospheric conditions is via decomposition[3,145,244,245,248]

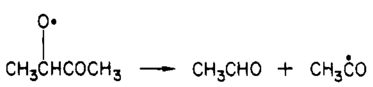

$$CH_3\overset{O\cdot}{C}HCOCH_3 \longrightarrow CH_3CHO + CH_3\dot{C}O$$

c. α,β-Unsaturated Carbonyls. For this class of oxygen-containing organics, the OH radical reaction can proceed via two pathways, namely, OH radical addition to the >C=C< bond or via H atom abstraction. For the α,β-unsaturated ketones this latter route, i.e., H atom abstraction, is expected to be negligible, and hence for this subclass OH radical addition will be the essentially exclusive reaction pathway, e.g.

$$OH + CH_2{=}CHCOCH_3 \rightarrow HOCH_2\dot{C}HCOCH_3 \text{ and } \dot{C}H_2CH(OH)COCH_3$$

However, for the α,β-unsaturated aldehydes the overall H atom abstraction pathway from the -CHO group is expected to be significant, e.g., for acrolein

$$OH + CH_2{=}CHCHO \rightarrow H_2O + CH_2{=}CH\dot{C}O \quad (a)$$

$$OH + CH_2{=}CHCHO \rightarrow HOCH_2\dot{C}HCHO \text{ and } \dot{C}H_2CH(OH)CHO \quad (b)$$

While no definitive product data for these α,β-unsaturated aldehydes are available, the kinetic data for the OH radical[223] and O_3[383] reactions and the observation of a peroxyacyl nitrate, presumed to be $CH_2{=}C(CH_3)C(O)OONO_2$, from the NO_x-air photooxidation of methacrolein[384] indicates that H atom abstraction is important. Thus while for acrolein the overall room-temperature OH radical rate constant is close to that for the aliphatic aldehydes, for crotonaldehyde and methacrolein the room-temperature rate constants are approximately a factor of 1.5–1.8 higher. Assuming that the rate constant for the H atom abstraction pathway is similar to those for acetaldehyde or 1-propanal, this suggests that the H atom abstraction pathway accounts for most of the overall reaction for acrolein and for ~55–70% of the overall reaction for crotonaldehyde and methacrolein. This conclusion is consistent with predictions from correlations between OH radical and O_3 reactions for this class of organics[383] (but see also ref 385).

The reaction mechanisms of methacrolein and methyl vinyl ketone under atmospheric conditions have been discussed by Lloyd et al.[14] and Killus and Whitten[15] as an integral part of the isoprene (2-methyl-1,3-butadiene) atmospheric degradation scheme. The reaction scheme of Lloyd et al. for methacrolein,[14] which is consistent with the chemical mechanisms discussed by Atkinson and Lloyd[3] for the various classes of organics, is used to illustrate the chemistry subsequent to the initial OH radical reaction.

As discussed above, the initial reaction almost certainly proceeds via the two pathways

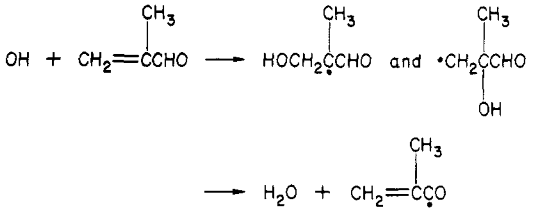

$$OH + CH_2{=}\overset{CH_3}{C}CHO \longrightarrow HOCH_2\underset{\bullet}{\overset{CH_3}{C}}CHO \text{ and } \cdot CH_2\underset{OH}{\overset{CH_3}{C}}CHO$$
$$\longrightarrow H_2O + CH_2{=}\overset{CH_3}{C}\underset{\bullet}{C}O$$

The subsequent fates of these radicals under atmospheric conditions in the presence of NO are analogous to those formed in the alkene and aldehyde reaction mechanisms, respectively. Thus, for example, for the OH radical addition pathway the reaction scheme is expected to be

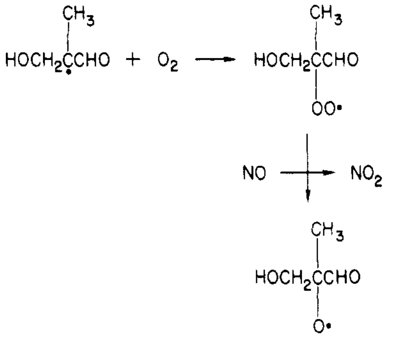

$$HOCH_2\underset{\bullet}{\overset{CH_3}{C}}CHO + O_2 \longrightarrow HOCH_2\underset{OO\cdot}{\overset{CH_3}{C}}CHO$$
$$\xrightarrow{NO \;\rightarrow\; NO_2} HOCH_2\underset{O\cdot}{\overset{CH_3}{C}}CHO$$

followed by decomposition of this alkoxy radical

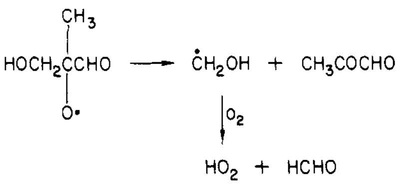

$$HOCH_2\underset{O\cdot}{\overset{CH_3}{C}}CHO \longrightarrow \dot{C}H_2OH + CH_3COCHO$$
$$\dot{C}H_2OH \xrightarrow{O_2} HO_2 + HCHO$$

A totally analogous reaction sequence, leading to the same products, is expected to occur for the $\cdot CH_2C(CH_3)(OH)CHO$ radical.

The expected reactions of the $CH_2{=}C(CH_3)\dot{C}O$ radical are as follows,[14] involving the rapid addition of O_2

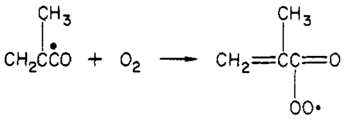

$$CH_2\overset{CH_3}{C}\dot{C}O + O_2 \longrightarrow CH_2{=}\overset{CH_3}{C}\underset{OO\cdot}{C}{=}O$$

followed by reaction with NO_2

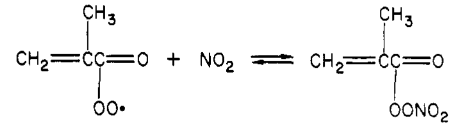

$$CH_2{=}\overset{CH_3}{C}\underset{OO\cdot}{C}{=}O + NO_2 \rightleftharpoons CH_2{=}\overset{CH_3}{C}\underset{OONO_2}{C}{=}O$$

to form a thermally unstable peroxyacyl nitrate, which has been tentatively observed,[384] and with NO

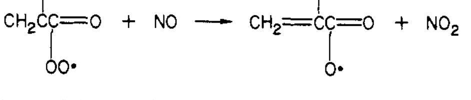

$$CH_2\overset{CH_3}{C}\underset{OO\cdot}{C}{=}O + NO \longrightarrow CH_2{=}\overset{CH_3}{C}\underset{O\cdot}{C}{=}O + NO_2$$

This $CH_2{=}C(CH_3)CO_2\cdot$ radical is expected to decompose to yield CO_2 and the $CH_2{=}\dot{C}CH_3$ radical, followed by the following speculative reactions of this $CH_2{=}\dot{C}CH_3$ radical with O_2 and NO:

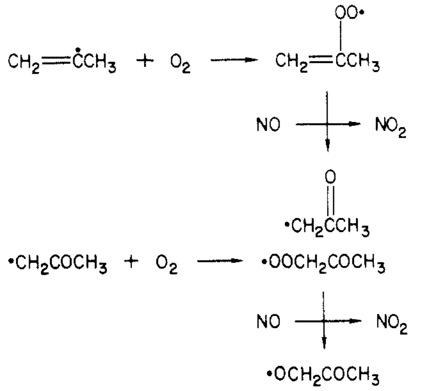

As discussed by Atkinson and Lloyd,[3] the $\cdot OCH_2COCH_3$ radical will react under atmospheric conditions with O_2 to yield methylglyoxal

$$CH_3COCH_2O\cdot + O_2 \rightarrow HO_2 + CH_3COCHO$$

Since for the α,β-unsaturated ketones the OH radical reaction involves solely addition to the >C=C< bond, the subsequent reaction sequences are analogous to those following OH radical addition to the α,β-unsaturated aldehydes. It should be noted, however, that multiple decomposition pathways may be available for the ketoalkoxy radicals. Thus for the reaction of OH radicals with methyl vinyl ketone, while the alkoxy radical $CH_3COCH(OH)CH_2\dot{O}$ decomposes as follows

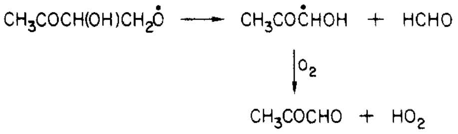

$CH_3COC(\dot{O})HCH_2OH$ can decompose via

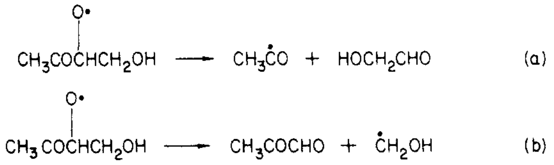

Pathway a is favored thermochemically, as observed experimentally.[139] Thus, in contrast to the alkenes, where identical products are formed after OH radical addition at either of the unsaturated carbon atoms, differing final products can be formed for the α,β-unsaturated carbonyls, depending on the position of initial OH radical addition to the >C=C< entity.

d. α-Dicarbonyls. The reactions of these organics subsequent to the initial OH radical reaction are expected to be analogous to those for the simple aldehydes and ketones. The initial reaction involves overall H atom abstraction from the –CHO group (glyoxal and methylglyoxal) or the $-CH_3$ group (biacetyl). The magnitude of the OH radical rate constants thus reflect the corresponding C–H bond energies, with those in biacetyl being similar to those in acetone and ethane.[165]

Taking glyoxal as an example, the initial reaction proceeds via

$$OH + (CHO)_2 \rightarrow HCO\dot{C}O + H_2O$$

Recently Niki et al.[386] have shown, from an FT-IR spectroscopic study of the Cl atom initiated reaction of glyoxal, that this initially formed $HCO\dot{C}O$ radical can either decompose or react with O_2:

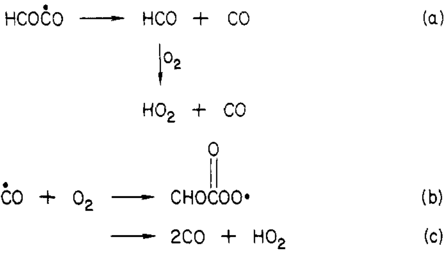

with $k_b \approx k_c$ and $k_a/k_b \approx 3.5 \times 10^{18}$ molecule cm^{-3}.[386] Thus at 298 K and 760-torr total pressure of air, O_2 addition occurs ~40% of the time, while formation of CO and HO_2 occurs the remaining ~60%. The $HCOCO_3$ radical is expected to react with NO_2 and NO analogous to RCO_3 (R = alkyl) radicals. Similar reaction schemes are expected for methylglyoxal.

e. Unsaturated 1,4-Dicarbonyls. The sole product and mechanistic study concerning this class of organics is that recently carried out by Tuazon et al.[352] using FT-IR absorption spectroscopy. While obviously for the 3-hexene-2,5-diones the OH radical reaction must proceed via OH radical addition to the >C=C< bond, the data obtained did not allow the mechanism to be elucidated, except to suggest that the alkoxy radical $CH_3COCH(OH)C(\dot{O})HCOCH_3$ isomerizes or reacts with O_2 rather than decomposing.[352] The expected atmospheric chemistry of this class of organics has been discussed in detail by Atkinson and Lloyd[3] and parallels very closely the chemistry of the unsaturated α,β-carbonyls. Further experimental data concerning the atmospheric chemistry of this class of organics are clearly necessary before any firm recommendations regarding the reactions subsequent to the initial OH radical reaction under atmospheric conditions can be made.

f. Alcohols. For the saturated alcohols, the reactions with OH radicals proceed via H atom abstraction from both the C–H and O–H bonds. On the basis of the thermochemistry of H atom abstraction from –OH bonds (with a bond dissociation energy of 100.9 ± 1.0[387] or 104.4 ± 1 kcal mol^{-1} [319]) and the C–H bonds in CH_3OH (of bond dissociation energy 94 ± 2 kcal mol^{-1} [319]), the predominant reaction process in CH_3OH is expected to be exclusively via H atom abstraction from the C–H bonds. This is consistent with the observations that the corresponding Cl atom reaction with CH_3OH proceeds solely via H atom abstraction from the C–H bonds[87,388]). For the higher saturated alcohols, H atom abstraction from the strong O–H bonds would be expected to be even less important.

However, the two recent studies of Hägele et al.[355] and Meier et al.[87,356] have elucidated the relative importance of pathways a and b

$$OH + CH_3OH \rightarrow H_2O + CH_3O\cdot \qquad (a)$$

$$OH + CH_3OH \rightarrow H_2O + \dot{C}H_2OH \qquad (b)$$

and derived, from LIF measurements of the $CH_3\dot{O}$ radical, ratios of $k_a/(k_a + k_b)$ at ~298 K of 0.11 ± 0.03[355] (increasing to 0.22 ± 0.07 at 393 K[355]) and 0.17 ± 0.08.[87,356]

Thus for CH_3OH it appears that H atom abstraction from both C–H and O–H bonds occurs, with that from the stronger O–H bonds increasing in importance with increasing temperature. However, since under atmospheric conditions both the $CH_3\dot{O}$ and $\dot{C}H_2OH$ radicals react with O_2 to yield HO_2 and HCHO[3,137,254]

$$CH_3\dot{O} + O_2 \rightarrow HCHO + HO_2$$

$$k(298\ K) \simeq 1.3 \times 10^{-15}\ cm^3\ molecule^{-1}\ s^{-1}\ {}^{3,246,247,389}$$

$$\dot{C}H_2OH + O_2 \rightarrow HCHO + HO_2$$

$$k(298\ K) \simeq (1\text{–}12) \times 10^{-12}\ cm^3\ molecule^{-1}\ s^{-1}\ {}^{253,255,256}$$

the ultimate products formed from the two reaction pathways are identical.

Interestingly, while the $\dot{C}H_2OH$ radical appears to react with O_2 via an overall abstraction reaction, the reaction of HO_2 radicals with HCHO leads to formation of the $HOCH_2O\dot{O}$ radical which would arise from O_2 addition to $\dot{C}H_2OH$. This occurs via initial HO_2 radical addition to HCHO, followed by isomerization of the initially formed $HO_2CH_2\dot{O}$ radical[3,390–392]

$$HO_2 + HCHO \rightleftarrows HO_2CH_2O\cdot \rightarrow [HOCH_2OO\cdot]^{*} \xrightarrow{M} HOCH_2OO\cdot$$

as evidenced by formation of the thermally labile peroxynitrate $HOCH_2OONO_2$.[392] While the formation of the $HOCH_2O\dot{O}$ radical obviously occurs, the reaction pathway to form this radical from $\dot{C}H_2OH$ and O_2 is exothermic by ~33 kcal mol^{-1}.[226,319] Under atmospheric conditions, it may be that elimination of HO_2 from the initially formed energy rich $HOCH_2OO\cdot$ radical competes with collisional stabilization.

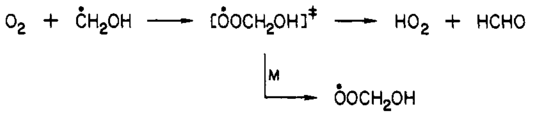

The higher alcohols, after reaction with OH radicals at the α-carbon atom, also yield exclusively, within the experimental error limits, the corresponding carbonyls and an HO_2 radical[252,254]

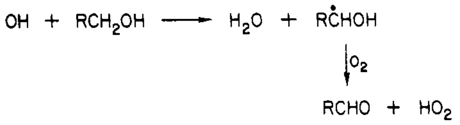

However, experimental data are available only up to the C_4 alcohols,[252] and on the basis of our above discussion, it is evident that further data are required for the higher $R\dot{C}HOH$ radicals before these observations can be extended to higher alcohols or to other classes of organics which yield $R\dot{C}HOH$ radicals during their atmospheric degradation pathways.

For ethanol, Meier et al.[356,359] have recently shown from a mass spectrometric investigation of the reaction products that the initial OH radical reaction forming the $CH_3\dot{C}HOH$ radical accounts for 75 ± 15% of the overall reaction at 300 K. For these higher alcohols, H atom abstraction from the carbon atoms other than the α-carbon is also expected to occur; the subsequent reactions are then analogous to those for the alkyl radicals.

For allyl alcohol, the magnitude of the OH radical reaction indicates, as expected, that this reaction occurs prodominantly via OH radical addition to the >C═C< bond.

g. Ethers. For the saturated ethers, the OH radical reactions apparently proceed via H atom abstraction from the C–H bonds. As noted above, the C–H bonds for CH_x (x = 1–3) groups adjacent to the oxygen atom have significantly lower bond dissociation energies than do the corresponding C–H bonds in the alkanes.[226,319,379] Since the bond dissociation energies per primary, secondary, or tertiary C–H bond are expected to increase as these CH_x groups become more distant from the oxygen atom,[363] the distribution of initially formed radicals from these OH radical reactions cannot as yet be reliably calculated for any but the simplest ethers (but see section IV below for presently available a priori predictions).

The subsequent reactions are expected to be totally analogous to those for the alkanes. Thus, for example, for dimethyl ether the reaction sequence under atmospheric conditions appears to be

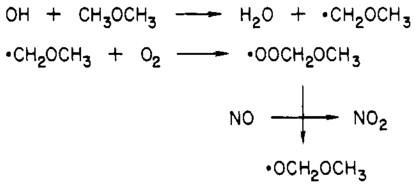

For this particular alkoxy radical, under atmospheric conditions, reaction with O_2 dominates over decomposition to yield methyl formate[393]

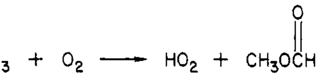

$$\ldots_3 + O_2 \longrightarrow HO_2 + CH_3O\overset{\overset{O}{\|}}{C}H$$

For vinyl methyl ether and furan, the magnitude of the rate constants and the negative temperature dependencies[363,365] indicate that the reaction of OH radicals with these unsaturated ethers proceed via initial OH radical addition to the >C═C< double bonds, e.g.

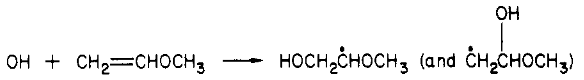

$$OH + CH_2{=}CHOCH_3 \longrightarrow HOCH_2\dot{C}HOCH_3\ (\text{and}\ \dot{C}H_2\overset{\overset{OH}{|}}{C}HOCH_3)$$

followed by

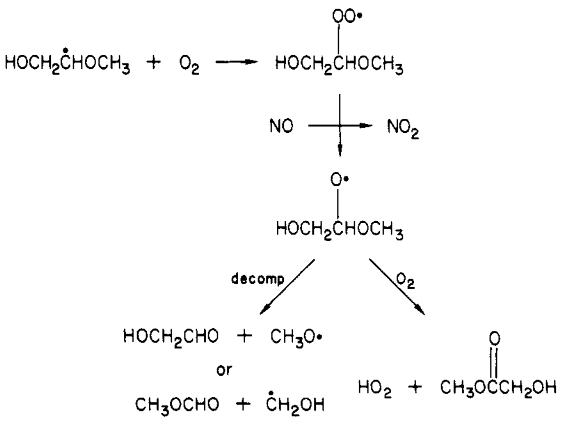

Obviously further product and mechanistic data under atmospheric conditions are necessary before anything approaching a complete understanding of these reaction sequences will become available.

h. Esters. As discussed above, the limited data set (which includes, as discussed elsewhere in this article, i.e., those sections dealing with the aldehydes and the

TABLE XII. Rate Constants *k* and Arrhenius Parameters for the Gas-Phase Reaction of OH Radicals with Sulfur-Containing Organics

organic	$10^{12}A$, cm^3 molecule^{-1} s^{-1}	*E*, cal mol^{-1}	$10^{12}k$, cm^3 molecule^{-1} s^{-1}	*T*, K	technique	ref	temp range covered, *K*
				Thiols			
methanethiol			33.9 ± 3.4	299.8	FP-RF	Atkinson et al.[394]	300–423
			27.3 ± 2.8	347.2			
	8.89	−790 ± 300	23.0 ± 2.3	423.1			
			97.0 ± 9.4[a]	297 ± 2	rel rate [rel to *k*(OH + ethene) = 8.58 × 10^{-12}][b]	Cox and Sheppard[395]	
			48.3 ± 9.8	244	FP-RF	Wine et al.[396]	244–366
			38.4 ± 5.8	270			
			33.7 ± 4.1	298			
			32.2 ± 6.2	333			
	11.5 ± 3.9	−672 ± 199	29.7 ± 4.7	366			
			21 ± 2	293	DF-EPR	Mac Leod et al.[397,398]	
			25.6 ± 4.4	296	DF-RF	Lee and Tang[399]	
			40.8 ± 4.2	254	FP-RF	Wine et al.[400]	254–430
			37.3 ± 4.3	272			
			32.2 ± 3.2	298			
			31.6 ± 4.3	298			
			30.4 ± 1.9	298			
			32.5 ± 0.9	298			
			30.9 ± 1.0	298			
			32.5 ± 2.8	299			
			32.3 ± 3.7	300			
			30.3 ± 2.6	322			
			24.9 ± 3.1	347			
			28.0 ± 2.8	375			
			23.9 ± 1.3	403			
	10.1 ± 1.9	−689 ± 117	22.5 ± 1.4	430			
methanethiol-*d*$_1$ (CH_3SD)			40.4 ± 2.2	253	FP-RF	Wine et al.[400]	253–429
			34.3 ± 3.9	268			
			34.1 ± 4.1	276			
			31.9 ± 2.8	295			
			30.8 ± 2.1	297			
			28.7 ± 1.8	346			
			24.3 ± 1.0	384			
			24.0 ± 1.8	412			
	11.2 ± 1.5	−616 ± 86	23.4 ± 0.7	429			
ethanethiol			27 ± 2	293	DF-EPR	Mac Leod et al.[397,398]	
			36.7 ± 1.8	296	DF-RF	Lee and Tang[399]	
			65.5 ± 5.1	252	FP-RF	Wine et al.[400]	252–425
			51.5 ± 3.5	278			
			45.2 ± 6.2	298			
			43.1 ± 6.1	298			
			42.1 ± 3.2	298			
			46.5 ± 2.9	300			
			40.2 ± 1.4	343			
			33.2 ± 3.6	381			
			34.1 ± 3.1	397			
	12.3 ± 3.3	−787 ± 167	33.2 ± 2.7	425			
1-propanethiol ($CH_3CH_2CH_2SH$)			63.1 ± 2.0	257	FP-RF	Wine et al.[400]	257–419
			45.6 ± 1.8	298			
			41.8 ± 5.7	298			

			45.5 ± 2.5	298			
			36.3 ± 1.6	353			
	8.89 ± 2.80	−972 ± 195	29.1 ± 0.9	419			
2-propanethiol ((CH$_3$)$_2$CHSH)			56.9 ± 9.0	256	FP-RF	Wine et al.[400]	256–429
			40.7 ± 3.7	297			
			42.2 ± 7.1	299			
			39.5 ± 4.4	300			
			31.2 ± 0.9	358			
			33.0 ± 3.4	380			
			35.5 ± 2.6	423			
	11.6 ± 5.5	−767 ± 308	25.1 ± 2.3	429			
1-butanethiol (CH$_3$CH$_2$CH$_2$CH$_2$SH)			43.8 ± 6.6	298	FP-RF	Wine et al.[400]	
2-methyl-1-propanethiol ((CH$_3$)$_2$CHCH$_2$SH)			41.8 ± 6.3	298	FP-RF	Wine et al.[400]	
2-butanethiol (CH$_3$CH$_2$C(CH$_3$)HSH)			39.8 ± 5.9	298	FP-RF	Wine et al.[400]	
2-methyl-2-propanethiol ((CH$_3$)$_3$CSH)			47.2 ± 2.3	257	FP-RF	Wine et al.[400]	257–409
			34.2 ± 1.3	298			
			35.7 ± 0.8	298			
			26.3 ± 4.2	348			
	6.22 ± 1.35	−1025 ± 133	22.7 ± 0.5	409			
				Sulfides			
dimethyl sulfide			9.8 ± 1.2	299.9	FP-RF	Atkinson et al.[401]	300–427
			9.3 ± 1.2	355.3			
	5.47	−355 ± 300	8.2 ± 1.2	426.5			
			10.98 ± 3.37	273	FP-RF	Kurylo[402]	273–400
			8.28 ± 0.87	296			
			10.75 ± 2.85	323			
			7.99 ± 1.37	362			
	6.25 ± 4.19	−260 ± 427	9.28 ± 2.01	400			
			9.78 ± 1.54[a]	297 ± 2	rel rate [rel to k(OH + ethene) = 8.58 × 10^{-12}][b]	Cox and Sheppard[395]	
			3.89 ± 0.38	248	FP-RF	Wine et al.[396]	248–363
			4.15 ± 0.55	271			
			4.26 ± 0.56	298			
			4.50 ± 0.68	334			
	6.8 ± 1.1	274 ± 91	4.67 ± 0.51	363			
			9.2 ± 0.6	373	DF-EPR	Mac Leod et al.[397,398]	373–573
			7.8 ± 1.0	573			
			9.7 ± 1.0[a]	296 ± 2	rel rate [rel to k(OH + n-hexane) = 5.53 × 10^{-12}][b]	Atkinson et al.[403]	
			3.6 ± 0.2	297	FP-RF	Wallington et al.[404]	297–400
			3.8 ± 0.7	320			
			3.7 ± 0.9	332			
			3.7 ± 0.4	359			
			3.4 ± 0.4	369			
			3.4 ± 0.4	377			
	$2.5^{+0.9}_{-0.6}$	−258 ± 203	3.3 ± 0.3	400			
	9.64 ± 2.10	465 ± 131	4.40 ± 0.66	298	FP-RF	Wine et al.[405]	248–397
			5.80 ± 0.16[c]	298	LP-LIF	Wine et al.[405]	
			3.80 ± 0.30	273	DF-EPR	Martin et al.[406]	
			3.22 ± 0.16	293			
			3.66 ± 0.19	318			
di(methyl-d_3) sulfide (CD$_3$SCD$_3$)	10.3 ± 1.7	990 ± 101	1.94 ± 0.27	298	FP-RF	Wine et al.[405]	253–418
methyl ethyl sulfide			8.50 ± 1.27	298	FP-RF	Wine et al.[405]	
diethyl sulfide	15.2 ± 1.5	0 ± 199	15.2 ± 2.3	298	FP-RF	Wine et al.[405]	255–370
			12 ± 1.4	293	DF-EPR	Martin et al.[406]	
di-*tert*-butyl sulfide ((CH$_3$)$_3$CSC(CH$_3$)$_3$)		*d*	7.51 ± 1.12	298	FP-RF	Wine et al.[405]	260–424

TABLE XII (Continued)

organic	$10^{12}A$, cm^3 $molecule^{-1}$ s^{-1}	E, cal mol^{-1}	$10^{12}k$, cm^3 $molecule^{-1}$ s^{-1}	T, K	technique	ref	temp range covered, K
dimethyl disulfide			240 ± 86[a]	297 ± 2	rel rate [rel to k(OH + ethene) = 8.58 × 10^{-12}][b]	Cox and Sheppard[395]	
			280 ± 18	249	FP-RF	Wine et al.[396]	249–367
			198 ± 18	298			
	59 ± 33	−755 ± 318	171 ± 25	367			
Thioethers							
tetrahydrothiophene			23.2 ± 1.3	255	FP-RF	Wine and Thompson[365]	255–377
			20.9 ± 1.9	255			
			19.8 ± 3.4	298			
			18.4 ± 1.0	298			
			18.8 ± 1.8	338			
			19.5 ± 0.6	377			
			16.2 ± 1.4	377			
	11.3 ± 3.5	−330 ± 193	17.4 ± 1.3	377			
			21.2 ± 1.6	293	DF-EPR	Martin et al.[406]	
thiophene			47.7 ± 6.3	295 ± 1	DF-RF	Lee and Tang[199]	
			9.37 ± 0.34	298 ± 2	rel rate [rel to k(OH + n-hexane) = 5.58 × 10^{-12}][b]	Atkinson et al.[217]	
			50 ± 4	293	DF-EPR	Mac Leod et al.[398,407]	293–473
			22 ± 2	333			
			12 ± 2	373			
	0.13 ± 0.08	−3477 ± 397	5.2 ± 0.5	473			
			11.4 ± 0.6	255	FP-RF	Wine and Thompson[365]	255–425
			11.5 ± 0.9	255			
			9.57 ± 1.15	298			
			9.37 ± 0.66	298			
			8.20 ± 0.68	353			
			7.28 ± 0.41	419			
			6.06 ± 0.37	425			
	3.20 ± 0.70	−646 ± 141	7.37 ± 0.41	425			
			10.1 ± 0.5	274	FP-RF	Wallington[408]	274–382
			8.9 ± 0.7	298 ± 2			
			6.1 ± 1.2	325			
			5.5 ± 0.3	349			
			6.3 ± 0.6	365			
			5.3 ± 0.5	379			
	$1.2^{+1.0}_{-0.6}$	−1160 ± 431	5.8 ± 0.5	382			
			12 ± 1	293	DF-EPR	Martin et al.[406]	

[a] At atmospheric pressure of air. [b] From the present recommendations (see text). [c] In the presence of 593 torr of air (see text). [d] Arrhenius plot exhibits curvature.[405]

alkyl nitrites, the possibly dubious data of Campbell and co-workers[159]) indicates that these OH radical reactions proceed via H atom abstraction from the -OR entity, e.g.

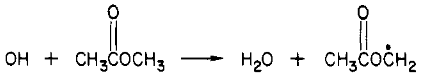

$$OH + CH_3C(O)CH_3 \rightarrow H_2O + CH_3C(O)\dot{C}H_2$$

The subsequent reactions under atmospheric conditions have not been elucidated but are expected to involve rapid O_2 addition, followed by reaction sequences such as that shown:

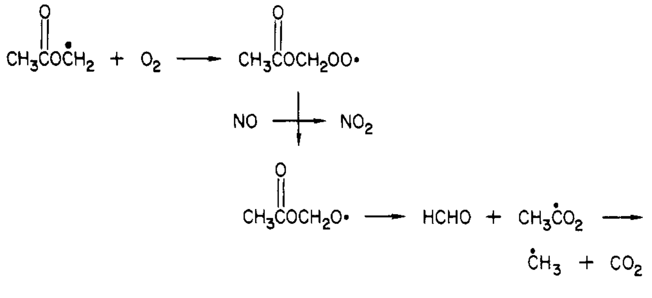

Again, further kinetic, mechanistic, and product data are needed before a complete understanding of the atmospheric chemistry of this class of organics becomes available.

i. Carboxylic Acids. The sole mechanistic information available for the reaction of OH radicals with the carboxylic acids arises from the study of Wine et al.[367] for formic acid. Using resonance fluorescence detection of H atoms, the H atom production yield was estimated[367] to be 0.75 ± 0.25, indicating that the major reaction pathway proceeds via

$$OH + HCOOH \rightarrow H_2O + CO_2 + H$$

The detailed reaction dynamics are not known, i.e., initial formation of a HO-HCOOH adduct followed by direct H atom production or subsequent decomposition to H_2O + HOCO* (followed by decomposition of this energized HOCO* radical) or by direct H atom abstraction to yield H_2O and HOCO. The lack of a kinetic deuterium isotope effect for the reaction of OH radicals with DCOOH and the observation of an essentially zero temperature dependence of the rate constant for HCOOH supports the initial formation of an HO-HCOOH adduct as the major reaction pathway.[367]

Again, it is clear that further kinetic, mechanistic, and product data for the higher carboxylic acids are needed.

j. Oxides. The kinetic data set for this class of organics, which are clearly a subset of the ethers, is limited (Table XI), and only for ethene oxide has a product and mechanistic study been carried out.[368] For all of the oxides studied to date, the initial reaction is expected to involve H atom abstraction, e.g.

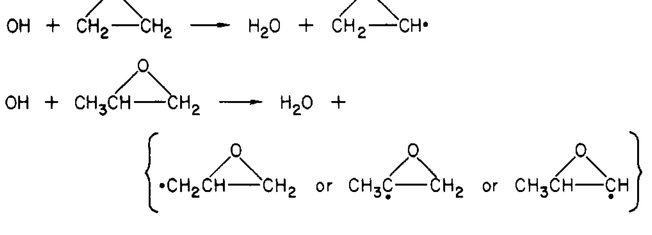

Due to the high ring strain energy of ~27 kcal mol^{-1},[226] the initially formed radical is expected to rapidly undergo ring cleavage, with or without a 1,2-H atom shift,[368] e.g.

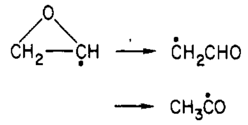

Lorenz and Zellner[368] have recently determined, by using LIF detection to monitor the vinoxy radical, $\dot{C}H_2CHO$ yields at 298 K of 0.08 ± 0.03 and 0.23 ± 0.08 at 10- and 60-torr total pressure of helium, respectively.

For the higher oxides, radicals such as $RCO\dot{C}H_2$ and $R\dot{C}HCHO$ may be formed; their subsequent reactions have been dealt with in the above discussions of other oxygen-containing organics.

k. Hydroperoxides. As shown in Table XI, kinetic data have been obtained only for CH_3OOH and $(CH_3)_3COOH$. For CH_3OOH, Niki and co-workers[370] have shown that both of the reaction channels

$$OH + CH_3OOH \rightarrow H_2O + \cdot CH_2OOH \quad (a)$$

$$OH + CH_3OOH \rightarrow H_2O + CH_3OO\cdot \quad (b)$$

are operative, with a rate constant ratio at room temperature of $k_a/(k_a + k_b) \approx 0.42 \pm 0.09$. The subsequent reactions of the CH_3O_2 radical have been dealt with previously, while the $\cdot CH_2OOH$ radical will decompose

$$\cdot CH_2OOH \rightarrow HCHO + OH$$

to regenerate an OH radical. Thus, interestingly, while the relative rate measurements yield the overall rate constant ($k_a + k_b$), absolute flash photolysis or discharge flow measurements may yield (depending on the lifetime of the $\cdot CH_2OOH$ radical, which may be short relative to the experimental measurement period) only the rate constant k_b.

For $(CH_3)_3COOH$, because of the stronger C-H bonds than the O-H bond, the reaction is expected to proceed mainly via H atom abstraction from the weak O-H bond

$$OH + (CH_3)_3COOH \rightarrow H_2O + (CH_3)_3COO\cdot$$

and this is consistent with the magnitude of the rate constant measured by Anastasi et al.[371] This $(CH_3)_3CO\dot{O}$ radical will react with NO as follows (together with a small amount of alkyl nitrate formation), followed by decomposition of the alkoxy radical:

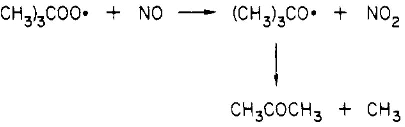

G. Sulfur-Containing Organics

1. *Kinetics*

The available kinetic data for this class of organic compounds are listed in Table XII. Most of these data deal with the reactions of OH radicals with thiols, sulfides and thioethers, and the sulfur-containing organics for which recommendations are made are discussed individually below.

a. Thiols. i. Methanethiol. The available kinetic data are listed in Table XII. Rate constants have been determined by Atkinson et al.,[394] Wine et al.,[396,400] Mac Leod et al.,[397,398] and Lee and Tang[399] using flash photolysis[394,396,400] and discharge flow[397-399] techniques and by Cox and Sheppard[395] using a relative rate technique. While the absolute rate constant data,[394,396-400] which were obtained in the absence of O_2 at total pressures of $\leq$200 torr, are in general agreement, the rate constant derived by Cox and Sheppard[395] from relative rate measurements in one atmosphere of synthetic air is a factor of ~3 higher. Although this could be due to an enhancement by oxygen, as observed for the reaction of OH radicals with CS_2,[409-411] Wine et al.[400] conclude, from their observations of exponential OH radical decays over the entire temperature range studied and the lack of a deuterium isotope effect, that any kinetic enhancement due to O_2 is unlikely. Thus the data obtained in the absence of O_2 should be applicable to atmospheric pressure.

Of the absolute rate constants obtained (plotted in Arrhenius form in Figure 44), the flash photolysis–resonance fluorescence data of Atkinson et al.[394] and Wine et al.[396,400] are in excellent agreement. However, these rate constants[394,396,400] are somewhat higher, by up to 50%, than the room-temperature values of Mac Leod et al.[397,398] and Lee and Tang.[399] Similar discrepancies occur for ethanethiol.

From a unit-weighted least-squares analysis of the flash photolysis–resonance fluorescence data of Atkinson et al.[394] and Wine et al.,[396,400] the Arrhenius expression

$$k(\text{methanethiol}) = (9.70^{+1.90}_{-1.58}) \times 10^{-12} e^{(366\pm56)/T} \text{ cm}^3 \text{ molecule}^{-1} \text{ s}^{-1}$$

is recommended, where the indicated errors are two least-squares standard deviations, and

$$k(\text{methanethiol}) = 3.31 \times 10^{-11} \text{ cm}^3 \text{ molecule}^{-1} \text{ s}^{-1} \text{ at } 298 \text{ K}$$

with an estimated uncertainty at 298 K of ±20%.

ii. Ethanethiol. Rate constants have been determined by Mac Leod et al.,[397,398] Lee and Tang,[399] and Wine et al.,[400] with the sole temperature dependence study being that of Wine et al.[400] These data are plotted in Arrhenius form in Figure 45. As for methanethiol, the two discharge flow studies[397-399] yield somewhat lower room-temperature rate constants. From a unit-weighted least-squares analysis of the rate constant data of Wine et al.,[400] the Arrhenius expression

$$k(\text{ethanethiol}) = (1.23^{+0.37}_{-0.29}) \times 10^{-11} e^{(396\pm84)/T} \text{ cm}^3 \text{ molecule}^{-1} \text{ s}^{-1}$$

is tentatively recommended, where the indicated error limits are two least-squares standard deviations, and

$$k(\text{ethanethiol}) = 4.65 \times 10^{-11} \text{ cm}^3 \text{ molecule}^{-1} \text{ s}^{-1} \text{ at } 298 \text{ K}$$

with an estimated uncertainty at 298 K of ±25%.

The remaining thiols for which data are available (Table XII) have been studied only by Wine et al.[400] These thiols (1- and 2-propanethiol, 1- and 2-butanethiol, 2-methyl-1-propanethiol, and 2-methyl-2-propanethiol) all have room-temperature rate constants and negative temperature dependencies similar to those for methanethiol and ethanethiol, indicating no significant effect of the alkyl side chain on the kinetics of these reactions. Furthermore, the rate constants for CH_3SD are virtually identical with those for CH_3SH,[400] indicating no kinetic deuterium isotope effect within the experimental error limits.

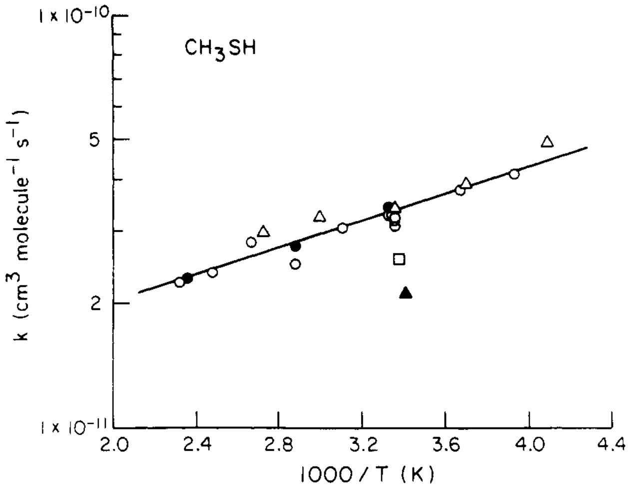

Figure 44. Arrhenius plot of the rate constants for the reaction of OH radicals with methanethiol: (●) Atkinson et al.;[394] (△) Wine et al.;[396] (▲) Mac Leod et al.;[397,398] (□) Lee and Tang;[399] (○) Wine et al.;[400] (—) recommendation (see text).

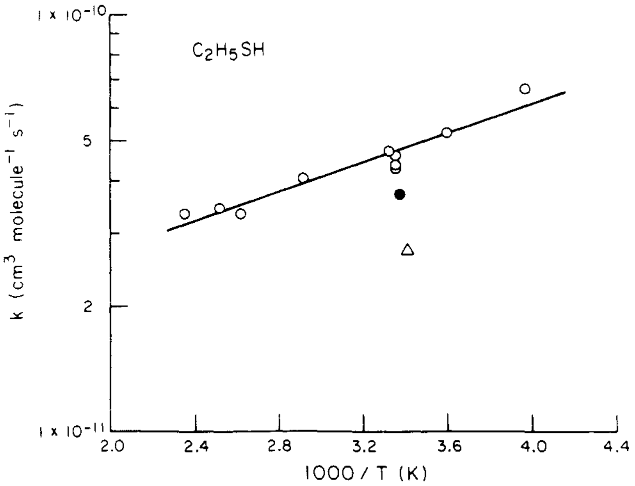

Figure 45. Arrhenius plot of the rate constants for the reaction of OH radicals with ethanethiol: (△) Mac Leod et al.;[397,398] (●) Lee and Tang;[399] (○) Wine et al.;[400] (—) recommendation (see text).

b. Sulfides. i. Dimethyl Sulfide. The available kinetic data are listed in Table XII. Rate constants have been obtained using absolute rate constant techniques in the absence of O_2[396-398,401,402,404-406] and by relative rate techniques at room-temperature and atmospheric pressure of air.[395,403,404] There are significant discrepancies in the measured rate constants within this data set, and this is approached by first evaluating the rate constants obtained in the absence of O_2 and then those in the presence of O_2 (for example, in one atmosphere of air).

In the absence of O_2 the available rate constants, plotted in Arrhenius form in Figure 46, have all been obtained by using absolute rate constant techniques and fall into two groups, namely, those of Atkinson et al.,[401] Kurylo,[402] and Mac Leod et al.[397,398] which exhibit a room-temperature rate constant of ~(9–10) × 10^{-12} cm^3 molecule^{-1} s^{-1} and a negative temperature dependence equivalent to an Arrhenius activation energy of approximately −0.6 kcal mol^{-1} and those of Wine et

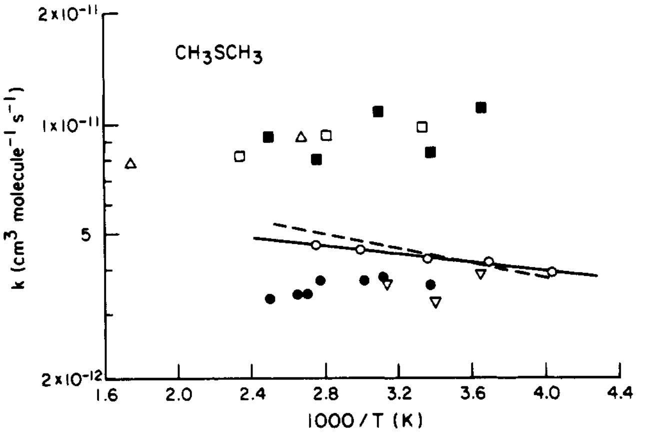

Figure 46. Arrhenius plot of the rate constants for the reaction of OH radicals with dimethyl sulfide in the absence of O_2: (□) Atkinson et al.;[401] (■) Kurylo;[402] (○) Wine et al.;[396] (△) MacLeod et al.;[397,398] (●) Atkinson et al.;[404] (- - -) Wine et al.;[405] (▽) Martin et al.;[406] (—) recommendation (see text).

al.,[396,405] Wallington et al.,[404] and Martin et al.[406] which have a room-temperature rate constant of ~4 × 10^{-12} cm^3 $molecule^{-1}$ s^{-1} and a zero or slightly positive temperature dependence.[396,404-406] For the reasons discussed below, the most recent data sets of Wine et al.,[396,405] Wallington et al.,[404] and Martin et al.[406] are used in the evaluation of this rate constant.

While even for this data set there are significant discrepancies, it is recommended that in the absence of O_2 the Arrhenius expression of Wine et al.[396] be used, i.e.

$$k(\text{dimethyl sulfide}) = (6.78^{+1.18}_{-1.01}) \times 10^{-12} e^{-(137\pm48)/T}\ \text{cm}^3\ \text{molecule}^{-1}\ \text{s}^{-1}$$

where the indicated error limits are two least-squares standard deviations

$$k(\text{dimethyl sulfide}) = 4.28 \times 10^{-12}\ \text{cm}^3\ \text{molecule}^{-1}\ \text{s}^{-1}\ \text{at}\ 298\ \text{K}$$

with an estimated uncertainty at 298 of ±30%.

The reported relative rate constant studies of Cox and Sheppard[395] and Atkinson et al.,[403] carried out in 1 atm of air, have derived a rate constant of ~9.7 × 10^{-12} cm^3 $molecule^{-1}$ s^{-1} at room temperature.[395,403] Since these data were obtained by monitoring the relative decay rates of dimethyl sulfide and a reference organic (ethene[395] or *n*-hexane[403]), problems associated with impurities can be discounted. The possibility of an O_2 effect has been investigated at 298 K by Wine et al.[405] using a laser photolysis–laser-induced fluorescence (LP–LIF) technique and by Wallington et al.[404] using two relative rate techniques at ~740-torr total pressure. Wine et al.[405] have observed that for M = air the rate constant does exhibit a small "O_2 effect", increasing from 4.8 × 10^{-12} cm^3 $molecule^{-1}$ s^{-1} in the absence of air to 5.18 × 10^{-12} and 5.8 × 10^{-12} cm^3 $molecule^{-1}$ s^{-1} in the presence of 343- and 593-torr total pressure of air, respectively.[405] In contrast, in the absence of O_2 the rate constant is independent of the diluent gas pressure,[396,401,402,404,405] up to 500-torr total pressure of SF_6.[405]

Recently Wallington et al.[404] have used two relative rate techniques to study the kinetics of this reaction at 296 ± 2 K as a function of the O_2 pressure (over the range 0–740 torr) at a constant total pressure of ~740 torr. The rate constants obtained from these relative rate measurements were observed to increase with increasing O_2 concentration.[404] However, for a given O_2 concentration the rate constants obtained by using the dark N_2H_4–O_3 reaction to generate OH radicals were lower by 10–25% than those obtained by using irradiated CH_3ONO–NO–air mixtures to generate OH radicals.[404] The rate constants at 740 torr total pressure of air were (8.5 ± 0.2) × 10^{-12} and (9.3 ± 0.7) × 10^{-12} cm^3 $molecule^{-1}$ s^{-1} for these two methods of generation of OH radicals, respectively. Extrapolation to zero O_2 leads[404] to a rate constant of (8.3 ± 0.7) × 10^{-12} cm^3 $molecule^{-1}$ s^{-1} for the irradiated CH_3ONO–NO–air system and (5.3 ± 0.5) × 10^{-12} cm^3 $molecule^{-1}$ s^{-1} for the dark N_2H_4–O_3 system.

These extrapolated rate constants in the absence of O_2 are lower than the room-temperature absolute values determined by Atkinson et al.,[401] Kurylo,[402] and Mac Leod et al.,[397,398] thus supporting the above recommendation of the lower absolute rate constants of Wine et al.,[396,405] Wallington et al.,[404] and Martin et al.[406] Furthermore, the discrepancies between the rate constants obtained by these two relative rate techniques, which at 740 torr total pressure of O_2 are well outside of the two standard deviation combined error limits, suggest that secondary reactions may be involved, leading to a stoichiometry factor in excess of unity for the disappearance of CH_3SCH_3 in these relative rate measurements. This possibility is further suggested by recent product data for the reactions of NO_3 radicals with CH_3SH[412] in air in the presence of part per million concentrations of NO_2, which show the formation of CH_3SSCH_3 from CH_3SH. These data[412] indicate that even in the presence of air CH_3S radicals can undergo self-recombination reactions. Thus it appears that the data from relative rate constant measurements involving the thiols, sulfides, and disulfides are probably suspect, leading to erroneously high rate constants. This may also impact the detailed elucidation of reaction mechanisms and products.

In view of the above discussion, it is recommended, based on the above recommendation for this reaction in the absence of O_2 and the LP–LIF measurements of Wine et al.[405] in the presence of O_2, that at 298 K

$$k(\text{dimethyl sulfide}) = 4.28 \times 10^{-12}(1 + 2.6 \times 10^{-3}P)\ \text{cm}^3\ \text{molecule}^{-1}\ \text{s}^{-1}$$

where P is the pressure of air in torr, and

$$k(\text{dimethyl sulfide}) = 6.3 \times 10^{-12}\ \text{cm}^3\ \text{molecule}^{-1}\ \text{s}^{-1}$$

at 760-torr total pressure of air. It is expected that any temperature dependence will be small. Clearly, further experimental studies are necessary to better define the kinetics of this reaction.

For the remaining sulfides, data are available only from the recent study of Wine et al.[405] for a series of sulfides and of Martin et al.[406] for diethyl sulfide, with the two room-temperature rate constants for this sulfide being in good agreement.[405,406] There is a significant isotope effect for dimethyl sulfide, with the room-temperature rate constant for CD_3SCD_3 being lower than that for CH_3SCH_3 by a factor of ~2.[405] For CH_3SCH_3, $CH_3SC_2H_5$, and $C_2H_5SC_2H_5$ the room-temperature rate constants increase with the size of the alkyl substituent groups, while for di-*tert*-butyl sulfide [$[(CH_3)_3C]_2S$]

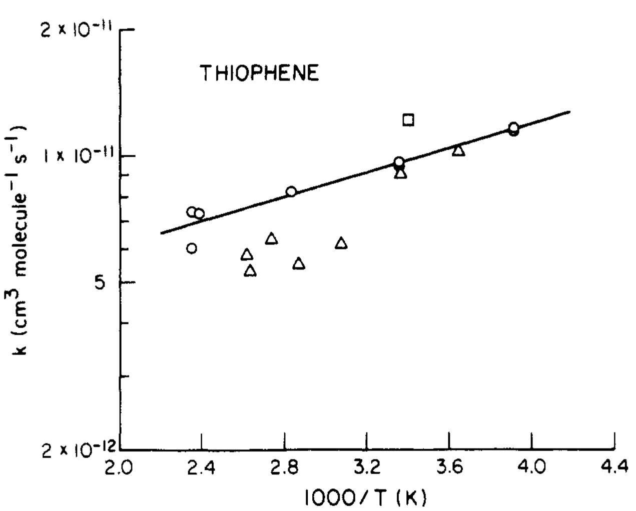

Figure 47. Arrhenius plot of the rate constants for the reaction of OH radicals with thiophene: (●) Atkinson et al.;[217] (○) Wine and Thompson;[365] (△) Wallington;[408] (□) Martin et al.;[406] (—) recommendation (see text).

non-Arrhenius behavior is observed, with a room-temperature rate constant similar to that for $CH_3SC_2H_5$, but with the rate constant increasing both above and below room temperature.[405]

c. Disulfides. The only kinetic data available for this class of sulfur-containing organics (Table XII) arise from the flash photolysis–resonance fluorescence rate constants determined by Wine et al.[396] and the room-temperature relative rate constant of Cox and Sheppard[395] for dimethyl disulfide. These room-temperature rate constants are in reasonable agreement within the error limits, and it is tentatively recommended, based upon the rate constant data of Wine et al.,[396] that

$$k(\text{dimethyl disulfide}) = (5.12^{+2.43}_{-1.65}) \times 10^{-11} e^{(414\pm112)/T}\ \text{cm}^3\ \text{molecule}^{-1}\ \text{s}^{-1}$$

where the indicated error limits are two least-squares standard deviations (note that this expression is different to that cited by Wine et al.[396] for unknown reasons)

$$k(\text{dimethyl disulfide}) = 2.05 \times 10^{-10}\ \text{cm}^3\ \text{molecule}^{-1}\ \text{s}^{-1}\ \text{at 298 K}$$

with an estimated uncertainty at 298 K of ±50%.

d. Thioethers. i. Thiophene. Rate constants have been determined for thiophene by Lee and Tang,[199] Atkinson et al.,[217] Mac Leod et al.,[398,407] Wine and Thompson,[365] Wallington,[408] and Martin et al.[406] The two earlier discharge flow measurements[199,398,407] yield room-temperature rate constants higher by a factor of ~5 than those determined from the flash photolysis,[365,408] the most recent discharge flow,[406] and the relative rate[217] studies. To some extent this situation is analogous to that for furan, and the rate constants of Lee and Tang[199] and Mac Leod et al.[398,407] are not used in the rate constant evaluation.

While the rate constants of Atkinson et al.,[217] Wine and Thompson,[365] Wallington,[408] and Martin et al.[406] (plotted in Arrhenius form in Figure 47) are in good agreement at temperatures ≤298 K, significant discrepancies arise between those of Wine and Thompson[365] and Wallington[408] at elevated temperatures. Since the Arrhenius preexponential factor for this reaction should be in the upper 10^{-12} cm³ molecule⁻¹ s⁻¹ region, it is recommended, based upon a unit-weighted least-squares analysis of the rate constant data of Atkinson et al.[217] and Wine and Thompson,[365] that

$$k(\text{thiophene}) = (3.20^{+0.73}_{-0.59}) \times 10^{-12} e^{(324\pm65)/T}\ \text{cm}^3\ \text{molecule}^{-1}\ \text{s}^{-1}$$

where the indicated error limits are two least-squares standard deviations, and

$$k(\text{thiophene}) = 9.49 \times 10^{-12}\ \text{cm}^3\ \text{molecule}^{-1}\ \text{s}^{-1}\ \text{at 298 K}$$

with an estimated uncertainty at 298 K of ±20%.

Two studies have been carried out for tetrahydrothiophene,[365,406] with good agreement at room temperature (the only temperature studied by Martin et al.[406]). However, no firm recommendation for this sulfur-containing organic is made.

2. Mechanisms and Subsequent Reactions under Atmospheric Conditions

a. Thiols. There are three possible pathways for the reaction of OH radicals with the thiols, taking methanethiol as an example:

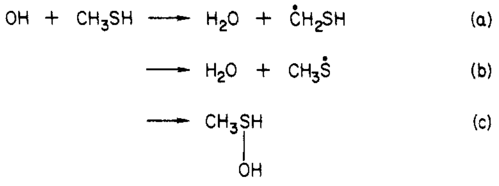

$$\mathrm{OH + CH_3SH \longrightarrow H_2O + \dot{C}H_2SH} \qquad (a)$$
$$\mathrm{\longrightarrow H_2O + CH_3\dot{S}} \qquad (b)$$
$$\mathrm{\longrightarrow CH_3\underset{\substack{|\\ OH}}{S}H} \qquad (c)$$

The observation that the room-temperature rate constants and the temperature dependencies are essentially invariant of the alkyl group, including the $(CH_3)_3C$– group (Table XII), shows that H atom abstraction from the C–H bonds cannot be the major reaction pathway.[400] Thus these reactions must proceed via either H atom abstraction from the weak S–H bonds (of bond dissociation energy 91 ± 1.5 kcal mol⁻¹ [319,413]) or by the formation of an OH–thiol adduct. While no definitive information is available concerning this issue, Wine et al.[400] conclude from the lack of a deuterium isotope kinetic effect for CH_3SH and CH_3SD and from the product data of Hatakeyama and Akimoto[177] that adduct formation involving OH radical addition to the sulfur atom is the primary reaction pathway.

Hatakeyama and Akimoto[177] observed the formation of CH_3SNO and ROH, with essentially identical formation yields, from the irradiation of CH_3SH–RONO–NO–air mixtures. The dark formation of CH_3SNO and ROH was observed to be of minor importance and based upon a series of control experiments, including the predominant formation of $CH_3S^{14}NO$ in irradiated CH_3SH–RONO–^{15}NO–air mixtures, Hatakeyama and Akimoto[177] concluded that the OH–thiol adduct reacted in their experimental system with RCH_2ONO:

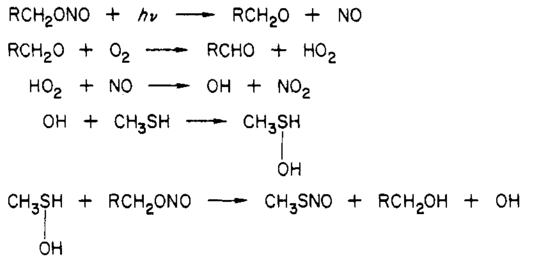

$$\mathrm{RCH_2ONO} + h\nu \longrightarrow \mathrm{RCH_2O + NO}$$
$$\mathrm{RCH_2O + O_2 \longrightarrow RCHO + HO_2}$$
$$\mathrm{HO_2 + NO \longrightarrow OH + NO_2}$$
$$\mathrm{OH + CH_3SH \longrightarrow CH_3\underset{\substack{|\\ OH}}{S}H}$$
$$\mathrm{CH_3\underset{\substack{|\\ OH}}{S}H + RCH_2ONO \longrightarrow CH_3SNO + RCH_2OH + OH}$$

followed by rapid photolysis of CH_3SNO to yield CH_3S radicals and NO:[414]

$$CH_3SNO + h\nu \rightarrow CH_3S + NO$$

Subsequent reactions of CH_3S with O_2 (probably via the formation of CH_3SO_2) were postulated to lead to SO_2 and HCHO, the major ultimate products.[177] Since irradiataion of CH_3SH-2-methyl-2-butene–NO–air mixtures give rise to the same yield (~29%) of SO_2[177] (though Grosjean[415] has reported a 100% SO_2 yield from irradiation of a CH_3SH–NO–air mixture), this implies that the CH_3S radical is also formed in this system, presumably from decomposition of the $CH_3S(OH)H$ adduct:

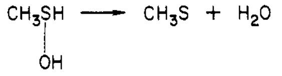

$$CH_3\underset{\displaystyle OH}{\underset{|}{S}}H \longrightarrow CH_3S + H_2O$$

Clearly, further experimental data are required concerning the dynamics of the initial OH radical with thiols and of the subsequent reaction pathways operative under atmospheric conditions.

b. Sulfides. The reaction of OH radicals with the sulfides, RSR, can proceed via either H atom abstraction from the C–H bonds (96 ± 1 kcal mol^{-1} in CH_3SCH_3[416]) or OH radical addition to the sulfur atom:

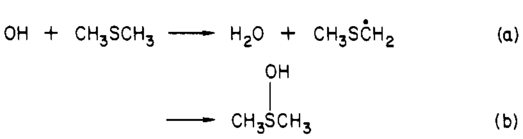

$$OH + CH_3SCH_3 \longrightarrow H_2O + CH_3S\dot{C}H_2 \qquad (a)$$

$$\longrightarrow CH_3\overset{\displaystyle OH}{\overset{|}{S}}CH_3 \qquad (b)$$

The most recent extensive kinetic study of Wine et al.[405] shows that in the absence of O_2 there is a significant deuterium isotope effect for dimethyl sulfide and that the room-temperature rate constant increases along the series CH_3SCH_3, $CH_3SC_2H_5$, and $C_2H_5SC_2H_5$.[405] This strongly suggests that for these particular sulfides, and in the absence of O_2, H atom abstraction from the C–H bonds is the dominant reaction pathway. For $(CH_3)_3CSC(CH_3)_3$ the Arrhenius plot shows marked curvature, with the rate constant increasing both above and below 298 K, thus exhibiting a minimum value at ~298 K.[405] This observation suggests[405] that OH radical addition to the sulfur atom may become significant for this sulfide for temperatures $\lesssim$298 K.

However, it is expected, by analogy with the $O(^3P)$ atom reactions with CH_3SH,[417-421] C_2H_5SH,[417-421] the higher thiols,[419] CH_3SCH_3,[417,418,420-423] and CH_3SSCH_3,[420,421,424] that if OH radical addition to the thiols occurs, then so would OH radical addition to the sulfides, with the addition rate constants for the sulfides being markedly higher than those for the thiols. [Thus these reactions all proceed via $O(^3P)$ atom addition to the sulfur atom[418,421,422] with rate constants which increase markedly from CH_3SH to CH_3SCH_3 to CH_3SSCH_3[420] but are to a first approximation invariant of the alkyl group in the thiols.[419]]

Indeed, the recent observation of an effect of O_2 on the rate constant for the reaction of OH radicals with dimethyl sulfide[405] shows that OH radical addition to this sulfide does occur, with the resulting $CH_3S(OH)CH_3$ adduct radical being intercepted by O_2:

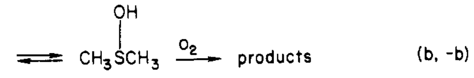

$$OH + CH_3SCH_3 \longrightarrow H_2O + CH_3S\dot{C}H_2 \qquad (a)$$

$$\rightleftharpoons CH_3\overset{\displaystyle OH}{\overset{|}{S}}CH_3 \xrightarrow{O_2} \text{products} \qquad (b, -b)$$

As discussed above, the kinetic data of Wine et al.[405] indicate that at 298 K the rate constant for the OH radical addition pathway increases approximately linearly with the O_2 concentration and has a value of ~2 × 10^{-12} cm^3 $molecule^{-1}$ s^{-1} at 760-torr total pressure of air. Thus at atmospheric pressure of air the H atom abstraction process accounts for ~70% of the overall reaction, with the initial OH radical addition process intercepted by O_2 accounting for the remainder.

Product data for the reaction of OH radicals with dimethyl sulfide under atmospheric conditions have been obtained from numerous studies,[177,178,415,425-427] with the major final products being HCHO, SO_2, and CH_3SO_3H, together with CH_3SNO as an intermediate product. While the most recent product studies[177,178,415] all postulate that the CH_3S radical is the main intermediate giving rise to SO_2 and CH_3SO_3H, the detailed reaction steps are still a matter of discussion.[177,178,415] The discussion above of the relative importance of the H atom abstraction and OH radical addition pathways indicates that the majority of the reaction (~70%) may proceed via

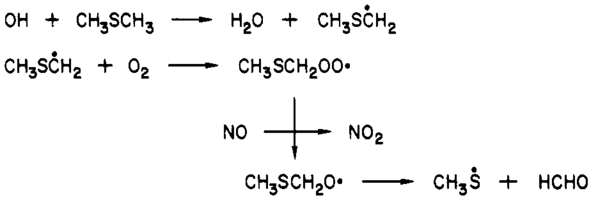

$$OH + CH_3SCH_3 \longrightarrow H_2O + CH_3S\dot{C}H_2$$

$$CH_3S\dot{C}H_2 + O_2 \longrightarrow CH_3SCH_2OO\cdot$$

$$CH_3SCH_2OO\cdot \xrightarrow{NO \,\to\, NO_2} CH_3SCH_2O\cdot$$

$$CH_3SCH_2O\cdot \longrightarrow CH_3\dot{S} + HCHO$$

with the CH_3S radical giving rise to SO_2 and CH_3SO_3H [as well as possibly being involved in secondary reactions with CH_3SCH_3 (see above)]. Although the products arising from the initial OH radical addition reaction are not presently known, the overall product distribution under atmospheric conditions (for example, the yield of SO_2) may be similar to that arising from the photolysis of CH_3SNO.[414] This indeed appears to be so, since the SO_2 yields (~21–22%)[177,178,425,427] are very similar to that observed from the irradiation of CH_3SNO–air mixtures.[414]

c. Disulfides. Only for dimethyl disulfide have kinetic[395,396] and product[177] data been reported. On the basis of these data, it appears that the initial reaction proceeds via OH radical addition to form an adduct,[177,395,396] followed by rapid decomposition of this adduct to CH_3S and CH_3SOH radicals[177]

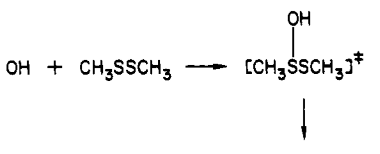

$$OH + CH_3SSCH_3 \longrightarrow [CH_3\overset{\displaystyle OH}{\overset{|}{S}}SCH_3]^{\ddagger} \longrightarrow CH_3SOH + CH_3S$$

Subsequent reactions of these CH_3SOH and CH_3S radicals then lead to the observed products (SO_2, HCHO, CH_3SO_3H).[177]

d. Thioethers. Kinetic data are available only for tetrahydrothiophene[365,406] and thiophene (ref 199, 217, 365, 398, 406–408) and no product studies have been carried out to date. Thus any assessments concerning the initial reaction pathways must be based on these kinetic data and analogies with the reaction mechanisms for other classes of organics.

For thiophene the initial reaction can proceed via OH radical addition to either the sulfur atom or the >C=

TABLE XIII. Rate Constants *k* and Arrhenius Parameters for the Gas-Phase Reaction of OH Radicals with Nitrogen- and Phosphorus-Containing Organics at the High-Pressure Limits

organic	$10^{12}A$, cm^3 molecule^{-1} s^{-1}	E, cal mol^{-1}	$10^{12}k$, cm^3 molecule^{-1} s^{-1}	T, K	technique	ref	temp range covered, K
Nitrogen-Containing Organics							
Amines							
methylamine			22.0 ± 2.2	299.0	FP-RF	Atkinson et al.[394]	299–426
			19.4 ± 2.0	353.9			
	10.2	−455 ± 300	17.5 ± 1.8	426.1			
ethylamine			27.7 ± 2.8	299.6	FP-RF	Atkinson et al.[428]	300–426
			24.9 ± 2.5	354.1			
	14.7	−375 ± 300	23.0 ± 2.3	425.8			
dimethylamine			65.4 ± 6.6	298.5	FP-RF	Atkinson et al.[428]	298–425
			58.3 ± 5.9	354.5			
	28.9	−490 ± 300	51.1 ± 5.2	425.4			
trimethylamine			60.9 ± 6.1	298.7	FP-RF	Atkinson et al.[428]	299–425
			53.7 ± 5.4	352.5			
	26.2	−500 ± 300	47.4 ± 4.8	424.7			
diethylhydroxylamine			101	308	PR-RA	Gorse et al.[429]	
2-dimethylaminoethanol			66.9 ± 15.0	269	FP-RF	Anderson and Stephens[430]	269–364
			78.9 ± 17.2	293			
			85.7 ± 7.8	333			
	80^{+20}_{-10}	0	79.4 ± 13.0	364			
			47 ± 12	300 ± 2	FP-RF	Harris and Pitts[431]	
2-amino-2-methyl-1-propanol			28 ± 5	300 ± 2	FP-RF	Harris and Pitts[431]	
N-nitrosodimethylamine			2.53 ± 0.21	298 ± 2	rel rate [rel to k(OH + dimethyl ether) = 2.98×10^{-12}][a]	Tuazon et al.[149]	
dimethylnitramine			3.84 ± 0.15	298 ± 2	rel rate [rel to k(OH + dimethyl ether) = 2.98×10^{-12}][a]	Tuazon et al.[149]	
Hydrazines							
hydrazine			22 ± 5	298	DF-EPR	Hack et al.[432]	
			65 ± 10	298 ± 1	FP-RF	Harris et al.[433]	298–424
			59 ± 9	355 ± 1			
	44	−230 ± 350	58 ± 9	424 ± 1			
	[61 ± 10	0]					
methylhydrazine	65 ± 13	0	65 ± 13	298	FP-RF	Harris et al.[433]	298–424
Nitrites							
methyl nitrite			1.42 ± 0.19	292 ± 2	rel rate [rel to k(OH + CO = 1.60×10^{-13}][b]	Campbell and Goodman[157]	
			1.08 ± 0.17	295 ± 3	rel rate [rel to k(OH + n-butane) = 2.48×10^{-12}][a]	Audley et al.[158]	
			0.21 ± 0.04	300 ± 3	rel rate [rel to k(OH + n-hexane) = 5.64×10^{-12}][a]	Tuazon et al.[143]	
			0.12 ± 0.03	300 ± 3	rel rate [rel to k(OH + dimethyl ether) = 3.01×10^{-12}][a]	Tuazon et al.[143]	
			1.00 ± 0.15	295	DF-RF	Baulch et al.[434]	
ethyl nitrite			1.75 ± 0.27	295 ± 3	rel rate [rel to k(OH + n-butane) = 2.48×10^{-12}][a]	Audley et al.[158]	
1-propyl nitrite [$CH_3(CH_2)_2ONO$]			2.38 ± 0.44	295 ± 3	rel rate [rel to k(OH + n-butane) = 2.48×10^{-12}][a]	Audley et al.[158]	

			2.31 ± 0.33	295	DF-RF	Baulch et al.[434]	
1-butyl nitrite [$CH_3(CH_2)_3ONO$]			5.2 ± 1.7	295 ± 3	rel rate [rel to k(OH + n-butane) = 2.48 × 10^{-12}]^a	Audley et al.[158]	
			4.80 ± 0.72	295	DF-RF	Baulch et al.[434]	
2-butyl nitrite [$CH_3CH_2C(CH_3)HONO$]			5.93 ± 0.70	295 ± 3	rel rate [rel to k(OH + n-butane) = 2.48 × 10^{-12}]^a	Audley et al.[158]	
3-methyl-1-propyl nitrite [$(CH_3)_2CH_2CH_2ONO$]			5.31 ± 0.64	295 ± 3	rel rate [rel to k(OH + n-butane) = 2.48 × 10^{-12}]^a	Audley et al.[158]	
2-methyl-2-propyl nitrite [$(CH_3)_3CONO$]			1.40 ± 0.20	295 ± 3	rel rate [rel to k(OH + n-butane) = 2.48 × 10^{-12}]^a	Audley et al.[158]	
			Nitrates				
2-propyl nitrate [$(CH_3)_2CHONO_2$]			0.18 ± 0.05	299 ± 2	rel rate [rel to k(OH + cyclohexane) = 7.41 × 10^{-12}]^a	Atkinson et al.[155]	
1-butyl nitrate [$CH_3(CH_2)_3ONO_2$]			1.39 ± 0.11	299 ± 2	rel rate [rel to k(OH + cyclohexane) = 7.41 × 10^{-12}]^a	Atkinson et al.[155]	
2-butyl nitrate [$CH_3CH_2C(CH_3)HONO_2$]			0.67 ± 0.10	299 ± 2	rel rate [rel to k(OH + cyclohexane) = 7.41 × 10^{-12}]^a	Atkinson et al.[155]	
2-pentyl nitrate [$CH_3(CH_2)_2C(CH_3)HONO_2$]			1.83 ± 0.12	299 ± 2	rel rate [rel to k(OH + cyclohexane) = 7.41 × 10^{-12}]^a	Atkinson et al.[155]	
3-pentyl nitrate [$(C_2H_5)_2CHONO_2$]			1.10 ± 0.20	299 ± 2	rel rate [rel to k(OH + cyclohexane) = 7.41 × 10^{-12}]^a	Atkinson et al.[155]	
2-methyl-3-butyl nitrate [$(CH_3)_2CHC(CH_3)HONO_2$]			1.72 ± 0.05	298 ± 2	rel rate [rel to k(OH + n-butane) = 2.53 × 10^{-12}]^a	Atkinson et al.[29]	
2,2-dimethyl-1-propyl nitrate [$(CH_3)_3CCH_2ONO_2$]			0.85 ± 0.20	298 ± 2	rel rate [rel to k(OH + n-butane) = 2.53 × 10^{-12}]^a	Atkinson et al.[29]	
2-hexyl nitrate [$CH_3C(ONO_2)H(CH_2)_3CH_3$]			3.13 ± 0.15	299 ± 2	rel rate [rel to k(OH + cyclohexane) = 7.41 × 10^{-12}]^a	Atkinson et al.[155]	
3-hexyl nitrate [$CH_3CH_2CH(ONO_2)(CH_2)_2CH_3$]			2.66 ± 0.21	299 ± 2	rel rate [rel to k(OH + cyclohexane) = 7.41 × 10^{-12}]^a	Atkinson et al.[155]	
cyclohexyl nitrate			3.29 ± 0.36	298 ± 2	rel rate [rel to k(OH + n-butane) = 2.53 × 10^{-12}]^a	Atkinson et al.[29]	
2-methyl-2-pentyl nitrate [$(CH_3)_2C(ONO_2)(CH_2)_2CH_3$]			1.71 ± 0.22	298 ± 2	rel rate [rel to k(OH + n-butane) = 2.53 × 10^{-12}]^a	Atkinson et al.[29]	
3-methyl-2-pentyl nitrate [$CH_3C(ONO_2)HCH(CH_3)CH_2CH_3$]			3.01 ± 0.08	298 ± 2	rel rate [rel to k(OH + n-butane) = 2.53 × 10^{-12}]^a	Atkinson et al.[29]	
3-heptyl nitrate [$C_2H_5C(ONO_2)H(CH_2)_3CH_3$]			3.64 ± 0.43	299 ± 2	rel rate [rel to k(OH + cyclohexane) = 7.41 × 10^{-12}]^a	Atkinson et al.[155]	
3-octyl nitrate [$C_2H_5C(ONO_2)H(CH_2)_4CH_3$]			3.82 ± 0.78	299 ± 2	rel rate [rel to k(OH + cyclohexane) = 7.41 × 10^{-12}]^a	Atkinson et al.[155]	
			Nitriles				
hydrogen cyanide	0.12 ± 0.05	795	0.03 ± 0.01	298	FP-RA	Fritz et al.[435,436]	296–433
acetonitrile [CH_3CN]			0.0494 ± 0.006	297.2	FP-RF	Harris et al.[437]	297–424
			0.0620 ± 0.007	348.0			
	0.586	1500 ± 250	0.105 ± 0.015	423.8			
			0.024 ± 0.003	295	FP-RF	Fritz et al.[435]	
			0.019 ± 0.002	296	FP-RF	Zetzsch[357]	
			0.0102 ± 0.0022	250	FP-RF	Kurylo and Knable[438]	250–363
			0.0146 ± 0.0015	273			
			0.0194 ± 0.0037	298			
	0.628	2047	0.0370 ± 0.0033	363			
			0.021 ± 0.003	295	DF-EPR	Poulet et al.[439]	
propionitrile [C_2H_5CN]			0.194 ± 0.020	298.2	FP-RF	Harris et al.[437]	298–423
			0.233 ± 0.025	350.8			
			0.362 ± 0.036	384.0			

TABLE XIII (Continued)

organic	$10^{12}A$, cm^3 $molecule^{-1}$ s^{-1}	E, cal mol^{-1}	$10^{12}k$, cm^3 $molecule^{-1}$ s^{-1}	T, K	technique	ref	temp range covered, K
	2.69	1590 ± 350	0.414 ± 0.040	423.0			
acrylonitrile [CH_2=CHCN]		~0	4.80 ± 0.50	298.7	FP-RF	Harris et al.[437]	299–423
			3.4 ± 0.5	296	FP-RF	Zetzsch[357]	
					Nitrogen-Containing Heterocycles		
aziridine			6.1 ± 0.5	295	FP-RF	Zetzsch[220]	
pyrrole			122 ± 4	295 ± 1	rel rate [rel to k(OH + propene) = 2.68 × 10^{-11}]^a	Atkinson et al.[440]	
			103 ± 6	298	FP-RF	Wallington[408]	298–440
			98 ± 20	325			
			83 ± 13	355			
	27^{+8}_{-6}	−801 ± 185	68 ± 10	440			
pyridine			0.49 ± 0.04	296 ± 2	rel rate [rel to k(OH + dimethyl ether) = 2.96 × 10^{-12}]^a	Atkinson et al.[441]	
1,3,5-triazine			0.15 ± 0.03	296 ± 2	rel rate [rel to k(OH + dimethyl ether) = 2.96 × 10^{-12}]^a	Atkinson et al.[441]	
					Miscellaneous		
peroxyacetyl nitrate			≤0.17	299 ± 1	FP-RF	Winer et al.[293]	
			0.113 ± 0.006	273 ± 2	FP-RF	Wallington et al.[442]	273–297
	1.23	1294 ± 455	0.137 ± 0.005	297 ± 2			
nitromethane			1.01 ± 0.10	292	rel rate [rel to k(OH + CO) = 1.60 × 10^{-13}]^b	Campbell and Goodman[157]	
CH_2=NOH			0.63 ± 0.31	300 ± 2	FP-KS	Horne and Norrish[106]	
CH_3CH=NOH			2.2 ± 1.1	300 ± 2	FP-KS	Horne and Norrish[106]	
					Phosphorus-Containing Organics		
trimethyl phosphate [$(CH_3O)_3PO$]			7.4 ± 0.74	296 ± 2	rel rate [rel to k(OH + dimethyl ether) = 2.96 × 10^{-12}]^a	Tuazon et al.[273]	

[a] From the recommendations (see text). [b] From the expression $k(OH + CO) = 1.50 \times 10^{-13} [(1 + 9.19 \times 10^{-4}P)/(1 + 2.24 \times 10^{-4}P)]$ cm^3 $molecule^{-1}$ s^{-1},[3] where P is the total pressure in torr.

C< bonds, while for tetrahydrothiophene the reaction can proceed via OH radical addition to the sulfur atom or by H atom abstraction from the C–H bonds. The available kinetic data do not allow unambiguous decisions to be made regarding these possibilities, except to note that the negative temperature dependence for the tetrahydrothiophene reaction[365] suggests that OH radical addition to the sulfur atom is an important route for this thioether.[365]

Since any discussion regarding the subsequent reactions under atmospheric purposes is purely speculative, we can only recommend that further product and mechanistic studies be carried out.

The observation that for thiophene at room temperature the rate constant obtained in the presence of one atmopshere of air[217] is in agreement with those obtained at lower total pressures of argon or SF_6 diluent gas[365,408] shows that there is no oxygen-enhancement effect and that the OH–thiophene adduct is collisionally thermalized at relatively low total pressures ($\lesssim$30 torr of argon). This, together with the well behaved OH radical kinetic behavior in the flash photolysis studies,[365,408] then shows that this OH–thiophene adduct is thermally stable for $\geq$0.1 s at temperatures $\lesssim$425 K.[365]

H. Nitrogen- and Phosphorus-Containing Organics

1. *Kinetics*

The available rate constants at the high-pressure second-order limit are given in Table XIII (only for HCN have rate constant data in the fall-off region between second- and third-order kinetics been obtained[435,436,443,444]). As can be seen from Table XIII, for most of these nitrogen-containing organics only a single kinetic study has been carried out, the exceptions being 2-(dimethylamino)ethanol, hydrazine, methyl nitrite, acetonitrile, acrylonitrile, and peroxyacetyl nitrate (PAN). For 2-(dimethylamino)ethanol, hydrazine, methyl nitrite, and acetonitrile there are significant discrepancies in the reported rate constant data, and only for acrylonitrile[357,437] and peroxyacetyl nitrate[293,442] are the studies carried out consistent, with, for peroxyacetyl nitrate, one of these yielding only an upper limit rate constant.[293]

Only for acetonitrile (CH_3CN) is a firm recommendation made, based upon the agreement between the room-temperature rate constants of Fritz et al.,[435] Zetzsch,[357] Kurylo and Knable,[438] and Poulet et al.,[439] and these data[357,435,438,439] are plotted in Arrhenius form in Figure 48. From a unit-weighted least-squares analysis of these rate constants of Fritz et al.,[435] Kurylo and Knable,[438] Zetzsch,[357] and Poulet et al.,[439] the Arrhenius expression

$$k(CH_3CN) = (6.78^{+7.37}_{-3.53}) \times 10^{-13} e^{-(1040\pm214)/T} \text{ cm}^3 \text{ molecule}^{-1} \text{ s}^{-1}$$

is recommended, where the indicated error limits are two least-squares standard deviations, and

$$k(CH_3CN) = 2.07 \times 10^{-14} \text{ cm}^3 \text{ molecule}^{-1} \text{ s}^{-1} \text{ at 298 K}$$

with an estimated uncertainty at 298 K of ±30%.

The reasons for the significantly higher rate constants obtained by Harris et al.,[437] using a similar experimental technique, are not presently known but may involve radical formation by the photolysis flash, leading to enhanced OH radical decay rates.

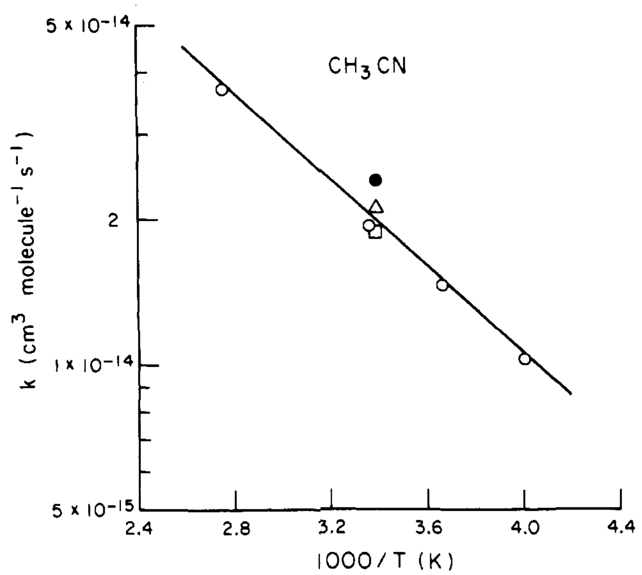

Figure 48. Arrhenius plot of the rate constants for the reaction of OH radicals with CH_3CN: (●) Fritz et al.;[435] (○) Kurylo and Knable;[438] (□) Zetzsch;[357] (△) Poulet et al.;[439] (—) recommendation (see text).

For the remaining nitrogen- and phosphorus-containing organics listed in Table XIII no firm recommendations are made. Since the trends of these rate constants along homologous series are used to assist in elucidating the reaction mechanisms in the section below, these kinetic data are not discussed any further in this section, except to note that for methyl nitrite there is a major discrepancy of a factor of ~7 between the rate constants obtained by Campbell and co-workers[157,158,434] and Tuazon et al.[143] The room-temperature rate constant determined by Tuazon et al.[143] is consistent with H atom abstraction from the C–H bonds and is of the general magnitude to that expected for CH_3ONO_2.[155] Clearly further work on the kinetic data for CH_3ONO and the higher alkyl nitrites is necessary, and indeed a thorough examination of the experimental technique used by Campbell and co-workers[135,157-160,216] is needed.

2. *Mechanisms and Subsequent Reactions under Atmospheric Conditions*

a. Amines. As shown in Table XIII, the OH radical reactions with the aliphatic amines are rapid, with room-temperature rate constants being in the range (2–6) × 10^{-11} cm^3 molecule^{-1} s^{-1} and with negative temperature dependencies equivalent to Arrhenius activation energies of ~–(0.4–0.5) kcal mol^{-1}. For the methyl-substituted amines, the trend of the room-temperature rate constants suggests that these reactions proceed via abstraction from the C–H bonds and, where possible, the N–H bonds. From the rate constants measured by Atkinson et al.[394,428] and the C–H (93.3 ± 2, 87 ± 2, and 84 ± 2 kcal mol^{-1} in CH_3NH_2, $(CH_3)_2NH$, and $(CH_3)_3N$, respectively[319]) and N–H bond strengths (100.0 ± 2.5 and 91.5 ± 2 kcal mol^{-1} in CH_3NH_2 and $(CH_3)_2NH$, respectively[319]), it is expected that for CH_3NH_2, and probably also $C_2H_5NH_2$, H atom abstraction from the C–H bonds predominates, while for $(CH_3)_2NH$, H atom abstraction from the N–H bond is competitive with H atom abstraction from the C–H bonds.[428]

Indeed, from a product study of irradiated HONO–$(CH_3)_2NH$–air mixtures, utilizing long path length FT-IR absorption spectroscopy, Lindley et al.[445] determined that at room temperature $k_a/(k_a + k_b) = 0.37 \pm 0.05$, where k_a and k_b are the rate constants for reaction pathways a and b, respectively

$$OH + (CH_3)_2NH \rightarrow H_2O + (CH_3)_2\dot{N} \quad (a)$$

$$OH + (CH_3)_2NH \rightarrow H_2O + \dot{C}H_2NHCH_3 \quad (b)$$

However, the observation of negative temperature dependencies for these reactions suggests that these OH radical reactions may proceed via the initial formation of an addition complex, which then rapidly decomposes to the observed products. Clearly, further experimental work concerning the reaction dynamics of these systems is needed.

For substituted amines, rate constants have been obtained for diethylhydroxylamine,[429] 2-(dimethylamino)ethanol,[430,431] 2-amino-2-methyl-1-propanol,[431] *N*-nitrosodimethylamine,[149] dimethylnitramine,[149] and aziridine.[220] While these reactions almost certainly proceed via overall H atom abstraction, the position of the H atom abstracted cannot be predicted in all cases, since the C–H and N–H bond strengths are not known. Obviously for *N*-nitrosodimethylamine and dimethylnitramine, any H atom abstraction must occur from the C–H bonds.

The subsequent reactions of the radicals formed from dimethylamine under atmospheric conditions are reasonably well understood.[445] The dimethylamino radicals are expected to react with O_2, NO, and NO_2.

$$\left.\begin{aligned} (CH_3)_2\dot{N} + O_2 &\xrightarrow{M} (CH_3)_2NOO\cdot \\ &\longrightarrow CH_3N{=}CH_2 + HO_2 \end{aligned}\right\} \quad (a)$$

$$(CH_3)_2\dot{N} + NO \xrightarrow{M} (CH_3)_2NNO \quad (b)$$

$$(CH_3)_2\dot{N} + NO_2 \xrightarrow{M} (CH_3)_2NNO_2 \quad (c)$$

$$\longrightarrow CH_3N{=}CH_2 + HONO \quad (d)$$

Lindley et al.[445] have shown, following the formation of $(CH_3)_2\dot{N}$ radicals from the photolysis of $(CH_3)_2NNO$ and $(CH_3)_2NN{=}NN(CH_3)_2$, that the reactions of the $(CH_3)_2\dot{N}$ radical with NO and NO_2 occur and that $k_d/k_c = 0.22 \pm 0.06$ at atmospheric pressure and room temperature. Furthermore, analogous to the situation for the NH_2 radical,[446,447] reaction with O_2 is extremely slow, with $k_a/k_c = (3.90 \pm 0.28) \times 10^{-7}$ and $k_a/k_b = (1.48 \pm 0.07) \times 10^{-7}$.[445] Thus at atmospheric pressure of air, reactions of the $(CH_3)_2\dot{N}$ radical with NO and NO_2 will predominate over reaction with O_2 for NO_x concentrations $\gtrsim 7 \times 10^{11}$ molecule cm^{-3} (30 ppb). For the $\dot{C}H_2NHCH_3$ radical, Lindley et al.[445] have shown that reaction with O_2 occurs to yield $CH_2{=}NCH_3$:

$$\dot{C}H_2NHCH_3 + O_2 \rightarrow HO_2 + CH_2{=}NCH_3$$

Pitts and co-workers,[448,449] utilizing GC-MS and FT-IR absorption spectroscopic techniques, have carried out product studies of irradiated NO_x–amine–air mixtures for the amines dimethylamine,[448,449] diethylamine,[448,449] trimethylamine,[448] and triethylamine.[449] A variety of products were identified, with, for example, large yields of acetaldehyde being observed from the NO_x–air photooxidations of di- and triethylamine.[448] Plausible reaction pathways for this and other products observed are as follows (taking diethylamine as an example)

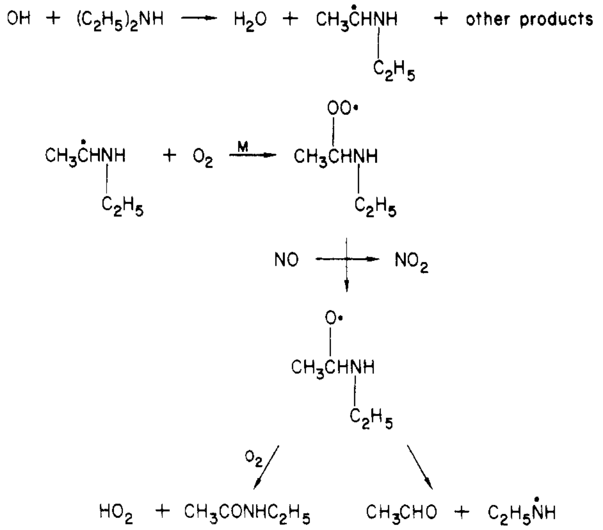

Clearly, only for the dimethylamino radical have the reaction pathways under atmospheric conditions been reasonably well delineated; for the other amines much further experimental data are needed.

b. Hydrazines. To date, only for hydrazine and methylhydrazine are kinetic data available for the OH radical reactions (Table XIII), and no unambiguous product data are available. The reactions of OH radicals with hydrazine and methylhydrazine are expected to occur via overall H atom abstraction from the weak N–H bonds (of bond strength $\sim$75 kcal mol^{-1} [226,450,451]). This is consistent with the magnitude of the rate constants observed,[433] although it is possible that the reaction proceeds via initial formation of an addition complex followed by rapid decomposition to the $RNH\dot{N}H$ or $R\dot{N}NH_2$ radical and H_2O. A general idea of the subsequent reactions of these radicals under atmospheric conditions arises from the studies of Tuazon et al.[452,453] While these product studies were concerned with the reactions of O_3 with these hydrazines, OH radicals were determined to be formed in these reactions,[453] and hence the observed products reflected the OH radical as well as the O_3 reactions. The radicals N_2H_3, $CH_3\dot{N}NH_2$, and $CH_3NH\dot{N}H$ were postulated to react under atmospheric conditions as follows[453]

$$R\dot{N}NH_2 + O_2 \rightarrow RN{=}NH + HO_2 \ (R = H \text{ or } CH_3)$$

$$CH_3NH\dot{N}H + O_2 \rightarrow CH_3N{=}NH + HO_2$$

followed by subsequent reactions of RN=NH with OH radicals or O_3.[453]

c. Nitrites. As noted above, there is a large discrepancy between the rate constants determined by Campbell and co-workers[157,158,434] and by Tuazon et al.[143] for CH_3ONO. These reactions may proceed via H atom abstraction from the C–H bonds, e.g.

$$\begin{tikzcd} OH + CH_3ONO \arrow[r] & H_2O + \dot{C}H_2ONO \arrow[d] \\ & HCHO + NO \end{tikzcd}$$

However, Cox et al.[389] and Zabarnick and Heicklen[454] have postulated from studies of alkyl nitrite photooxidations, using the rate constants of Campbell and co-workers,[157,158] that OH radical addition also occurs to a significant extent. This postulate is open to reexamination depending upon the magnitude of the rate constants, and, while it is possible that the overall reaction solely involves H atom abstraction from the C–H bonds, for the $\geq C_2$ alkyl nitrites the C–H bond from which H atom abstraction occurs cannot be a priori predicted.

Thus, since no product data are presently available, no reliable assessment of the initial reaction pathway can be made until more reliable kinetic or unambiguous product data are available. However, since the alkyl nitrites photolyze rapidly,[3] these OH radical reactions are of limited importance under atmospheric conditions.

d. Nitrates. No product or direct mechanistic data are available for this class of organics, and mechanistic information can only be based upon the kinetic data of Atkinson et al.[29,155] H atom abstraction from the C–H bonds appears to be the only reaction pathway,[29,155] with the $-ONO_2$ group severely decreasing the rate constant for H atom abstraction from $>CH-$ or $-CH_2-$ groups bonded to the $-ONO_2$ group[155] and decreasing those for the β $>CH-$, $-CH_2-$, or $-CH_3$ groups.[29,155] While significant uncertainties remain, at room temperature the expected reaction pathways for OH radical reaction with, for example, 2-pentyl nitrate are[155]

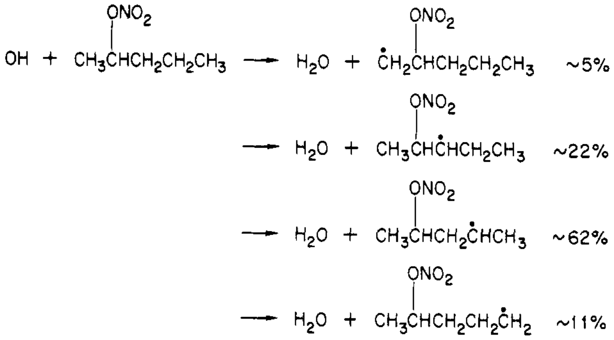

$$OH + CH_3CH(ONO_2)CH_2CH_2CH_3 \rightarrow H_2O + \dot{C}H_2CH(ONO_2)CH_2CH_2CH_3 \quad \sim 5\%$$
$$\rightarrow H_2O + CH_3CH(ONO_2)\dot{C}HCH_2CH_3 \quad \sim 22\%$$
$$\rightarrow H_2O + CH_3CH(ONO_2)CH_2\dot{C}HCH_3 \quad \sim 62\%$$
$$\rightarrow H_2O + CH_3CH(ONO_2)CH_2CH_2\dot{C}H_2 \quad \sim 11\%$$

followed by subsequent reactions of these radicals. For the above radicals, reaction with O_2 followed by reaction of the resulting peroxy radicals to yield the corresponding alkoxy radical and NO_2 (neglecting reaction to yield dinitrates, which is of unknown importance) is expected. The $\cdot OCH_2CH(ONO_2)CH_2CH_2CH_3$ and $CH_3CH(ONO_2)CH(\dot{O})CH_2CH_3$ radicals are expected to rapidly decompose

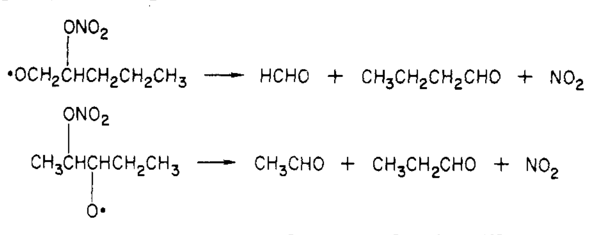

$$\cdot OCH_2CH(ONO_2)CH_2CH_2CH_3 \rightarrow HCHO + CH_3CH_2CH_2CHO + NO_2$$
$$CH_3CH(ONO_2)CH(O\cdot)CH_2CH_3 \rightarrow CH_3CHO + CH_3CH_2CHO + NO_2$$

while the remaining two alkoxy radicals will react via more complex reaction pathways. However, it is likely that these reactions of OH radicals with the alkyl nitrates (at least for the smaller alkyl nitrates for which isomerization of the alkoxy radicals cannot occur) will ultimately yield NO_2 together with aldehydes. These reactions are of importance for long-range transport and acid deposition computer modeling studies, since alkyl nitrates are formed in significant yields from the atmospheric photooxidation of the parent alkanes.[28,29,241]

e. Nitriles. As shown in Table XIII, rate constant data have been obtained for HCN, CH_3CN, C_2H_5CN, and $CH_2{=}CHCN$. For HCN, at temperatures between 296 and 433 K the rate constants are in the fall-off region between second- and third-order kinetics below ~400 torr of N_2 diluent,[435,436,443] with bimolecular rate constants which extrapolate to zero (within the experimental error limits) as the total pressure approaches zero.[443] This shows that this OH radical reaction with HCN must proceed via initial OH radical addition to HCN,[435,436,455] to form an initially energized adduct which can back decompose to reactants or be collisionally stabilized

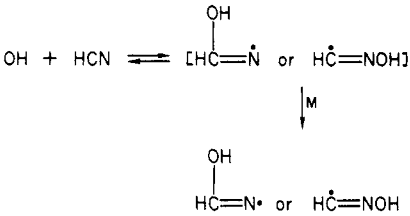

$$OH + HCN \rightleftharpoons [HC(OH){=}\dot{N} \text{ or } H\dot{C}{=}NOH]^{\ddagger} \xrightarrow{M} HC(OH){=}N\cdot \text{ or } H\dot{C}{=}NOH$$

followed by subsequent reactions of this HO–HCN adduct under atmospheric conditions.[435,436,455] For the higher nitriles such as CH_3CN and C_2H_5CN not containing $>C{=}C<$ bonds, the higher Arrhenius activation energies (with respect to that for HCN) and the dramatic increase in the room-temperature rate constant from CH_3CN to C_2H_5CN strongly suggests that these reactions proceed via H atom abstraction from the C–H bonds.

For nitriles containing $>C{=}C<$ double bonds, OH radical addition to the $>C{=}C<$ bond is expected. This is totally consistent with the observed pressure dependent rate constant and essentially zero temperature dependence for $CH_2{=}CHCN$[437] and with the recent product data of Hashimoto et al.[456] In this product study, Hashimoto et al.[456] utilized long pathlength FT-IR absorption spectroscopy to investigate the reactions of $CH_2{=}CHCN$, $CH_2{=}C(CH_3)CN$, and $CH_2{=}CHCH_2CN$ with OH radicals in the presence of NO. Formaldehyde was observed as a major product for all three reactions, together with CH_3COCN from $CH_2{=}C(CH_3)CN$, HCOCN from $CH_2{=}CHCN$, and $HCOCH_2CN$ from $CH_2{=}CHCH_2CN$. The high yields of these products (for example, unit yields of HCHO and CH_3COCN being determined for the reaction of OH radicals with $CH_2{=}C(CH_3)CN$[456]) and the observation that approximately two molecules of NO were consumed per molecule of nitrile reacted for $CH_2{=}CHCN$ and $CH_2{=}C(CH_3)CN$ indicates that these reactions proceed via pathways analogous to those for the alkenes.[456] For example, the postulated reaction pathways for the reaction of OH radicals with $CH_2{=}C(CH_3)CN$ are[456]

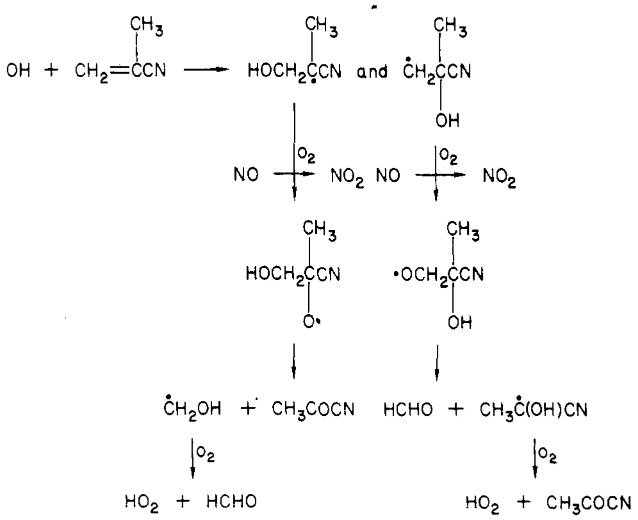

TABLE XIV. Rate Constants *k* for the Gas-Phase Reaction of OH Radicals with Aromatic Compounds at the High-Pressure Limit

aromatic	$10^{12}k$, cm^3 $molecule^{-1}$ s^{-1}	*T*, K	technique	ref	temp range covered, K
benzene	1.59 ± 0.12	298	FP-RF	Davis et al.[457]	
	≤2.62	304 ± 1	rel rate [rel to *k*(OH + *n*-butane) = 2.62 × 10^{-12}]^b	Doyle et al.[133]	
	1.24 ± 0.12	298	FP-RF	Hansen et al.[458]	
	1.20 ± 0.15	297.6	FP-RF	Perry et al.[313]	298–422
	1.32 ± 0.30	304.4			
	1.33 ± 0.25	305.8			
	1.66 ± 0.25	322.7			
	1.37 ± 0.20^a	331.9			
	1.66^a	333.2			
	1.04^a	350.6			
	0.63^a	354.7			
	1.00^a	355.2			
	1.00^a	361.2			
	0.31^a	364.8			
	0.31^a	380.8			
	0.26 ± 0.15	396.2			
	0.34 ± 0.07	396.4			
	0.34 ± 0.12	405.8			
	0.45 ± 0.07	422.0			
	0.85	300	rel rate [rel to *k*(OH + ethene) = 8.45 × 10^{-12}]^b	Cox et al.[139]	
	1.04 ± 0.08	250	FP-RF	Tully et al.[459]	250–1017
	1.20 ± 0.09	270			
	1.24 ± 0.09	298			
	0.7^a	352			
	0.3^a	390			
	0.4^a	442			
	0.543 ± 0.023	542			
	0.639 ± 0.029	621			
	0.682 ± 0.074	630			
	0.606 ± 0.034	653			
	1.02 ± 0.04	715			
	1.20 ± 0.16	742			
	1.59 ± 0.09	817			
	1.90 ± 0.20	895			
	2.26 ± 0.13	917			
	2.35 ± 0.23	981			
	2.20 ± 0.34	1017			
	0.93	~300	rel rate [rel to *k*(OH + ethene) = 8.45 × 10^{-12}]^b	Barnes et al.[141]	
	0.76 ± 0.15	244	LP-RF	Lorenz and Zellner[121,460]	244–870
	1.16 ± 0.25	298 ± 2			
	1.26 ± 0.25	336			
	0.83 ± 0.17	373			
	0.50 ± 0.10	384			
	0.40 ± 0.08	453			
	0.48 ± 0.16	522			
	0.43 ± 0.08	523			
	0.75 ± 0.20	567			
	0.46 ± 0.10	604			
	0.76 ± 0.25	665			
	1.28 ± 0.16	720			
	1.13 ± 0.25	803			
	2.16 ± 0.50	870			
	0.88 ± 0.04	295	FP-RF	Wahner and Zetzsch[461]	
	1.02 ± 0.20	296	FP-RF	Rinke and Zetzsch[462]	

benzene-d_6	1.08 ± 0.05	250	FP-RF	Tully et al.[459]	250–1150
	1.19 ± 0.05	298			
	0.4[a]	498			
	0.227 ± 0.030	568			
	0.424 ± 0.045	630			
	0.300 ± 0.032	653			
	0.430 ± 0.023	675			
	0.481 ± 0.019	734			
	0.720 ± 0.046	830			
	1.04 ± 0.03	917			
	1.08 ± 0.10	981			
	1.47 ± 0.07	1002			
	1.91 ± 0.28	1150			
	1.10 ± 0.22	298	LP-RF	Lorenz and Zellner[121]	298–524
	1.00 ± 0.20	336			
	0.76 ± 0.15	380			
	0.48 ± 0.10	398			
	0.28 ± 0.05	436			
	0.25 ± 0.05	524			
toluene	6.11 ± 0.40	298	FP-RF	Davis et al.[457]	
	3.7 ± 1.6	304 ± 1	rel rate [rel to $k(\text{OH} + n\text{-butane}) = 2.62 \times 10^{-12}$][b]	Doyle et al.[133]	
	5.78 ± 0.58	298	FP-RF	Hansen et al.[458]	
	6.40 ± 0.64	297.9	FP-RF	Perry et al.[313]	298–473
	4.90 ± 0.60	323.7			
	4.99 ± 0.6[a]	325.2			
	4.04[a]	334.6			
	5.36 ± 0.9[a]	338.5			
	1.51[a]	339.7			
	1.66 ± 0.25[a]	352.6			
	1.19[a]	354.2			
	1.38 ± 0.17[a]	364.0			
	1.35[a]	366.0			
	1.22 ± 0.14[a]	378.4			
	1.49 ± 0.22	379.3			
	1.58 ± 0.24	394.2			
	1.69 ± 0.25	408.7			
	1.76 ± 0.18	424.4			
	1.71 ± 0.20	472.7			
	7.6	300	rel rate [rel to $k(\text{OH} + \text{ethene}) = 8.45 \times 10^{-12}$][b]	Cox et al.[139]	
	8.20 ± 0.54	213	FP-RF	Tully et al.[459]	213–1046
	8.73 ± 0.39	231			
	7.97 ± 0.56	250			
	8.53 ± 0.37	260			
	7.44 ± 0.55	270			
	6.36 ± 0.69	298			
	6.3 ± 0.6[a]	320			
	5.4 ± 1.1[a]	332			
	3.6[a]	352			
	1.4[a]	397			
	1.7[a]	442			
	2.16 ± 0.08	504			
	2.45 ± 0.05	568			
	2.49 ± 0.12	568			
	3.26 ± 0.29	666			

TABLE XIV (Continued)

aromatic	$10^{12}k$, cm^3 molecule^{-1} s^{-1}	T, K	technique	ref	temp range covered, K
	3.58 ± 0.16	694			
	4.67 ± 0.19	793			
	5.54 ± 0.27	868			
	6.87 ± 0.23	958			
	9.5 ± 1.0	1046			
toluene-d_3 ($C_6H_5CD_3$)	5.62 ± 0.52	250	FP-RF	Tully et al.[459]	250–1002
	5.97 ± 0.17	270			
	5.63 ± 0.30	298			
	0.8[a]	383			
	1.23 ± 0.09	518			
	1.32 ± 0.08	568			
	1.41 ± 0.06	568			
	1.46 ± 0.09	568			
	1.40 ± 0.08	568			
	2.10 ± 0.07	653			
	3.01 ± 0.10	742			
	3.59 ± 0.13	817			
	4.55 ± 0.34	895			
	5.92 ± 0.42	966			
	8.54 ± 1.21	1002			
toluene-d_5 ($C_6D_5CH_3$)	6.11 ± 0.40	250	FP-RF	Tully et al.[459]	250–1002
	6.02 ± 1.68	270			
	6.47 ± 0.65	298			
	3.0[a]	358			
	1.1[a]	412			
	1.66 ± 0.10	470			
	2.04 ± 0.14	518			
	2.52 ± 0.14	568			
	2.69 ± 0.28	630			
	3.29 ± 0.25	653			
	4.53 ± 0.52	742			
	5.08 ± 0.32	793			
	6.48 ± 0.41	895			
	6.52 ± 0.91	996			
	7.97 ± 0.73	1002			
toluene-d_8 ($C_6D_5CD_3$)	6.13 ± 0.63	298.1	FP-RF	Perry et al.[313]	298–432
	4.78[a]	323.6			
	3.56[a]	324.2			
	0.38 ± 0.06	385.2			
	0.51 ± 0.07	397.0			
	0.70 ± 0.07	432.2			
	6.04 ± 0.48	250	FP-RF	Tully et al.[459]	250–1150
	6.36 ± 0.52	270			
	6.40 ± 0.20	298			
	0.5[a]	390			
	0.73 ± 0.07	470			
	1.17 ± 0.09	498			
	1.27 ± 0.03	542			
	1.15 ± 0.05	568			
	1.97 ± 0.12	621			
	2.35 ± 0.16	700			
	2.18 ± 0.10	715			

	3.53 ± 0.28	793			
	2.76 ± 0.14	842			
	3.18 ± 0.30	842			
	4.05 ± 0.30	868			
	4.52 ± 0.25	966			
	6.91 ± 1.32	1017			
	6.51 ± 1.50	1150			
ethylbenzene	7.0 ± 1.4	305 ± 2	rel rate [rel to k(OH + n-butane) = 2.63 × 10^{-12}][b]	Lloyd et al.[144]	
	7.95 ± 0.50	298	FP-RF	Ravishankara et al.[294]	
o-xylene	11.3 ± 3.4	304 ± 1	rel rate [rel to k(OH + n-butane) = 2.62 × 10^{-12}][b]	Doyle et al.[133]	
	15.3 ± 1.5	298.0	FP-RF	Hansen et al.[458]	
	14.3 ± 1.5	298.5	FP-RF	Perry et al.[313]	298–432
	12.9[a]	313.5			
	14.0 ± 2.0	319.0			
	12.3[a]	332.1			
	9.27[a]	348.2			
	4.98[a]	367.7			
	3.76[a]	372.8			
	3.25 ± 0.45	379.5			
	3.35 ± 0.46	395.6			
	3.27 ± 0.46	414.6			
	3.63 ± 0.43	425.3			
	3.34 ± 0.35	432.4			
	12.4 ± 1.2	298	FP-RF	Ravishankara et al.[294]	
	14.0	300	rel rate [rel to k(OH + ethene) = 8.45 × 10^{-12}][b]	Cox et al.[139]	
	14.2 ± 1.7	298	FP-RF	Nicovich et al.[463]	298–970
	15.8 ± 1.8	320			
	5.1[a]	357			
	2.39 ± 0.20	400			
	4.19 ± 0.48	508			
	5.42 ± 0.45	576			
	6.87 ± 0.91	647			
	10.20 ± 0.91	757			
	12.8 ± 1.1	886			
	15.7 ± 1.3	970			
m-xylene	19.7 ± 1.3	304 ± 1	rel rate [rel to k(OH + n-butane) = 2.62 × 10^{-12}][b]	Doyle et al.[133]	
	23.6 ± 2.4	297.3	FP-RF	Hansen et al.[458]	
	18.9 ± 3.8	305 ± 2	rel rate [rel to k(OH + n-butane) = 2.63 × 10^{-12}][b]	Lloyd et al.[144]	
	24.0 ± 2.5	298.3	FP-RF	Perry et al.[313]	298–427
	24.4 ± 3.6	314.5			
	20.5[a]	320.0			
	13.1[a]	327.8			
	2.81[a]	354.9			
	1.68[a]	365.2			
	2.19[a]	373.8			
	2.21 ± 0.33	379.1			
	2.23 ± 0.33	390.9			
	2.49 ± 0.36	403.5			
	2.86 ± 0.38	414.0			
	3.02 ± 0.30	427.0			
	20.6 ± 1.3	298	FP-RF	Ravishankara et al.[294]	
	19.6	300	rel rate [rel to k(OH + ethene) = 8.45 × 10^{-12}][b]	Cox et al.[139]	
	26.5 ± 2.5	250	FP-RF	Nicovich et al.[463]	250–960
	25.6 ± 4.3	269			
	25.4 ± 3.5	298			
	5.2[a]	330			

TABLE XIV (Continued)

aromatic	$10^{12}k$, cm^3 molecule^{-1} s^{-1}	T, K	technique	ref	temp range covered, K
	2.47 ± 0.41	400			
	3.44 ± 0.34	508			
	4.60 ± 0.54	576			
	6.2 ± 1.1	684			
	9.3 ± 1.1	757			
	10.1 ± 1.5	875			
	14.6 ± 3.1	960			
	21.1 ± 1.4	299 ± 2	rel rate [rel to k(OH + cyclohexane) = 7.41×10^{-12}][b]	Atkinson et al.[224]	
p-xylene	10.7 ± 2.4	304 ± 1	rel rate [rel to k(OH + *n*-butane) = 2.62×10^{-12}][b]	Doyle et al.[133]	
	12.2 ± 1.2	297.3	FP-RF	Hansen et al.[458]	
	15.3 ± 1.7	298.0	FP-RF	Perry et al.[313]	298–428
	18.2 ± 2.2	306.3			
	18.2 ± 2.2	310.7			
	17.3 ± 2.2	313.2			
	16.7[a]	315.0			
	14.9 ± 2.0[a]	324.2			
	15.3[a]	330.2			
	11.7[a]	352.7			
	5.49[a]	358.7			
	3.39[a]	369.6			
	2.50[a]	372.1			
	2.66 ± 0.40	383.8			
	2.43 ± 0.32	385.3			
	2.67 ± 0.36	387.1			
	2.96 ± 0.40	392.8			
	3.17 ± 0.43	400.0			
	3.29 ± 0.40	404.3			
	3.68 ± 0.45	412.6			
	3.56 ± 0.55	422.4			
	3.29 ± 0.33	428.4			
	10.5 ± 1.0	298	FP-RF	Ravishankara et al.[294]	
	13.5 ± 1.4	298	FP-RF	Nicovich et al.[463]	298–960
	13.8 ± 1.1	320			
	12.5 ± 1.3	335			
	4.3[a]	357			
	1.71 ± 0.28	400			
	3.70 ± 0.64	484			
	3.40 ± 0.48	526			
	5.03 ± 0.88	576			
	6.01 ± 0.59	647			
	9.66 ± 0.85	757			
	11.6 ± 1.6	886			
	14.6 ± 1.9	960			
xylenes (mixture of isomers)	18.7	298	DF-MS	Morris and Niki[102]	
n-propylbenzene	5.4 ± 1.1	305 ± 2	rel rate [rel to k(OH + *n*-butane) = 2.63×10^{-12}][b]	Lloyd et al.[144]	
	5.86 ± 0.50	298	FP-RF	Ravishankara et al.[294]	
isopropylbenzene	5.3 ± 1.1	305 ± 2	rel rate [rel to k(OH + *n*-butane) = 2.63×10^{-12}][b]	Lloyd et al.[144]	
	7.79 ± 0.50	298	FP-RF	Ravishankara et al.[294]	
o-ethyltoluene	12.0 ± 2.4	305 ± 2	rel rate [rel to k(OH + *n*-butane) = 2.63×10^{-12}][b]	Lloyd et al.[144]	
m-ethyltoluene	17.1 ± 3.4	305 ± 2	rel rate [rel to k(OH + *n*-butane) = 2.63×10^{-12}][b]	Lloyd et al.[144]	
p-ethyltoluene	11.4 ± 2.3	305 ± 2	rel rate [rel to k(OH + *n*-butane) = 2.63×10^{-12}][b]	Lloyd et al.[144]	
1,2,3-trimethylbenzene	19.9 ± 4.2	304 ± 1	rel rate [rel to k(OH + *n*-butane) = 2.62×10^{-12}][b]	Doyle et al.[133]	

	26.4 ± 2.6	297.1	FP-RF	Hansen et al.[458]	
	33.3 ± 4.5	296.9	FP-RF	Perry et al.[313]	297–421
	27.6^a	317.5			
	24.5 ± 3.7	325.1			
	19.4^a	338.6			
	4.32^a	374.4			
	3.54^a	377.4			
	4.28 ± 0.64	388.6			
	4.89 ± 0.74	396.8			
	6.00 ± 0.80	420.7			
1,2,4-trimethylbenzene	28.8 ± 5.2	304 ± 1	rel rate [rel to k(OH + n-butane) = 2.62 × 10^{-12}]^b	Doyle et al.[133]	
	33.5 ± 3.4	296.9	FP-RF	Hansen et al.[458]	
	40.0 ± 4.5	298.2	FP-RF	Perry et al.[313]	298–430
	37.3 ± 4.8	314.3			
	32.4 ± 4.8	323.4			
	15.2^a	340.2			
	4.56^a	370.9			
	2.47^a	374.1			
	3.34 ± 0.44	383.7			
	4.82 ± 0.63	397.7			
	4.75 ± 0.62	400.3			
	5.31 ± 0.69	423.5			
	5.24 ± 0.60	429.5			
1,3,5-trimethylbenzene	44.5 ± 5.2	304 ± 1	rel rate [rel to k(OH + n-butane) = 2.62 × 10^{-12}]^b	Doyle et al.[133]	
	47.2 ± 4.8	297.1	FP-RF	Hansen et al.[458]	
	62.4 ± 7.5	298.3	FP-RF	Perry et al.[313]	298–420
	51.9 ± 6.3	318.4			
	52.1^a	322.5			
	3.16^a	368.0			
	3.38 ± 0.45	372.4			
	3.45 ± 0.45	381.0			
	3.82 ± 0.50	390.1			
	5.03 ± 0.60	420.1			
styrene ($C_6H_5CH{=}CH_2$)	52 ± 5	298	rel rate [rel to k(OH + 2,2,4-trimethylpentane) = 3.66 × 10^{-12}]^b	Bignozzi et al.[464]	
α-methylstyrene [$C_6H_5C(CH_3){=}CH_2$]	52 ± 6	298	rel rate [rel to k(OH + 2,2,4-trimethylpentane) = 3.66 × 10^{-12}]^b	Bignozzi et al.[464]	
β-methylstyrene [$C_6H_5CH{=}CHCH_3$]	59 ± 6	298	rel rate [rel to k(OH + 2,2,4-trimethylpentane) = 3.66 × 10^{-12}]^b	Bignozzi et al.[464]	
β-dimethylstyrene [$C_6H_5CH{=}C(CH_3)_2$]	32 ± 5	298	rel rate [rel to k(OH + 2,2,4-trimethylpentane) = 3.66 × 10^{-12}]^b	Chiorboli et al.[348]	
phenol	28.3 ± 5.7	296	FP-RF	Rinke and Zetzsch[462]	
methoxybenzene	19.6 ± 2.4	299.9	FP-RF	Perry et al.[312]	300–435
	17.3 ± 2.6	309.0			
	17.5 ± 2.6	309.7			
	17.5 ± 2.6	318.5			
	17.8 ± 2.7	321.7			
	12.7^a	329.5			
	6.7^a	357.4			
	3.0^a	370.4			
	3.33 ± 0.50	385.5			
	3.25 ± 0.50	392.3			
	3.31 ± 0.50	404.1			
	3.90 ± 0.56	413.2			
	2.85 ± 0.43	417.9			
	3.30 ± 0.40	422.0			
	2.76 ± 0.41	428.7			
	2.72 ± 0.41	435.3			
o-cresol	34.1 ± 6.8	299.4	FP-RF	Perry et al.[312]	299–423
	29.3 ± 5.9	310.6			
	29.8 ± 6.0	322.0			

TABLE XIV (Continued)

aromatic	$10^{12}k$, cm^3 $molecule^{-1}$ s^{-1}	T, K	technique	ref	temp range covered, K
	26.8 ± 5.4	330.7			
	25.5 ± 5.1	335.4			
	18.5[a]	344.4			
	15.0[a]	356.5			
	6.4[a]	385.8			
	6.0[a]	392.8			
	5.6 ± 1.1	400.6			
	5.4 ± 1.1	407.8			
	6.2 ± 1.2	423.1			
	42 ± 4	300 ± 1	rel rate [rel to k(OH + n-butane) − k(OH + neopentane) = 1.69 × 10^{-12}][b]	Atkinson et al.[465]	
m-cresol	57 ± 7	300 ± 1	rel rate [rel to k(OH + *o*-cresol) = (4.0 ± 0.4) × 10^{-11}][b]	Atkinson et al.[465]	
p-cresol	44 ± 5	300 ± 1	rel rate [rel to k(OH + *o*-cresol) = (4.0 ± 0.4) × 10^{-11}][b]	Atkinson et al.[465]	
fluorobenzene	0.54 ± 0.05	296	FP-RF	Zetzsch[466]	
chlorobenzene	0.67 ± 0.05	296	FP-RF	Zetzsch[357,466]	
	0.94 ± 0.12	299 ± 2	rel rate [rel to k(OH + benzene) = 1.29 × 10^{-12}][b]	Atkinson et al.[156]	
bromobenzene	0.70 ± 0.07	296	FP-RF	Zetzsch[357]	
iodobenzene	0.93 ± 0.05	296	FP-RF	Zetzsch[357]	
benzotrifluoride [$C_6H_5CF_3$]	0.48 ± 0.12	299 ± 2	rel rate [rel to k(OH + benzene) = 1.29 × 10^{-12}][b]	Atkinson et al.[156]	
aniline	119 ± 24	296	FP-RF	Rinke and Zetzsch[462]	
	112 ± 12	265	FP-RF	Atkinson et al.[441]	265–455
	118 ± 10	283			
	118 ± 11	298			
	92[a]	310			
	67[a]	325			
	47.8 ± 5.3	342			
	36.3 ± 6.1	382			
	39.6 ± 7.5	391			
	29.7 ± 1.2	426			
	29.7 ± 5.4	455			
N,*N*-dimethylaniline	151 ± 31	278	FP-RF	Atkinson et al.[441]	278–464
	148 ± 11	298			
	119 ± 6	303			
	57[a]	318			
	29[a]	329			
	5.8[a]	361			
	1.75 ± 0.25	421			
	2.20 ± 0.51	425			
	2.09 ± 0.30	437			
	2.85 ± 0.24	460			
	3.12 ± 0.34	464			
benzonitrile	0.33 ± 0.03	296	FP-RF	Zetzsch[357,466]	
nitrobenzene	0.21 ± 0.05	296	FP-RF	Zetzsch[357,466]	
	<0.7	296 ± 2	rel rate [rel to k(OH + dimethyl ether) = 2.96 × 10^{12}][b]	Atkinson et al.[441]	
4-chlorobenzotrifluoride	0.25 ± 0.08	299 ± 2	rel rate [rel to k(OH + benzene) = 1.29 × 10^{-12}][b]	Atkinson et al.[156]	
o-dichlorobenzene	0.42 ± 0.02	295	FP-RF	Wahner and Zetzsch[461]	
m-dichlorobenzene	0.72 ± 0.02	295	FP-RF	Wahner and Zetzsch[461]	
p-dichlorobenzene	0.32 ± 0.02	295	FP-RF	Wahner and Zetzsch[461]	
p-chloroaniline	83.0 ± 4.2	295	FP-RF	Wahner and Zetzsch[461]	
o-nitrophenol	0.90 ± 0.02[c]	294	FP-RF	Zetzsch[357]	273–353
1,2,4-trichlorobenzene	0.497 ± 0.036	273	FP-RF	Rinke and Zetzsch[462]	273–368
	0.532 ± 0.050	296			
	0.631 ± 0.082	323			
	0.706 ± 0.054	348			

	0.712 ± 0.083	368			
hexafluorobenzene	0.219 ± 0.016	298	FP-RF	Ravishankara et al.[294]	
n-propylpentafluorobenzene	3.06 ± 0.24	298	FP-RF	Ravishankara et al.[294]	
biphenyl	5.8 ± 0.8	296	FP-RF	Zetzsch[466]	
	7.76 ± 0.68	294 ± 1	rel rate [rel to k(OH + n-nonane) = 1.03×10^{-11}]^b	Atkinson et al.[148]	
	8.2 ± 0.8	295 ± 1	rel rate [rel to k(OH + cyclohexane) = 7.28×10^{-12}]^b	Atkinson and Aschmann[467]	
2-chlorobiphenyl	2.8 ± 0.4	295 ± 1	rel rate [rel to k(OH + cyclohexane) = 7.28×10^{-12}]^b	Atkinson and Aschmann[467]	
3-chlorobiphenyl	5.2 ± 0.8	295 ± 1	rel rate [rel to k(OH + cyclohexane) = 7.28×10^{-12}]^b	Atkinson and Aschmann[467]	
4-chlorobiphenyl	3.8 ± 0.7	295 ± 1	rel rate [rel to k(OH + cyclohexanee) = 7.28×10^{-12}]^b	Atkinson and Aschmann[467]	
naphthalene	18.6 ± 1.0	300	LP-RF	Lorenz and Zellner[121,460]	300–873
	14.6 ± 5.0	337			
	11.0 ± 4.3	358			
	10.1 ± 4.0	378 ± 2			
	11.6 ± 3.0	404			
	10.5 ± 4.0	407			
	6.3 ± 2.0	452			
	4.3 ± 1.5	476			
	1.3 ± 0.5	502			
	1.2 ± 0.3	525 ± 1			
	0.7 ± 0.2	528			
	0.6 ± 0.1	531			
	1.1 ± 0.1	636			
	1.1 ± 0.2	665			
	1.4 ± 0.2	727			
	3.0 ± 0.5	873			
	23.3 ± 1.6	294 ± 1	rel rate [rel to k(OH + n-nonane) = 1.03×10^{-11}]^b	Atkinson et al.[148]	
	23.5 ± 0.6	298 ± 1	rel rate [rel to k(OH + propene) = 2.63×10^{-11}]^b	Biermann et al.[154]	
	25.9 ± 2.4	295 ± 1	rel rate [rel to k(OH + 2-methyl-1,3-butadiene) = 1.02×10^{-10}]^b	Atkinson and Aschmann[468]	
2-methylnaphthalene	52.3 ± 4.2	295 ± 1	rel rate [rel to k(OH + 2-methyl-1,3-butadiene) = 1.02×10^{-10}]^b	Atkinson and Aschmann[468]	
2,3-dimethylnaphthalene	76.8 ± 4.8	295 ± 1	rel rate [rel to k(OH + 2-methyl-1,3-butadiene) = 1.02×10^{-10}]^b	Atkinson and Aschmann[468]	
phenanthrene	34 ± 12	298 ± 1	rel rate [rel to k(OH + propene) = $4.85 \times 10^{-12}e^{504/T}$]^b	Biermann et al.[154]	298–319
	28 ± 6	319 ± 1			
	15.6 ± 2.0	338	LP-RF	Lorenz and Zellner[460]	338–748
	16.1 ± 2.0	355			
	19.1 ± 2.5	387			
	12.0 ± 1.7	399			
	8.3 ± 0.8	431			
	4.0 ± 0.7	492			
	2.8 ± 0.7	526			
	1.2 ± 0.2	597			
	1.2 ± 0.4	648			
	2.2 ± 0.5	748			
anthracene	112 ± 9	325 ± 1	rel rate [rel to k(OH + propene) = 2.29×10^{-11}]^b	Biermann et al.[154]	

[a] Nonexponential OH radical decays observed (see text). [b] From the present recommendations (see text). [c] A temperature-dependent rate constant of $k = (4.2 \pm 0.5) \times 10^{-13}e^{(217\pm60)/T}$ cm^3 molecule^{-1} s^{-1} is reported[357] over the temperature range 273–353 K.

Totally analogous reaction sequences can explain the primary products observed from $CH_2{=}CHCN$ and $CH_2{=}CHCH_2CN$.[456]

I. Aromatic Compounds

1. Kinetics

The available kinetic data are listed in Table XIV. Perhaps surprisingly, these rate constant data, obtained from both absolute and rate constant studies, are generally in reasonably good agreement. Room-temperature rate constant data are available for a wide variety of aromatic hydrocarbons and substituted aromatics. Additionally, temperature dependence studies have been carried out for benzene,[121,313,459,460] toluene,[313,459] the xylene isomers,[313,463] the trimethylbenzene isomers,[313] methoxybenzene,[312] *o*-cresol,[312] aniline,[441] *N,N*-dimethylaniline,[441] *o*-nitrophenol,[357] 1,2,4-trichlorobenzene,[462] naphthalene,[121,460] and phenanthrene[460] and for benzene-d_6,[121,459] toluene-d_3,[459] toluene-d_5,[459] and toluene-d_8.[313,459]

For the aromatic hydrocarbons, methoxybenzene, *o*-cresol, aniline, and *N,N*-dimethylaniline, three distinct temperature regimes have been observed with the flash or laser photolysis techniques employed to date:[121,312,313,441,459,460,463] (a) at low temperatures, i.e., ≲325 K for the monocyclic aromatic hydrocarbons and ≲410 K for naphthalene and phenanthrene, exponential OH radical decays are observed, and the rate constants change only slightly with temperature, with negative temperature dependencies being obtained in many cases; (b) at elevated temperatures, ≳400–450 K for the monocyclic aromatic hydrocarbons and ≳600 K for naphthalene and phenanthrene, exponential OH radical decays are also observed. Except for aniline[441] the derived rate constants increase rapidly with increasing temperature, with the values at ~400–450 K (or ~600 K for naphthalene and phenanthrene) being typically a factor of 5–10 lower than those at ~325 K; and (c) at intermediate temperatures of ~325–400 K for the monocyclic aromatics, and ~410–600 K for naphthalene and phenanthrene, nonexponential decays of OH radicals are observed,[121,312,313,441,459,463] with the decay rate decreasing with the reaction time. In this temperature regime any rate data obtained are a combination of the forward and reverse reaction steps (see below) and are dependent on the experimental conditions (for example, the observation time) employed.

As discussed below, for the aromatic hydrocarbons, methoxybenzene, *o*-cresol, and *N,N*-dimethylaniline, the available kinetic and mechanistic data show that in the low-temperature regime, OH radical addition is the dominant reaction pathway, while at elevated temperatures H atom abstraction (or a direct reaction involving H atom or substituent group elimination) occurs. The intermediate temperature regime where nonexponential OH radical decays occur is characterized by formation and redissociation of the OH–aromatic adducts. Furthermore, this precise intermediate temperature range where nonexponential decays are observed is dependent to some extent on the time resolution of the experimental technique. For these reasons we do not discuss the reported kinetic data in this intermediate temperature regime, apart from tabulating in Table XIV these data as reported.

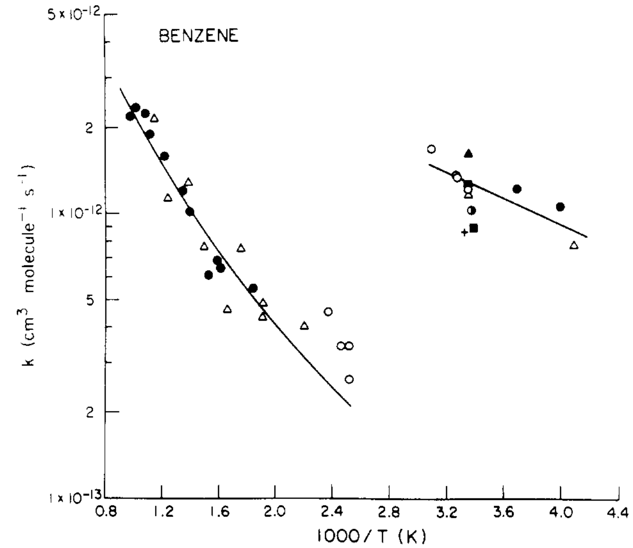

Figure 49. Arrhenius plot of the rate constants for the reaction of OH radicals with benzene: (▲) Davis et al.;[457] (□) Hansen et al.;[458] (○) Perry et al.;[313] (+) Cox et al.;[139] (●) Tully et al.;[459] (△) Lorenz and Zellner;[121,460] (■) Wahner and Zetzsch;[461] (◑) Rinke and Zetzsch[462] (for the flash or laser photolysis techniques, only rate constants derived from exponential OH radical decays are plotted); (—) recommendations (see text).

Furthermore, although exponential OH radical decays were observed by Perry et al.[312,313] for the monocyclic aromatics for temperature ≳380 K, Tully et al.[459] report that the OH radical addition process continues to contribute to the high-temperature reaction pathway up to ~450 K. Hence in our discussion and derivation of temperature-dependent rate constants for the individual aromatic compounds in the sections below, we have utilized rate constants in the temperature regimes ≲325 and ≳450 K for the monocyclic aromatics and ≲410 and ≳600 K for naphthalene and phenanthrene.

a. Benzene. The available rate constant data are listed in Table XIV. The most recent kinetic data show that at room temperature this reaction is at the second-order high-pressure limit for total pressures of argon diluent ≳40–50 torr[121,458,459,461] and for total pressures of helium diluent ≳25 torr.[459,462] This finding is contrary to the earlier observations of Davis et al.,[457] where the rate constant at 298 K was reported to be pressure dependent up to 100-torr total pressure of helium diluent. Hence the limiting high-pressure rate constants given in Table XIV will be applicable for tropospheric conditions.

The limiting high-pressure rate constants of Davis et al.,[457] Hansen et al.,[458] Perry et al.,[313] Cox et al.,[139] Tully et al.,[459] Lorenz and Zellner,[121,460] Wahner and Zetzsch,[461] and Rinke and Zetzsch[462] are plotted in Arrhenius form in Figure 49. At room temperature the reported rate constants exhibit a significant scatter of almost a factor of 2. The reasons for these discrepancies are not known but may be due, at least in part, to the relatively low magnitude of this rate constant. The recommendations are based on the flash and laser photolysis–resonance fluorescence studies of Hansen et al.,[458] Perry et al.,[313] Tully et al.,[459] and Lorenz and Zellner.[121,460] For temperatures ≤325 K, from a unit-weighted least-squares analysis of the rate constants from these studies, the Arrhenius expression

$$k(\text{benzene}, T \le 325\ \text{K}) = (7.57^{+7.72}_{-3.82}) \times 10^{-12} e^{-(529\pm201)/T}\ \text{cm}^3\ \text{molecule}^{-1}\ \text{s}^{-1}$$

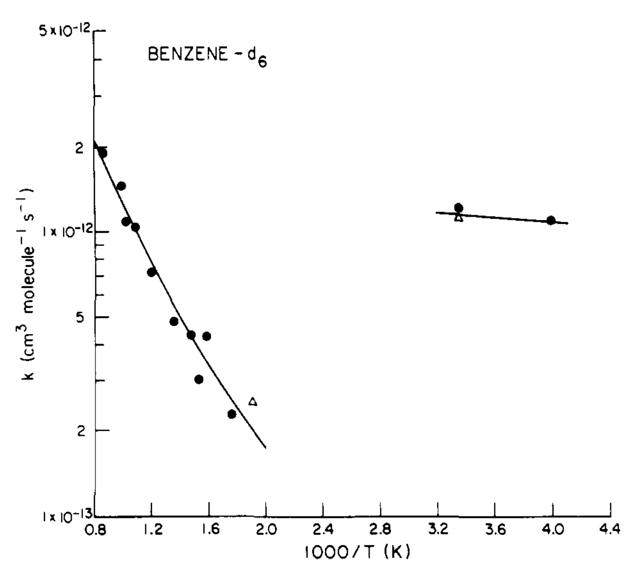

Figure 50. Arrhenius plot of the rate constants for the reaction of OH radicals with benzene-d_6: (●) Tully et al.;[459] (△) Lorenz and Zellner[121] (only the rate constants derived from exponential OH radical decays are plotted); (—) recommendations (see text).

is recommended, where the indicated error limits are two least-squares standard deviations [the relatively high uncertainties in the Arrhenius preexponential factor and activation energy arise largely from the small temperature range (250–325 K) considered]

$$k(\text{benzene}) = 1.28 \times 10^{-12}\ \text{cm}^3\ \text{molecule}^{-1}\ \text{s}^{-1}\ \text{at}\ 298\ \text{K}$$

with an estimated uncertainty at 298 K of ±30%.

At temperatures ≥450 K the only reported rate constants are those of Tully et al.[459] and Lorenz and Zellner,[121,460] and these are in good agreement. Consistent with the recommendations for the alkanes and haloalkanes, these data have been unit-weighted least squares fitted to the expression $k = A'T^2e^{-E'/RT}$ to yield the recommendation of

$$k(\text{benzene}, T \geq 450\ \text{K}) = (3.25^{+1.53}_{-1.03}) \times 10^{-18}T^2e^{-(344\pm253)/T}\ \text{cm}^3\ \text{molecule}^{-1}\ \text{s}^{-1}$$

where the error limits are two least-squares standard deviations. The rate constants reported by Perry et al.[313] between 396 and 422 K are, as expected,[459] somewhat higher than predicted from this recommendation, though within agreement within the experimental errors.

b. Benzene-d_6. The rate constants reported by Tully et al.[459] and Lorenz and Zellner[121] are listed in Table XIV, and the rate constants in the low and elevated temperature regimes (as discussed above) are plotted in Arrhenius form in Figure 50. It can be seen that the rate constants obtained by Lorenz and Zellner[121] at 298 and 524 K are in excellent agreement with those of Tully et al.[459]

A unit-weighted least-squares analysis of these rate constants over the temperature range 250–298 K yields the recommended Arrhenius expression

$$k(\text{benzene-}d_6, T \leq 325\ \text{K}) = (1.54^{+1.76}_{-0.82}) \times 10^{-12}e^{-(90\pm212)/T}\ \text{cm}^3\ \text{molecule}^{-1}\ \text{s}^{-1}$$

where the indicated error limits are two least-squares standard deviations

$$k(\text{benzene-}d_6) = 1.14 \times 10^{-12}\ \text{cm}^3\ \text{molecule}^{-1}\ \text{s}^{-1}\ \text{at}\ 298\ \text{K}$$

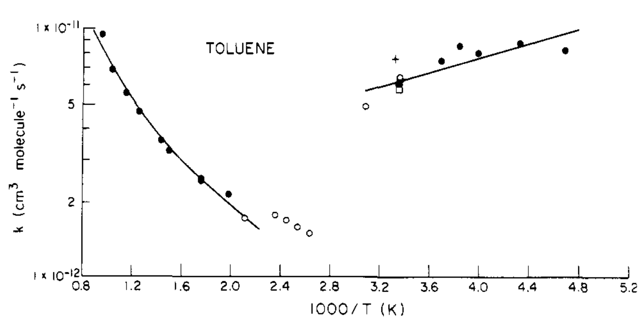

Figure 51. Arrhenius plot of the rate constants for the reaction of OH radicals with toluene: (▲) Davis et al.;[457] (□) Hansen et al.;[458] (○) Perry et al.;[313] (+) Cox et al.;[139] (●) Tully et al.[459] (for the flash photolysis techniques, only rate constants derived from exponential OH radical decays are plotted); (—) recommendations (see text).

with an estimated uncertainty at 298 K of ±30%. Again, the significant uncertainties in the above Arrhenius parameters are largely due to the small temperature range (250–298 K) covered.

At elevated temperatures, using the criteria discussed above, the recommendation is based on the rate constants obtained at temperatures >450 K. From a unit-weighted least-squares fit of these data[121,459] to the expression $k = A'T^2e^{-E'/RT}$, it is recommended that

$$k(\text{benzene-}d_6, T \geq 450\ \text{K}) = (2.23^{+1.14}_{-0.75}) \times 10^{-18}T^2e^{-(582\pm298)/T}\ \text{cm}^3\ \text{molecule}^{-1}\ \text{s}^{-1}$$

where the indicated error limits are two least-squares standard deviations.

It can be seen from Table XIV and Figures 49 and 50 that at temperatures ≲325 K the rate constants for benzene and benzene-d_6 are essentially identical within the experimental errors. However, for temperatures ≥450 K the rate constants for benzene-d_6 are significantly lower than those for benzene-h_6. As discussed below, these observations are totally consistent with OH radical addition to the aromatic ring dominating for temperatures ≲325 K, while H atom abstraction (or a direct reaction involving H atom elimination) dominates for temperatures ≥450 K, with the corresponding expected kinetic isotope effect.

c. Toluene. The available limiting second-order high-pressure rate constants are listed in Table XIV, and those of Davis et al.,[457] Hansen et al.,[458] Perry et al.,[313] Cox et al.,[139] and Tully et al.[459] are plotted in Arrhenius form in Figure 51 for the temperature regimes for which exponential OH radical decays have been observed in the two temperature-dependent flash photolysis studies.[313,459] Davis et al.[457] and Tully et al.[459] have reported that at room temperature this reaction is in the fall-off kinetic regime between second- and third-order kinetics below ~100-torr total pressure of helium[457,459] or argon[459] diluent.

For temperatures ≲325 K, a unit-weighted least-squares analysis of the flash photolysis–resonance fluorescence data of Hansen et al.,[458] Perry et al.,[313] and Tully et al.[459] (the rate constant of Davis et al.[457] has not been included since the corresponding rate constant for benzene appears to be anomalously high; see above) yields the recommended Arrhenius expression

$$k(\text{toluene}, T \leq 325\ \text{K}) = (2.10^{+1.59}_{-0.90}) \times 10^{-12}e^{(322\pm149)/T}\ \text{cm}^3\ \text{molecule}^{-1}\ \text{s}^{-1}$$

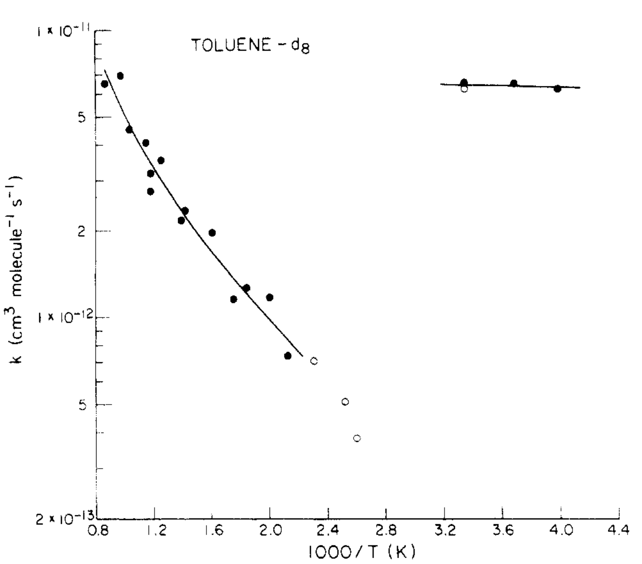

Figure 52. Arrhenius plot of the rate constants (obtained from exponential OH radical decays) for the reaction of OH radicals with toluene-d_8: (○) Perry et al.;[313] (●) Tully et al.;[459] (—) recommendations (see text).

where the indicated errors are two least-squares standard deviations

k(toluene) =

$$6.19 \times 10^{-12} \text{ cm}^3 \text{ molecule}^{-1} \text{ s}^{-1} \text{ at } 298 \text{ K}$$

with an estimated overall uncertainty at 298 K of ±20%.

For temperatures ≥450 K, a unit-weighted least-squares fit of the rate constants obtained by Perry et al.[313] and Tully et al.[459] to the expression $k = A'T^2e^{-E'/RT}$ yields the recommendation of

k(toluene, $T \geq 450$ K) =

$$(7.58^{+1.35}_{-1.14}) \times 10^{-18}T^2e^{(11\pm106)/T} \text{ cm}^3 \text{ molecule}^{-1} \text{ s}^{-1}$$

(i.e., essentially a pure T^2 dependence), where the indicated errors are two least-squares standard deviations. It may be noted that, although the rate constant obtained by Perry et al.[313] at 473 K is in good agreement with those of Tully et al.,[459] the rate constants of Perry et al.[313] at temperatures between 378 and 424 K are ~25% higher than predicted from the above expression. This may well be due to a continuing (but decreasing with increasing temperature) contribution of the addition process to the observed overall rate constant, as discussed by Tully et al.[459]

d. Toluene-d_8. Rate constants have been obtained for toluene-d_8 at the high-pressure limit by Perry et al.[313] and Tully et al.[459] These data are listed in Table XIV, and the rate constants obtained in the temperature regimes corresponding to exponential OH radical decays are plotted in Arrhenius form in Figure 52. The rate constants from these two studies[313,459] are in excellent agreement. At temperatures ≤325 K, a unit-weighted least-squares analysis of these rate constants yields the recommended Arrhenius expression

k(toluene-d_8, $T \leq 325$ K) =

$$(7.31^{+3.62}_{-2.42}) \times 10^{-12}e^{-(44\pm112)/T} \text{ cm}^3 \text{ molecule}^{-1} \text{ s}^{-1}$$

where the indicated errors are two least-squares standard deviations

k(toluene-d_8) =

$$6.31 \times 10^{-12} \text{ cm}^3 \text{ molecule}^{-1} \text{ s}^{-1} \text{ at } 298 \text{ K}$$

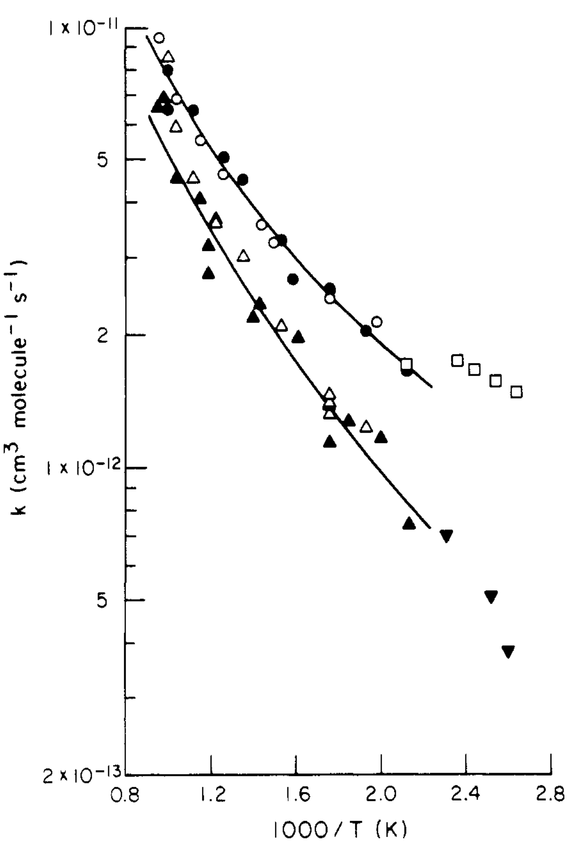

Figure 53. Arrhenius plot of the elevated (≥378 K) temperature rate constants (obtained from exponential OH radical decays) for the reactions of OH radicals with toluene, toluene-d_3, toluene-d_5, and toluene-d_8. For $C_6H_5CH_3$: (○) Tully et al.;[459] (□) Perry et al.[313] For $C_6H_5CD_3$: (△) Tully et al.[459] For $C_6D_5CH_3$: (●) Tully et al.[459] For $C_6D_5CD_3$: (▲) Tully et al.;[459] (▽) Perry et al.;[313] (—) recommendations for $C_6H_5CH_3$ and $C_6D_5CD_3$ (see text).

with an estimated overall uncertainty at 298 K of ±20%.

For temperatures ≥450 K, a unit-weighted least-squares fit of the rate constants of Tully et al.[459] to the expression $k = A'T^2e^{-E'/RT}$ yields the recommendation

k(toluene-d_8, $T \geq 450$ K) =

$$(6.85^{+2.55}_{-1.85}) \times 10^{-18}T^2e^{-(276\pm215)/T} \text{ cm}^3 \text{ molecule}^{-1} \text{ s}^{-1}$$

where the indicated errors are two least-squares standard deviations.

As for benzene and benzene-d_6, the rate constants at ≤325 K for toluene and toluene-d_8 are essentially identical, consistent with the dominance of OH radical addition to the aromatic ring. However, for temperatures ≥450 K the OH radical rate constant for toluene-d_8 is significantly lower than that for toluene-h_8. This is shown more clearly in Figure 53, in which the reported elevated temperature (≥378 K) rate constants for toluene,[313,459] toluene-d_3[459] ($C_6H_5CD_3$), toluene-d_5[459] ($C_6D_5CH_3$), and toluene-d_8[313,459] are plotted in Arrhenius form, together with the recommended expressions for toluene and toluene-d_8 for temperatures ≥450 K. It can be seen that to a first approximation these data fall into two sets, those for $C_6H_5CH_3$ and $C_6D_5CH_3$, and those for $C_6H_5CD_3$ and $C_6D_5CD_3$, with the rate constants for toluene and toluene-d_5 being significantly higher than those for toluene-d_3 and toluene-d_8 (at least up to 1000 K). While there may be consistent differences between the rate constants for toluene and toluene-d_5 and between those for toluene-d_3 and toluene-d_8, these are

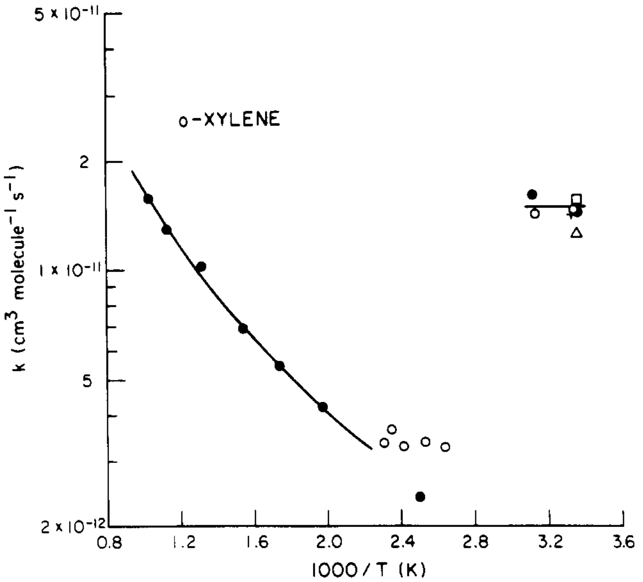

Figure 54. Arrhenius plot of the rate constants for the reaction of OH radicals with *o*-xylene: (□) Hansen et al.;[458] (○) Perry et al.;[313] (△) Ravishankara et al.;[294] (+) Cox et al.;[139] (●) Nicovich et al.[463] (for the flash photolysis studies, only rate constants obtained from exponential OH radical decays are plotted); (—) recommendations (see text).

minor and are probably within the experimental errors. This deuterium isotope substitution behavior shows that in this temperature regime the OH radical reaction must proceed predominantly via H (or D) atom abstraction from the substituent $-CH_3$ (or $-CD_3$) group.[1,313,459]

e. *o*-Xylene. The available limiting high-pressure second-order rate constants are listed in Table XIV, and those of Hansen et al.,[458] Perry et al.,[313] Ravishankara et al.,[294] Cox et al.,[139] and Nicovich et al.[463] are plotted in Arrhenius form in Figure 54. In general, the agreement between these studies is good. The somewhat lower rate constant obtained by Ravishankara et al.[294] at 298 K in their flash photolysis–resonance fluorescence study may have been due to *o*-xylene losses to the walls in the static reaction vessel used.[463] Thus this rate constant (and the corresponding rate constants for *m*- and *p*-xylene[294]) are not used in the evaluations.

For temperatures ≤325 K rate constants have been reported only over the very limited temperature range 298–320 K with, within the experimental error limits, a zero or near-zero temperature dependence. Hence a unit-weighted average of the absolute rate constants of Hansen et al.,[458] Perry et al.[313] and Nicovich et al.[463] yields the recommendation of

$$k(o\text{-xylene}, 298 \le T \le 320\text{ K}) = 1.47 \times 10^{-11}\text{ cm}^3\text{ molecule}^{-1}\text{ s}^{-1}$$

independent of temperature over the range 298–320 K, with an estimated overall uncertainty over this temperature range of ±25%. At room temperature, this rate constant is at the limiting high-pressure value at total pressures of helium or argon diluent of ≳20 torr.[294]

For temperatures ≥450 K, a unit-weighted least-squares fit of the ≥450 K rate constants of Nicovich et al.[463] to the expression $k = A'T^2e^{-E'/RT}$ yields the recommendation of

$$k(o\text{-xylene}, T \ge 450\text{ K}) = (1.75^{+0.25}_{-0.22}) \times 10^{-17}T^2e^{-(35\pm90)/T}\text{ cm}^3\text{ molecule}^{-1}\text{ s}^{-1}$$

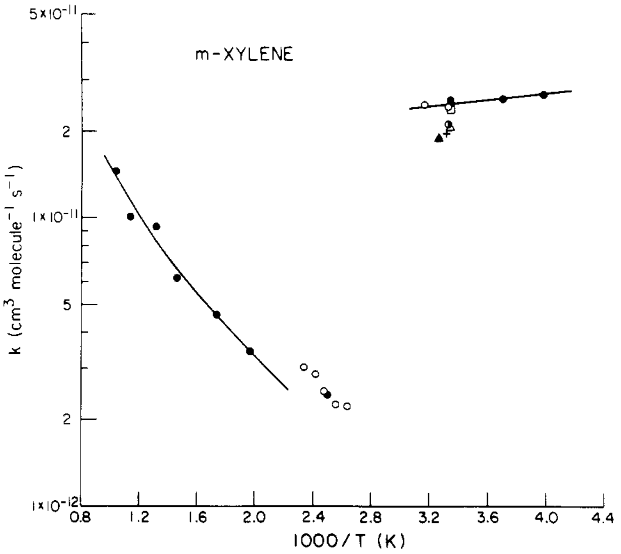

Figure 55. Arrhenius plot of the rate constants for the reaction of OH radicals with *m*-xylene: (□) Hansen et al.;[458] (▲) Lloyd et al.;[144] (○) Perry et al.;[313] (△) Ravishankara et al.;[294] (+) Cox et al.;[139] (●) Nicovich et al.;[463] (◑) Atkinson et al.[224] (for the flash photolysis studies, only rate constants obtained from exponential OH radical decays are plotted); (—) recommendations (see text).

where the indicated errors are two least-squares standard deviations. Again, as is the case for *m*- and *p*-xylene (see below) the rate constants determined by Perry et al.[313] over the small temperature range ~379–432 K are somewhat higher (by up to ~50%) than predicted from the recommended ≥450 K expression.

f. *m*-Xylene. The available limiting second-order high-pressure rate constants are listed in Table XIV, and those of Hansen et al.,[458] Lloyd et al.,[144] Perry et al.,[313] Ravishankara et al.,[294] Cox et al.,[139] Nicovich et al.,[463] and Atkinson et al.[224] are plotted in Arrhenius form in Figure 55. Ravishankara et al.[294] have shown that at 298 K this reaction is in the fall-off regime between second- and third-order kinetics at 3-torr total pressure of argon, with the limiting high-pressure value being attained at ~20-torr total pressure of helium or argon.[294]

For temperatures ≤325 K, a unit-weighted least-squares analysis of the absolute rate constant data of Hansen et al.,[458] Perry et al.,[313] and Nicovich et al.[463] (that of Ravishankara et al.[294] has been omitted for the reasons discussed above) yields the recommended Arrhenius expression of

$$k(m\text{-xylene}, T \le 325\text{ K}) = (1.66^{+0.58}_{-0.39}) \times 10^{-11}e^{(116\pm87)/T}\text{ cm}^3\text{ molecule}^{-1}\text{ s}^{-1}$$

where the indicated errors are two least-squares standard deviations

$$k(m\text{-xylene}) = 2.45 \times 10^{-11}\text{ cm}^3\text{ molecule}^{-1}\text{ s}^{-1}\text{ at 298 K}$$

with an estimated uncertainty at 298 K of ±25%. It should be noted that the more recent relative rate constants of Lloyd et al.,[144] Cox et al.,[139] and Atkinson et al.[224] are somewhat lower (by up to ~20%) than this expression.

For temperatures ≥450 K, a unit-weighted least-squares fit of the data of Nicovich et al.[463] to the expression $k = A'T^2e^{-E'/RT}$ yields the recommendation

$$k(m\text{-xylene}, T \ge 450\text{ K}) = (1.71^{+0.71}_{-0.50}) \times 10^{-17}T^2e^{-(127\pm235)/T}\text{ cm}^3\text{ molecule}^{-1}\text{ s}^{-1}$$

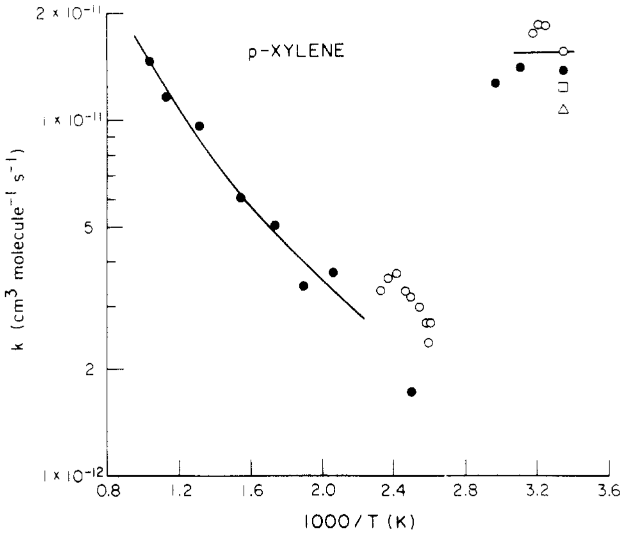

Figure 56. Arrhenius plot of the rate constants (obtained from exponential OH radical decays) for the reaction of OH radicals with *p*-xylene: (□) Hansen et al.;[458] (○) Perry et al.;[313] (△) Ravishankara et al.;[294] (●) Nicovich et al.;[463] (—) recommendations (see text).

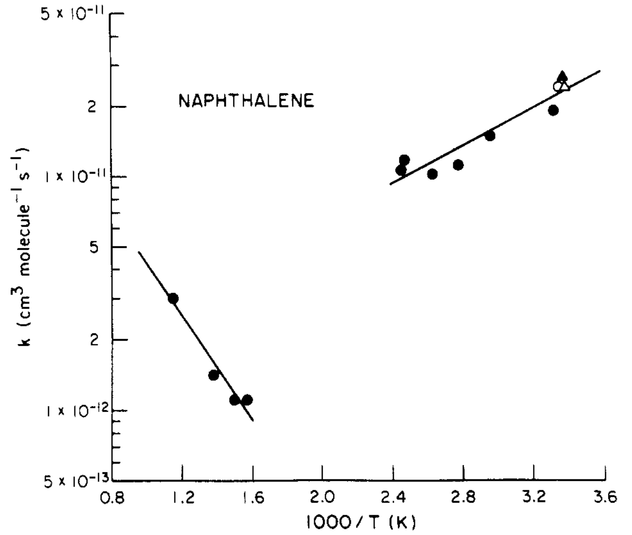

Figure 57. Arrhenius plot of the rate constants for the reaction of OH radicals with naphthalene: (●) Lorenz and Zellner;[121,460] (△) Atkinson et al.;[148] (○) Biermann et al.;[154] (▲) Atkinson and Aschmann[468] (for the laser photolysis study of Lorenz and Zellner,[121,460] only rate constants obtained at temperatures <410 and >600 K are plotted; see text); (—) recommendations (see text).

where the indicated errors are two least-squares standard deviations.

g. *p*-Xylene. The available limiting high-pressure rate constants are listed in Table XIV, and those of Hansen et al.,[458] Perry et al.,[313] Ravishankara et al.,[294] and Nicovich et al.[463] are plotted in Arrhenius form in Figure 56. As for *m*-xylene, Ravishankara[294] have reported that at 298 K the rate constant for this reaction is in the fall-off regime between second- and third-order kinetics at 3-torr total pressure of argon, with the rate constants at 20-torr total pressure of helium or argon being in the high-pressure kinetic regime. Omitting the rate constant determined by Ravishankara et al.[294] for the reasons discussed above, a unit-weighted average of the limiting high-pressure rate constants at temperatures ≤325 K determined by Hansen et al.,[458] Perry et al.,[313] and Nicovich et al.[463] yields the recommended value of

$$k(p\text{-xylene}, 297 \le T \le 320\ \text{K}) = 1.52 \times 10^{-11}\ \text{cm}^3\ \text{molecule}^{-1}\ \text{s}^{-1}$$

over the temperature range 297–320 K, with an estimated overall uncertainty of ±35%.

At temperatures ≥450 K, a unit-weighted least-squares fit of the rate constants reported by Nicovich et al.[463] to the expression $k = A'T^2e^{-E'/RT}$ yields the recommendation

$$k(p\text{-xylene}, T \ge 450\ \text{K}) = (1.74^{+0.70}_{-0.50}) \times 10^{-17}T^2e^{-(99\pm215)/T}\ \text{cm}^3\ \text{molecule}^{-1}\ \text{s}^{-1}$$

where the indicated errors are two least-squares standard deviations.

h. Naphthalene. The available limiting high-pressure rate constants are listed in Table XIV and are plotted in Arrhenius form in Figure 57. Lorenz and Zellner[121] have shown that at 378 ± 2 K the rate constant for this reaction is in the fall-off region between second- and third-order kinetics below ~50 torr total pressure of helium but that no such fall-off behavior is observed at 525 ± 1 K.

At temperatures ≤410 K the rate constants obtained by Lorenz and Zellner[121,460] and Atkinson and coworkers[148,154,468] are in good agreement, and a unit-weighted least-squares analysis of these data[121,148,154,460,468] yields the recommended Arrhenius expression

$$k(\text{naphthalene}, T \le 410\ \text{K}) = (1.05^{+1.11}_{-0.54}) \times 10^{-12}e^{(902\pm240)/T}\ \text{cm}^3\ \text{molecule}^{-1}\ \text{s}^{-1}$$

where the indicated errors are two least-squares standard deviations

$$k(\text{naphthalene}) = 2.17 \times 10^{-11}\ \text{cm}^3\ \text{molecule}^{-1}\ \text{s}^{-1}\ \text{at 298 K}$$

with an estimated overall uncertainty of ±30% at 298 K.

It should be noted that this negative temperature dependence, equivalent to an Arrhenius activation energy of −1.8 kcal mol⁻¹, is the most negative encountered for the reactions of OH radicals with organics, and, when compared to other recommended negative Arrhenius activation energies of ~−1 kcal mol⁻¹, may indicate an erroneously high temperature dependence in this temperature regime for this reaction rate constant.

At elevated temperatures, ≥600 K for this particular aromatic hydrocarbon,[121] the only rate constants available are those of Lorenz and Zellner,[460] and a unit-weighted least-squares fit of these to the expression $k = A'T^2e^{-E'/RT}$ yields the tentative recommendation of

$$k(\text{naphthalene}, T \ge 600\ \text{K}) = (1.12^{+2.12}_{-0.73}) \times 10^{-17}T^2e^{-(969\pm752)/T}\ \text{cm}^3\ \text{molecule}^{-1}\ \text{s}^{-1}$$

where the indicated errors are two least-squares standard deviations.

For the remaining aromatic compounds, fewer data are available, and in many of these cases only tentative recommendations can be made.

i. Ethylbenzene. Only two rate constants[144,294] are available (Table XIV) at around room temperature. Within the experimental error limits these are in agreement, and it is tentatively recommended that

$$k(\text{ethylbenzene}) = 7.5 \times 10^{-12}\ \text{cm}^3\ \text{molecule}^{-1}\ \text{s}^{-1}$$

at ~298–305 K, with an estimated overall uncertainty of ~±35%.

j. *n*-Propylbenzene. The room-temperature rate constants of Lloyd et al.[144] and Ravishankara et al.[294] are in good agreement (Table XIV), and it is tentatively recommended that

$$k(n\text{-propylbenzene}) = 5.7 \times 10^{-12}\ \text{cm}^3\ \text{molecule}^{-1}\ \text{s}^{-1}$$

at ~298–305 K, with an estimated overall uncertainty of ±30%.

k. Isopropylbenzene. Again, the only two measurements of this rate constant are those of Lloyd et al.[144] and Ravishankara et al.[294] (Table XIV). However, in this case the agreement is not good, with a discrepancy of ~50% being evident. A room-temperature (298–305 K) rate constant of ~6.6 × 10^{-12} cm^3 molecule^{-1} s^{-1} is indicated.

These room-temperature rate constants for ethylbenzene, *n*-propylbenzene, and isopropylbenzene are similar to that for toluene and thus indicate that the rate constants for toluene are reasonably applicable to the higher monoalkylbenzenes.

l. *o*-, *m*-, and *p*-Ethyltoluene. While only a single room-temperature rate constant study has been carried out for each of these isomers,[144] the rate constants at ~305 K are similar to those for *o*-, *m*-, and *p*-xylene, respectively. This again indicates that to a first approximation the rate constants depend on the number of alkyl substituent groups, and not on their identity [as expected since (see below) OH radical addition to the aromatic ring is the dominant reaction pathway for the aromatic hydrocarbons].

m. *o*-, *m*-, and *p*-Cresol. Only for the ortho cresol isomer has more than a single kinetic study been carried out. The room-temperature rate constants for this isomer[312,465] show a discrepancy of ~20%, although they agree within the combined experimental error limits. As noted by Atkinson et al.,[465] the rate constants determined by Perry et al.[312] may have been somewhat low due to wall adsorption problems (especially in the small optical calibration cells used). Since the higher overall error limits assigned by Perry et al.[312] take into account (at least in part) such adsorption problems, a weighted least-squares analysis of these room-temperature rate constants[312,465] yields the recommendation that at 300 ± 1 K

$$k(o\text{-cresol}) = 4.0 \times 10^{-11}\ \text{cm}^3\ \text{molecule}^{-1}\ \text{s}^{-1}$$

with an estimated overall uncertainty of ±30%.

On the basis of this recommendation, it is recommended that the rate constants for *o*-cresol as a function of temperature be those of Perry et al.[312] multiplied by a factor of 1.17. [Because of the small temperature ranges covered for which exponential OH radical decays were observed (299–335 K and 393–423 K), no temperature dependent expressions are recommended.] For *m*- and *p*-cresol the recommendations at 300 ± 1 K then become

$$k(m\text{-cresol}) = 5.7 \times 10^{-11}\ \text{cm}^3\ \text{molecule}^{-1}\ \text{s}^{-1}$$

$$k(p\text{-cresol}) = 4.4 \times 10^{-11}\ \text{cm}^3\ \text{molecule}^{-1}\ \text{s}^{-1}$$

both with estimated overall uncertainties of ±35%.

n. Phenanthrene. Rate constants have been determined only by Biermann et al.[154] at 298 and 319 K and by Lorenz and Zellner[460] at temperatures ≥338 K, and these are plotted for temperatures <410 and >600 K in Figure 58. Although the rate constants obtained by Lorenz and Zellner[460] exhibit a significant degree of scatter, these rate constants, together with those of Biermann et al.[154] at 298 and 319 K, are uniformly higher than those for naphthalene by ~30% in both of the temperature regimes, <400 and >600 K, as shown by the dashed lines in Figure 58. While no definite recommendation is made, the above discussion indicates the magnitude of the OH radical reaction rate constants for this three-ring polycyclic aromatic hydrocarbon.

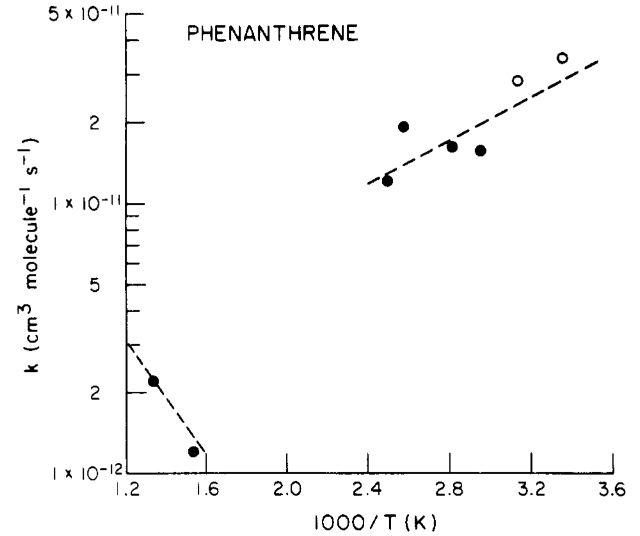

Figure 58. Arrhenius plot of the rate constants at <410 and >600 K for the reaction of OH radicals with phenanthrene: (●) Lorenz and Zellner;[460] (○) Biermann et al.;[154] (- - -) rate constants recommended for naphthalene increased by a factor of 1.3 (see text).

o. Biphenyl. Three room-temperature rate constant studies have been carried out for biphenyl.[148,466,467] These reported rate constants are in reasonably good agreement, considering the difficulties of working with such relatively low volatility organics.[148] On the basis of these data, it is recommended that

$$k(\text{biphenyl}) = (7 \pm 2) \times 10^{-12}\ \text{cm}^3\ \text{molecule}^{-1}\ \text{s}^{-1} \text{ at } 298\ \text{K}$$

For the remaining aromatic compounds for which rate constants have been reported, no firm recommendations are made.

Rate constants as a function of temperature have been determined by using the flash photolysis-resonance fluorescence technique for the trimethylbenzenes,[313] methoxybenzene,[312] aniline,[441] *N*,*N*-dimethylaniline,[441] *o*-nitrophenol,[357] and 1,2,4-trichlorobenzene.[462] For the trimethylbenzenes,[313] methoxybenzene,[312] and *N*,*N*-dimethylaniline[441] the reported temperature dependencies are qualitatively similar to those discussed above for the aromatic hydrocarbons. Because of the small temperature ranges over which exponential OH radical decays were observed, recommendations regarding the temperature dependencies are not warranted.

In the case of aniline, the room-temperature rate constants obtained by Rinke and Zetzsch[462] and Atkinson et al.[441] are in good agreement. However, while the general temperature-dependent behavior of this rate constant is similar to those described above for the aromatic hydrocarbons, the elevated temperature (≳350

K) rate constants continue to decrease with increasing temperature,[441] with an extrapolated rate constant at 298 K of ~55% of that measured. While further data are clearly necessary, this may suggest that two reaction pathways, involving OH radical addition to the aromatic ring and interaction with the $-NH_2$ group, are occurring with approximately equal probability at room temperature.

For *o*-nitrophenol and 1,2,4-trichlorobenzene, the reported rate constants[357,462] vary monotonically with temperature over the relatively limited temperature ranges studied. Additional data at higher temperatures are necessary before conclusions concerning the temperature dependencies and the resulting implications for the mechanisms of these reactions can be drawn.

2. Mechanism

The available kinetic[121,133,154,294,312,313,441,457–463,465–468] and product and mechanistic (ref 1, 3, 12, 13, 16, 17, 165–169, 172, 174, 180, 469–479) data show that in general two reaction pathways are operative at around room temperature: namely, OH radical addition to the aromatic ring to form an initially energy rich OH–aromatic adduct, e.g.

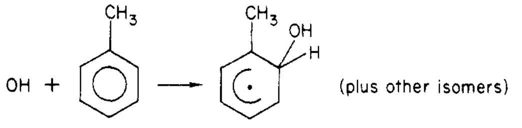

and a direct reaction involving either H atom abstraction

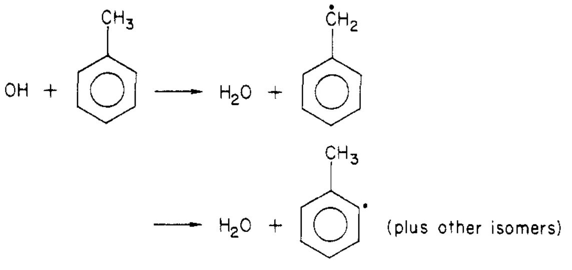

or substituent group (including H atom) elimination

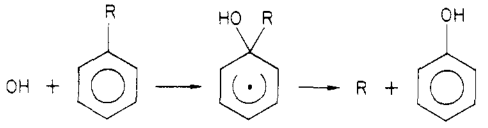

The OH radical addition pathway yields an initially energy rich OH–aromatic adduct which, for the case of benzene, has very recently been observed in the gas phase by Fritz et al.[479] using long path length ultraviolet laser absorption at 308 nm. This adduct can either decompose back to the reactants or be collisionally stabilized[1,3,313,457]

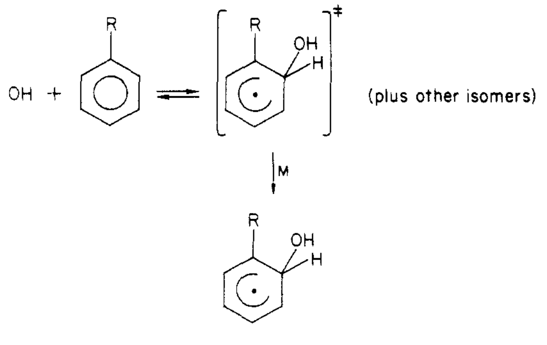

A further reaction step involves the unimolecular decomposition of this thermalized OH–aromatic adduct back to the reactants

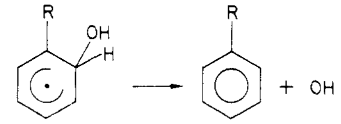

and this reaction pathway obviously becomes more rapid as the temperature increases.

Indeed, it is this thermal back-decomposition of the OH–aromatic adduct which gives rise to the observed nonexponential OH radical decays in the flash or laser photolysis kinetic studies[121,312,313,441,459,461,463] and to the occurrence of distinct temperature regimes with differing kinetic behavior.[121,312,313,441,459,463] Since the OH–aromatic adducts were rapidly deactivated to an essentially thermal energy population at the total pressures used in the studies of Perry et al.,[312,313] Tully et al.,[459] Nicovich et al.,[463] and Lorenz and Zellner,[121] the thermal back-decomposition rate constant, k_d, is given by

$$k_d = A_d e^{-E_d/RT}$$

In the flash photolysis studies of Perry et al.,[313] Tully et al.,[459] and Nicovich et al.[463] of the kinetics of the reactions of the reactions of the OH radical with the aromatic hydrocarbons, OH radical concentrations were monitored for ~1–30 ms after the flash. Significant nonexponentialities of the OH radical decay curves were observed at temperatures from ~320 to 380 K in the study of Perry et al.[313] and from ~320 to 400–450 K in those of Tully et al.[459] and Nicovich et al.[463] Hence the half-life of the OH–aromatic adduct was of the order of ~5–10 ms in this temperature range, corresponding to $k_d \approx 100\ s^{-1}$ at 350 K.[313] For an assumed preexponential factor of $A_d = 3 \times 10^{13}\ s^{-1}$,[313] the Arrhenius activation energy for thermal decomposition of the OH–aromatic adducts is then $E_d \approx 18$ kcal mol^{-1} for benzene,[313] toluene,[313] the xylene isomers,[313] the trimethylbenzene isomers,[313] methoxybenzene,[312] and *o*-cresol.[312] Since OH radical addition to the aromatic ring has no significant temperature dependence, this value of ~18 kcal mol^{-1} is essentially that for the C–OH bond dissociation energy in these OH–aromatic adducts.[3,313]

Recently, Wahner and Zetzsch[461] have directly monitored the equilibrium behavior of the OH radical–benzene–hydroxycyclohexadienyl radical system and determined values of $k_d = 1.95 \pm 0.2\ s^{-1}$ at 298 K and $11.5 \pm 1\ s^{-1}$ at 312 ± 3 K. The Arrhenius activation energy for decomposition of the hydroxycyclohexadienyl radical derived from these data of $E_d = 17.8 \pm 1.4$ kcal mol^{-1} (using the assumed preexponential factor of $A_d = 3 \times 10^{13}\ s^{-1}$)[313,461] is in excellent agreement with those derived by Perry et al.[313] using the quite different (and more indirect) procedure described above.

For naphthalene, Lorenz and Zellner[121] have estimated an Arrhenius activation energy for the thermal decomposition of the OH–naphthalene adduct of $E_d = 22.7 \pm 1.5$ kcal mol^{-1} using the same procedure as Perry et al.[312,313] For benzene and the monocyclic aromatic hydrocarbons, the thermalized hydroxycyclohexadienyl and methyl-substituted hydroxycyclohexadienyl radicals are then calculated to have lifetimes of ~0.5 s at 298 K, ~0.04 s at 325 K, ~0.8 ms at 380 K, and ~0.2

ms at 400 K. These lifetimes are then totally consistent with the above discussion of the reaction dynamics of these OH radical reactions.

Thus, at around room temperature, i.e., ≤325 K, OH radical addition to the aromatic ring dominates, while for temperatures ≳450 K (~600 K for the OH–naphthalene adduct[121]) back-dissociation of the OH–aromatic adducts becomes so rapid that on the time scale of the flash or laser photolysis studies carried out to date only the direct reaction involving H atom abstraction or H atom, or other substituent group, elimination is observed.

At elevated temperatures these reaction pathways are, for example, for benzene

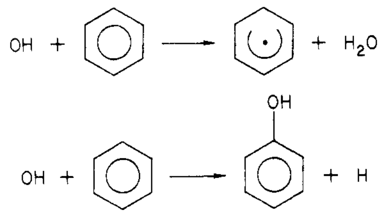

On the basis of the heat of formation of the hydroxycyclohexadienyl radical[313,461] and the observation[480] that the Arrhenius activation energies for H atom addition to a series of substituted benzenes are ~3–4 kcal mol^{-1},[480] it can be estimated that H atom elimination from the thermalized hydroxycyclohexadienyl radical is endothermic by ~21–22 kcal mol^{-1}. Hence the direct H atom elimination reaction will have a barrier height of only 3–4 kcal mol^{-1}. Indeed, for benzene Lin and Lin[335] have calculated that at elevated temperatures (≳400 K) it is the H atom elimination process which has been observed in the kinetic studies carried out to date[313,459] with a rate constant of

$$k = 1.84 \times 10^{-18} T^{2.11} e^{-449/T} \text{ cm}^3 \text{ molecule}^{-1} \text{ s}^{-1}$$

which is in good agreement with the above recommendation for temperatures >450 K. The calculations of Lin and Lin[335] show that the H atom abstraction pathway is insignificant at temperatures below at least 1000 K. Analogous elimination processes, for example, elimination of a Cl atom, possibly occur in the reaction of OH radicals with chloro-[461] and bromo benzenes, for example

$$OH + C_6H_5Cl \rightarrow C_6H_5OH + Cl$$

For the methyl-substituted benzenes, Atkinson et al.[1] have estimated that direct elimination of a $-CH_3$ group is exothermic by ~6 kcal mol^{-1}. However, phenol has not been detected (an upper limit yield of <1% has been reported[481]) at room temperature from the reaction of OH radicals with toluene, and hence this direct elimination pathway is, at least for toluene, very minor. Rather, for the alkyl-substituted benzenes the kinetic and product data show that H atom abstraction from the alkyl substituent groups occurs, and this process is almost certainly the major contributor to the reaction rate constants measured at temperatures ≥450 K. Thus for toluene, benzaldehyde is observed as a product under atmospheric conditions with a yield of ~7% at room temperature[17,475] and can only arise following H atom abstraction from the substituent $-CH_3$ group. The kinetic data for toluene and the deuterated toluenes totally supports this observation (see above and Figure 53).

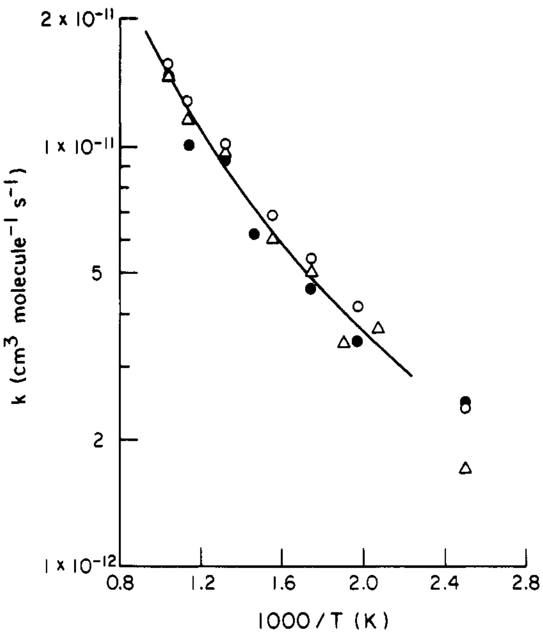

Figure 59. Arrhenius plot of the rate constants obtained at temperatures ≥400 K obtained by Nicovich et al.[463] for the reaction of OH radicals with *o*-xylene (○), *m*-xylene (●), and *p*-xylene (△).

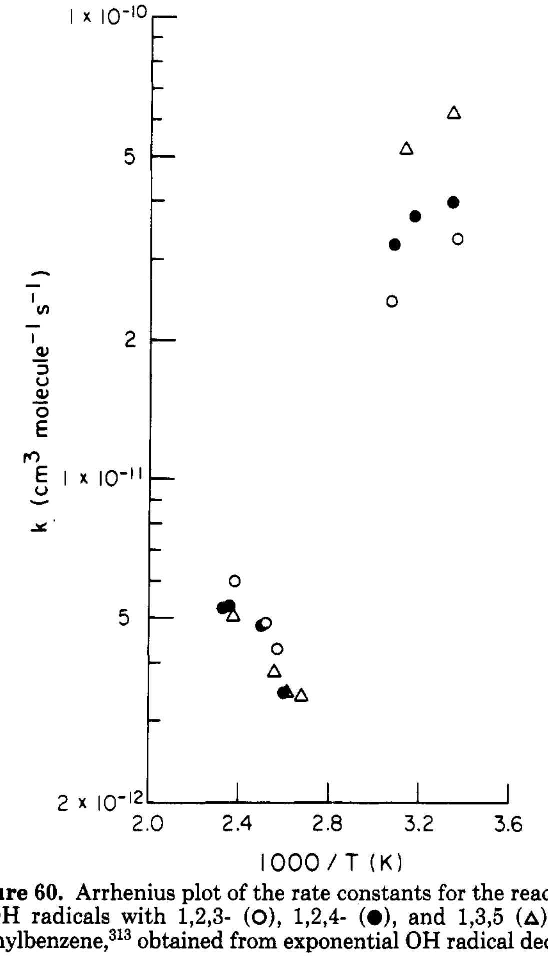

Figure 60. Arrhenius plot of the rate constants for the reaction of OH radicals with 1,2,3- (○), 1,2,4- (●), and 1,3,5 (△) trimethylbenzene,[313] obtained from exponential OH radical decays.

Furthermore, as seen in Figures 59 and 60, the elevated temperature rate constants for the three xylene isomers are essentially identical, as are those for the three trimethylbenzene isomers. The observed rate constants for the xylene isomers are almost exactly a factor of 2 higher than those for toluene-h_8 and toluene-d_5 ($C_6D_5CH_3$) over the temperature range 450–1000 K. A unit-weighted least-squares analysis of the rate constants of Nicovich et al.[463] for temperatures ≥450 K to the expression $k = A'T^2e^{-E'/RT}$ yields

$$k(\text{xylenes}, T \geq 450\ \text{K}) = (1.74^{+0.39}_{-0.32}) \times 10^{-17}T^2e^{-(89\pm134)/T}\ \text{cm}^3\ \text{molecule}^{-1}\ \text{s}^{-1}$$

where the errors are two least-squares standard deviations.

For the trimethylbenzenes, rate constants (which may be somewhat high[459]) in this temperature regime are available only at ~400 K[313] and are a factor of ~4 higher than that for toluene at this temperature, consistent with the above discussion. The available kinetic data for *o*-cresol suggests that H atom abstraction from the -OH substituent group occurs ~8% of the overall reaction of room temperature.[3,312]

For benzaldehyde the available kinetic data[3] (Table XI) show that the H atom abstraction pathway dominates at room temperature, and this is expected to be the case over a wide temperature range. This is also expected to be the case for the other aromatic aldehydes and possibly for certain other substituted aromatics such as aniline and other aromatic amines.[441]

Table XV gives estimated rate constant ratios $k_a/(k_a + k_b)$ at 298 K for benzene, the substituted benzenes and naphthalene and phenanthrene for which estimates can be made, where k_b and k_a are the rate constants for the OH radical addition reaction and the H atom abstraction/substituent elimination reaction, respectively. Apart from toluene, these estimates are derived from extrapolations of the elevated temperature (generally ≥450 K) rate constants, using the recommendations discussed above or previous literature estimates.

TABLE XV. Rate Constant Ratios $k_a/(k_a + k_b)$ at 298 K for the Gas-Phase Reaction of OH Radicals with a Series of Aromatic Compounds

aromatic	$k_a/(k_a + k_b)$ at 298 K[a]
benzene	0.07, 0.05[b]
benzene-d_6	0.02
toluene	0.11, 0.08[c]
toluene-d_8	0.08
o-xylene	0.09
m-xylene	0.04
p-xylene	0.07
1,2,3-trimethylbenzene	0.05,[d] 0.04[e]
1,2,4-trimethylbenzene	0.04,[d] 0.03[e]
1,3,5-trimethylbenzene	0.03,[d] 0.02[e]
methoxybenzene	0.20[f]
o-cresol	0.08[f]
aniline	~0.5[g]
N,N-dimethylaniline	~0.001[g]
naphthalene	0.002
phenanthrene	~0.002

[a] From extrapolation of the elevated temperature rate constant data to 298 K, using the recommendations (see text) for the rate constants k_a and k_b, unless indicated. These extrapolated values are expected to be subject to uncertainties of the order of ±50%. [b] From Lin and Lin,[335] using a calculated rate constant for the reaction OH + $C_6H_6 \rightarrow C_6H_5OH$ + H of $k_a = 1.84 \times 10^{-18}T^{2.11}e^{-449/T}$ cm^3 molecule^{-1} s^{-1} [which can be compared to the ≥450 K recommendation above of $k_a = 3.25 \times 10^{-18}T^2e^{-344/T}$ cm^3 molecule^{-1} s^{-1} for the direct (and unspecified) reaction pathway]. [c] From the product study of Atkinson et al.[475] (see also Akinson and Lloyd[3]). [d] Calculated by multiplying the direct reaction rate constant for the three xylene isomers of $k_a = (1.74^{+0.39}_{-0.32}) \times 10^{-17}T^2e^{-(89\pm134)/T}$ cm^3 molecule^{-1} s^{-1} = 1.15×10^{-12} cm^3 molecule^{-1} s^{-1} at 298 K), by a factor of 1.5 to take into account the number of substituent -CH_3 groups. [e] As given by Perry et al.[313] from extrapolation of their rate constants at ≥380 K to 298 K. [f] As given by Perry et al.[312] from extrapolation of their rate constants at >385 K (methoxybenzene) and >400 K (*o*-cresol) to 298 K. [g] From Atkinson et al.,[441] from extrapolation of rate constants to 298 K.

3. Mechanisms under Atmospheric Conditions

The reaction mechanisms of the OH radical reactions with the aromatic compounds subsequent to the initial reaction under atmospheric conditions are presently incompletely understood. For the aromatic hydrocarbons toluene and *m*-xylene a detailed discussion has been given by Atkinson and Lloyd,[3] and this review should be consulted for details. To date, only for benzene, toluene, the xylene isomers, and the trimethylbenzene isomers are product and mechanistic data available, and in this section the present status of this topic is summarized, concentrating on toluene since to date this is the most studied aromatic.

As discussed above, for the aromatic hydrocarbons at room temperature the initial OH radical reaction proceeds via two pathways; namely, OH radical addition to the aromatic ring

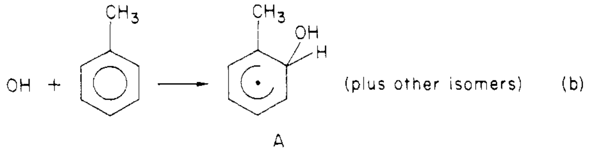

A

to yield a hydroxycyclohexadienyl radical,[479] and H atom abstraction (for the alkyl-substituted benzenes) or H atom elimination (for benzene and presumably naphthalene and the higher polycyclic aromatic hydrocarbons), i.e.

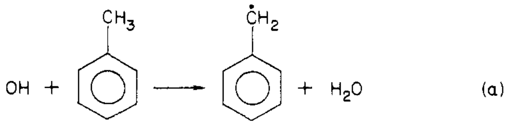

[or for benzene

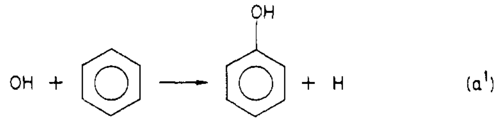

although this postulate needs to be experimentally confirmed]. The rate constant ratios, $k_a/(k_a + k_b)$ or $k_a^1/(k_a^1 + k_b)$, or estimates thereof are given in Table XV.

The reaction pathways subsequent to the H atom abstraction reaction pathway a are reasonably well understood.[3] Thus the benzyl radical is expected to react under atmospheric conditions via the following sequence of reactions

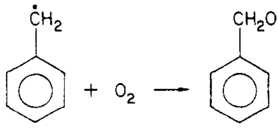

(with a rate constant of 1.0×10^{-12} cm^3 molecule^{-1} s^{-1},[482,483] independent of temperature,[483] with similar rate constants for the *o*- and *p*-methylbenzyl radicals[482])

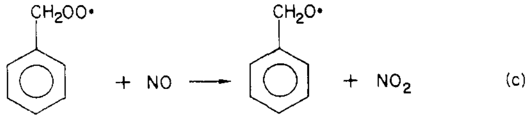

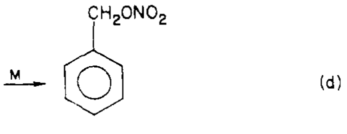

TABLE XVI. Formation Yields of the α-Dicarbonyls, Glyoxal, Methylglyoxal, and Biacetyl, from Benzene and the Methyl-Substituted Benzenes at Room Temperature

aromatic	α-dicarbonyl yield[a] glyoxal	methylglyoxal	biacetyl	ref
benzene	0.207 ± 0.019			478
toluene	0.15 ± 0.04	0.14 ± 0.04		476
	0.111 ± 0.013	0.146 ± 0.014		180
	0.105 ± 0.019	0.146 ± 0.006		478
o-xylene			0.18 ± 0.04	165
			0.260 ± 0.102	166
			0.137 ± 0.016	475
	0.08 ± 0.01	0.23 ± 0.03	0.10 ± 0.02	476
	0.087 ± 0.012	0.246 ± 0.020		478
m-xylene	0.13 ± 0.03	0.42 ± 0.05		476
	0.104 ± 0.020	0.265 ± 0.035		180
	0.086 ± 0.011	0.319 ± 0.009		478
p-xylene	0.24 ± 0.02	0.12 ± 0.02		476
	0.120 ± 0.020	0.111 ± 0.015		180
	0.225 ± 0.039	0.105 ± 0.034		478
1,2,3-trimethylbenzene	0.072 ± 0.001	0.18 ± 0.01	0.45 ± 0.02	476
	0.057 ± 0.008	0.152 ± 0.025	0.316 ± 0.036	478
1,2,4-trimethylbenzene	0.078 ± 0.005	0.37 ± 0.01	0.11 ± 0.01	476
	0.048 ± 0.005	0.357 ± 0.017	0.048 ± 0.009	478
1,3,5-trimethylbenzene		0.64 ± 0.03		476
		0.602 ± 0.033		478

[a] Indicated error limits are two standard deviations.

with $k_d/(k_c + k_d) \approx 0.1$ at atmospheric pressure and room temperature,[470] followed by reaction of the $C_6H_5CH_2O\cdot$ radical with O_2 to yield benzaldehyde and an HO_2 radical:

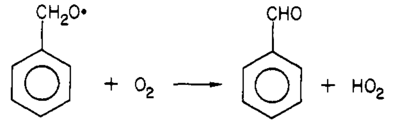

Analogous reaction pathways are expected to be applicable to the other aromatic hydrocarbons, after H atom abstraction from the substituent alkyl groups.[3]

The major area of uncertainty concerns the reaction mechanisms of the OH–aromatic adducts (A) [i.e., the hydroxycyclohexadienyl and alkylhydroxycyclohexadienyl radicals] under atmospheric conditions. Two pathways, involving reaction with O_2, have been postulated.[1,3,12,13,16,17] One leads to the formation of phenol and its homologues

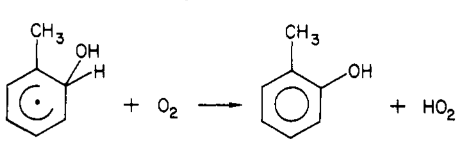

although this reaction may well be more complex than the simple H atom abstraction route shown above (see, for example, the liquid-phase ^{18}O incorporation study of Narita and Tezuka[484]). This overall reaction does occur, as evidenced by the observation of *o*-, *m*-, and *p*-cresol from the photooxidation of toluene,[167,470,475] with a total yield of ~16% (~13% *o*-cresol[475] together with much smaller amounts of *p*- and *m*-cresol[167,470]) under atmospheric conditions. For the other aromatic hydrocarbons, the hydroxyaromatic yields are not reliably known at present.

Clearly a major portion of the reaction pathways are not accounted for by these above reaction sequences (for example, ~80% for the case of toluene), and the available data show that other reactions of the OH–aromatic adducts (A), leading to ring cleavage, occur. This is evidenced by the observation of significant yields of the α-dicarbonyls glyoxal, methylglyoxal, and biacetyl from benzene and the alkyl-substituted benzenes[165,166,180,475,476,478] (given in Table XVI) and by the observation of the unsaturated 1,4-dicarbonyls butene-1,4-dial from toluene[168] and 3-hexene-2,5-dione from *p*-xylene and 1,2,4-trimethylbenzene[474] (though in small yields).

The actual reaction pathways leading to these α-dicarbonyls are not known but have been postulated[3,12] to proceed via, taking toluene as an example:

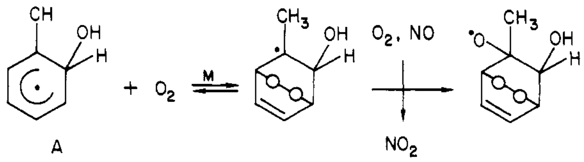

followed by decomposition of this alkoxy radical

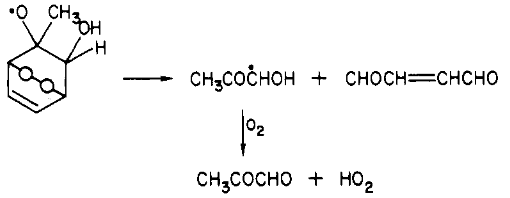

However, other reaction pathways may well be involved. The α-dicarbonyl yields given in Table XVI show that the total α-dicarbonyl yields are appreciably less than unity, being ~21% for benzene, 25–29% for toluene, ~40% for the three xylene isomers, and ~50–60% for the three trimethylbenzene isomers. For toluene, this then leads to only ~50% of the reaction pathways being accounted for, and the two recent product studies of Shepson et al.[169] and Dumdei and O'Brien,[477] utilizing GC-MS[169] and MS-MS[477] analytical techniques, have identified a wide variety of other ring cleavage products, including $CH_3COCOCH{=}CH_2$,[169] $CHOCOCH{=}CH_2$,[169] $CH_3COCH{=}CH_2$,[477] $CH_3COCH{=}CHCH{=}CH_2$,[477] $CHOC(OH){=}CHCHO$,[477] and $CH_3COCH{=}CHCH{=}CHCHO$.[477] Possible reaction schemes have been proposed by Dumdei and O'Brien.[477]

TABLE XVII. Rate Constants k for the Gas-Phase Reaction of OH Radicals with Organometallic Compounds

organometallic	$10^{12}k$, cm^3 molecule^{-1} s^{-1}	T, K	technique	ref
dimethylmercury	19.7 ± 1.5	~300	rel rate [rel to k(OH + ethene) = 8.45×10^{-12}]^a	Niki et al.[179]
	18.5 ± 1.5	~300	rel rate [rel to k(OH + propene) = 2.60×10^{-11}]^a	Niki et al.[179]
tetramethyllead	9.4	295 ± 3	rel rate [rel to k(OH + toluene) = 6.26×10^{-12}]^a	Harrison and Laxen[487]
	6.3 ± 1.3	296	PR-RA	Nielsen et al.[488]
tetraethyllead	83.1	295 ± 3	rel rate [rel to k(OH + m-xylene) = 2.45×10^{-11}]^a	Harrison and Laxen[487]
	11.6 ± 1.7	296	PR-RA	Nielsen et al.[488]

[a] From the present recommendations (see text).

Recent experimental studies of Zellner et al.[485] concerning the reactions of the hydroxycyclohexadienyl radical (HCHD) with NO, NO_2, and O_2 have shown that this radical reacts with NO and NO_2 with room-temperature (298 K) rate constants of

$$k(\mathrm{NO + HCHD}) = (1.0 \pm 0.5) \times 10^{-12}\ \mathrm{cm^3\ molecule^{-1}\ s^{-1}}$$

$$k(\mathrm{NO_2 + HCHD}) = (8.5 \pm 2.1) \times 10^{-12}\ \mathrm{cm^3\ molecule^{-1}\ s^{-1}}$$

Clearly, even for toluene (to date the most studied aromatic) the reaction mechanisms and products formed under atmospheric conditions are incompletely understood. This is more so for benzene and the other methyl-substituted benzenes, and, apart from benzaldehyde which reacts by pathways analogous to the aliphatic aldehydes,[3,12,486] essentially no product and mechanistic data subsequent to the initial OH radical reaction are available for other substituted aromatics.

For styrene and its homologues $C_6H_5C(R_1){=}CR_2R_3$ (where R_{1-3} = H or CH_3), the studies of Chiorboli et al.[348] and Bignozzi et al.[464] have shown that OH radical reaction proceeds via addition to the olefinic double bond:

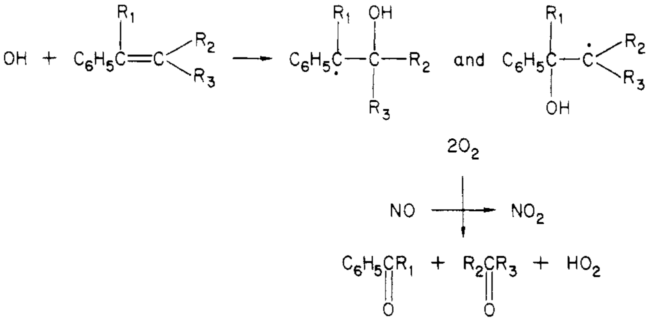

as evidenced by the observations of the formation of benzaldehyde in essentially unit yield from styrene and β-dimethylstyrene and of acetone from β-dimethylstyrene.

J. Organometallic Compounds

1. Kinetics

The available rate constant data are listed in Table XVII. Only three organometallics have been studied to date and for tetramethyl- and tetraethyllead two kinetic studies have been carried out at room temperature by Harrison and Laxen[487] and Nielsen et al.[488] However, the two rate constants reported for tetraethyllead[487,488] disagree by a factor of ~7. Although the two rate constants for tetramethyllead (obtained from the same studies as those for tetraethyllead[487,488]) are in reasonable agreement, we do not make any recommendations.

However, the room-temperature rate constants are higher, by factors of ~50,[179] ~9,[488] and ~2,[488] than those for the corresponding alkanes containing the same numbers of primary and secondary C–H bonds.[214]

2. Mechanisms and Reaction Products under Atmospheric Conditions

The sole product study carried out concerning the reactions of OH radicals with organometallic compounds under atmospheric conditions is that of Niki et al.[179] for CH_3HgCH_3. It was concluded[179] from this FT-IR absorption spectroscopic study that the initial reaction proceeds via

$$\mathrm{OH + CH_3HgCH_3 \rightarrow CH_3HgOH + CH_3}$$

followed by subsequent oxidation of CH_3 radicals to formaldehyde and other minor products and by further homogeneous and/or heterogeneous reactions of CH_3HgOH to yield compounds such as $[(CH_3Hg)_3O]NO_3$.[179] The occurrence of such a displacement reaction is consistent with the magnitude of the rate constant observed.[179] Clearly, a temperature dependence study would be useful to further confirm this postulate.

For the tetraalkyllead compounds studied, neither the initial reaction pathways nor the products under atmospheric conditions are known, although again displacement mechanisms leading to the initial formation of $(CH_3)_3PbOH$ and $(C_2H_5)_3PbOH$ are possible.

IV. Discussion and Conclusions

A. Rate Constant Trends and Correlations

As can be seen from the above sections, kinetic data are available for the gas-phase reactions of the OH radical with a wide variety of organics. For certain classes of organics, these data allow possible rate constant trends and correlations to be examined. In the following sections, discussion and evaluations of OH radical rate constant trends, correlations with other electrophilic reactants such as $O(^3P)$ atoms, NO_3 radicals, and O_3, and a priori predictive techniques are given for the classes of organics for which sufficient kinetic data are available.

1. Correlation with $O(^3P)$ Atom, NO_3 Radical, and O_3 Rate Constants

As noted previously,[1] the OH radical is electrophilic in character, as are $O(^3P)$ atoms, NO_3 radicals, and O_3, and it may be expected that the rate constants for the addition reactions of these species to unsaturated car-

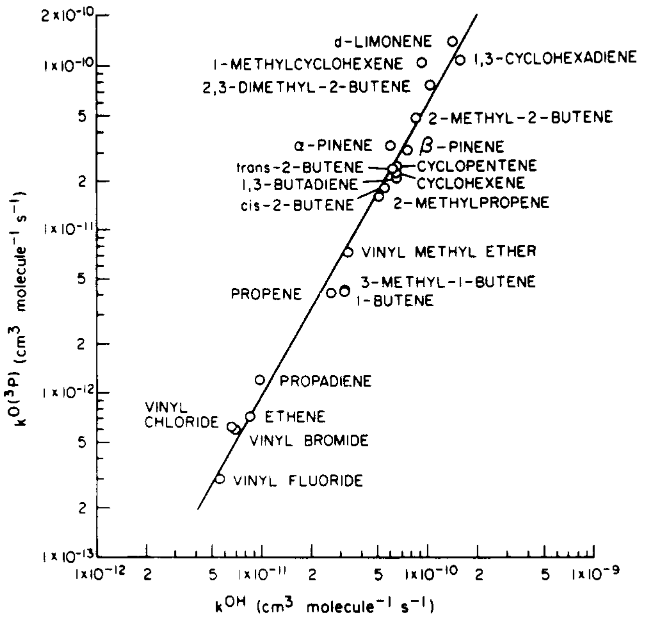

Figure 61. Linear free energy plot of log $k^{O(^3P)}$ against log k^{OH} at room temperature for a series of acyclic and cyclic alkenes and dialkenes, vinyl methyl ether, and the vinyl halides [the OH radical rate constants are from this work, while the $O(^3P)$ atom reaction rate constants are from ref 300 and 489 through 501].

bon–carbon bonds will exhibit some degree of correlation. Figures 61, 62, and 63 show such correlations of $O(^3P)$ atom, NO_3 radical, and O_3 reaction rate constants with the corresponding OH radical reaction rate constants for a series of unsaturated organics. It can be seen that the correlation between the OH radical and $O(^3P)$ atom reaction rate constants is excellent, with a least-squares expression of (with the rate constants in cm^3 $molecule^{-1}$ s^{-1} units)

$$\ln k^{O(^3P)} = -4.09 + 1.76 \ln k^{OH}$$

Similar correlations have been presented and discussed previously,[151,227,298,489,508] and it is evident that this correlation between OH radical and $O(^3P)$ atom reaction rate constants is sufficiently good for the estimation of OH radical reaction rate constants for alkenes, cycloalkenes, and a variety of other organics containing >C=C< bonds.

However, for the correlations of the OH radical and NO_3 radical or O_3 reaction rate constants, a considerable amount of scatter is evident, although obviously correlations do occur. The correlation between O_3 and OH radical reaction rate constants is made more complex by the observed effects of ring strain energy on the O_3 reaction rate constants[509] and by the observation that the rate constants for the reaction of O_3 with conjugated di- and trialkenes are significantly lower than may be expected based upon the monoalkenes and nonconjugated dialkenes.[303,506] These effects, which give rise, at least in part, to the significant degree of scatter in the plot shown in Figure 63 and which are largely incidental with the present discussion, have been discussed in more detail by Atkinson and Carter.[506]

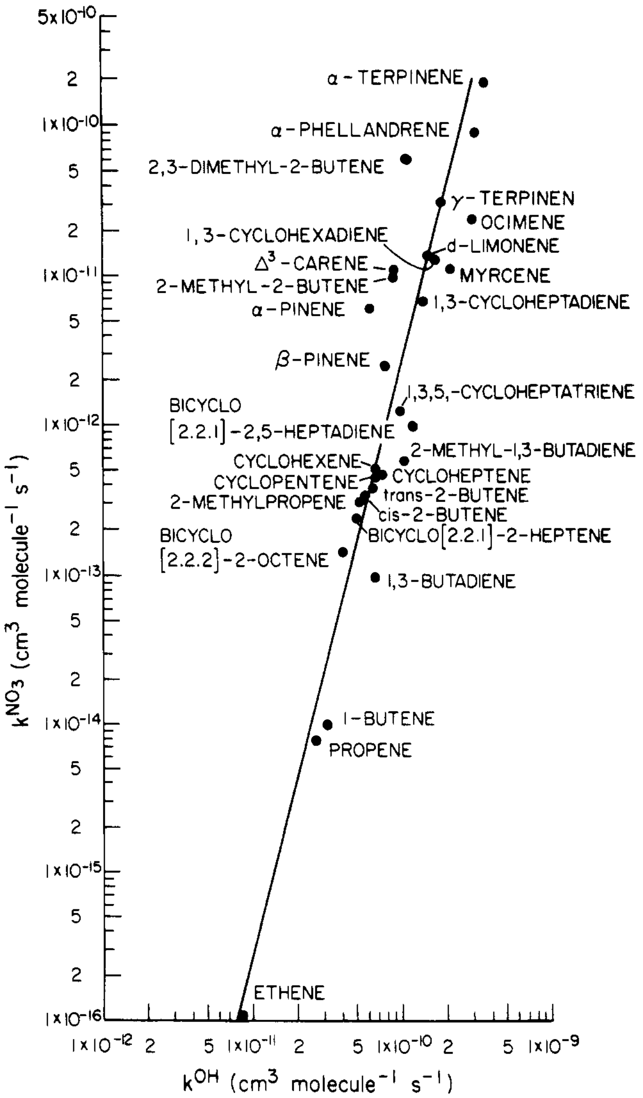

Figure 62. Linear free-energy plot of log k^{NO_3} against log k^{OH} at room temperature for a series of acyclic and cyclic alkenes, dialkenes and trialkenes [the OH radical rate constants are from this work; the NO_3 radical reaction rate constants are from ref 502 through 505]. The line drawn is merely to indicate the trend of the data.

The observation that the correlations of $O(^3P)$ atom (and to a lesser extent of NO_3 radical) reaction rate constants are significantly better than the corresponding correlation between O_3 and OH radical reaction rate constants is expected due to the different reaction pathways occurring.[506] Thus $O(^3P)$ atom, NO_3 radicals, and OH radicals react with the >C=C< double bonds to form a radical (or in the case of $O(^3P)$ atoms, a biradical) species, e.g.

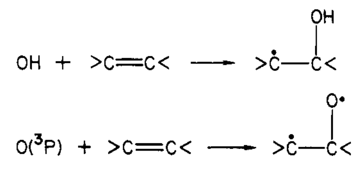

$$OH + {>}C{=}C{<} \longrightarrow {>}\dot{C}{-}\overset{OH}{C}{<}$$

$$O(^3P) + {>}C{=}C{<} \longrightarrow {>}\dot{C}{-}\overset{O\cdot}{C}{<}$$

while O_3 adds across the unsaturated >C=C< (or –C≡C–) bond to form a nonradical ozonide

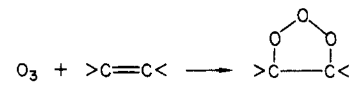

The O_3 reactions are hence not totally analogous to either the $O(^3P)$ atom or OH radical reactions.[506]

While there is an excellent correlation between the $O(^3P)$ atom and OH radical reaction rate constants for the acyclic and cyclic alkenes and dialkenes, certain other classes of organics with unsaturated >C=C< bonds, and for organics where the reactions proceed via

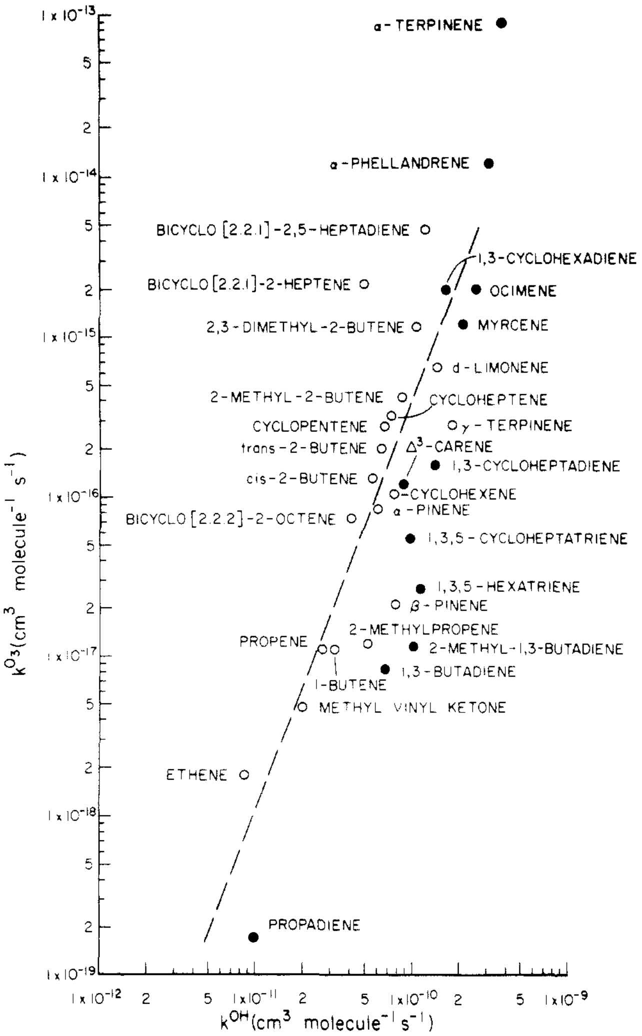

Figure 63. Linear free energy plot of log k^{O_3} against log k^{OH} at room temperature for a series of acyclic and cyclic alkenes, dialkenes, and trialkenes and methyl vinyl ether [the OH radical rate constants are from this work; the O_3 reaction rate constants are from Atkinson and Carter[506] and Bahta et al.[507]]. The line drawn is merely to indicate the trend of the data for the non-conjugated alkenes.

H atom abstraction pathways,[508] it should be noted that such correlations should in general only be used for use within homologous series. Thus Atkinson[227] has shown that $O(^3P)$ atom and OH radical correlations are significantly different for the alkenes and the aromatic hydrocarbons. Furthermore, in the use of these correlations, care must be exercised to make sure that the reaction mechanisms are the same (i.e., abstraction or addition) for both reactant species. Clearly, this may not always be the case. Thus, for example, it appears that the reactions of OH radicals and $O(^3P)$ atoms with the α,β-unsaturated aldehydes proceed via both overall H atom abstraction from the –CHO group and addition to the >C=C< bond, but with these reaction pathways being of significantly differing importance for these two reactants.[227,383,385]

2. Further Correlations Involving OH Radical Rate Constants

In order to carry out the above correlations, a knowledge of the corresponding $O(^3P)$ atom, NO_3 radical, and/or O_3 reaction rate constants is necessary for a given homologous series of organic reactions, and hence such correlations cannot be considered as a priori predictive techniques. However, a number of other correlations between OH radical reaction rate constants and physical or chemical properties of the organic reactants have been investigated.

Thus, for example, OH radical addition reaction rate constants have been observed to correlate well with the ionization potential for unsaturated[508,510,511] and saturated[511] organics, including polycyclic aromatic hydrocarbons.[154] Furthermore, for aromatic compounds the OH radical rate constants for addition to the ring correlate well with the Hammett electrophilic substituent constants, σ^+.[156,466] Clearly, as discussed in detail in these references,[154,156,466,508,510,511] these predictive techniques are of great utility in the a priori prediction of OH radical addition rate constants. In particular, the correlation between the room-temperature rate constants for the addition of OH radicals to aromatic compounds and the electrophilic substituent constants of Brown and Okamoto[512] is used below in the development of an a priori predictive scheme for OH radical rate constants with organic compounds.

For OH radical reactions which proceed via H atom abstraction, the most used correlation to date has been that between the OH radical rate constant and the C–H bond dissociation energy[1,21,138,191,221,225,227,270,508,513,514] or the (sometimes[257]) related quantity, the C–H bond stretching frequencies γ_{C-H}.[257,270] The first application of this essentially a priori predictive technique was that of Greiner,[21] who derived the rate constants for the reactions of the OH radical with a series of alkanes based upon the numbers of primary, secondary, and tertiary C–H bonds. This approach assumed that the C–H bond dissociation energies are essentially identical for all primary, secondary, and tertiary C–H bonds, respectively, and that

$$k_{\text{total}} = N_{\text{prim}}k_{\text{prim}} + N_{\text{sec}}k_{\text{sec}} + N_{\text{tert}}k_{\text{tert}}$$

where N_{prim}, N_{sec}, and N_{tert} are the numbers of primary, secondary, and tertiary C–H bonds, respectively, and k_{prim}, k_{sec}, and k_{tert} are the corresponding rate constants for the reaction of OH radicals with these C–H bonds. For the alkanes, the original equation due to Greiner[21] was slightly modified by Darnall et al.[1,138] to take into account more recent (through late 1978) kinetic data. This approach, though of great utility to the acyclic alkanes and the non-strained cycloalkanes (e.g., cyclohexane), is now known to be somewhat too simplistic in its assumption that all primary, secondary, and tertiary C–H bonds have correspondingly identical bond dissociation energies, even within the alkanes.

In more recent such a priori approaches to estimating (or rationalizing) H atom abstraction rate constants by OH radicals, Atkinson,[227] Heicklen,[513] Cohen,[225] Atkinson et al.,[29,155,207,214,224,349] Martin and Paraskevopoulos,[270] and Jolly et al.[221] have extended this earlier method[1,21,138] to take into account the dependence of differing C–H bond dissociation energies on the particular C–H bonds from which H atom abstraction occurs. In certain of these studies, use has been made of literature C–H bond dissociation energies,[221,225,227,270,513] while in the extensive studies of Atkinson et al. concerning the alkanes,[207,214,224] ketones,[349] and alkyl nitrates,[29,155] $-CH_3$, $-CH_2-$, and >CH– group rate constants have been derived from the experimental kinetic data.

It has been shown (see, for example, Atkinson,[227] Heicklen,[513] and Jolly et al.[221]) that the H abstraction rate constant per C–H bond by OH radicals for a wide variety of organics correlates extremely well with the C–H bond dissociation energies. While similar correlations using the C–H bond stretching frequencies have been shown to apply,[257,270] this approach is of less utility than that employing the corresponding C–H bond dissociation energies because of the limited number of C–H bond stretching frequencies available,[221] and, in general, the complexity of this approach for any but the simpler organics.[270]

While several of the above approaches have used literature C–H bond dissociation energies in their analyses,[221,225,227,270] Heicklen[513] has used the available literature kinetic data to develop the following expression allowing the C–H bond dissociation energies, and hence the overall H atom abstraction rate constants, to be estimated

$$k_{\text{total}} = \left(\frac{8\pi\kappa T}{\mu}\right)^{1/2} \sigma_R^2 \sum_i \gamma_i \exp\left\{\frac{-a[D_i - D_0(T)]}{RT}\right\}$$

where μ is the reduced mass, κ is Boltzmann's constant, σ_R is the reaction radius for reaction of an OH radical with a C–H bond ($\sim 1.5 \times 10^{-8}$ cm[513]), γ_i the number of equivalent C–H bonds of each type, D_i is the C–H bond dissociation energy at 298 K for each type of C–H bond, $a = 0.323$, and D_0 is given by

$$D_0^{-1}\ (\text{kcal mol}^{-1}) = 1.062 \times 10^{-2} + 3.52 \times 10^{-6} T\ (\text{K})$$

This approach,[513] which is one of the most general presented to date,[513,514] appears to be able to yield OH radical reaction rate constants proceeding via H atom abstraction which are reliable to within ± a factor of ~3 for the alkanes and oxygenates, but of significant less accuracy (approximately an order of magnitude) for the haloalkanes, aromatic hydrocarbons, and alkenes.

In this context, it should be noted that this general method of relating the H atom abstraction rate constant to the C–H bond dissociation energy greatly overestimates the contribution of H atom abstraction to the overall OH radical reaction rate constants for the alkenes and the aromatic hydrocarbons,[221] unless rather drastic and arbitrary correction factors are included.[513]

The more recent, and to date more restricted, approach of Atkinson et al.[29,155,207,214,224,349] has been aimed at deriving, from the experimentally observed overall rate constants, the group rate constants for H atom abstraction appropriate to the alkanes,[207,214,224] alkyl nitrates,[29,155] and ketones.[349] While to date this technique has been restricted in its application, it yields more accurate predictions for a given homologous series than does the more general a priori predictive methods exemplified by that of Heicklen.[513]

Güsten et al.[515] have proposed another predictive technique based upon the observed correlation between gas-phase and aqueous-phase OH radical rate constants, with an estimated overall uncertainty of ± a factor of ~5.

Kaufman and co-workers[186,516] and Cohen[225] have derived, from transition-state theory[186,225,516] (including tunneling effects calculated from the bond energy–bond order (BEBO) model[186,516]), Arrhenius preexponential factors for a series of alkanes and haloalkanes. Cohen[225] has combined these calculated Arrhenius preexponential factors with the experimental room-temperature rate constants to extrapolate the existing rate constants for the reactions of the OH radical with a series of alkanes to high (≥2000 K) temperatures. Again, while this technique[225] clearly has great utility, it has to reply on either experimental or a priori predicted rate constants at one temperature in order to "calibrate" the reaction rate constants.

Thus in these recent investigations involving the development of predictive techniques,[225,513,514] reliance has been placed upon the experimental determination or the a priori prediction of H atom abstraction rate constants by OH radicals. In the following sections, the available a priori predictive techniques for the estimation of OH radical reaction rate constants are discussed by the class of organic compound, and an up-to-date and extended predictive technique is presented.

B. Estimation of OH Radical Rate Constants

In the following sections, the available a priori techniques advanced for the prediction of OH radical reaction rate constants with the various classes or organic compounds are discussed. At the present time these techniques have been applied to only a limited number of classes of organic compounds, and their extension to a wider variety of organic compounds is explored in the sections below.

1. H-Atom Abstraction from Alkanes, Carbonyls, Alkyl Nitrates, and Other Saturated Organics

A relatively wide kinetic data base is available for the reaction of OH radicals with alkanes (Table I), haloalkanes (Table V), carbonyls (Table XI), alkyl nitrates (Table XIII), and other saturated organics. The following discussion of a priori predictive techniques is analogous to that developed by Atkinson et al.[29,155,207,214,224,349] and is based upon the estimation of CH_3–, –CH_2–, and –CH< group rate constants. This approach, which is analogous to the group additivity thermochemical technique of Benson,[226] is complementary to the OH radical estimation technique of Heicklen[513] based upon measured or estimated C–H bond dissociation energies. However, the technique described by Heicklen[513] only considers the effects of substituent groups or atoms on the α-carbon, whereas the methods of Hendry and Kenley[514] and of Atkinson et al.[349] takes into account, at least in certain cases, the effects of β-substituents, although at the expense of the need for a much larger data base.

This a priori estimation technique is based upon the premise that the –CH_3, –CH_2–, and >CH– group rate constants depend on the identity of the α- and β-substituents. In the simplest case, for example in the n-alkane series, the room-temperature –CH_2– group rate constants are dependent on the neighboring groups, increasing from a –CH_2– group bonded to two –CH_3 groups through a –CH_2– group bonded to one –CH_3 and one –CH_2– group to a –CH_2– group bonded to two –CH_2– groups.[207]

In the most general symbolism, these group rate constants are given by, at room temperature

$$k(\text{CH}_3\text{—X}) = k^0_{\text{prim}} F(\text{X})$$

$$k(\text{Y—CH}_2\text{—X}) = k^0_{\text{sec}} F(\text{X}) F(\text{Y})$$

$$k(\text{X—CH(Z)—Y}) = k^0_{\text{tert}} F(\text{X}) F(\text{Y}) F(\text{Z})$$

TABLE XVIII. Group Rate Constants, k^0, and Substituent Factors, F(X), at 298 K Derived from the Available Kinetic Data (See Text)

group rate constants, k^0	$10^{12}k$, cm^3 molecule^{-1} s^{-1}
k^0_{primary}	0.144
$k^0_{\text{secondary}}$	0.838
k^0_{tertiary}	1.83
$k^0_{\text{-OH}}$	0.13[a]
substituent group, X	factor F(X)
$-CH_3$	1.00[b]
$-CH_2-$ $>CH-$ $>C<$	1.29[c]
$-F$	0.099
$-Cl$	0.38
$-Br$	~0.30[d]
$-CH_2Cl$ $-CHCl_2$ $-CH_2Br$	0.57[e]
$-CCl_3$	~0.083[f]
$-CH_2F$	~0.85[g]
$-CHF_2$	~0.10[h]
$-CF_2Cl$	~0.025[i]
$-CF_3$	0.075
$=O$	8.8
$-CHO$ $-C(O)-$	0.76[j]
$-CH_2C(O)-$	4.4
$>CHC(O)-$ $>CC(O)-$	4.4[k]
$-C_6H_5$	~1.0[l]
$-OH$	3.6
$-O-$	8.3
$-C(O)OR$	~0.0
$-OC(O)R$	1.3
$-CH_2ONO_2$ $>CHONO_2$ $>CONO_2$	0.34[m]
$-ONO_2$	0.050
$>C{=}C<$ $-C{\equiv}C-$	$\lesssim$1[n]
$-CN$	0.14[o]
$-CH_2CN$	0.5[o]
three-membered ring	0.017
four-membered ring	0.22
five-membered ring	0.80
six-membered ring	1.00
seven-membered ring	~1.0

[a] Derived from the product analysis data for CH_3OH.[87,355,356] [b] By definition (see text). [c] A non-linear least squares fit, with $F(-CH_2-) \neq F(>CH-) \neq F(>C<)$ yielded similar values of these group factors, with no trend along the group. The factor given arises from assuming that $F(-CH_2-) = F(>CH-) = F(>C<)$. [d] Derived from the recommended rate constants for CH_3Br and CH_2BrCH_2Br. [e] Because of lack of data, $F(-CH_2Cl)$, $F(-CHCl_2)$, and $F(-CH_2Br)$ are assumed to be equal. [f] Derived from the recommended rate constant for CH_3CCl_3. [g] Derived from the available rate constants for CH_3CH_2F and CH_2FCH_2F. [h] Derived from the available rate constants for CH_3CHF_2 and CH_2FCHF_2. [i] Derived from the recommended rate constant for CH_3CF_2Cl. [j] $F(-CHO)$ assumed to be identical with $F(-C(=O)-)$, which is derived from the product data of Cox et al.[145] [k] Assumed equal due to paucity of data. [l] Approximate value to fit the rate constant for benzaldehyde and the abstraction rate constants derived from the data in Table XV. [m] Because of lack of wide data base, assumed equal. [n] Based upon observation of negligible H atom abstraction from allylic C–H bonds (see text). [o] Derived from the recommendation for acetonitrile (CH_3CN) and the reported rate constant for CH_3CH_2CN.

where k^0_{prim}, k^0_{sec}, and k^0_{tert} are the rate constants per $-CH_3$, $-CH_2-$, and $>CH-$ group for a given "standard" substituent, X, Y, and Z are the substituent groups, and F(X), F(Y), and F(Z) are the corresponding group factors. While obviously the values of k^0_{prim}, k^0_{sec}, and k^0_{tert} can be adjusted for any given substituent group X (= Y = Z), the most appropriate standard substituents are H– or CH_3– groups. For practical use, X ≡ $-CH_3$ is clearly the most useful, leading to $F(-CH_3) = 1.00$ by definition.

Using the recommended rate constants at 298 K together with the other available room-temperature rate constants given in the relevant data tabulations, nonlinear least-squares analyses of these kinetic data have been carried out, minimizing the sum of the percentage errors, to derive values of F(X) for a variety of substituent groups. Because the available kinetic data generally involve only single types of substituent groups, with few data available for difunctional and polyfunctional organics, the kinetic data have been analyzed sequentially for the various classes of organic compounds, i.e., alkanes, haloalkanes, aldehydes, carbonyls, alcohols, ethers, esters, and nitrates, etc., separately. The more extensive data set for the alkanes has been first analyzed to obtain k^0_{prim}, k^0_{sec}, and k^0_{tert} and $F(-CH_2-)$, $F(>CH-)$, and $F(>C<)$, and these quantities have then been used to derive values of F(X) for other substituent groups. Values of F(X), where, for example, X = $-CH_2-$, $>CH-$, $>C<$, $-F$, $-Cl$, $-Br$, $-CH_2F$, $-CH_2Cl$, $-CH_2Br$, $-CHF_2$, $-CHCl_2$, $-CF_3$, $-CF_2Cl$, $-CCl_3$, $=O$, $-CHO$, $-C_6H_5$, $-C(O)-$, $-CH_2C(O)-$, $-O-$, $-OC(O)-$, $-C(O)O-$, $-OH$, $-ONO_2$, and $-CN$ are derived, as discussed below.

a. Alkanes. In a manner analogous to the recent study of Atkinson et al.,[214] the recommended room-temperature rate constants for the acyclic alkanes and for cyclohexane (the sole essentially strain-free cycloalkane[226] for which a recommendation has been made) have been used to carry out a nonlinear least-squares fit to the general equation

$$k_{\text{total}} = \sum[k^0_{\text{prim}}F(\text{X})] + \sum[k^0_{\text{sec}}F(\text{X})F(\text{Y})] + \sum[k^0_{\text{tert}}F(\text{X})F(\text{Y})F(\text{Z})]$$

As an example, the expression for 2,2,4-trimethylpentane is

$$k_{\text{total}} = 3k^0_{\text{prim}}F(>C<) + 2k^0_{\text{prim}}F(>CH-) + k^0_{\text{sec}}F(>C<)F(>CH-) + k^0_{\text{tert}}\{F(-CH_3)\}^2\,F(-CH_2-)$$

with $F(-CH_3) = 1.00$, by definition (see above).

The values of k^0_{prim}, k^0_{sec}, k^0_{tert}, $F(-CH_2-)$, $F(>CH-)$, and $F(>C<)$ obtained at ~298 K are given in Table XVIII, and these quantities are used in an extension of this predictive approach to other classes of organic compounds. The experimental and predicted room-temperature rate constants for the acyclic alkanes and for cyclohexane (which has essentially zero ring strain energy[226]) are compared in Table XIX. The agreement between the experimental and predicted rate constants is seen to within ±50%.

b. Haloalkanes. Analogous to the situation for the alkanes discussed above, the values of k^0_{prim}, k^0_{sec}, k^0_{tert}, $F(-CH_2-)$, $F(>CH-)$, and $F(>C<)$ derived above and the recommended room-temperature rate constants for the haloalkanes have been used to obtain from a nonlinear least-squares analysis the factors F(X) given in Table XVIII. The experimental and predicted room-temperature rate constants are compared in Table XIX, and again the agreement is seen to be good, typically to within ± a factor of 2, except for CHF_3 and CH_3CF_3, for which the discrepancies are factors of ~11 and ~6, respectively.

TABLE XIX. Comparison of Experimental and Calculated Room-Temperature Rate Constants for the Reactions of OH Radicals with a Series of Organic Compounds Which Proceed via Overall H Atom Abstraction (Underlined Rate Constants are Those Used in Derivation of the Group Rate Constants and Factors Given in Table XVIII)

	$10^{12}k_{\text{total}}$, cm^3 molecule^{-1} s^{-1}	
organic	calcd	exptl
Alkanes		
ethane	0.288	$\underline{0.274}$
propane	1.21	$\underline{1.18}$
n-butane	2.53	$\underline{2.53}$
2-methylpropane	2.39	$\underline{2.37}$
n-pentane	3.93	$\underline{4.04}$
2-methylbutane	4.00	$\underline{3.9}$
2,2-dimethylpropane	0.743	$\underline{0.852}$
n-hexane	5.32	$\underline{5.58}$
2-methylpentane	5.39	$\underline{5.5}$
3-methylpentane	5.76	$\underline{5.6}$
2,2-dimethylbutane	1.82	2.6
2,3-dimethylbutane	5.46	$\underline{6.2}$
n-heptane	6.72	$\underline{7.2}$
2,4-dimethylpentane	6.86	5.1
2,2,3-trimethylbutane	3.29	$\underline{4.1}$
n-octane	8.11	$\underline{8.72}$
2,2,4-trimethylpentane	4.68	$\underline{3.66}$
2,2,3,3-tetramethylbutane	1.11	$\underline{1.06}$
n-nonane	9.51	$\underline{10.0}$
n-decane	10.9	$\underline{11.2}$
n-undecane	12.3	13.3
n-dodecane	13.7	13.9
n-tridecane	15.1	15.5
cyclopropane	0.07	0.07
cyclobutane	1.2	1.2
cyclopentane	5.58	5.2
cyclohexane	8.37	$\underline{7.38}$
1-methylcyclohexane	10.2	10.3
cycloheptane	9.8	13.1
bicyclo[2.2.1]heptane	9.5	5.42
bicyclo[2.2.2]octane	16.2	14.5
bicyclo[3.3.0]octane	10.4	10.9
cis-bicyclo[4.3.0]nonane	14.1	17.0
trans-bicyclo[4.3.0]nonane	14.1	17.4
cis-bicyclo[4.4.0]decane	19.0	19.6
trans-bicyclo[4.4.0]decane	19.0	20.2
tricyclo[5.2.1.0^{2,6}]decane	12.3	11.2
tricyclo[3.3.1.1^{3,7}]decane	22.1	22.7
Haloalkanes		
CH_3F	0.014	$\underline{0.0168}$
CH_3Cl	0.055	$\underline{0.0436}$
CH_3Br	0.043	$\underline{0.0393}$
CH_2F_2	0.0082	$\underline{0.0109}$
CH_2FCl	0.032	$\underline{0.0441}$
CH_2Cl_2	0.12	$\underline{0.142}$
CHF_3	0.0018	0.00020
CHF_2Cl	0.0068	$\underline{0.00468}$
$CHFCl_2$	0.026	$\underline{0.0303}$
$CHCl_3$	0.100	$\underline{0.103}$
CH_3CH_2F	0.21[a]	0.23
CH_3CH_2Cl	0.40	$\underline{0.40}$
CH_3CHF_2	0.032	$\underline{0.034}$
CH_2FCH_2F	0.14	0.11
CH_3CHCl_2	0.35	0.26
CH_2ClCH_2Cl	0.36	0.22
CH_2BrCH_2Br	0.29	$\underline{0.25}$
CH_3CF_3	0.011	~0.002
CH_2FCHF_2	0.024	0.018
CH_3CF_2Cl	0.0036	$\underline{0.00358}$
CH_3CCl_3	0.012	$\underline{0.0119}$
$CH_2ClCHCl_2$	0.33	$\underline{0.328}$
CH_2FCF_3	0.0062	$\underline{0.00854}$
CH_2ClCF_3	0.024	$\underline{0.0162}$
CH_2ClCF_2Cl	0.0080	≤ 0.019
CHF_2CF_3	0.0013	0.0025
$CHFClCF_3$	0.0052	0.0102
$CHCl_2CF_3$	0.020	0.0335
Aldehydes		
formaldehyde	7.4	$\underline{9.0}$
acetaldehyde	16.2	$\underline{16.2}$
1-propanal	22.0	$\underline{19.6}$
1-butanal	25.5	23
2-methyl-1-propanal	23.4	27
1-pentanal	27.6	27
3-methyl-1-butanal	30.0	27
2,2-dimethyl-1-propanal	21.3	27
benzaldehyde	16.1	$\underline{13.0}$
Ketones		
acetone	0.22	$\underline{0.23}$
2-butanone	1.38	$\underline{1.0}$
2-pentanone	4.8	$\underline{4.64}$
3-pentanone	2.5	$\underline{1.82}$
2-hexanone	7.0	$\underline{8.97}$
3-hexanone	6.0	$\underline{6.81}$
2,4-dimethyl-3-pentanone	5.3	$\underline{5.31}$
4-methyl-2-pentanone	9.4	$\underline{14.1}$
2,6-dimethyl-4-heptanone	18.5	$\underline{27.1}$
α-Dicarbonyls		
glyoxal	24.5	11.2
methylglyoxal	12.3	16.9
biacetyl	0.22	0.24
Alcohols		
methanol	0.65	$\underline{0.9}$
ethanol	3.3	$\underline{2.9}$
1-propanol	5.3	$\underline{5.3}$
2-propanol	7.1	$\underline{6.2}$
1-butanol	6.7	7.3
2-methyl-2-propanol	0.69	$\underline{1.09}$
Glycols		
1,2-ethanediol	8.0	7.7
1,2-propanediol	12.8	12
dihydroxyethylether	26.0	30
2-chloroethanol	2.3	1.4
Ethers		
dimethyl ether	2.4	$\underline{2.98}$
diethyl ether	14.3	$\underline{13.4}$
di-*n*-propyl ether	20.5	$\underline{16.8}$
methyl *tert*-butyl ether	1.8	$\underline{2.64}$
tetrahydrofuran	16.6	15
ethene oxide	0.31	0.07
propene oxide	0.67	0.52
1,2-butene oxide	1.8	2.1
1-chloro-2,3-epoxypropane	0.99	0.44
Esters		
methyl acetate	0.19	$\underline{0.17}$
ethyl acetate	1.3	$\underline{1.82}$
n-propyl acetate	2.7	$\underline{4.2}$
sec-butyl acetate	4.1	$\underline{5.4}$
methyl propionate	0.37	$\underline{0.27}$
ethyl propionate	1.5	$\underline{1.66}$
Nitrates		
2-propyl nitrate	0.19	$\underline{0.18}$
1-butyl nitrate	1.7	$\underline{1.39}$
2-butyl nitrate	0.64	$\underline{0.67}$
2-pentyl nitrate	1.8	$\underline{1.83}$
3-pentyl nitrate	1.1	$\underline{1.10}$
2-methyl-3-butyl nitrate	1.2	$\underline{1.72}$
2,2-dimethyl-1-propyl nitrate	0.61	$\underline{0.85}$
2-hexyl nitrate	3.2	$\underline{3.13}$
3-hexyl nitrate	2.3	$\underline{2.66}$
cyclohexyl nitrate	5.1	$\underline{3.29}$
2-methyl-2-pentyl nitrate	1.7	$\underline{1.71}$
3-methyl-2-pentyl nitrate	2.4	$\underline{3.01}$
3-heptyl nitrate	3.7	$\underline{3.64}$
3-octyl nitrate	5.0	$\underline{3.82}$
Nitriles		
CH_3CN	0.020	$\underline{0.021}$
CH_3CH_2CN	0.19	$\underline{0.19}$

[a] While this overall rate constant agrees well with that experimentally observed,[257] the calculated distribution of H atom abstraction from the α- and β-carbon atoms do not. Thus only ~42% H atom abstraction from the α-carbon is calculated, compared with the experimental observation of 85 ± 3%.[517]

c. Oxygen- and Nitrogen-Containing Organics. The recommended room-temperature rate constants for formaldehyde, acetaldehyde, and 1-propanal have been used to derive a value of $F(=\mathrm{O})$. Since the earlier kinetic study of Atkinson et al.[349] concerning the ketones showed that the $-\mathrm{C(O)}-$ group affects the β-substituents as well as the α-substituents, the factors $F(-\mathrm{C(O)}-)$, $F(-\mathrm{CH_2C(O)}-)$, $F(>\mathrm{CHC(O)}-)$, and $\mathrm{F}(\gg\mathrm{CC(O)}-)$ have been utilized in the present estimation technique. Due to the limited data base available, it has been assumed that $F(-\mathrm{CH_2C(O)}-) = F(>\mathrm{CHC(O)}-) = F(\gg\mathrm{CC(O)}-)$ in the derivation of these factors. The recommendations for 2-butanone, 4-methyl-2-pentanone, and 2,6-dimethyl-4-heptanone and the rate constants of Atkinson et al.[349] for a series of ketones have been used to derive these factors. Similarly, the rate constants for the ethers, esters, alcohols, nitrates, and nitriles have been used to derive the factors $F(-\mathrm{O}-)$, $F(-\mathrm{OC(O)}-)$, $F(-\mathrm{C(O)O}-)$, $F(-\mathrm{OH})$, $F(-\mathrm{ONO_2})$, $F(-\mathrm{CH_2ONO_2})$, $F(>\mathrm{CHONO_2})$, $F(\gg\mathrm{CONO_2})$ and $F(-\mathrm{CN})$ given in Table XVIII. The calculated rate constants at ~298 K using these factors for a series of organics are compared with the experimental values in Table XIX, and good agreement, typically to within a factor of ~2, is seen.

d. Alkenes, Alkynes, and Aromatics. The observations that at room-temperature H atom abstraction from propene and 1-butene are negligible (<2%[173] and <10%,[176,317] respectively) allow upper limit values of $F(>\mathrm{C{=}C}<)$ to be derived. Since H atom abstraction from C–H bonds in the $>\mathrm{CHC{\equiv}C}-$ structural unit is expected to be less important than from C–H bonds in $>\mathrm{CHC{=}C}<$, we use this latter value for abstraction from the $>\mathrm{CHC{\equiv}C}-$ unit also. Similarly, for the aromatic hydrocarbons, the rate constants for H atom abstraction from the substituent $-\mathrm{CH_3}$ groups (Table XV) allow the factor $F(-\mathrm{C_6H_5})$ to be derived.

e. Effects of Ring Strain. Atkinson et al.[224] and Jolly et al.[221] have shown that in the cycloalkanes the presence of a ring strain energy of ≥5 kcal $\mathrm{mol^{-1}}$[224] leads to a decrease of the experimental rate constants, compared to those predicted in the absence of ring strain. This is primarily due to the fact that the C–H bond dissociation energies in these strained cycloalkanes are significantly higher than those in the acyclic alkanes,[319] and hence a knowledge of the precise bond dissociation energies in these cycloalkanes again allows the H atom abstraction rate constants to be reliably estimated.[221] However, such data are available for only a small number of cycloalkanes, and for a priori predictive purposes a more parametric approach is necessary.

Atkinson et al.[224] have shown that a total ring strain energy in excess of ~5 kcal $\mathrm{mol^{-1}}$ leads to a decrease in the observed room-temperature rate constants for a series of bi- and tricycloalkanes, over those predicted in the absence of ring strain, with $k_{\mathrm{obsd}}/k_{\mathrm{calcd}}$ decreasing approximately exponentially with increasing ring strain energies. Since for polycyclic systems the overall ring strain energies are approximately the sum of the ring strain energies per ring,[226] a correction factor per ring can be derived. For polycyclic systems these correction factors, F_{ring}, are then multiplicative. For example, for bicyclo[4.3.0]nonane the rate constant is given by

$$k_{\mathrm{total}} = \{3k^0_{\mathrm{sec}}[F(-\mathrm{CH_2}-)]^2 + 4k^0_{\mathrm{sec}}F(-\mathrm{CH_2}-)F(>\mathrm{CH}-) + 2k^0_{\mathrm{tert}}[F(-\mathrm{CH_2}-)]^2\,F(>\mathrm{CH}-)\}F_5F_6$$

where F_6 and F_5 are the correcton factors for six-membered and five-membered rings, respectively. From an analysis of the room-temperature rate constants for the $\mathrm{C_3}$–$\mathrm{C_7}$ cycloalkanes, and the bi- and tricycloalkanes studied by Atkinson et al.,[224] the ring correction factors given in Table XVIII are derived. These ring strain correction factors then allow the estimation of H atom abstraction rate constants for strained ring systems. Furthermore, since the ring strain energies for ring systems containing O, N, and S heteroatoms are similar to the corresponding cycloalkane rings,[226] they can be used for the estimation of H atom abstraction rate constants for heteroatom-containing rings, such as the oxides and cycloethers.

However, the strained $\mathrm{C_3}$–$\mathrm{C_7}$ alkanes and the bi- and tricycloalkanes from which these ring correction factors were obtained contain no substituent side chains. Thus it is expected that these correction factors F_3 through F_7 are applicable only to the $-\mathrm{CH_2}-$ and $>\mathrm{CH}-$ groups involved in the ring(s), with the group rate constants for nonring $-\mathrm{CH_3}$, $-\mathrm{CH_2}-$, and $>\mathrm{CH}-$ groups being calculated without the ring correction. For example, for ethylcyclopentane

$$k_{\mathrm{total}} = \{2k^0_{\mathrm{sec}}[F(-\mathrm{CH_2}-)]^2 + 2k^0_{\mathrm{sec}}F(-\mathrm{CH_2}-)F(>\mathrm{CH}-) + k^0_{\mathrm{tert}}[F(-\mathrm{CH_2}-)]^3\}F_5 + k^0_{\mathrm{sec}}F(>\mathrm{CH}-) + k^0_{\mathrm{prim}}F(-\mathrm{CH_2}-)$$

Clearly, for organics involving six-membered rings (for example, methylcyclohexane) this is immaterial since $F_6 = 1.00$.

A comparison of the experimentally observed and calculated room-temperature rate constants is given in Table XIX for the OH radical reactions which proceed via H atom abstraction. Of the 138 organics listed, only for five do the experimental and calculated rate constants disagree by more than a factor of 2.

There are only a limited number or organics (all alkanes) for which OD radical rate constants are available and which proceed via H atom abstraction. From these data, assuming that deuterium isotope substitution leads to a constant decrease in the abstraction rate constant per $-\mathrm{CD_3}$, $-\mathrm{CD_2}-$, and $>\mathrm{CD}-$ groups, relative to the corresponding $-\mathrm{CH_3}$, $-\mathrm{CH_2}$, and $>\mathrm{CH}-$ groups, this factor is 0.28 at room temperature. Thus (in units of 10^{-12} $\mathrm{cm^3}$ $\mathrm{molecule^{-1}}$ $\mathrm{s^{-1}}$), at room temperature $k^0_{\mathrm{primary}}(-\mathrm{CD_3}) = 0.04$; $k^0_{\mathrm{secondary}}(-\mathrm{CD_2}-) = 0.23$, and $k^0_{\mathrm{tertiary}}(>\mathrm{CH}-) = 0.51$, with $F(-\mathrm{CD_2}-) = F(>\mathrm{CD}-) = 1.29$ being set equal to the corresponding factors for $F(-\mathrm{CH_2}-) = F(>\mathrm{CH}-)$. These group rate constants fit the room-temperature rate constants of Paraskevopoulos and Nip[211] and Tully et al.[203,208,215] for n-$\mathrm{C_4D_{10}}$,[211] $\mathrm{(CD_3)_3CH}$,[208] $\mathrm{(CH_3)_3CD}$,[208] $\mathrm{(CD_3)_3CD}$,[208] and $\mathrm{(CD_3)_4C}$[203,215] to within ~30%.

2. OH Radical Addition to Unsaturated $>\mathrm{C{=}C}<$ and $-\mathrm{C{\equiv}C}-$ Bonds

a. Alkenes and Alkynes. The a priori prediction of room-temperature OH radical reaction rate constants involving OH radical addition to alkenes has been discussed recently by Ohta[142,152] and Atkinson and coworkers.[151,153] The approach used by these authors is analogous to that presented earlier by Hendry and Kenley[514] and is based upon the number of unconjugated double bonds or conjugated double-bond systems and the degree, identity and configuration of substitution around these double bonds.[151] As an example, 2-methyl-1,4-pentadiene ($CH_2{=}C(CH_3)CH_2CH{=}CH_2$) contains a 1,1-dialkyl-substituted double bond ($CH_2{=}C<$) plus a monoalkyl-substituted double bond ($CH_2{=}CH-$) and the overall rate constant is given by the sum of the rate constants for 2-methylpropene (for $CH_2{=}C<$) and propene (for $CH_2{=}CH-$).[151]

For the conjugated dialkenes the approaches used by Ohta[142,152] and Atkinson et al.[151] differ somewhat but yield similar results for the data set presently available. Atkinson et al.[151] consider the $>C{=}C{-}C{=}C<$ moiety as a single unit with the rate constant depending solely on the number of alkyl substituents around this structural unit. Thus, for example, for 2-methyl-6-methylene-2,7-octadiene [$(CH_3)_2C{=}CHCH_2CH_2C({=}CH_2)CH{=}CH_2$] the overall OH radical addition rate constant is given by the sum of the rate constants for 2-methylpropene ($CH_2{=}C<$) and the $CH_2{=}CH{-}C{=}CH_2$ entity. Ohta[142,152] rather considers this conjugated $>C{=}C{-}C{=}C<$ unit as being comprised of the individual $>C{=}C-$ and $-C{=}C<$ monoalkene units, with the rate constants for the corresponding monoalkene units multiplied by a factor of 1.24.[142] Thus, for example, the rate constant for 2-methyl-1,3-butadiene [$CH_2{=}CHC(CH_3){=}CH_2$] is derived from that for the $CH_2{=}CH-$ unit (propene) plus that for $CH_2{=}C<$ (2-methylpropene), multiplied by 1.24.

Both approaches yield similar results (see Table XX) and both are equally applicable. Only when kinetic data become available for non-alkyl-substituted $>C{=}C{-}C{=}C<$ systems will it become evident which of these two approaches to the a priori prediction of addition rate constants for conjugated dialkene systems is superior.

The group rate constants, their derivations, and a comparison of predicted and experimental room-temperature rate constants for the acyclic and cyclic monoalkenes and conjugated dialkenes are given in Table XX. For the dialkenes and cyclodialkenes containing nonconjugated $>C{=}C<$ bonds and for other alkenes and cycloalkenes containing both $>C{=}C<$ and $>C{=}C{-}C{=}C<$ units, calculated and experimental data are given in Table XXI. These experimental data utilized include those given in Tables VI, VII, and VIII (the recommendations whenever possible, otherwise the rate constants determined by Ohta,[142,152] and Atkinson et al.[151,303,304] and Atkinson and Aschmann[153]), together with the rate constants derived from the NO_x photooxidation rates of Grimsrud et al.[308] at 301 ± 1 K. These latter data[308] must be viewed as semiquantitative only[292,304] since their use assumes that the OH radical concentrations were identical in the separate NO–organic–air irradiations and that O_3 reactions were negligible.

The agreement between the calculated and experimental room-temperature rate constants is seen to be generally excellent. Furthermore, for the alkenes containing $>C{=}C{-}C{=}C<$ structural units, the use of the techniques advanced by Ohta[142,152] and Atkinson et al.[151] yield very similar predicted rate constants. The use of either is recommended. For use at temperatures other than room temperature, a temperature dependence equivalent to an Arrhenius activation energy of −1.0 kcal mol^{-1} should be used.

Insufficient data exist for reliable a priori predictions for the 1,2-dialkenes and the alkynes, since only the group rate constants $CH_2{=}C{=}CH-$, $CH_2{=}C{=}C<$, and $HC{\equiv}C-$ can be derived from the rate constants presently available. These group rate constants are included in Table XX and are used for comparison with the experimental data in Table XX. While the conjugated trialkenes are not dealt with due to insufficient data, the general technique of Ohta[142] may be applicable to this class of alkenes.

b. Haloalkenes and Oxygen-Containing Organics with Unsaturated >C=C< Bonds. In order to predict the rate constants for the haloalkenes and for various classes of oxygenates containing $>C{=}C<$ double bonds, factors are employed to account for the bonding of halogen and oxygen atoms and of carbonyl groups to the $>C{=}C<$ double bond. The use of these factors is illustrated as follows: the rate constant for vinyl chloride ($CH_2{=}CHCl$) is that for $CH_2{=}CH-$ (i.e., propene) multiplied by the factor C(Cl); that for trichloroethene ($CHCl{=}CCl_2$) is that for $-CH{=}C<$ (i.e., 2-methyl-2-butene) × $[C(Cl)]^3$.

The factors derived from the fairly limited data set available [the haloalkenes, including those studied by Howard,[78] $CH_2{=}CHOCH_3$, $CH_2{=}CHCOCH_3$, $CH_2{=}CHCN$, *cis*- and *trans*-1,3-dichloropropene, $CH_2{=}C(CH_2Cl)_2$, and *cis*- and *trans*-$CH_3COCH{=}CHCOCH_3$ (the α,β-unsaturated aldehydes such as $CH_2{=}CHCHO$ cannot be used directly due to the concurrent reaction pathway involving H atom abstraction from the –CHO group)] are given in Table XX. A comparison of calculated and experimentally determined rate constants is given in Table XXI. It should be noted that since most of the available data have been utilized in deriving these factors, the observed reasonable agreement may be fortuitous. For the –CHO group an approximate factor has been estimated which yields OH radical addition (and hence by difference the H atom abstraction) rate constants for $CH_2{=}CHCHO$, $CH_3CH{=}CHCHO$, and $CH_2{=}C(CH_3)CHO$ consistent with the discussion above dealing with these α,β-unsaturated aldehydes.

3. OH Radical Addition to Aromatic Rings

On the basis of the literature data, the optimum approach to the a priori prediction of room-temperature rate constants for OH radical addition to the aromatic ring appears to be that of Zetzsch.[466] This a priori predictive technique utilizes the excellent correlation[156,466] between the OH radical rate constants for addition to the aromatic ring, k^{add}, and the sum of the electrophilic substituent constants, $\sum\sigma^+$, of Brown and Okamoto.[512] Thus Zetzsch[466] reported that for benzene, a series of substituted monocyclic aromatics (excluding benzaldehyde since H atom abstraction is the major reaction pathway for this aromatic) and biphenyl

$$\log k^{add}(\text{cm}^3\ \text{molecule}^{-1}\ \text{s}^{-1}) = -11.4 - 1.39\sum\sigma^+$$

In Table XXII the available room-temperature rate constants for the addition of OH radicals to benzene, substituted monocyclic aromatics, and biphenyl are listed (using the recommended values where possible). Benzaldehyde has been omitted from this list since H atom abstraction is the major reaction route for this compound and aniline, *p*-chloroaniline, and *n*-propylpentafluorobenzene were not used in the correlation, since significant, and presently unknown, amounts of the OH radical reactions with these substituted aromatics may proceed via H atom abstraction from the

TABLE XX. Comparison of Room-Temperature Recommended, Experimentally Observed and Calculated Rate Constants for the Addition of OH Radicals to Monoalkenes, Conjugated Dialkenes, and Alkynes with Varying Degrees and Configuration of Alkyl Substitution and Factors for Non-Alkyl Substituents

general structure	$10^{11}k$[recommended], cm^3 molecule^{-1} s^{-1}	alkene or alkyne	$10^{11}k$[obsd], cm^3 molecule^{-1} s^{-1}
$CH_2{=}CHR$	2.63[a]	propene	2.63
		1-butene	3.14
		1-pentene	3.14
		3-methyl-1-butene	3.18
		1-hexene	3.7
		3,3-dimethyl-1-butene	2.84
		1-heptene	4.0
$CH_2{=}CR_2$	5.14[b]	2-methylpropene	5.14
		2-methy-2-butene	6.07
		2-methyl-1-pentene	6.26
		β-pinene	7.82
cis-$RCH{=}CHR$	5.61[c]	*cis*-2-butene	5.61
		cis-2-pentene	6.51
		cyclopentene	6.70
		cyclohexene	6.74
		cycloheptene	7.41
		bicyclo[2.2.1]-2-heptene	4.91
		bicyclo[2.2.2]-2-octene	4.06
trans-$RCH{=}CHR$	6.37[d]	*trans*-2-butene	6.37
		trans-2-pentene	6.7
		trans-4-methyl-2-pentene	6.08
		trans-4,4-dimethyl-2-pentene	5.48
$RCH{=}CR_2$	8.69[e]	2-methyl-2-butene	8.69
		2-methyl-2-pentene	8.88
		α-pinene	5.32
		1-methylcyclohexene	9.5
		Δ^3-carene	8.70
		carvomethene	12.7[f]
$R_2C{=}CR_2$	11.0[g]	2,3-dimethyl-2-butene	11.0
		2,3-dimethyl-2-pentene	10.8
$H_2C{=}CHCH{=}CHR$		*cis*-1,3-pentadiene	10.1 (10.2)[i]
	10.5[h]	2-methyl-1,3-butadiene	10.1 (9.6)
$H_2C{=}CHCR{=}CH_2$		*trans*-1,3-hexadiene	11.3 (10.2)
$H_2C{=}CHCR{=}CHR$		*cis*- and *trans*-2,4-hexadiene	13.5 (14.9)
		2-methyl-1,3-pentadiene	13.7 (~13.8)
$H_2C{=}CRCH{=}CHR$		4-methyl-1,3-pentadiene	13.7 (14.0)
	13.5[h]	2,3-dimethyl-1,3-butadiene	12.2 (12.7)
$H_2C{=}CRCR{=}CH_2$		1,3-cyclohexadiene	16.3 (13.9)
		1,3-cycloheptadiene	13.9 (13.9)
$RHC{=}CHCH{=}CHR$		β-phellandrene	11.4[f] (13.3)
$H_2C{=}CHCR{=}CR_2$			(16.9)
$H_2C{=}CRCH{=}CR_2$			(17.1)
$RHC{=}CHCH{=}CR_2$	18[j]		(~18.2)
$H_2C{=}CRCR{=}CHR$			(17.1)
$RHC{=}CRCH{=}CHR$		α-phellandrene	31 (17.7)
$R_2C{=}CHCH{=}CR_2$		α-terpinene	36 (21.6)
		2,5-dimethyl-2,4-hexadiene	21.1
$RHC{=}CRCH{=}CR_2$	23[j]		(21.6)
$RHC{=}CRCR{=}CHR$			(21.6)
$H_2C{=}CRCR{=}CR_2$			(20.0)
$H_2C{=}C{=}CHR$	3.1[h]	1,2-butadiene	2.6
		1,2-pentadiene	3.56
$H_2C{=}C{=}CR_2$	5.7[h]	3-methyl-1,2-butadiene	5.71
$HC\equiv CR$	0.7[h]	propyne	0.61
		1-butyne	0.80

group	factor *C*	group	factor *C*
-F		-CN	0.15[m]
-Cl	0.25[k]	-CHO	~0.2[n]
-Br		$-COCH_3$	0.9[o]
$-CH_2Cl$	0.8[l]	$-OCH_3$	1.3[p]

[a] Derived from propene. [b] Derived from 2-methylpropene. [c] Derived from *cis*-2-butene. [d] Derived from *trans*-2-butene. [e] Derived from 2-methyl-2-butene. [f] Derived from the NO–air photooxidation data of Grimsrud et al.[308] (see text and ref 151 and 304). [g] Derived from 2,3-dimethyl-2-butene. [h] Derived from the dialkenes or alkynes shown. [i] Rate constants in parentheses are those calculated by the technique described by Ohta[142,152] (see text). [j] No experimental data available; derived by multiplying the rate constant for the two-substituent $>C{=}C{-}C{=}C<$ structure by a factor of 1.3 per alkyl substituent based upon the recommendations for the one and two alkyl-substituted $>C{=}C{-}C{=}C<$ entities. [k] Derived from the rate constants for $CH_2{=}CHF$, $CH_2{=}CHCl$, $CH_2{=}CHBr$, CH_2CF_2, $CHCl{=}CCl_2$, $CCl_2{=}CCl_2$ and $CFCl{=}CF_2$. [l] Derived from fitting experimental and calculated rate constants for *cis*- and *trans*-1,3-dichloropropene and 2-(chloromethyl)-3-chloro-1-propene. [m] Derived from the rate constant for $CH_2{=}CHCN$. [n] Derived from the rate constants for $CH_2{=}CHCHO$, $CH_3CH{=}CHCHO$, and $CH_2{=}C(CH_3)CHO$, consistent with the discussion in the text. [o] Derived from the rate constants for $CH_2{=}CHCOCH_3$ and *cis*- and *trans*-3-hexene-2,5-dione. [p] Derived from the rate constant for $CH_2{=}CHOCH_3$.

TABLE XXI. Comparison of Experimental and Calculated Room-Temperature Rate Constants for Alkenes Containing Multiple >C=C< or >C=CC=C< Structural Units and for Heteroatom-Containing Alkenes

alkene or substituted alkene	$10^{11}k$, cm^3 $molecule^{-1}$ s^{-1} calcd	obsd
1,4-pentadiene	5.26	5.33
trans-1,4-hexadiene	9.00	9.1
1,5-hexadiene	5.26	6.2
2-methyl-1,4-pentadiene	7.77	7.9
2-methyl-1,5-hexadiene	7.77	9.6
2,5-dimethyl-1,5-hexadiene	10.3	12.0
1,4-cyclohexadiene	11.2	9.9
bicyclo[2.2.1]-2,5-heptadiene	11.2	12.0
d-limonene	13.8	16.9
γ-terpinene	17.4	17.6
3,7-dimethyl-1,6-octadiene	11.3	18[a]
3-methylene-7-methyl-1,6-octadiene	19.2 (18.3)[b]	21.3
cis-3,7-dimethyl-1,3,6-octatriene	22.2 (22.7)[b]	25.0
terpinolene	19.7	66[a,c]
vinyl fluoride	0.66	0.556
vinyl chloride	0.66	0.660
vinyl bromide	0.66	0.681
1,1-difluoroethene	0.32	0.2–0.25
trichloroethene	0.14	0.24
tetrachloroethene	0.042	0.017
chlorotrifluoroethene	0.042	~0.7
cis-1,3-dichloropropene	1.1	0.75
trans-1,3-dichloropropene	1.3	1.26
2-(chloromethyl)-3-chloro-1-propene	3.3	4.0
methyl vinyl ketone	2.4	1.85
cis-3-hexene-2,5-dione	4.5	6.3
trans-3-hexene-2,5-dione	5.2	5.3
acrylonitrile (CH_2=CHCN)	0.39	~0.4
vinyl methyl ether	3.4	3.35

[a] Derived from the NO photooxidation study of Grimsrud et al.[308] (see text). [b] Calculated by using the technique of Ohta[142,152] (see text). [c] Probably high due to contribution from O_3 reaction.

TABLE XXII. Comparison of Experimentally Observed and Calculated Room-Temperature Rate Constants for the Addition of OH Radicals to Benzene, Biphenyl, and a Series of Substituted Monocyclic Aromatics

aromatic	$\sum\sigma^+$	$10^{12}k_{addition}$, cm^3 $molecule^{-1}$ s^{-1} obsd[a]	calcd
benzene	0	1.19	2.3
toluene	−0.311	5.7	5.9
o-xylene	−0.377	13.4	7.1
m-xylene	−0.622	23.5	15.0
p-xylene	−0.377	14.1	7.1
1,2,3-trimethylbenzene	−0.688	31.6	18.3
1,2,4-trimethylbenzene	−0.688	38.4	18.3
1,3,5-trimethylbenzene	−0.933	60.5	38.2
ethylbenzene	−0.295	7.5	5.6
n-propylbenzene	−0.295	5.7	5.6
isopropylbenzene	−0.280	6.6	5.3
phenol	−0.92	28.3	36.7
methoxybenzene	−0.778	15.7	23.9
o-cresol	−0.986	37	44.8
m-cresol	−1.231	54	93.9
p-cresol	−0.986	41	44.8
o-ethyltoluene	−0.375	12.0	7.1
m-ethyltoluene	−0.606	17.1	14.3
p-ethyltoluene	−0.375	11.4	7.1
fluorobenzene[b]	−0.073	0.54	2.9
chlorobenzene	0.114	0.94	1.6
bromobenzene[b]	0.150	0.70	1.5
iodobenzene[b]	0.135	0.93	1.5
benzotrifluoride	0.520	0.48	0.48
aniline[b]	−1.3	~60	116
N,N-dimethylaniline	−1.7	148	386
benzonitrile	0.562	0.33	0.42
nitrobenzene	0.674	0.21	0.30
4-chlorobenzotrifluoride	0.634	0.25	0.34
o-dichlorobenzene	0.513	0.42	0.49
m-dichlorobenzene	0.228	0.72	1.15
p-dichlorobenzene	0.513	0.32	0.49
p-chloroaniline[b]	−0.901	83.0	34.7
o-nitrophenol[b]	−0.13	0.90	3.4
1,2,4-trichlorobenzene	0.627	0.532	0.35
n-propylpentafluorobenzene[b]	0.419	3.06	0.65
hexafluorobenzene	0.837	0.219	0.18
biphenyl (per ring)	−0.179	3.5	3.9

[a] Account has been taken, wherever possible, for the H atom abstraction pathway using the data in Table XV. [b] Not used in deriving the correlation (see text).

substituent groups. Furthermore, because of the limited information available, the reported data for fluorobenzene, bromobenzene, iodobenzene, and *o*-nitrophenol were also not used in the derivation of the best-fit correlation. The observed overall OH radical reaction rate constants for the contribution due to the H atom abstraction pathway have been corrected, wherever possible, by use of the data in Table XV. Additionally, the recommended rate constant for biphenyl has been divided by a factor of 2 to take into account the two identical aromatic rings to which OH radical addition can take place.

The values of $\sum\sigma^+$ listed in Table XXII were calculated as described by Zetzsch,[466] i.e., (a) steric hindrance was neglected and the electrophilic substituent constant of the ortho position was set equal to that for the para position, (b) the total substituent constant $\sum\sigma^+$ was the sum of all substituent constants of the substituents connected to the aromatic ring, (c) the OH radical adds to the position yielding the most negative value for $\sum\sigma^+$ (preferably a free position), and (d) if all positions are occupied, the ipso position was treated as a meta position.

A unit-weighted least-squares analysis of these values of k^{add} and $\sum\sigma^+$ yields the expression

$$\log k^{add}\ (cm^3\ molecule^{-1}\ s^{-1}) = -11.64 - 1.31\sum\sigma^+$$

which is only slightly different from that given by Zetzsch.[466]

The OH radical addition rate constants at room temperature calculated from this equation are compared to the experimental values in Table XXII and Figure 64, and it can be seen that only for 1,2,4-trimethylbenzene, fluorobenzene, bromobenzene, *N,N*-dimethylaniline, *p*-chloroaniline, *o*-nitrophenol, and *n*-propylpentafluorobenzene are the discrepancies between the measured and calculated value of k^{add} greater than a factor of 2. For the other 31 aromatics given in Table XXII, the estimated values of k^{add} are within a factor of 2 of the measured rate constants, even though the absolute magnitude of these measured rate constants vary by a factor of ~700.

Clearly, this correlation can be used to a priori predict the room-temperature rate constants for the addition of OH radicals to the aromatic ring to within ± a factor of typically $\lesssim 2$. As an example of interest, this correlation predicts room temperature rate constants for OH radical addition to aniline and *p*-chloroaniline of 1.2×10^{-10} and 3.5×10^{-11} cm^3 $molecule^{-1}$ s^{-1}, respectively, which can be compared to the measured overall rate constants of 1.2×10^{-10} and 8.3×10^{-11} cm^3 $molecule^{-1}$ s^{-1}, respectively. This suggests that the OH radical addition process is dominant for aniline and significant for *p*-chloroaniline. For aniline the sole data available[441] indicate that the room-temperature rate constant for

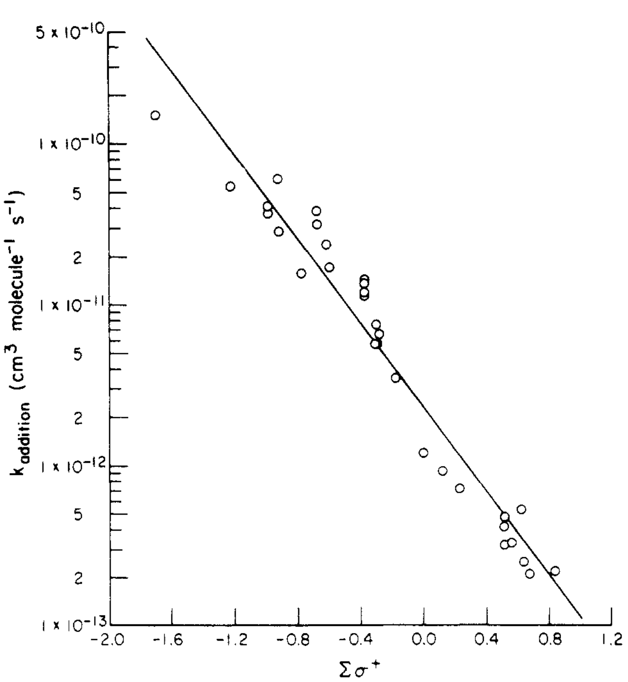

Figure 64. Plot of log k_{addition} against the overall electrophilic substituent constants for a series of aromatic compounds (see text).

OH radical addition to the aromatic ring is $\sim 6 \times 10^{-11}$ cm^3 molecule^{-1} s^{-1}, a factor of $\sim$2 lower than the predicted value.

The use of the above a priori predictive techniques, namely, those applicable to H atom abstraction from C–H (and, to a lesser extent from O–H) bonds, and OH radical addition to double and triple carbon–carbon bonds and to aromatic rings, enables OH radical reaction rate constants to be estimated with apparently reasonable reliability. It should, however, be noted that the available kinetic data base for sulfur-, nitrogen, and phosphorus-containing organics, and for organometallics, is presently insufficient for the extension of the predictive techniques discussed above to these important classes of organics. Hopefully, this deficiency will be reduced with the development of the necessary data base in future years. However, the present predictive technique appears to be able to estimate, solely from the chemical structure of the organic compound, room-temperature rate constants to within a factor of <5 (and often to within a factor of 2 or better) for a number of classes of organic compounds.

C. Atmospheric Lifetimes

The lifetimes of organic chemicals with respect to reaction with the OH radical, τ_{OH}, can be determined from a knowledge of the OH radical reaction rate constant k^{OH} and the atmospheric OH radical concentration, [OH], from the equation

$$\tau_{\text{OH}} = (k^{\text{OH}}[\text{OH}])^{-1}$$

However, in general this equation only yields the instantaneous lifetime, since the OH radical concentration exhibits seasonal, altitudinal, diurnal, and geographical variations, and k^{OH} typically varies with temperature, which decreases with increasing altitude in the troposphere. Variations in k^{OH} due to pressure are expected to be minor, except possibly for HCN and acetylene, since most organic compounds studied to date are in the limiting high-pressure second-order kinetic regime at total pressures of $\sim$200 torr of air or lower.

Chang and Kaufman[265] and Altshuller[518] have discussed the derivation of atmospheric OH radical lifetimes for a series of organics. As discussed,[265,518] differing assumptions of tropospheric OH radical concentration profiles as a function of altitude affect the resulting calculated lifetimes. Altshuller[518] used a weighted average tropospheric temperature of 265 K to calculate lifetimes due to reaction with OH radicals and an average OH radical concentration derived from tropospheric halocarbon measurements. While this use of an average tropospheric temperature of 265 K is reasonably appropriate for the alkanes and other organics which exhibit positive temperature dependencies, its use may lead to discrepancies for those organics whose temperature dependencies are negative (an obvious example being trichloroethene).

As discussed earlier in this paper, based upon the recent modeling study of Crutzen,[32] seasonally and diurnally averaged tropospheric northern and southern hemispheric OH radical concentrations are $\sim 5 \times 10^5$ and $\sim 6 \times 10^5$ molecule cm^{-3}, respectively. These estimates are in good agreement with previous estimates based upon, for example, the observed concentrations of $CHCl_3$ and CH_3CCl_3[56–58,60,65,66,71,72] and of ^{14}CO[61] and can be used to derive the lifetimes due to OH radical reaction of organics which are well-mixed throughout the troposphere. For organics which have lifetimes short with respect to the tropospheric mixing time, for example, of the order of a few days or less, the use of averaged temperatures and OH radical concentrations will lead to errors. However, since the actual instantaneous OH radical concentrations are not known to within at least a factor of 2, such errors may not be significant at the present time.[519]

Of course, in addition to reaction with OH radicals, organic compounds can be homogeneously removed from the troposphere by photolysis and reaction with NO_3 radicals and O_3 (and for certain basic amines and hydrazines[453] and other nitrogen-containing heterocycles,[441] by reaction with gas-phase HNO_3). While for the majority of organic compounds the reaction with OH radicals is expected to be the major homogeneous tropospheric loss process, these other reactions can dominate over OH radical reaction for certain classes of organics, e.g., photolysis for the alkyl nitrites[3,389] and nitrosamines,[149] reaction with O_3 for the higher alkenes (including the monoterpenes),[506] reaction with the NO_3 radical for the higher alkenes[502,520] (including the monoterpenes[503,504,521]), dimethyl sulfide[403] and the lower thiols,[412] furan and pyrrole,[522] and the hydroxy-substituted aromatics.[523,524]

As an illustrative example, Table XXIII gives calculated atmospheric lifetimes for a series of organics for reaction with OH and NO_3 radicals and with O_3. For these approximate estimates, the room-temperature O_3 and NO_3 and OH radical rate constants and OH radical, NO_3 radical, and O_3 concentrations of 5×10^5 molecule cm^{-3},[32] 2.4×10^8 molecule cm^{-3} (over continental areas),[525–531] and 7.2×10^{11} molecule cm^{-3} [532,533] have been used.

These estimated, and approximate, lifetimes are consistent with our above discussion and show that the OH radical reactions are the major tropospheric loss process for the alkanes, haloalkanes, the lower alkenes,

TABLE XXIII. Comparison of Room-Temperature Rate Constants and Loss Rates of Selected Organics in the Presence of 7.2 × 10^{11} molecule cm^{-3} of O_3, 5 × 10^5 molecule cm^{-3} of OH Radicals, and 2.4 × 10^8 molecule cm^{-3} of NO_3 Radicals

	OH		O_3		NO_3	
Organic	k^{OH},[a] cm^3 molecule^{-1} s^{-1}	loss rate, day^{-1}	k^{O_3},[b] cm^3 molecule^{-1} s^{-1}	loss rate, day^{-1}	k^{NO_3},[c] cm^3 molecule^{-1} s^{-1}	loss rate, day^{-1}
			Alkanes and Haloalkanes			
n-butane	2.5 × 10^{-12}	0.11	<10^{-23}	<6 × 10^{-7}	3.6 × 10^{-17}	0.0007
1,2-dibromoethane	2.5 × 10^{-13}	0.01	<10^{-23}	<6 × 10^{-7}		
			Alkenes and Haloalkenes			
ethene	8.5 × 10^{-12}	0.37	1.8 × 10^{-18}	0.11	1.1 × 10^{-16}	0.002
propene	2.6 × 10^{-11}	1.1	1.1 × 10^{-17}	0.7	7.6 × 10^{-15}	0.16
2-methyl-2-butene	8.7 × 10^{-11}	3.8	4.2 × 10^{-16}	25	9.9 × 10^{-12}	205
d-limonene	1.7 × 10^{-10}	7.3	6 × 10^{-16}	36	1.4 × 10^{-11}	290
trichloroethene	2.4 × 10^{-12}	0.10	<3 × 10^{-20}	<0.002		
			Alkynes			
acetylene	7.8 × 10^{-13}	0.03	7.8 × 10^{-21}	0.0005		
			O, S, N Containing			
acetaldehyde[d]	1.6 × 10^{-11}	0.7	≤6 × 10^{-21}	≤0.0004	2.5 × 10^{-15}	0.05
methyl vinyl ketone	1.8 × 10^{-11}	0.8	4.8 × 10^{-18}	0.3		
furan	4.0 × 10^{-11}	1.7	2.4 × 10^{-18}	0.15	1.4 × 10^{-12}	29
dimethyl sulfide	6.3 × 10^{-12}	0.27	<8 × 10^{-19}	<0.05	9.7 × 10^{-13}	20
thiophene	9.7 × 10^{-12}	0.4	<6 × 10^{-20}	<0.004	3.2 × 10^{-14}	0.7
dimethylamine[e]	6.5 × 10^{-11}	2.8	2.6 × 10^{-18}	0.16		
hydrazine[e]	6.5 × 10^{-11}	2.8	~3 × 10^{-17}	~2		
pyrrole	1.2 × 10^{-10}	5.2	1.6 × 10^{-17}	1.0	4.9 × 10^{-11}	1000
			Aromatics			
toluene	6.2 × 10^{-12}	0.27	<1 × 10^{-20}	<0.0006	3.6 × 10^{-17}	0.0007
o-cresol	4.0 × 10^{-11}	1.7	2.6 × 10^{-19}	0.02	2.2 × 10^{-11}	450

[a] From this work. [b] From Atkinson and Carter.[506] [c] From ref 228, 403, 502, 503, 522, and 524. [d] Photolysis will also occur, but OH radical reaction will be dominant. [e] Reaction with gas-phase HNO_3 will also occur[453] and may be the dominant loss process in urban atmospheres.

the aromatic hydrocarbons, and a majority of the oxygen-containing organics. The recent review article of Atkinson and Carter,[506] dealing with the kinetics and mechanisms of O_3 reactions under atmospheric conditions, and ref 228, 403, 502–505, 520, 522–524, 534, and 535, dealing with NO_3 radical reaction rate constants, should be consulted for the available kinetic data concerning O_3 and NO_3 radical reactions with organic compounds.

V. Conclusions

In the above sections the available kinetic and mechanistic data concerning the reactions of OH radicals with organic compounds under atmospheric conditions have been compiled and evaluated, and previous a priori predictive schemes have been extended to develop an up-to-date estimation procedure which will hopefully prove useful for room-temperature rate constant and atmospheric lifetime calculations. Since our earlier review,[1] which covered the literature through mid-1978, a large number of experimental kinetic product and mechanistic studies have been carried out. While these have, of course, greatly enlarged the available data base, it is an attribute to the earlier studies that few major changes have occurred in the past 7 years. Rather these recent years have proved to be a time of refinement in the area dealing with the kinetics of OH radical reactions and a beginning of reliable product and mechanistic studies and of the development of techniques for studying even more difficult to handle (for example, those of low volatility) organic compounds. Hopefully, this process will continue.

VI. Addendum

Since the revision of this paper in mid-1985 and the end of 1985, data have been published concerning the reactions of the OH radical with organic compounds which were not included in this review. These data are briefly discussed here by the same organic compound classes as in the text. For further details, the references cited should be consulted.

A. Alkanes

In addition to determining rate constants for the reaction of OH radicals with C_2H_6 over the temperature range 292.5–705 K (Table I), Tully and co-workers[203] have determined OH radical reaction rate constants for CH_3CD_3 and C_2D_6 over the temperature range 293–705 K by LP-LIF. The room temperature rate constants obtained are given in Table XXIV, and the following temperature dependent expressions are given by Tully and co-workers[203]

$$k_{C_2H_3D_3} = 7.65 \times 10^{-19} T^{2.38} e^{-411/T} \text{ cm}^3 \text{ molecule}^{-1} \text{ s}^{-1}$$

$$k_{C_2D_6} = 2.43 \times 10^{-19} T^{2.56} e^{-663/T} \text{ cm}^3 \text{ molecule}^{-1} \text{ s}^{-1}$$

Using a PR-RA technique, Nielsen et al.[536] have studied the kinetics of the reaction of OH radicals with ethane over the temperature range 300–400 K. The 300 K rate constant, which is in reasonable agreement with the recommendation, is given in Table XXIV. The Arrhenius expression cited[536] is

$$k_{C_2H_6} = 1.61 \times 10^{-11} e^{-1173/T} \text{ cm}^3 \text{ molecule}^{-1} \text{ s}^{-1}$$

in good agreement with that of Greiner[21] over a similar temperature range.

TABLE XXIV. Rate Constants k for the Gas-Phase Reaction of OH Radicals with Organic Compounds

compd	$10^{12}k$, cm^3 molecule^{-1} s^{-1}	T, K	technique	ref
CH_3CD_3	0.142 ± 0.007	293	LP-LIF	Tully et al.[203]
C_2D_6	0.0523 ± 0.0060	293	LP-LIF	Tully et al.[203]
C_2H_6	0.324	300	PR-RA	Nielsen et al.[536]
CH_3Cl	0.0714	300	PR-RA	Nielsen et al.[536]
CH_2Cl_2	0.146	300	PR-RA	Nielsen et al.[536]
$CHFCl_2$	0.00515	300	PR-RA	Nielsen et al.[536]
CH_3CCl_3	0.0087	298 ± 3	rel rate [rel to k(OH + CH_3Cl) = 4.36×10^{-14}][a]	Nelson et al.[537]
CCl_3CHO	1.95	298 ± 3	rel rate [rel to k(OH + $CH_3C(O)OC_2H_5$) = 1.8×10^{-12}][b]	Nelson et al.[537]
CH_3CClO	0.068	298 ± 3	rel rate [rel to k(OH + $CHCl_3$) = 1.03×10^{-13}][a]	Nelson et al.[537]
acetylene	0.85 ± 0.18[c]	297 ± 2	rel rate [rel to k(OH + cyclohexane) = 7.34×10^{-12}][a]	Hatakeyama et al.[539]
propyne	5.53 ± 0.14[c]	297 ± 2	rel rate [rel to k(OH + cyclohexane) = 7.34×10^{-12}][a]	Hatakeyama et al.[539]
2-butyne	29.2 ± 2.6[c]	297 ± 2	rel rate [rel to k(OH + cyclohexane) = 7.34×10^{-12}][a]	Hatakeyama et al.[539]
acetaldehyde	14.7 ± 2.8	298	DF-RF	Michael et al.[540]
propanal	≤26	296	rel rate [rel to k(OH + HONO) = 6.6×10^{-12}]	Kerr and Stocker[541]
ketene	17 ± 2[c]	299 ± 2	rel rate [rel to k(OH + cyclohexane) = 7.41×10^{-12}][a]	Hatakeyama et al.[542]
methylketene	59 ± 13[c]	299 ± 2	rel rate [rel to k(OH + cyclohexane) = 7.41×10^{-12}][a]	Hatakeyama et al.[542]
	79 ± 13[c]	299 ± 2	rel rate [rel to k(OH + propene) = 2.62×10^{-11}][a]	Hatakeyama et al.[542]
ethylketene	118 ± 29[c]	299 ± 2	rel rate [rel to k(OH + propene) = 2.62×10^{-11}][a]	Hatakeyama et al.[542]
dimethylketene	107 ± 29[c]	299 ± 2	rel rate [rel to k(OH + propene) = 2.62×10^{-11}][a]	Hatakeyama et al.[542]
thiophene	9.6 ± 1.5	300	rel rate [rel to k(OH + propene) = 2.60×10^{-11}][a]	Barnes et al.[543]
benzene	1.45 ± 0.06	~298	rel rate [rel to k(OH + n-hexane) = 5.58×10^{-12}][a]	Ohta and Ohyama[549]
toluene	6.03 ± 0.17	~298	rel rate [rel to k(OH + n-hexane) = 5.58×10^{-12}][a]	Ohta and Ohyama[549]
ethylbenzene	6.47 ± 0.28	~298	rel rate [rel to k(OH + n-hexane) = 5.58×10^{-12}][a]	Ohta and Ohyama[549]
isopropylbenzene	6.25 ± 0.34	~298	rel rate [rel to k(OH + n-hexane) = 5.58×10^{-12}][a]	Ohta and Ohyama[549]
propylbenzene	6.58 ± 0.22	~298	rel rate [rel to k(OH + n-hexane) = 5.58×10^{-12}][a]	Ohta and Ohyama[549]
tert-butylbenzene	4.58 ± 0.45	~298	rel rate [rel to k(OH + n-hexane) = 5.58×10^{-12}][a]	Ohta and Ohyama[549]
o-xylene	12.5 ± 0.6	~298	rel rate [rel to k(OH + n-hexane) = 5.58×10^{-12}][a]	Ohta and Ohyama[549]
2-ethyltoluene	12.4 ± 1.2	~298	rel rate [rel to k(OH + n-hexane) = 5.58×10^{-12}][a]	Ohta and Ohyama[549]
m-xylene	22.2 ± 0.6	~298	rel rate [rel to k(OH + n-hexane) = 5.58×10^{-12}][a]	Ohta and Ohyama[549]
3-ethyltoluene	21.2 ± 1.0	~298	rel rate [rel to k(OH + n-hexane) = 5.58×10^{-12}][a]	Ohta and Ohyama[549]
p-xylene	12.9 ± 0.6	~298	rel rate [rel to k(OH + n-hexane) = 5.58×10^{-12}][a]	Ohta and Ohyama[549]
4-ethyltoluene	12.8 ± 1.2	~298	rel rate [rel to k(OH + n-hexane) = 5.58×10^{-12}][a]	Ohta and Ohyama[549]
1,2,3-trimethylbenzene	29.6 ± 4.1	~298	rel rate [rel to k(OH + n-hexane) = 5.58×10^{-12}][a]	Ohta and Ohyama[549]
1,2,4-trimethylbenzene	31.5 ± 1.2	~298	rel rate [rel to k(OH + n-hexane) = 5.58×10^{-12}][a]	Ohta and Ohyama[549]
1,3,5-trimethylbenzene	38.7 ± 5.2	~298	rel rate [rel to k(OH + n-hexane) = 5.58×10^{-12}][a]	Ohta and Ohyama[549]
fluorobenzene	0.89 ± 0.11	~298	rel rate [rel to k(OH + n-hexane) = 5.58×10^{-12}][a]	Ohta and Ohyama[549]
methoxybenzene	14.1 ± 0.6	~298	rel rate [rel to k(OH + n-hexane) = 5.58×10^{-12}][a]	Ohta and Ohyama[549]

[a] From recommendations. [b] From Table XI. [c] At 1 atm of air.

B. Haloalkanes and Other Halo Organics

Nielsen et al.[536] have determined rate constants for the reactions of the OH radical with CH_3Cl, CH_2Cl_2, and $CHFCl_2$ over the temperature range 300–400 K, using a PR-RA technique. The 300 K rate constants are given in Table XXIV, and the cited Arrhenius expressions are

$$k(CH_3Cl) = 5.3 \times 10^{-12}e^{-1263/T} \text{ cm}^3 \text{ molecule}^{-1} \text{ s}^{-1}$$

$$k(CH_2Cl_2) = 6.8 \times 10^{-12}e^{-1117/T} \text{ cm}^3 \text{ molecule}^{-1} \text{ s}^{-1}$$

$$k(CHFCl_2) = 1.8 \times 10^{-12}e^{-1787/T} \text{ cm}^3 \text{ molecule}^{-1} \text{ s}^{-1}$$

While these rate constants for CH_2Cl_2 and $CHFCl_2$ are in reasonable agreement with the other literature data discussed above, the rate constants for CH_3Cl are higher, by a factor of approximately 1.7 at 300 K, possibly due to initial fragmentation of CH_3Cl by the radiolysis source.[536]

Nelson et al.[537] have used a relative rate method to measure the OH radical rate constants for CH_3CCl_3, CH_3CClO, and CCl_3CHO at 298 ± 3 K. For CH_3CCl_3 their rate constant is in agreement with previous room temperature data[71,72,186] and the recommendation. For the other two halo organics studied no previous literature measurements are available for comparison.

C. Alkenes

Shepson et al.[538] have identified and measured the yields of hydroxy nitrates from the reaction of the OH radical with propene in the presence of NO at atmospheric pressure of air. These hydroxy nitrates [$CH_3CHOHCH_2ONO_2$ and $CH_3CH(ONO_2)CH_2OH$] were shown to be formed from the corresponding RO_2 radicals via reaction with NO, with formation yields of 0.015–0.017. These nitrate formation yields are a factor of ~2 lower than those for alkyl nitrate formation from secondary C_3-alkylperoxy radicals.

D. Alkynes

Using a relative rate method, Hatakeyama et al.,[539] have determined rate constants at 297 ± 2 K for the reaction of OH radicals with acetylene, propyne, and 2-butyne in 1 atm of air (Table XXIV). The rate constants for acetylene and propyne are in good agreement with those of Atkinson and Aschmann.[328] The increase in the room temperature rate constant with the degree of alkyl substitution around the carbon–carbon triple bond is expected for an initial OH radical addition reaction. Hatakeyama et al.[539] also investigated the products of these reactions under atmospheric conditions, and showed that glyoxal, methylglyoxal, and biacetyl are formed in relatively high yields in both the presence and absence of NO.

E. Oxygen-Containing Organics

Rate constants, or upper limits, have been reported for the reactions of the OH radical with acetaldehyde,[540] propanal,[541] and a series of ketenes.[542] The room temperature rate constants obtained are listed in Table XXIV. Michael et al.[540] have used a DF-RF technique to determine the rate constants for acetaldehyde over the temperature range 244–528 K, with k(acetaldehyde) = $5.52 \times 10^{-12}\ e^{307/T}$ cm^3 molecule^{-1} s^{-1}. These rate constants are in good agreement with the FP-RF data of Atkinson and Pitts[340] and the recommendation. The data of Hatakeyama et al.[542] for the ketenes are given in Table XXIV, and these rate constants indicate that these reactions proceed via OH radical addition to the $>C{=}C<$ bond. Products were also studied under simulated atmospheric conditions.[542]

F. Sulfur-Containing Organics

Barnes et al.[543] have used relative rate techniques to study the kinetics of the reactions of the OH radical with several sulfur-containing organics at 300 K and atmospheric pressure in the presence of varying O_2 concentrations. For CH_3SH and CH_3SCH_3, the rate constants were observed to increase with the O_2 concentrations, yielding rate constants in 1 atm of air of $\sim 1.2 \times 10^{-10}$ cm^3 molecule^{-1} s^{-1} and $\sim 5 \times 10^{-11}$ cm^3 molecule^{-1} s^{-1}, respectively.[543] On the basis of the discussions above concerning the kinetics and mechanisms of these reactions, it is almost certain that these anomolously high rate constants are due to the occurrence of secondary reactions leading to an enhanced consumption of the sulfur-containing compounds in the relative rate systems utilized. However, for thiophene no dependence of the observed rate constant on the O_2 concentration was observed,[543] and the value of 9.6×10^{-12} cm^3 molecule^{-1} s^{-1} at 300 K in 1 atm of air is in good agreement with the recommendation.

G. Aromatics

The product data reported by Bandow et al.[476] have been published.[544-546] In addition to the α-dicarbonyl yields from toluene, the xylenes, and the trimethylbenzenes (given in Table XVI), data are presented for the hydroxy aromatic yields from toluene[544] and the xylenes.[545] Product data for toluene have also been reported by Gery et al.[547]

Kinetic studies have been carried out by Madronich and Felder[548] and Ohta and Ohyama.[549] Madronich and Felder[548] obtained rate constants for the reaction of OH radicals with benzene over the temperature range 787–1409 K using a FP-RF method. The rate constants determined are ~30% higher than those of Tully et al.[459] However, of particular interest is the evidence presented to show that at these elevated temperatures the reaction proceeds predominantly via H atom abstraction from the aromatic ring, rather than by an elimination reaction as proposed by Lin and Lin.[335]

Ohta and Ohyama[549] have used a relative rate method to obtain rate constants for the reaction of the OH radical with a series of aromatic compounds at room temperature (Table XXIV). For benzene, toluene, and the xylenes these rate constants are in reasonable agreement with, though those for the xylenes are somewhat lower than, the recommendations and previous data. However, for the trimethylbenzenes and methoxybenzene these rate constants of Ohta and Ohyama[549] are significantly lower than the previous literature data, and this may indicate wall adsorption/desorption problems in this recent study.[549]

Using a FP-RF technique, Witte and Zetzsch[550] have determined absolute rate constants for the reaction of OH radicals with benzene, aniline, and nitrobenzene over the temperature range 239–359 K. Nonexponential OH radical decays were observed, even at room temperature, and the initial OH radical reaction rate constants and the OH–aromatic adduct decay rates were obtained. For the initial OH radical reactions, the following Arrhenius expressions were obtained

$$k(\text{benzene}) = 2.3 \times 10^{-12} e^{-192/T}\ \text{cm}^3\ \text{molecule}^{-1}\ \text{s}^{-1}$$

$$k(\text{aniline}) = 1.7 \times 10^{-11} e^{553/T}\ \text{cm}^3\ \text{molecule}^{-1}\ \text{s}^{-1}$$

$$k(\text{nitrobenzene}) = 6 \times 10^{-13} e^{-445/T}\ \text{cm}^3\ \text{molecule}^{-1}\ \text{s}^{-1}$$

These rate constants for benzene and aniline are in reasonable agreement with the previous data discussed above. Those for nitrobenzene are the first temperature dependent data reported, and the previous rate constant of Zetzsch[466] has been reevaluated to take into account a new determination of the vapor pressure for this compound.[550]

VII. Acknowledgment

The author gratefully acknowledges the financial support of the U.S. Environmental Protection Agency through Cooperative Agreement CR809247-03 (Project Officer, Bruce W. Gay, Jr.). I thank Drs. George Le Bras, Th. Just, James J. Margitan, Hiromi Niki, Frank P. Tully, Paul H. Wine, Reinhard Zellner, Cornelius Zetzsch, and their co-workers for communicating their data prior to publication and for helpful discussions, Dr. William P. L. Carter for helpful discussions, Ms. Virpi T. Lindfors and Ms. Minn P. Poe for carrying out the nonlinear least-squares analyses, and, especially, Ms. Christy J. LaClaire for her long-suffering efforts in preparing this manuscript. Although the research described in this article have been wholly funded by the U.S. Environmental Protection Agency, it has not been subjected to agency review and therefore does not necessarily reflect the view of the agency and no official endorsement should be inferred.

Registry No. Hydroxyl, 3352-57-6.

VIII. References

(1) Atkinson, R.; Darnall, K. R.; Lloyd, A. C.; Winer, A. M.; Pitts, J. N., Jr. *Adv. Photochem.* **1979**, *11*, 375.
(2) Logan, J. A.; Prather, M. J.; Wofsy, S. C.; McElroy, M. B. *J. Geophys. Res.* **1981**, *86*, 7210.
(3) Atkinson, R.; Lloyd, A. C. *J. Phys. Chem. Ref. Data* **1984**, *13*, 315.
(4) Atkinson, R.; Bull, D. C.; Shuff, P. J. *Combust. Flame* **1980**, *39*, 287.
(5) Westbrook, C. K. *Combust. Flame* **1982**, *46*, 191.
(6) Westbrook, C. K. *Combust. Sci. Technol.* **1982**, *29*, 67.
(7) Fairchild, P. W.; Smith, G. P.; Crosley, D. R., 19th International Symposium on Combustion, 1982, The Combustion Institute, 1982, pp 107–115.
(8) Westbrook, C. K.; Dryer, F. L.; Schug, K. P., 19th International Symposium on Combustion, 1982, The Combustion Institute, 1982, pp 153–166.
(9) Miller, J. A.; Mitchell, R. E.; Smooke, M. D.; Kee, R. J., 19th International Symposium on Combustion, 1982, The Combustion Institute, 1982, pp 181–196.
(10) Warnatz, J.; Bockhorn, H.; Möser, A.; Wenz, H. W., 19th International Symposium on Combustion, 1982, The Com-

bustion Institute, 1982, pp 197–209.
(11) Carter, W. P. L.; Lloyd, A. C.; Sprung, J. L.; Pitts, J. N., Jr. *Int. J. Chem. Kinet.* **1979**, *11*, 45.
(12) Atkinson, R.; Carter, W. P. L.; Darnall, K. R.; Winer, A. M.; Pitts, J. N., Jr. *Int. J. Chem. Kinet.* **1980**, *12*, 779.
(13) Killus, J. P.; Whitten, G. Z. *Atmos. Environ.* **1982**, *16*, 1973.
(14) Lloyd, A. C.; Atkinson, R.; Lurmann, F. W.; Nitta, B. *Atmos. Environ.* **1983**, *17*, 1931.
(15) Killus, J. P.; Whitten, G. Z. *Environ. Sci. Technol.* **1984**, *18*, 142.
(16) Leone, J. A.; Seinfeld, J. H. *Int. J. Chem. Kinet.* **1984**, *16*, 159.
(17) Leone, J. A.; Flagan, R. C.; Grosjean, D.; Seinfeld, J. H. *Int. J. Chem. Kinet.* **1985**, *17*, 177.
(18) Leighton, P. A. "Photochemistry of Air Pollution"; Academic Press: New York, NY, 1961.
(19) Greiner, N. R. *J. Chem. Phys.* **1967**, *46*, 2795.
(20) Greiner, N. R. *J. Chem. Phys.* **1967**, *46*, 3389.
(21) Greiner, N. R. *J. Chem. Phys.* **1970**, *53*, 1070.
(22) Heicklen, J.; Westberg, K.; Cohen, N. Report No. 115-69; Center for Air Environment Studies, Pennsylvania State University: University Park, PA, 1969.
(23) Stedman, D. H.; Morris, E. D., Jr.; Daby, E. E.; Niki, H.; Weinstock, B., 160th National Meeting of the American Chemical Society, Chicago, IL, Sept 1970; American Chemical Society: Washington, D.C., 1970.
(24) Niki, H.; Daby, E. E.; Weinstock, B. *Adv. Chem. Ser.* **1972**, *No. 113*, 16.
(25) Demerjian, K. L.; Kerr, J. A.; Calvert, J. G. *Adv. Environ. Sci. Technol.* **1974**, *4*, 1.
(26) Dodge, M. C.; Bufalini, J. *Adv. Chem. Ser.* **1972**, *No. 113*, 232.
(27) Calvert, J. G.; Demerjian, K. L.; Kerr, J. A. *Environ. Lett.* **1973**, *4*, 281.
(28) Atkinson, R.; Aschmann, S. M.; Carter, W. P. L.; Winer, A. M.; Pitts, J. N., Jr. *J. Phys. Chem.* **1982**, *86*, 4563.
(29) Atkinson, R.; Aschmann, S. M.; Carter, W. P. L.; Winer, A. M.; Pitts, J. N., Jr. *Int. J. Chem. Kinet.* **1984**, *16*, 1085.
(30) DeMore, W. B.; Margitan, J. J.; Molina, M. J.; Watson, R. T.; Golden, D. M.; Hampson, R. F.; Kurylo, M. J.; Howard, C. J.; Ravishankara, A. R. "Chemical Kinetics and Photochemical Data for Use in Stratospheric Modeling"; Evaluation No. 7, Jet Propulsion Laboratory Publication 85–37, July 1985.
(31) Baulch, D. L.; Cox, R. A.; Hampson, R. F., Jr.; Kerr, J. A.; Troe, J.; Watson, R. T. *J. Phys. Chem. Ref. Data* **1980**, *9*, 295; **1982**, *11*, 327; **1984**, *13*, 1259.
(32) Crutzen, P. J. In "Atmospheric Chemistry"; Goldberg, D. G., Ed.; Ann Arbor Press: Ann Arbor, MI, 1982; pp 313–328.
(33) Wofsy, S. C.; McConnell, J. C.; McElroy, M. B. *J. Geophys. Res.* **1972**, *77*, 4477.
(34) Crutzen, P. J.; Isaksen, I. S. A.; McAfee, J. R. *J. Geophys. Res.* **1978**, *83*, 345.
(35) Johnston, H. S. *Adv. Environ. Sci. Technol.* **1974**, *4*, 263.
(36) Crutzen, P. J. *Can. J. Chem.* **1974**, *52*, 1569.
(37) Nicolet, M. *Can. J. Chem.* **1974**, *52*, 1381.
(38) Wofsy, S. C.; McElroy, M. B. *Can. J. Chem.* **1974**, *52*, 1582.
(39) Nicolet, M. *Rev. Geophys. Space Phys.* **1975**, *13*, 593.
(40) Wang, C. C.; Davis, L. I., Jr. *Phys. Rev. Lett.* **1974**, *32*, 349.
(41) Wang, C. C.; Davis, L. I., Jr.; Wu, C. H.; Japar, S.; Niki, H.; Weinstock, B. *Science (Washington, D.C.)* **1975**, *189*, 797. Selzer, P. M.; Wang, C. C. *J. Chem. Phys.* **1979**, *71*, 3786.
(42) Anderson, J. G. *Geophys. Res. Lett.* **1976**, *3*, 165.
(43) Anderson, J. G., Proceedings of the NATO Advanced Study Institute on Atmospheric Ozone, Oct 1979, pp 233–251, Report FAA-EE-80-20, May 1980.
(44) Davis, D. D.; Heaps, W.; McGee, T. *Geophys. Res. Lett.* **1976**, *3*, 331.
(45) Perner, D.; Ehhalt, D. H.; Pätz, H. W.; Platt, U.; Röth, E. P.; Volz, A. *Geophys. Res. Lett.* **1976**, *3*, 466.
(46) Campbell, M. J.; Sheppard, J. C.; Au, B. F. *Geophys. Res. Lett.* **1979**, *6*, 175.
(47) Davis, D. D.; Heaps. W.; Philen, D.; McGee, T. *Atmos. Environ.* **1979**, *13*, 1197.
(48) Wang, C. C.; Davis, L. I., Jr.; Selzer, P. M.; Munoz, R. *J. Geophys. Res.* **1981**, *86*, 1181.
(49) Heaps, W. S.; McGee, T. J.; Hudson, R. D.; Caudill, L. O. *Appl. Optics* **1982**, *21*, 2265.
(50) Heaps, W. S.; McGee, T. J. *J. Geophys. Res.* **1983**, *88*, 5281.
(51) Ortgies, G.; Comes, F. J. *Appl. Phys. B* **1984**, *33*, 103.
(52) Hübler, G.; Perner, D.; Platt, U.; Tönnissen, A.; Ehhalt, D. H. *J. Geophys. Res.* **1984**, *89*, 1309.
(53) Hard, T. M.; O'Brien, R. J.; Chan, C. Y.; Mehrabzadeh, A. A. *Environ. Sci. Technol.* **1984**, *18*, 768.
(54) Hoell, J. M.; Gregory, G. L.; Carroll, M. A.; McFarland, M.; Ridley, B. A.; Davis, D. D.; Bradshaw, J.; Rodgers, M. O.; Torres, A. L.; Sachse, G. W.; Hill, G. F.; Condon, E. P.; Rasmussen, R. A.; Campbell, M. C.; Farmer, J. C.; Sheppard, J. C.; Wang, C. C.; Davis, L. I. *J. Geophys. Res.* **1984**, *89*, 11819.
(55) Calvert, J. G. *Environ. Sci. Technol.* **1976**, *10*, 256.
(56) Singh, H. B. *Geophys. Res. Lett.* **1977**, *4*, 101.
(57) Singh, H. B. *Geophys. Res. Lett.* **1977**, *4*, 453.
(58) Lovelock, J. E. *Nature (London)* **1977**, *267*, 32.
(59) Crutzen, P. J.; Fishman, J. *Geophys. Res. Lett.* **1977**, *4*, 321.
(60) Neely, W. B.; Plonka, J. H. *Environ. Sci. Technol.* **1978**, *12*, 317.
(61) Volz, A.; Ehhalt, D. H.; Derwent, R. G. *J. Geophys. Res.* **1981**, *86*, 5163.
(62) Chameides, W. L.; Tan, A. *J. Geophys. Res.* **1981**, *86*, 5209.
(63) Allam, R. J.; Groves, K. S.; Tuck, A. F. *J. Geophys. Res.* **1981**, *86*, 5303.
(64) Pyle, J. A.; Zavody, A. M.; Harries, J. E.; Moffat, P. H. *Nature (London)* **1983**, *305*, 690.
(65) Khalil, M. A. K.; Rasmussen, R. A. *Tellus* **1984**, *36B*, 317.
(66) Khalil, M. A. K.; Rasmussen, R. A. *Chemosphere* **1984**, *13*, 789.
(67) Roberts, J. M.; Fehsenfeld, F. C.; Liu, S. C.; Bollinger, M. J.; Hahn, C.; Albritton, D. L.; Sievers, R. E. *Atmos. Environ.* **1984**, *18*, 2421.
(68) Ortgies, G.; Gericke, K.-H.; Comes, F. J. *Geophys. Res. Lett.* **1980**, *7*, 905.
(69) Ortgies, G.; Gericke, K.-H.; Comes, F. J. *Z. Naturforsch.* **1981**, *36A*, 177.
(70) Gericke, K.-H.; Comes, F. J. *Z. Naturforsch.* **1982**, *37A*, 559.
(71) Jeong, K.-M.; Kaufman, F. *Geophys. Res. Lett.* **1979**, *6*, 757.
(72) Kurylo, M. J.; Anderson, P. C.; Klais, O. *Geophys. Res. Lett.* **1979**, *6*, 760.
(73) Oldenberg, O. *J. Chem. Phys.* **1935**, *3*, 266.
(74) Avramenko, L. I.; Lorenzo, R. V. *Dokl. Akad. Nauk SSR* **1949**, *67*, 867.
(75) Kaufman, F.; Del Greco, F. P. *J. Chem. Phys.* **1961**, *35*, 1895.
(76) Del Greco, F. P.; Kaufman, F. *Discuss. Faraday Soc.* **1962**, *33*, 128.
(77) Kaufman, F.; Del Greco, F. P., "9th International Symposium on Combustion"; Academic Press: New York, 1963; p 659.
(78) Howard, C. J. *J. Chem. Phys.* **1976**, *65*, 4771.
(79) Howard, C. J. *J. Phys. Chem.* **1979**, *83*, 3.
(80) Kaufman, F. *J. Phys. Chem.* **1984**, *88*, 4909.
(81) Anderson, J. G.; Kaufman, F. *Chem. Phys. Lett.* **1972**, *16*, 375.
(82) Westenberg, A. A. *J. Chem. Phys.* **1965**, *43*, 1544.
(83) Westenberg, A. A.; deHaas, N. *J. Chem. Phys.* **1965**, *43*, 1550.
(84) Dixon-Lewis, G.; Wilson, W. E.; Westenberg, A. A. *J. Chem. Phys.* **1966**, *44*, 2877.
(85) Morris, E. D., Jr.; Stedman, D. H.; Niki, H. *J. Am. Chem. Soc.* **1971**, *93*, 3570.
(86) Howard, C. J.; Evenson, K. M. *J. Chem. Phys.* **1974**, *61*, 1943.
(87) Meier, U.; Grotheer, H. H.; Just, Th. *Chem. Phys. Lett.* **1984**, *106*, 97.
(88) Westenberg, A. A.; deHaas, N. *J. Chem. Phys.* **1967**, *46*, 490.
(89) Anderson, J. G.; Margitan, J. J.; Kaufman, F. *J. Chem. Phys.* **1974**, *60*, 3310.
(90) Sridharan, U. C.; Reimann, B.; Kaufman, F. *J. Chem. Phys.* **1980**, *73*, 1286.
(91) Keyser, L. F. *J. Phys. Chem.* **1984**, *88*, 4750.
(92) Sie, B. K. T.; Simonaitis, R.; Heicklen, J. *Int. J. Chem. Kinet.* **1976**, *8*, 85.
(93) Cox, R. A.; Derwent, R. G.; Holt, P. M. *J. Chem. Soc., Faraday Trans. 1* **1976**, *72*, 2031.
(94) Chan, W. H.; Uselman, W. M.; Calvert, J. G.; Shaw, J. H. *Chem. Phys. Lett.* **1977**, *45*, 240.
(95) Overend, R.; Paraskevopoulos, G. *Chem. Phys. Lett.* **1977**, *49*, 109.
(96) Perry, R. A.; Atkinson, R.; Pitts, J. N., Jr. *J. Chem. Phys.* **1977**, *67*, 5577.
(97) Paraskevopoulos, G.; Irwin, R. S. *J. Chem. Phys.* **1984**, *80*, 259.
(98) Hofzumahaus, A.; Stuhl, F. *Ber. Bunsen-Ges. Phys. Chem.* **1984**, *88*, 557.
(99) Niki, H.; Maker, P. D.; Savage, C. M.; Breitenbach, L. P. *J. Phys. Chem.* **1984**, *88*, 2116.
(100) Wahner, A.; Zetzsch, C., 8th International Symposium on Gas Kinetics, University of Nottingham, Nottingham, U.K., July 15–20, 1984.
(101) DeMore, W. B. *Int. J. Chem. Kinet.* **1984**, *16*, 1187.
(102) Morris, E. D., Jr.; Niki, H. *J. Phys. Chem.* **1971**, *75*, 3640.
(103) Morris, E. D., Jr.; Niki, H. *J. Chem. Phys.* **1971**, *55*, 1991.
(104) Norrish, R. G. W.; Porter, G. *Nature (London)* **1949**, *164*, 658.
(105) Horne, D. G.; Norrish, R. G. W. *Nature (London)* **1967**, *215*, 1373.
(106) Horne, D. G.; Norrish, R. G. W. *Proc. R. Soc. London, Ser. A* **1970**, *315*, 287.
(107) Greiner, N. R. *J. Chem. Phys.* **1966**, *45*, 99.
(108) Greiner, N. R. *J. Chem. Phys.* **1968**, *48*, 1413.
(109) Greiner, N. R. *J. Phys. Chem.* **1968**, *72*, 406.
(110) Greiner, N. R. *J. Chem. Phys.* **1969**, *51*, 5049.
(111) Greiner, N. R. *J. Chem. Phys.* **1970**, *53*, 1284.
(112) Morley, C.; Smith, I. W. M. *J. Chem. Soc., Faraday Trans. 2* **1972**, *68*, 1016.
(113) Stuhl, F.; Niki, H. *J. Chem. Phys.* **1972**, *57*, 3671.
(114) Stuhl, F.; Niki, H. *J. Chem. Phys.* **1972**, *57*, 3677.

(115) Michael, J. V.; Lee, J. H. *J. Phys. Chem.* **1979**, *83*, 10.

(116) Anastasi, C.; Bemand, P. P.; Smith, I. M. W. *Chem. Phys. Lett.* **1976**, *37*, 370.

(117) Ravishankara, A. R.; Kreutter, N. M.; Shah, R. C.; Wine, P. H. *Geophys. Res. Lett.* **1980**, *7*, 861.

(118) Smith, I. W. M.; Zellner, R. *J. Chem. Soc., Faraday Trans. 2* **1973**, *69*, 1617.

(119) Overend, R.; Paraskevopoulos, G. *J. Chem. Phys.* **1977**, *67*, 674.

(120) Kurylo, M. J. *Chem. Phys. Lett.* **1973**, *23*, 467.

(121) Lorenz, K.; Zellner, R. *Ber. Bunsen-Ges. Phys. Chem.* **1983**, *87*, 629.

(122) Tully, F. P. *Chem. Phys. Lett.* **1983**, *96*, 148.

(123) Robertshaw, J. S.; Smith, I. W. M. *J. Phys. Chem.* **1982**, *86*, 785.

(124) Atkinson, R.; Hansen, D. A.; Pitts, J. N., Jr. *J. Chem. Phys.* **1975**, *62*, 3284.

(125) Tully, F. P.; Ravishankara, A. R. *J. Phys. Chem.* **1980**, *84*, 3126.

(126) Schmidt. V.; Zhu, G. Y.; Becker, K. H.; Fink, E. H. *Ber. Bunsen-Ges. Phys. Chem.* **1985**, *89*, 321.

(127) Ravishankara, A. R.; Nicovich, J. M.; Thompson, R. L.; Tully, F. P. *J. Phys. Chem.* **1981**, *85*, 2498.

(128) Madronich, S.; Felder, W., 20th International Symposium on Combustion, 1984, The Combustion Institute, 1985, pp 703–713.

(129) Gordon, S.; Mulac, W. A. *Int. J. Chem. Kinet.* **1975**, *Symp. 1*, 289.

(130) Harker, A. B.; Burton, C. S. *Int. J. Chem. Kinet.* **1975**, *7*, 907.

(131) Gorse, R. A.; Volman, D. H. *J. Photochem.* **1972**, *1*, 1.

(132) Simonaitis, R.; Heicklen, J. *Int. J. Chem. Kinet.* **1973**, *5*, 231.

(133) Doyle, G. J.; Lloyd, A. C.; Darnall, K. R.; Winer, A. M.; Pitts, J. N., Jr. *Environ. Sci. Technol.* **1975**, *9*, 237.

(134) Cox, R. A. *J. Photochem.* **1974/1975**, *3*, 291.

(135) Campbell, I. M.; Handy, B. J.; Kirby, R. M. *J. Chem. Soc., Faraday Trans. 1* **1975**, *71*, 867.

(136) Wu, C. H.; Japar, S. M.; Niki, H. *J. Environ. Sci. Health* **1976**, *A11*, 191.

(137) Niki, H.; Maker, P. D.; Savage, C. M.; Breitenbach, L. P. *J. Phys. Chem.* **1978**, *82*, 132.

(138) Darnall, K. R.; Atkinson, R.; Pitts, J. N., Jr. *J. Phys. Chem.* **1978**, *82*, 1581.

(139) Cox, R. A.; Derwent, R. G.; Williams, M. R. *Environ. Sci. Technol.* **1980**, *14*, 57.

(140) Atkinson, R.; Carter, W. P. L.; Winer, A. M.; Pitts, J. N., Jr. *J. Air Pollut. Contr. Assoc.* **1981**, *31*, 1090.

(141) Barnes, I.; Bastian, V.; Becker, K. H.; Fink, E. H. and Zabel, F. *Atmos. Environ.* **1982**, *16*, 545.

(142) Ohta, T. *J. Phys. Chem.* **1983**, *87*, 1209.

(143) Tuazon, E. C.; Carter, W. P. L.; Atkinson, R.; Pitts, J. N., Jr. *Int. J. Chem. Kinet.* **1983**, *15*, 619.

(144) Lloyd, A. C.; Darnall, K. R.; Winer, A. M.; Pitts, J. N., Jr. *J. Phys. Chem.* **1976**, *80*, 789.

(145) Cox, R. A.; Patrick, K. F.; Chant, S. A. *Environ. Sci. Technol.* **1981**, *15*, 587.

(146) Niki, H.; Maker, P. D.; Savage, C. M.; Breitenbach, L. P. *J Phys. Chem.* **1978**, *82*, 135.

(147) Atkinson, R.; Aschmann, S. M.; Winer, A. M.; Pitts, J. N., Jr. *Int. J. Chem. Kinet.* **1982**, *14*, 507.

(148) Atkinson, R.; Aschmann, S. M.; Pitts, J. N., Jr. *Environ. Sci. Technol.* **1984**, *18*, 110.

(149) Tuazon, E. C.; Carter, W. P. L.; Atkinson, R.; Winer, A. M.; Pitts, J. N., Jr. *Environ. Sci. Technol.* **1984**, *18*, 49.

(150) Plum, C. N.; Sanhueza, E.; Atkinson, R.; Carter, W. P. L.; Pitts, J. N., Jr. *Environ. Sci. Technol.* **1983**, *17*, 479.

(151) Atkinson, R.; Aschmann, S. M.; Carter, W. P. L. *Int. J. Chem. Kinet.* **1983**, *15*, 1161.

(152) Ohta, T. *Int. J. Chem. Kinet.* **1984**, *16*, 879.

(153) Atkinson, R.; Aschmann, S. M. *Int. J. Chem. Kinet.* **1984**, *16*, 1175.

(154) Biermann, H. W.; Mac Leod, H.; Atkinson, R.; Winer, A. M.; Pitts, J. N., Jr. *Environ. Sci. Technol.* **1985**, *19*, 244.

(155) Atkinson, R.; Aschmann, S. M.; Carter, W. P. L.; Winer, A. M. *Int. J. Chem. Kinet.* **1982**, *14*, 919.

(156) Atkinson, R.; Aschmann, S. M.; Winer, A. M.; Pitts, J. N., Jr. *Arch. Environ. Contam. Toxicol.* **1985**, *14*, 417.

(157) Campbell, I. M.; Goodman, K. *Chem. Phys. Lett.* **1975**, *36*, 382.

(158) Audley, G. J.; Baulch, D. L.; Campbell, I. M.; Waters, D. J.; Watling, G. *J. Chem. Soc., Faraday Trans. 1* **1982**, *78*, 611.

(159) Campbell, I. M.; Parkinson, P. E. *Chem. Phys. Lett.* **1978**, *53*, 385.

(160) Audley, G. J.; Baulch, D. L.; Campbell, I. M. *J. Chem. Soc., Faraday Trans. 1* **1981**, *77*, 2541.

(161) Henri, J. P. L.; Carr, R. W., Jr. *J. Photochem.* **1975**, *5*, 69.

(162) Cvetanovic, R. J., 12th International Symposium on Free Radicals, Laguna Beach, CA, Jan 1976.

(163) Meagher, J. F.; Heicklen, J. *J. Phys. Chem.* **1976**, *80*, 1645.

(164) Niki, H.; Maker, P. D.; Savage, C. M.; Breitenbach, L. P. *Chem. Phys. Lett.* **1981**, *80*, 499.

(165) Darnall, K. R.; Atkinson, R.; Pitts, J. N., Jr. *J. Phys. Chem.* **1979**, *83*, 1943.

(166) Takagi, H.; Washida, N.; Akimoto, H.; Nagasawa, K.; Usui, Y.; Okuda, M. *J. Phys. Chem.* **1980**, *84*, 478.

(167) Kenley, R. A.; Davenport, J. E.; Hendry, D. G. *J. Phys. Chem.* **1981**, *85*, 2740.

(168) Besemer, A. C. *Atmos. Environ.* **1982**, *16*, 1599.

(169) Shepson, P. B.; Edney, E. O.; Corse, E. W. *J. Phys. Chem.* **1984**, *88*, 4122.

(170) Kanofsky, J. R.; Lucas, D.; Pruss, F.; Gutman, D. *J. Phys. Chem.* **1974**, *78*, 311.

(171) Slagle, I. R.; Gilbert, J. R.; Graham, R. E.; Gutman, D. *Int. J. Chem. Kinet.* **1975**, *Symp. 1*, 317.

(172) Sloane, T. M. *Chem. Phys. Lett.* **1978**, *54*, 269.

(173) Hoyermann, K.; Sievert, R. *Ber. Bunsen-Ges. Phys. Chem.* **1979**, *83*, 933.

(174) Sloane, T. M.; Brudzynski, R. J. *J. Chem. Phys.* **1980**, *72*, 4394.

(175) Biermann, H. W.; Harris, G. W.; Pitts, J. N., Jr. *J. Phys. Chem.* **1982**, *86*, 2958.

(176) Hoyermann, K.; Sievert, R. *Ber. Bunsen-Ges. Phys. Chem.* **1983**, *87*, 1027.

(177) Hatakeyama, S.; Akimoto, H. *J. Phys. Chem.* **1983**, *87*, 2387.

(178) Niki, H.; Maker, P. D.; Savage, C. M.; Breitenbach, L. P. *Int. J. Chem. Kinet.* **1983**, *15*, 647.

(179) Niki, H.; Maker, P. D.; Savage, C. M.; Breitenbach, L. P. *J. Phys. Chem.* **1983**, *87*, 4978.

(180) Tuazon, E. C.; Atkinson, R.; Mac Leod, H.; Biermann, H. W.; Winer, A. M.; Carter, W. P. L.; Pitts, J. N., Jr. *Environ. Sci. Technol.* **1984**, *18*, 981.

(181) Westenberg, A. A.; deHaas, N. *J. Chem. Phys.* **1973**, *58*, 4061.

(182) Davis, D. D.; Fischer, S.; Schiff, R. *J. Chem. Phys.* **1974**, *61*, 2213.

(183) Vandooren, J.; Peeters, J.; Van Tiggelen, P. J., 15th International Symposium on Combustion, 1974, The Combustion Institute, 1975, pp 745–753.

(184) Ravishankara, A. R.; Thompson, R. L. *Chem. Phys. Lett.* **1983**, *99*, 377.

(185) Jonah, C. D.; Mulac, W. A.; Zeglinski, P. *J. Phys. Chem.* **1984**, *88*, 4100.

(186) Jeong, K.-M.; Hsu, K.-J.; Jeffries, J. B.; Kaufman, F. *J. Phys. Chem.* **1984**, *88*, 1222.

(187) Zellner, R. *J. Phys. Chem.* **1979**, *83*, 18.

(188) Wilson, W. E.; Westenberg, A. A., 11th International Symposium on Combustion, 1966, The Combustion Institute, 1967; pp 1143–1150.

(189) Margitan, J. J.; Kaufman, F.; Anderson, J. G. *Geophys. Res. Lett.* **1974**, *1*, 80.

(190) Overend, R. P.; Paraskevopoulos, G.; Cvetanovic, R. J. *Can. J. Chem.* **1975**, *53*, 3374.

(191) Howard, C. J.; Evenson, K. M. *J. Chem. Phys.* **1976**, *64*, 197.

(192) Zellner, R.; Steinert, W. *Int. J. Chem. Kinet.* **1976**, *8*, 397.

(193) Jeong, K.-M.; Kaufman, F. *J. Phys. Chem.* **1982**, *86*, 1808.

(194) Baulch, D. L.; Craven, R. J. B.; Din, M.; Drysdale, D. D.; Grant, S.; Richardson, D. J.; Walker, A.; Watling, G. *J. Chem. Soc., Faraday Trans. 1* **1983**, *79*, 689.

(195) Rust, F.; Stevens, C. M. *Int. J. Chem. Kinet.* **1980**, *12*, 371.

(196) Howard, C. J.; Evenson, K. M. *J. Chem. Phys.* **1976**, *64*, 4303.

(197) Leu, M.-T. *J. Chem. Phys.* **1979**, *70*, 1662.

(198) Anderson, L. G.; Stephens, R. D., 15th Informal Conference on Photochemistry, Stanford, CA, June 27–July 1, 1982; Report GMR-4087, ENV #130, General Motors Research Laboratories, Warren, MI, 1982.

(199) Lee, J. H.; Tang, I. N. *J. Chem. Phys.* **1982**, *77*, 4459.

(200) Margitan, J. J.; Watson, R. T. *J. Phys. Chem.* **1982**, *86*, 3819.

(201) Tully, F. P.; Ravishankara, A. R.; Carr, K. *Int. J. Chem. Kinet.* **1983**, *15*, 1111.

(202) Smith, C. A.; Molina, L. T.; Lamb, J. J.; Molina, M. J. *Int. J. Chem. Kinet.* **1984**, *16*, 41.

(203) Tully, F. P.; Droege, A. T.; Koszykowski, M. L.; Melius, C. F. *J. Phys. Chem.* **1986**, *90*, 691.

(204) Baulch, D. L.; Campbell, I. M.; Saunders, S. M. *J. Chem. Soc., Faraday Trans. 1* **1985**, *81*, 259.

(205) Bradley, J. N.; Hack, W.; Hoyermann, K.; Wagner, H. Gg. *J. Chem. Soc., Faraday Trans. 1* **1973**, *69*, 1889.

(206) Gorse, R. A.; Volman, D. H. *J. Photochem.* **1974**, *3*, 115.

(207) Atkinson, R.; Aschmann, S. M.; Carter, W. P. L.; Winer, A. M.; Pitts, J. N., Jr. *Int. J. Chem. Kinet.* **1982**, *14*, 781.

(208) Tully, F. P., and co-workers, private communication, 1985.

(209) Stuhl, F. *Z. Naturforsch.* **1973**, *28A*, 1383.

(210) Perry, R. A.; Atkinson, R.; Pitts, J. N., Jr. *J. Chem. Phys.* **1976**, *64*, 5314.

(211) Paraskevopoulos, G.; Nip, W. S. *Can. J. Chem.* **1980**, *58*, 2146.

(212) Behnke, W.; Nolting, F.; Zetzsch, C., 8th International Symposium on Gas Kinetics, University of Nottingham, Nottingham, U.K., July 15–20, 1984.

(213) Butler, R.; Solomon, I. J.; Snelson, A. *Chem. Phys. Lett.* **1978**, *54*, 19.

(214) Atkinson, R.; Carter, W. P. L.; Aschmann, S. M.; Winer, A. M.; Pitts, J. N., Jr. *Int. J. Chem. Kinet.* **1984**, *16*, 469.

(215) Tully, F. P.; Koszykowski, M. L.; Brinkley, J. S. 20th Inter-

national Symposium on Combustion, 1984, The Combustion Institute, 1985, pp 715–721.

(216) Campbell, I. M.; McLaughlin, D. F.; Handy, B. J. *Chem. Phys. Lett.* **1976**, *38*, 362.

(217) Atkinson, R.; Aschmann, S. M.; Carter, W. P. L. *Int. J. Chem. Kinet.* **1983**, *15*, 51.

(218) Klein, Th.; Barnes, I.; Becker, K. H.; Fink, E. H.; Zabel, F. *J. Phys. Chem.* **1984**, *88*, 5020.

(219) Darnall, K. R.; Winer, A. M.; Lloyd, A. C.; Pitts, J. N., Jr. *Chem. Phys. Lett.* **1976**, *44*, 415.

(220) Zetzsch, C., presented at Bunsen Colloquium, Göttingen, West Germany, October 9, 1980; private communication, 1985.

(221) Jolly, G. S.; Paraskevopoulos, G.; Singleton, D. L. *Int. J. Chem. Kinet.* **1985**, *17*, 1.

(222) Volman, D. H. *Int. J. Chem. Kinet.* **1975**, *Symp. 1*, 358.

(223) Atkinson, R.; Aschmann, S. M.; Pitts, J. N., Jr. *Int. J. Chem. Kinet.* **1983**, *15*, 75.

(224) Atkinson, R.; Aschmann, S. M.; Carter, W. P. L. *Int. J. Chem. Kinet.* **1983**, *15*, 37.

(225) Cohen, N. *Int. J. Chem. Kinet.* **1982**, *14*, 1339.

(226) Benson, S. W. "Thermochemical Kinetics", 2nd ed.; Wiley: New York, 1976.

(227) Atkinson, R. *Int. J. Chem. Kinet.* **1980**, *12*, 761.

(228) Atkinson, R.; Plum, C. N.; Carter, W. P. L.; Winer, A. M.; Pitts, J. N., Jr. *J. Phys. Chem.* **1984**, *88*, 2361.

(229) Lenhardt, T. M.; McDade, C. E.; Bayes, K. D. *J. Chem. Phys.* **1980**, *72*, 304.

(230) Plumb, I. C.; Ryan, K. R. *Int. J. Chem. Kinet.* **1981**, *13*, 1011.

(231) Smith, M. J. C.; Pilling, M. J.; Bayes, K. D. 8th International Symposium on Free Radicals, University of Nottingham, Nottingham, U.K., July 15–20, 1984.

(232) Ruiz, R. P.; Bayes, K. D. *J. Phys. Chem.* **1984**, *88*, 2592.

(233) Schiff, H. I.; Pepper, D.; Ridley, B. A. *J. Geophys. Res.* **1979**, *84*, 7895.

(234) Stedman, D. H.; McEwan, M. J. *Geophys. Res. Lett.* **1983**, *10*, 168.

(235) Logan, J. A. *J. Geophys. Res.* **1983**, *88*, 10785.

(236) Johnston, P. V.; McKenzie, R. L. *Geophys. Res. Lett.* **1984**, *11*, 69.

(237) Bollinger, M. J.; Hahn, C. J.; Parrish, D. D.; Murphy, P. C.; Albritton, D. L.; Fehsenfeld, F. C. *J. Geophys. Res.* **1984**, *89*, 9623.

(238) Dickerson, R. R. *Atmos. Environ.* **1984**, *18*, 2585.

(239) McFarland, M.; Kley, D.; Drummond, J. W.; Schmeltekopf, A. L.; Winkler, R. H. *Geophys. Res. Lett.* **1979**, *6*, 605.

(240) Darnall, K. R.; Carter, W. P. L.; Winer, A. M.; Lloyd, A. C.; Pitts, J. N., Jr. *J. Phys. Chem.* **1976**, *80*, 1948.

(241) Atkinson, R.; Carter, W. P. L.; Winer, A. M. *J. Phys. Chem.* **1983**, *87*, 2012.

(242) Carter, W. P. L.; Atkinson, R. *J. Atmos. Chem.* **1985**, *3*, 377.

(243) Atkinson, R.; Lloyd, A. C. In "Oxygen and Oxy-Radicals in Chemistry and Biology"; Rodgers, M. A. J., Powers, E. L., Eds.; Academic Press: New York, 1981; pp 559–592.

(244) Baldwin, A. C.; Barker, J. R.; Golden, D. M.; Hendry, D. G. *J. Phys. Chem.* **1977**, *81*, 2483.

(245) Batt, L. Proceedings, 1st European Symposium on the "Physico-Chemical Behavior of Atmospheric Pollutants"; Ispra, October 16–18, 1979; Comm. Europ. Commut., 1980; pp 167–184.

(246) Gutman, D.; Sanders, N.; Butler, J. E. *J. Phys. Chem.* **1982**, *86*, 66.

(247) Lorenz, K.; Rhäsa, D.; Zellner, R.; Fritz, B. *Ber. Bunsen-Ges. Phys. Chem.* **1985**, *89*, 341.

(248) Batt, L. *Int. J. Chem. Kinet.* **1979**, *11*, 977.

(249) Choo, K. Y.; Benson, S. W. *Int. J. Chem. Kinet.* **1981**, *13*, 833.

(250) Carter, W. P. L.; Darnall, K. R.; Lloyd, A. C.; Winer, A. M.; Pitts, J. N., Jr. *Chem. Phys. Lett.* **1976**, *42*, 22.

(251) Niki, H.; Maker, P. D.; Savage, C. M.; Breitenbach, L. P. *J. Phys. Chem.* **1981**, *85*, 2698.

(252) Carter, W. P. L.; Darnall, K. R.; Graham, R. A.; Winer, A. M.; Pitts, J. N., Jr. *J. Phys. Chem.* **1979**, *83*, 2305.

(253) Radford, H. E. *Chem. Phys. Lett.* **1980**, *71*, 195.

(254) Ohta, T.; Bandow, H.; Akimoto, H. *Int. J. Chem. Kinet.* **1982**, *14*, 173.

(255) Wang, W. C.; Suto, M.; Lee, L. C. *J. Chem. Phys.* **1984**, *81*, 3122.

(256) Grotheer, H.-H.; Riekert, G.; Meier, U.; Just, Th. *Ber. Bunsen-Ges. Phys. Chem.* **1985**, *89*, 187.

(257) Nip, W. S.; Singleton, D. L.; Overend, R.; Paraskevopoulos, G. *J. Phys. Chem.* **1979**, *83*, 2440.

(258) Perry, R. A.; Atkinson, R.; Pitts, J. N., Jr. *J. Chem. Phys.* **1976**, *64*, 1618.

(259) Davis, D. D.; Machado, G.; Conaway, B.; Oh, Y.; Watson, R. *J. Chem. Phys.* **1976**, *65*, 1268.

(260) Paraskevopoulos, G.; Singleton, D. L.; Irwin, R. S. *J. Phys. Chem.* **1981**, *85*, 561.

(261) Clyne, M. A. A.; Holt, P. M. *J. Chem. Soc., Faraday Trans. 2* **1979**, *75*, 582.

(262) Watson, R. T.; Machado, G.; Conaway, B.; Wagner, S.; Davis, D. D. *J. Phys. Chem.* **1977**, *81*, 256.

(263) Handwerk, V.; Zellner, R. *Ber. Bunsen-Ges. Phys. Chem.* **1978**, *82*, 1161.

(264) Atkinson, R.; Hansen, D. A.; Pitts, J. N., Jr. *J. Chem. Phys.* **1975**, *63*, 1703.

(265) Chang, J. S.; Kaufman, F. *J. Chem. Phys.* **1977**, *66*, 4989.

(266) Clyne, M. A. A.; Holt, P. M. *J. Chem. Soc., Faraday Trans. 2* **1979**, *75*, 569.

(267) Le Bras, G.; Combourieu, J. *Int. J. Chem. Kinet.* **1978**, *10*, 1205.

(268) Garraway, J.; Donovan, R. J. *J. Chem. Soc., Chem. Comm.* **1979**, 1108.

(269) Chang, J. S.; Kaufman, F. *Geophys. Res. Lett.* **1977**, *4*, 192.

(270) Martin, J.-P.; Paraskevopoulos, G. *Can. J. Chem.* **1983**, *61*, 861.

(271) Watson, R. T.; Ravishankara, A. R.; Machado, G.; Wagner, S.; Davis, D. D. *Int. J. Chem. Kinet.* **1979**, *11*, 187.

(272) Tuazon, E. C.; Atkinson, R.; Winer, A. M.; Pitts, J. N., Jr. *Arch. Environ. Contamin. Toxicol.* **1984**, *13*, 691.

(273) Tuazon, E. C.; Atkinson, R.; Aschmann, S. M.; Sweetman, J. A.; Winer, A. M.; Pitts, J. N., Jr. *Environ. Sci. Technol.*, submitted for publication.

(274) Cox, R. A.; Derwent, R. G.; Eggleton, A. E. J.; Lovelock, J. E. *Atmos. Environ.* **1976**, *10*, 305.

(275) Butler, R.; Solomon, I. J.; Snelson, A. *J. Air Pollut. Contr. Assoc.* **1978**, *28*, 1131.

(276) Ryan, K. R.; Plumb, I. C. *J. Phys. Chem.* **1982**, *86*, 4678.

(277) Caralp, F.; Lesclaux, R. *Chem. Phys. Lett.* **1983**, *102*, 54.

(278) Caralp, F.; Dognon, A. M.; Lesclaux, R. 8th International Symposium on Gas Kinetics, University of Nottingham, Nottingham, U.K., July 15–20, 1984.

(279) Cooper, R.; Cumming, J. B.; Gordon, S.; Mulac, W. A. *Radiat Phys. Chem.* **1980**, *16*, 169.

(280) Ryan, K. R.; Plumb, I. C. *Int. J. Chem. Kinet.* **1984**, *16*, 591.

(281) Simonaitis, R.; Glavas, S.; Heicklen, J. *Geophys. Res. Lett.* **1979**, *6*, 385.

(282) Simonaitis, R.; Heicklen, J. *Chem. Phys. Lett.* **1979**, *62*, 473; **1979**, *68*, 245.

(283) Lesclaux, R.; Caralp, F. *Int. J. Chem. Kinet.* **1984**, *16*, 1117.

(284) Jayanty, R. K. M.; Simonaitis, R.; Heicklen, J. *J. Photochem.* **1975**, *4*, 381.

(285) Gillespie, H. M.; Garraway, J.; Donovan, R. J. *J. Photochem.* **1977**, *7*, 29.

(286) Suong, J. Y.; Carr, R. W., Jr. *J. Photochem.* **1982**, *19*, 295.

(287) Atkinson, R.; Perry, R. A.; Pitts, J. N., Jr. *J. Chem. Phys.* **1977**, *66*, 1197.

(288) Zellner, R.; Lorenz, K. *J. Phys. Chem.* **1984**, *88*, 984.

(289) Stuhl, F. *Ber. Bunsen-Ges. Phys. Chem.* **1973**, *77*, 674.

(290) Pastrana, A. V.; Carr, R. W., Jr. *J. Phys. Chem.* **1975**, *79*, 765.

(291) Atkinson, R.; Pitts, J. N., Jr. *J. Chem. Phys.* **1975**, *63*, 3591.

(292) Winer, A. M.; Lloyd, A. C.; Darnall, K. R.; Pitts, J. N., Jr. *J. Phys. Chem.* **1976**, *80*, 1635.

(293) Winer, A. M.; Lloyd, A. C.; Darnall, K. R.; Atkinson, R.; Pitts, J. N., Jr. *Chem. Phys. Lett.* **1977**, *51*, 221.

(294) Ravishankara, A. R.; Wagner, S.; Fischer, S.; Smith, G.; Schiff, R.; Watson, R. T.; Tesi, G.; Davis, D. D. *Int. J. Chem. Kinet.* **1978**, *10*, 783.

(295) Nip, W. S.; Paraskevopoulos, G. *J. Chem. Phys.* **1979**, *71*, 2170.

(296) Smith, R. H. *J. Phys. Chem.* **1983**, *87*, 1596.

(297) Tully, F. P.; Goldsmith, J. E. M. *Chem. Phys. Lett.* **1985**, *116*, 345.

(298) Atkinson, R.; Perry, R. A.; Pitts, J. N., Jr. *J. Chem. Phys.* **1977**, *67*, 3170.

(299) Atkinson, R.; Perry, R. A.; Pitts, J. N., Jr. *Chem. Phys. Lett.* **1976**, *38*, 607.

(300) Atkinson, R.; Pitts, J. N., Jr. *J. Chem. Phys.* **1978**, *68*, 2992.

(301) Atkinson, R.; Darnall, K. R.; Pitts, J. N., Jr. **1978**, cited in ref 1.

(302) Perry, R. A. Ph.D. Thesis, University of California, Riverside, 1977.

(303) Atkinson, R.; Aschmann, S. M.; Carter, W. P. L. *Int. J. Chem. Kinet.* **1984**, *16*, 967.

(304) Atkinson, R.; Aschmann, S. M.; Pitts, J. N., Jr. *Int. J. Chem. Kinet.*, in press.

(305) Tully, F. P., and co-workers, private communication, 1985.

(306) Kleindienst, T. E.; Harris, G. W.; Pitts, J. N., Jr. *Environ. Sci. Technol.* **1982**, *16*, 844.

(307) Cox, R. A. *Int. J. Chem. Kinet.* **1975**, *Symp. 1*, 379.

(308) Grimsrud, E. P.; Westberg, H. H.; Rasmussen, R. A. *Int. J. Chem. Kinet.* **1975**, *Symp. 1*, 183.

(309) Davis, D. D.; Fischer, S.; Schiff, R.; Watson, R. T.; Bollinger, W. *J. Chem. Phys.* **1975**, *63*, 1707.

(310) Palmer, H. B. *J. Chem. Phys.* **1976**, *64*, 2699.

(311) Farquharson, G. K.; Smith, R. H. *Aust. J. Chem.* **1980**, *33*, 1425.

(312) Perry, R. A.; Atkinson, R.; Pitts, J. N., Jr. *J. Phys. Chem.* **1977**, *81*, 1607.

(313) Perry, R. A.; Atkinson, R.; Pitts, J. N., Jr. *J. Phys. Chem.* **1977**, *81*, 296.

(314) Smith, G. P.; Fairchild, P. W.; Jeffries, J. B.; Crosley, D. R. *J. Phys. Chem.* **1985**, *89*, 1269.

(315) Mozurkewich, M.; Benson, S. W. *J. Phys. Chem.* **1984**, *88*, 6429.

(316) Bartels, M.; Hoyermann, K.; Sievert, R. 19th International Symposium on Combustion, 1982, The Combustion Institute 1982; pp 61–72.

(317) Atkinson, R.; Tuazon, E. C.; Carter, W. P. L. *Int. J. Chem. Kinet.* **1985**, *17*, 725.

(318) Ohta, T. *Int. J. Chem. Kinet.* **1984**, *16*, 1495.

(319) McMillen, D. F.; Golden, D. M. *Annu. Rev. Phys. Chem.* **1982**, *33*, 493.

(320) Melius, C. F.; Binkley, J. S.; Koszykowski, M. L. 8th International Symposium on Free Radicals, University of Nottingham, Nottingham, U.K., July 15–20, 1984.

(321) Golden, D. M. In "Chemical Kinetic Data Needs for Modeling the Lower Troposphere"; NBS Special Publication 557, Aug 1979, pp 51–61.

(322) Perry, R. A.; Atkinson, R.; Pitts, J. N., Jr. *J. Chem. Phys.* **1977**, *67*, 458.

(323) Davis, D. D.; Machado, U.; Smith, G.; Wagner, S.; Watson, R. T., unpublished data, cited in ref 78 and 265.

(324) Kirchner, K. *Chimia*, **1983**, *37*, 1.

(325) Pitts, J. N., Jr.; Atkinson, R.; Winer, A. M.; Biermann, H. W.; Carter, W. P. L.; Mac Leod, H.; Tuazon, E. C. Formation and Fate of Toxic Chemicals in California's Atmosphere, Final Report to California Air Resources Board Contract No. A2-115-32, July, 1984.

(326) Michael, J. V.; Nava, D. F.; Borkowski, R. P.; Payne, W. A.; Stief, L. J. *J. Chem. Phys.* **1980**, *73*, 6108.

(327) Perry, R. A.; Williamson, D. *Chem. Phys. Lett.* **1982**, *93*, 331.

(328) Atkinson, R.; Aschmann, S. M. *Int. J. Chem. Kinet.* **1984**, *16*, 259.

(329) Wahner, A.; Zetzsch, C. *Ber. Bunsen-Ges. Phys. Chem.* **1985**, *89*, 323.

(330) Homann, K. H.; Schottler, M.; Warnatz, J., unpublished data cited in ref 10.

(331) Atkinson, R.; Aschmann, S. M. *Combust. Flame* **1984**, *58*, 217.

(332) Perry, R. A. *Combust. Flame* **1984**, *58*, 221.

(333) Breen, J. E.; Glass, G. P. *Int. J. Chem. Kinet.* **1971**, *3*, 145.

(334) Pastrana, A.; Carr, R. W., Jr. *Int. J. Chem. Kinet.* **1974**, *6*, 587.

(335) Lin, C.-Y.; Lin, M. C., presented at the Fall Technical Meeting, Eastern Section, The Combustion Institute, 1984.

(336) Hack, W.; Hoyermann, K.; Sievert, R.; Wagner, H. Gg. *Oxid. Commun.* **1983**, *5*, 101.

(337) Smith, G. P.; Fairchild, P. W.; Crosley, D. R. *J. Chem. Phys.* **1984**, *81*, 2667.

(338) Gutman, D.; Nelson, H. H. *J. Phys. Chem.* **1983**, *87*, 3902.

(339) Herron, J. T.; Penzhorn, R. D. *J. Phys. Chem.* **1969**, *73*, 191.

(340) Atkinson, R.; Pitts, J. N., Jr. *J. Chem. Phys.* **1978**, *68*, 3581.

(341) Stief, L. J.; Nava, D. F.; Payne, W. A.; Michael, J. V. *J. Chem. Phys.* **1980**, *73*, 2254.

(342) Temps, F.; Wagner, H. Gg. *Ber. Bunsen-Ges. Phys. Chem.* **1984**, *88*, 415.

(343) Niki, H.; Maker, P. D.; Savage, C. M.; Breitenbach, L. P. *J. Phys. Chem.* **1984**, *88*, 5342.

(344) Cox, R. A.; Derwent, R. G.; Holt, P. M.; Kerr, J. A. *J. Chem. Soc., Faraday Trans. 1* **1976**, *72*, 2061.

(345) Kerr, J. A.; Sheppard, D. W. *Environ. Sci. Technol.* **1981**, *15*, 960.

(346) Semmes, D. H.; Ravishankara, A. R.; Gump-Perkins, C. A.; Wine, P. H. *Int. J. Chem. Kinet.* **1985**, *17*, 303.

(347) Zetzsch, C. 7th International Symposium on Gas Kinetics, University of Göttingen, Göttingen, West Germany, August 23–28, 1982.

(348) Chiorboli, C.; Bignozzi, C. A.; Maldotti, A.; Giardini, P. F.; Rossi, A.; Carassiti, V. *Int. J. Chem. Kinet.* **1983**, *15*, 579.

(349) Atkinson, R.; Aschmann, S. M.; Carter, W. P. L.; Pitts, J. N., Jr. *Int. J. Chem. Kinet.* **1982**, *14*, 839.

(350) Maldotti, A.; Chiorboli, C.; Bignozzi, C. A.; Bartocci, C.; Carassiti, V. *Int. J. Chem. Kinet.* **1980**, *12*, 905.

(351) Faubel, C.; Wagner, H. Gg.; Hack, W. *Ber. Bunsen-Ges. Phys. Chem.* **1977**, *81*, 689.

(352) Tuazon, E. C.; Atkinson, R.; Carter, W. P. L. *Environ. Sci. Technol.* **1985**, *19*, 265.

(353) Overend, R.; Paraskevopoulos, G. *J. Phys. Chem.* **1978**, *82*, 1329.

(354) Ravishankara, A. R.; Davis, D. D. *J. Phys. Chem.* **1978**, *82*, 2852.

(355) Hägele, J.; Lorenz, K.; Rhäsa, D.; Zellner, R. *Ber. Bunsen-Ges. Phys. Chem.* **1983**, *87*, 1023.

(356) Meier, U.; Grotheer, H. H.; Riekert, G.; Just, Th. *Ber. Bunsen-Ges. Phys. Chem.* **1985**, *89*, 325.

(357) Zetzsch, C., report to Bundeminister für Forschung und Technologie, Projekttrager für unweltchemikalien, 1982.

(358) Cox, R. A.; Goldstone, A. Proceedings, 2nd European Symposium on the "Physico-Chemical Behavior of Atmospheric Pollutants"; Varese, Italy, Sept 29–Oct 1, 1981; D. Riedel Publishing Co.: Dorecht, Holland 1982; pp 112–119.

(359) Meier, U.; Grotheer, H. H.; Riekert, G.; Just, Th. *Chem. Phys. Lett.* **1985**, *115*, 221.

(360) Lorenz, K.; Rhäsa, D.; Zellner, R. **1984**, private communication.

(361) Lloyd, A. C.; Darnall, K. R.; Winer, A. M.; Pitts, J. N., Jr. *Chem. Phys. Lett.* **1976**, *42*, 205.

(362) Weidelmann, A.; Zetzsch, C., presented at Bunsentagung, Ulm and Neu-Ulm, May 20–22, 1982.

(363) Perry, R. A.; Atkinson, R.; Pitts, J. N., Jr. *J. Chem. Phys.* **1977**, *67*, 611.

(364) Tully, F. P., and co-workers, private communication, 1985.

(365) Wine, P. H.; Thompson, R. J. *Int. J. Chem. Kinet.* **1984**, *16*, 867.

(366) Zetzsch, C.; Stuhl, F. Proceedings, 2nd European Symposium on the "Physico-Chemical Behavior of Atmospheric Pollutants"; Varese, Italy, Sept 29–Oct 1, 1981; D. Riedel: Boston, 1982; pp 129–137; private communication, 1985.

(367) Wine, P. H.; Astalos, R. J.; Mauldin, R. L., III *J. Phys. Chem.* **1985**, *89*, 2620.

(368) Lorenz, K.; Zellner, R. *Ber. Bunsen-Ges. Phys. Chem.* **1984**, *88*, 1228.

(369) Winer, A. M.; Darnall, K. R.; Atkinson, R.; Pitts, J. N., Jr., unpublished results, 1978, cited in ref 1.

(370) Niki, H.; Maker, P. D.; Savage, C. M.; Breitenbach, L. P. *J. Phys. Chem.* **1983**, *87*, 2190.

(371) Anastasi, C.; Smith, I. W. M.; Parkes, D. A. *J. Chem. Soc., Faraday Trans. 1* **1978**, *74*, 1693.

(372) Smith, R. H. *Int. J. Chem. Kinet.* **1978**, *10*, 519.

(373) Blundell, R. V.; Cook, W. G. A.; Hoare, D. E.; Milne, G. S. 10th International Symposium on Combustion, 1964, The Combustion Institute, 1965; pp 445–452.

(374) Westenberg, A. A.; Fristrom, R. M. 10th International Symposium on Combustion, 1964, The Combustion Institute, 1965; pp 473–487.

(375) Hoare, D. E. *Proc. R. Soc. London, Ser. A* **1966**, *291*, 73.

(376) Hoare, D. E.; Peacock, G. B. *Proc. R. Soc. London, Ser. A* **1966**, *291*, 85.

(377) Peeters, J.; Mahnen, G. 14th International Symposium on Combustion, 1972, The Combustion Institute, 1973; pp 133–146.

(378) Osif, T. L.; Simonaitis, R.; Heicklen, J. *J. Photochem.* **1975**, *4*, 233.

(379) Kondo, O.; Benson, S. W. *Int. J. Chem. Kinet.* **1984**, *16*, 949.

(380) Morrison, B. M., Jr.; Heicklen, J. *J. Photochem.* **1980**, *13*, 189.

(381) Singleton, D. L.; Irwin, R. S.; Cvetanovic, R. J. *Can. J. Chem.* **1977**, *55*, 3321.

(382) Solly, R. K.; Golden, D. M.; Benson, S. W. *Int. J. Chem. Kinet.* **1970**, *2*, 381.

(383) Atkinson, R.; Aschmann, S. M.; Winer, A. M.; Pitts, J. N., Jr. *Int. J. Chem. Kinet.* **1981**, *13*, 1133.

(384) Carter, W. P. L.; Atkinson, R.; Winer, A. M.; Pitts, J. N., Jr., unpublished data, cited in ref 223.

(385) Gaffney, J. S.; Levine, S. Z. *Int. J. Chem. Kinet.* **1982**, *14*, 1281.

(386) Niki, H.; Maker, P. D.; Savage, C. M.; Breitenbach, L. P. *Int. J. Chem. Kinet.* **1985**, *17*, 547.

(387) Engelking, P. C.; Ellison, G. B.; Lineberger, W. C. *J. Chem. Phys.* **1978**, *69*, 1826.

(388) Michael, J. V.; Nava, D. F.; Payne, W. A.; Stief, L. J. *J. Chem. Phys.* **1979**, *70*, 3652.

(389) Cox, R. A.; Derwent, R. G.; Kearsey, S. V.; Batt, L.; Patrick, K. G. *J. Photochem.* **1980**, *13*, 149.

(390) Su, F.; Calvert, J. G.; Shaw, J. H.; Niki, H.; Maker, P. D.; Savage, C. M.; Breitenbach, L. D. *Chem. Phys. Lett.* **1979**, *65*, 221.

(391) Su, F.; Calvert, J. G.; Shaw, J. H. *J. Phys. Chem.* **1979**, *83*, 3185.

(392) Niki, H.; Maker, P. D.; Savage, C. M.; Breitenbach, L. P. *Chem. Phys. Lett.* **1980**, *72*, 71.

(393) Tuazon, E. C.; Carter, W. P. L.; Atkinson, R., unpublished data.

(394) Atkinson, R.; Perry, R. A.; Pitts, J. N., Jr. *J. Chem. Phys.* **1977**, *66*, 1578.

(395) Cox, R. A.; Sheppard, D. *Nature (London)* **1980**, *284*, 330.

(396) Wine, P. H.; Kreutter, N. M.; Gump, C. A.; Ravishankara, A. R. *J. Phys. Chem.* **1981**, *85*, 2660.

(397) Mac Leod, H.; Poulet, G.; Le Bras, G. *J. Chim. Phys.* **1983**, *80*, 287.

(398) Mac Leod, H.; Jourdain, J. L.; Poulet, G.; Le Bras, G. *Atmos. Environ.* **1984**, *18*, 2621.

(399) Lee, J. H.; Tang, I. N. *J. Chem. Phys.* **1983**, *78*, 6646.

(400) Wine, P. H.; Thompson, R. J.; Semmes, D. H. *Int. J. Chem. Kinet.* **1984**, *16*, 1623.

(401) Atkinson, R.; Perry, R. A.; Pitts, J. N., Jr. *Chem. Phys. Lett.* **1978**, *54*, 14.

(402) Kurylo, M. J. *Chem. Phys. Lett.* **1978**, *58*, 233.

(403) Atkinson, R.; Pitts, J. N., Jr.; Aschmann, S. M. *J. Phys. Chem.* **1984**, *88*, 1584.

(404) Wallington, T. J.; Atkinson, R.; Tuazon, E. C.; Aschmann, S. M. *Int. J. Chem. Kinet.*, in press.

(405) Wine, P. H., private communication, 1985.

(406) Martin, D.; Jourdain, J. L.; Le Bras, G. *Int. J. Chem. Kinet.* **1985**, *17*, 1247.
(407) Mac Leod, H.; Jourdain, J. L.; Le Bras, G. *Chem. Phys. Lett.* **1983**, *98*, 381.
(408) Wallington, T. J. *Int. J. Chem. Kinet.*, in press.
(409) Jones, B. M. R.; Burrows, J. P.; Cox, R. A.; Penkett, S. A. *Chem. Phys. Lett.* **1982**, *88*, 372.
(410) Barnes, I.; Becker, K. H.; Fink, E. H.; Reimer, A.; Zabel, F.; Niki, H. *Int. J. Chem. Kinet.* **1983**, *15*, 631.
(411) Jones, B. M. R.; Cox, R. A.; Penkett, S. A. *J. Atmos. Chem.* **1983**, *1*, 65.
(412) Mac Leod, H.; Aschmann, S. M.; Atkinson, R.; Tuazon, E. C.; Sweetman, J. A.; Winer, A. M.; Pitts, J. N., Jr. *J. Geophys. Res.*, in press.
(413) Benson, S. W. *Chem. Rev.* **1978**, *78*, 23.
(414) Niki, H.; Maker, P. D.; Savage, C. M.; Breitenbach, L. P. *J. Phys. Chem.* **1983**, *87*, 7.
(415) Grosjean, D. *Environ. Sci. Technol.* **1984**, *18*, 460.
(416) Shum, L. G. S.; Benson, S. W. *Int. J. Chem. Kinet.* **1985**, *17*, 277.
(417) Slagle, I. R.; Graham, R. E.; Gutman, D. *Int. J. Chem. Kinet.* **1976**, *8*, 451.
(418) Slagle, I. R.; Baiocchi, F.; Gutman, D. *J. Phys. Chem.* **1978**, *82*, 1333.
(419) Kirchner, K.; Vettermann, R.; Indruch, H. *Ber. Bunsen-Ges. Phys. Chem.* **1978**, *82*, 1223.
(420) Nip, W. S.; Singleton, D. L.; Cvetanovic, R. J. *J. Am. Chem. Soc.* **1981**, *103*, 3526.
(421) Cvetanovic, R. J.; Singleton, D. L.; Irwin, R. S. *J. Am. Chem. Soc.* **1981**, *103*, 3530.
(422) Lee, J. H.; Timmons, R. B.; Stief, L. J. *J. Chem. Phys.* **1976**, *64*, 300.
(423) Lee, J. H.; Tang, I. N.; Klemm, R. B. *J. Chem. Phys.* **1980**, *72*, 1793.
(424) Lee, J. H.; Tang, I. N. *J. Chem. Phys.* **1980**, *72*, 5718.
(425) Hatakeyama, S.; Okuda, M.; Akimoto, H. *Geophys. Res. Lett.* **1982**, *9*, 583.
(426) Grosjean, D.; Lewis, R. *Geophys. Res. Lett.* **1982**, *9*, 1203.
(427) Hatakeyama, S.; Izumi, K.; Akimoto, H. *Atmos. Environ.* **1985**, *19*, 135.
(428) Atkinson, R.; Perry, R. A.; Pitts, J. N., Jr. *J. Chem. Phys.* **1978**, *68*, 1850.
(429) Gorse, R. A. Jr.; Lii, R. R.; Saunders, B. B. *Science (Washington, D.C.)* **1977**, *197*, 1365.
(430) Anderson, L. G.; Stephens, R. D. 14th Int. Conf. Photochem., Newport Beach, CA, April, 1980.
(431) Harris, G. W.; Pitts, J. N., Jr. *Environ. Sci. Technol.* **1983**, *17*, 50.
(432) Hack, W.; Hoyermann, K.; Wagner, H. Gg. *Ber. Bunsen-Ges. Phys. Chem.* **1974**, *78*, 386.
(433) Harris, G. W.; Atkinson, R.; Pitts, J. N., Jr. *J. Phys. Chem.* **1979**, *83*, 2557.
(434) Baulch, D. L.; Campbell, I. M.; Saunders, S. M. *Int. J. Chem. Kinet.* **1985**, *17*, 355.
(435) Fritz, B.; Lorenz, K.; Steinert, W.; Zellner, R. Proceedings, 2nd European Symposium on the "Physico-Chemical Behavior of Atmospheric Pollutants"; Varese, Italy, Sept 29–Oct 1, 1981; D. Riedel: Boston, 1982; pp 192–202.
(436) Fritz, B.; Lorenz, K.; Steinert, W.; Zellner, R. *Oxid. Commun.* **1984**, *6*, 363.
(437) Harris, G. W.; Kleindienst, T. E.; Pitts, J. N., Jr. *Chem. Phys. Lett.* **1981**, *80*, 479.
(438) Kurylo, M. J.; Knable, G. L. *J. Phys. Chem.* **1984**, *88*, 3305.
(439) Poulet, G.; Laverdet, G.; Jourdain, J. L.; Le Bras, G. *J. Phys. Chem.* **1984**, *88*, 6259.
(440) Atkinson, R.; Aschmann, S. M.; Winer, A. M.; Carter, W. P. L. *Atmos. Environ.* **1984**, *18*, 2105.
(441) Atkinson, R.; Tuazon, E. C.; Wallington, T. J.; Aschmann, S. M.; Sweetman, J. A.; Winer, A. M.; Pitts, J. N., Jr., submitted for publication in *Environ. Sci. Technol.*
(442) Wallington, T. J.; Atkinson, R.; Winer, A. M. *Geophys. Res. Lett.* **1984**, *11*, 861.
(443) Phillips, L. F. *Chem. Phys. Lett.* **1978**, *57*, 538.
(444) Phillips, L. F. *Aust. J. Chem.* **1979**, *32*, 2571.
(445) Lindley, C. R. C.; Calvert, J. G.; Shaw, J. H. *Chem. Phys. Lett.* **1979**, *67*, 57.
(446) Lesclaux, R.; Demissy, M. *Nouv. J. Chem.* **1977**, *1*, 443.
(447) Lozovsky, V. A.; Ioffe, M. A.; Sarkisov, O. M. *Chem. Phys. Lett.* **1984**, *110*, 651.
(448) Pitts, J. N., Jr.; Grosjean, D.; Van Cauwenberghe, K.; Schmid, J. P.; Fitz, D. R. *Environ. Sci. Technol.* **1978**, *12*, 946.
(449) Tuazon, E. C.; Winer, A. M.; Graham, R. A.; Schmid, J. P.; Pitts, J. N., Jr. *Environ. Sci. Technol.* **1978**, *12*, 954.
(450) Foner, S. N.; Hudson, R. L. *J. Chem. Phys.* **1958**, *29*, 442.
(451) Dibeler, V. H.; Franklin, J. L.; Reese, R. M. *J. Am. Chem. Soc.* **1959**, *81*, 68.
(452) Tuazon, E. C.; Carter, W. P. L.; Winer, A. M.; Pitts, J. N., Jr. *Environ. Sci. Technol.* **1981**, *15*, 823.
(453) Tuazon, E. C.; Carter, W. P. L.; Brown, R. V.; Atkinson, R.; Winer, A. M.; Pitts, J. N., Jr. "Atmospheric Reaction Mechanisms of Amine Fuels"; Final Report ESL-TR-82-17, Mar 1982.
(454) Zabarnick, S.; Heicklen, J. *Int. J. Chem. Kinet.* **1985**, *17*, 455, 477, 503.
(455) Cicerone, R. J.; Zellner, R. *J. Geophys. Res.* **1983**, *88*, 10689.
(456) Hashimoto, S.; Bandow, H.; Akimoto, H.; Weng, J.-H.; Tang, X.-Y. *Int. J. Chem. Kinet.* **1984**, *16*, 1385.
(457) Davis, D. D.; Bollinger, W.; Fischer, S. *J. Phys. Chem.* **1975**, *79*, 293.
(458) Hansen, D. A.; Atkinson, R.; Pitts, J. N., Jr. *J. Phys. Chem.* **1975**, *79*, 1763.
(459) Tully, F. P.; Ravishankara, A. R.; Thompson, R. L.; Nicovich, J. M.; Shah, R. C.; Kreutter, N. M.; Wine, P. H. *J. Phys. Chem.* **1981**, *85*, 2262.
(460) Lorenz, K.; Zellner, R., private communication, 1985.
(461) Wahner, A.; Zetzsch, C. *J. Phys. Chem.* **1983**, *87*, 4945.
(462) Rinke, M.; Zetzsch, C. *Ber. Bunsen-Ges. Phys. Chem.* **1984**, *88*, 55.
(463) Nicovich, J. M.; Thompson, R. L.; Ravishankara, A. R. *J. Phys. Chem.* **1981**, *85*, 2913.
(464) Bignozzi, C. A.; Maldotti, A.; Chiorboli, C.; Bartocci, C.; Carassiti, V. *Int. J. Chem. Kinet.* **1981**, *13*, 1235.
(465) Atkinson, R.; Darnall, K. R.; Pitts, J. N., Jr. *J. Phys. Chem.* **1978**, *82*, 2759.
(466) Zetzsch, C. 15th Informal Conference on Photochemistry, Stanford, CA, June 27–July 1, 1982.
(467) Atkinson, R.; Aschmann, S. M. *Environ. Sci. Technol.* **1985**, *19*, 462.
(468) Atkinson, R.; Aschmann, S. M. *Int. J. Chem. Kinet.*, in press.
(469) Kenley, R. A.; Davenport, J. E.; Hendry, D. G. *J. Phys. Chem.* **1978**, *82*, 1095.
(470) Hoshino, M.; Akimoto, H.; Okuda, M. *Bull. Chem. Soc. Jpn.* **1978**, *51*, 718.
(471) Mulder, P.; Louw, R. *Tetrahedron Lett.* **1982**, *23*, 2605.
(472) O'Brien, R. J.; Green, P. J.; Doty, R. M. In "Chemical Kinetic Data Needs for Modeling the Lower Troposphere"; NBS Special Publication 557, 1979, pp 93–95.
(473) O'Brien, R. J.; Green, P. J.; Doty, R. A.; Vanderzanden, J. W.; Easton, R. R.; Irwin, R. P. In "Nitrogenous Air Pollutants"; Grosjean, D., Ed.; Ann Arbor Press: Ann Arbor, MI, 1979, pp 189–210.
(474) Takagi, H.; Washida, N.; Akimoto, H.; Okuda, M. *Spectrosc. Lett.* **1982**, *15*, 145.
(475) Atkinson, R.; Carter, W. P. L.; Winer, A. M. *J. Phys. Chem.* **1983**, *87*, 1605.
(476) Bandow, H.; Washida, N.; Akimoto, H. 11th International Conference on Photochemistry, University of Maryland, College Park, MA, Aug 21–26, 1983.
(477) Dumdei, B. E.; O'Brien, R. J. *Nature (London)* **1984**, *311*, 248.
(478) Tuazon, E. C.; Mac Leod, H.; Atkinson, R.; Carter, W. P. L. *Environ. Sci. Technol.*, in press.
(479) Fritz, B.; Handwerk, V.; Preidel, M.; Zellner, R. *Ber. Bunsen-Ges. Phys. Chem.* **1985**, *89*, 343.
(480) Sauer, M. C., Jr.; Mani, I. *J. Phys. Chem.* **1970**, *74*, 59.
(481) Spicer, C. W.; Jones, P. W. *J. Air Pollut. Control Assoc.* **1977**, *27*, 1122.
(482) Ebata, T.; Obi, K.; Tanaka, I. *Chem. Phys. Lett.* **1981**, *77*, 480.
(483) Nelson, H. H.; McDonald, J. R. *J. Phys. Chem.* **1982**, *86*, 1242.
(484) Narita, N.; Tezuka, T. *J. Am. Chem. Soc.* **1982**, *104*, 7316.
(485) Zellner, R.; Fritz, B.; Preidel, M. *Chem. Phys. Lett.* **1985**, *121*, 412.
(486) Niki, H.; Maker, P. D.; Savage, C. M.; Breitenbach, L. P. In "Nitrogeneous Air Pollutants"; Grosjean, D., Ed.; Ann Arbor Press: Ann Arbor, MI, 1979, pp 1–16.
(487) Harrison, R. M.; Laxen, D. P. H. *Environ. Sci. Technol.* **1978**, *12*, 1384.
(488) Nielsen, O. J.; Nielsen, T.; Pagsberg, P. "Direct Spectrokinetic Investigation of the Reactivity of OH with Tetraalkyllead Compounds in the Gas Phase. Estimate of Lifetimes of Tetraalkyllead Compounds in Ambient Air"; Riso-R-463, Riso National Laboratory, Roskilde, Denmark, May, 1982.
(489) Cvetanovic, R. J. *Adv. Photochem.* **1963**, *1*, 115.
(490) Slagle, I. R.; Gutman, D.; Gilbert, J. R. *Chem. Phys. Lett.* **1974**, *26*, 111.
(491) Slagle, I. R.; Gutman, D.; Gilbert, J. R. 15th International Symposium on Combustion, 1974, The Combustion Institute, 1975; pp 785–793.
(492) Singleton, D. L.; Furuyama, S.; Cvetanovic, R. J.; Irwin, R. S. *J. Chem. Phys.* **1975**, *63*, 1003.
(493) Gaffney, J. S.; Atkinson, R.; Pitts, J. N., Jr. *J. Am. Chem. Soc.* **1975**, *97*, 5049.
(494) Singleton, D. L.; Cvetanovic, R. J. *J. Am. Chem. Soc.* **1976**, *98*, 6812.
(495) Atkinson, R.; Pitts, J. N., Jr. *J. Chem. Phys.* **1977**, *67*, 38.
(496) Atkinson, R.; Pitts, J. N., Jr. *J. Chem. Phys.* **1977**, *67*, 2488.
(497) Atkinson, R.; Pitts, J. N., Jr. *J. Chem. Phys.* **1977**, *67*, 2492.
(498) Nip, W. S.; Singleton, D. L.; Cvetanovic, R. J. *Can. J. Chem.*

1979, *57*, 949.

(499) Nicovich, J. M.; Ravishankara, A. R. 19th International Symposium on Combustion, 1982. The Combustion Institute, 1982, pp 23–30.

(500) Perry, R. A. *J. Chem. Phys.* **1984**, *80*, 153.

(501) Park, J.-Y.; Sawyer, P. F.; Heaven, M. C.; Gutman, D. *J. Phys. Chem.* **1984**, *88*, 2821.

(502) Atkinson, R.; Plum, C. N.; Carter, W. P. L.; Winer, A. M.; Pitts, J. N., Jr. *J. Phys. Chem.* **1984**, *88*, 1210.

(503) Atkinson, R.; Aschmann, S. M.; Winer, A. M.; Pitts, J. N., Jr. *Environ. Sci. Technol.* **1984**, *18*, 370.

(504) Atkinson, R.; Aschmann, S. M.; Winer, A. M.; Pitts, J. N., Jr. *Environ. Sci. Technol.* **1985**, *19*, 159.

(505) Atkinson, R.; Aschmann, S. M.; Long, W. D.; Winer, A. M. *Int. J. Chem. Kinet.* **1985**, *17*, 957.

(506) Atkinson, R.; Carter, W. P. L. *Chem. Rev.* **1984**, *84*, 437.

(507) Bahta, A.; Simonaitis, R.; Heicklen, J. *Int. J. Chem. Kinet.* **1984**, *16*, 1227.

(508) Gaffney, J. S.; Levine, S. Z. *Int. J. Chem. Kinet.* **1979**, *11*, 1197.

(509) Atkinson, R.; Aschmann, S. M.; Carter, W. P. L.; Pitts, J. N., Jr. *Int. J. Chem. Kinet.* **1983**, *15*, 721.

(510) Rinke, M.; Wahner, A.; Zetzsch, C.; *J. Photochem.* **1981**, *17*, 142.

(511) Güsten, H.; Klasinc, L.; Marić, D. *J. Atmos. Chem.* **1984**, *2*, 83.

(512) Brown, H. C.; Okamoto, Y. *J. Am. Chem. Soc.* **1958**, *80*, 4979.

(513) Heicklen, J. *Int. J. Chem. Kinet.* **1981**, *13*, 651.

(514) Hendry, D. G.; Kenley, R. A. "Atmospheric Reaction Products of Organic Compounds"; EPA-560/12-79-001, June 1979.

(515) Güsten, H.; Filby, W. G.; Schoof, S. *Atmos. Environ.* **1981**, *15*, 1763.

(516) Jeong, K.-M.; Kaufman, F. *J. Phys. Chem.* **1982**, *86*, 1816.

(517) Singleton, D. L.; Paraskevopoulos, G.; Irwin, R. S. *J. Phys. Chem.* **1980**, *84*, 2339.

(518) Altshuller, A. P. *Adv. Environ. Sci. Technol.* **1980**, *10*, 181.

(519) Hewitt, C. N.; Harrison, R. M. *Atmos. Environ.* **1985**, *19*, 545.

(520) Japar, S. M.; Niki, H. *J. Phys. Chem.* **1975**, *79*, 1629.

(521) Winer, A. M.; Atkinson, R.; Pitts, J. N., Jr. *Science (Washington, D.C.)* **1984**, *224*, 156.

(522) Atkinson, R.; Aschmann, S. M.; Winer, A. M.; Carter, W. P. L. *Environ. Sci. Technol.* **1985**, *19*, 87.

(523) Carter, W. P. L.; Winer, A. M.; Pitts, J. N., Jr. *Environ. Sci. Technol.* **1981**, *15*, 829.

(524) Atkinson, R.; Carter, W. P. L.; Plum, C. N.; Winer, A. M.; Pitts, J. N., Jr. *Int. J. Chem. Kinet.* **1984**, *16*, 887.

(525) Platt, U.; Perner, D.; Winer, A. M.; Harris, G. W.; Pitts, J. N., Jr. *Geophys. Res. Lett.* **1980**, *7*, 89.

(526) Noxon, J. F.; Norton, R. B.; Marovich, E. *Geophys. Res. Lett.* **1980**, *7*, 125.

(527) Platt, U.; Perner, D.; Schröder, J.; Kessler, C.; Toennissen, A. *J. Geophys. Res.* **1981**, *86*, 11965.

(528) Platt, U.; Perner, D.; Kessler, C. Proceedings, 2nd European Symposium; "Composition of the Nonurban Troposphere"; Williamsburg, VA, May 25–28, 1982, pp 21–24.

(529) Platt, U. F.; Winer, A. M.; Biermann, H. W.; Atkinson, R.; Pitts, J. N., Jr. *Environ. Sci. Technol.* **1984**, *18*, 365.

(530) Pitts, J. N., Jr.; Biermann, H. W.; Atkinson, R.; Winer, A. M. *Geophys. Res. Lett.* **1984**, *11*, 557.

(531) Perner, D.; Schmeltekopf, A.; Winkler, R. H.; Johnston, H. S.; Calvert, J. G.; Cantrell, C. A.; Stockwell, W. R. *J. Geophys. Res.* **1985**, *90*, 3807.

(532) Singh, H. B.; Ludwig, F. L.; Johnson, W. B. *Atmos. Environ.* **1978**, *12*, 2185.

(533) Oltmans, S. J. *J. Geophys. Res.* **1981**, *86*, 1174.

(534) Morris, E. D., Jr.; Niki, H. *J. Phys. Chem.* **1974**, *78*, 1337.

(535) Cantrell, C. A.; Stockwell, W. R.; Anderson, L. G.; Busarow, K. L.; Perner, D.; Schmeltekopf, A.; Calvert, J. G.; Johnston, H. S. *J. Phys. Chem.* **1985**, *89*, 139.

(536) Nielsen, O. J.; Pagsberg, P.; Sillesen, A. Proceedings, 3rd European Symposium on the Physico-Chemical Behaviour of Atmospheric Pollutants, Varese, Italy, April 10–12, 1984; Riedel: Boston, 1984; pp 283–292.

(537) Nelson, L.; Treacy, J. J.; Sidebottom, H. W. Proceedings, 3rd European Symposium on the Physico-Chemical Behaviour of Atmospheric Pollutants, Varese, Italy, April 10–12, 1984; Riedel: Boston, pp 258–263.

(538) Shepson, P. B.; Edney, E. O.; Kleindienst, T. E.; Pittman, J. H.; Namie, G. R.; Cupitt, L. T. *Environ. Sci. Technol.* **1985**, *19*, 849.

(539) Hatakeyama, S.; Washida, N.; Akimoto, H. *J. Phys. Chem.* **1986**, *90*, 173.

(540) Michael, J. V.; Keil, D. G.; Klemm, R. B. *J. Chem. Phys.* **1985**, *83*, 1630.

(541) Kerr, J. A.; Stocker, D. W. *J. Photochem.* **1985**, *28*, 475.

(542) Hatakeyama, S.; Honda, S.; Washida, N.; Atkimoto, H. *Bull. Chem. Soc. Jpn.* **1985**, *58*, 2157.

(543) Barnes, I.; Bastian, V.; Becker, K. H.; Fink, E. H. Proceedings, 3rd European Symposium on the Physico-Chemical Behaviour of Atmospheric Pollutants, Varese, Italy, April 10–12, 1984; Riedel: Boston, 1984; pp 149–157.

(544) Bandow, H.; Washida, N.; Akimoto, H. *Bull. Chem. Soc. Jpn.* **1985**, *58*, 2531.

(545) Bandow, H.; Washida, N. *Bull. Chem. Soc. Jpn.* **1985**, *58*, 2541.

(546) Bandow, H.; Washida, N. *Bull. Chem. Soc. Jpn.* **1985**, *58*, 2549.

(547) Gery, M. W.; Fox, D. L.; Jeffries, H. E.; Stockburger, L.; Weathers, W. S. *Int. J. Chem. Kinet.* **1985**, *17*, 931.

(548) Madronich, S.; Felder, W. *J. Phys. Chem.* **1985**, *89*, 3556.

(549) Ohta, T.; Ohyama, T. *Bull. Chem. Soc. Jpn.* **1985**, *58*, 3029.

(550) Witte, F.; Zetzsch, C. Proceedings, 3rd European Symposium on the Physico-Chemical Behaviour of Atmospheric Pollutants, Varese, Italy, April 10–12, 1984; Riedel: Boston, 1984; pp 168–176.